The American Mineralogist

Journal of the Mineralogical Society of America

Vol. 37 MAY-JUNE, 1952 Nos. 5 and 6

Contents

Contributions to Canadian Mineralogy

Volume 5, Part 4

Sponsored by The Walker Mineralogical Club

Edited by L. G. Berry, *Kingston*

Published bi-monthly by the Society

Mineralogical Society of America

ASSOCIATED WITH THE GEOLOGICAL SOCIETY OF AMERICA

President: **Michael Fleischer,** U. S. Geological Survey, Washington 25, D. C.

Vice President: **J. D. H. Donnay,** The Johns Hopkins University, Baltimore, Maryland.

Secretary: **C. S. Hurlbut, Jr.,** Harvard University, Cambridge, Massachusetts.

Treasurer: **Earl Ingerson,** U. S. Geological Survey, Washington 25, D. C.

Editor: **Walter F. Hunt,** University of Michigan, Ann Arbor, Michigan.

Councillors: **Lewis S. Ramsdell,** University of Michigan, Ann Arbor, Michigan.
E. F. Osborn, School of Mineral Industries, Pennsylvania State College, Pennsylvania.
George T. Faust, U. S. Geological Survey, Washington 25, D. C.
Victor T. Allen, Institute of Geophysical Technology, St. Louis, Missouri.
Adolf Pabst, University of California, Berkeley, California

The enlarged issues of this journal for 1952 are made possible by a grant from the Penrose Fund of the Geological Society of America.

The American Mineralogist—Journal of the Mineralogical Society of America

A journal containing articles on mineralogy, crystallography, petrography, and allied sciences, is issued every two months. Contributions are invited from everyone.

Office of Publication, Mineralogical Laboratory, Ann Arbor, Mich.

The general conduct of the journal is in the hands of the editor, **Walter F. Hunt,** Ann Arbor, Michigan, to whom all manuscripts should be submitted. To assist the editor the council of the Mineralogical Society has appointed **Lewis S. Ramsdell,** Ann Arbor, Michigan, assistant editor, and the following board of associate editors:

Michael Fleischer, U. S. Geological Survey, Washington, D. C.
Esper S. Larsen, Jr., U. S. Geological Survey, Washington, D. C.
Austin F. Rogers, 2412 Durant Ave., Berkeley, California.
George Tunell, University of California at Los Angeles, California.

Contributors of leading articles are given without charge 100 reprints (without covers) of their article. If additional reprints are desired these can be purchased at the following rates:

Pages	*1–4*	*5–8*	*9–12*	*13–16*	*17–20*	*21–24*	*25–28*	*29–32*	*Covers*
Copies									
25	$3.50	$5.00	$ 8.00	$ 9.50	$11.00	$13.00	$15.00	$16.00	$4.90
50	3.80	5.55	8.80	10.40	12.10	14.20	16.40	17.50	5.50
75	4.10	6.10	9.60	11.30	13.20	15.40	17.80	19.00	6.10
100	4.00	6.65	10.40	12.20	14.30	16.60	19.20	20.50	6.70
Addl. C's	1.20	2.20	3.20	3.60	4.40	4.80	5.60	6.00	2.40

Cover Composition $1.55.

Sent to all members and fellows of the Mineralogical Society of America. Subscription price, $4.00 per year (single copies of normal issues, $1.00 plus postage).

Entered as second class matter at the post office at Menasha, Wis., under Act of March 3, 1879. Acceptance for mailing at the special rate of postage provided for in section 1103, Act of Oct. 3, 1917, paragraph 4 section 429 P. L. & R. authorized March 13, 1922.

Notice of change of address, orders, and remittances should be sent to Dr. Earl Ingerson, U. S. Geological Survey, Washington 25, D. C.

Printed by the George Banta Publishing Company, Menasha, Wisconsin
Printed in the United States of America

THE AMERICAN MINERALOGIST

JOURNAL OF THE MINERALOGICAL SOCIETY OF AMERICA

Vol. 37 MAY-JUNE, 1952 Nos. 5 and 6

STUDIES OF RADIOACTIVE COMPOUNDS: IV—PITCHBLENDE FROM LAKE ATHABASKA, CANADA[1]

E. J. BROOKER, *Geological Survey of Canada, Ottawa*

AND

E. W. NUFFIELD, *University of Toronto, Toronto, Canada*

ABSTRACT

Six specimens of pitchblende have been analyzed for their U^4 and U^6 content and x-ray powder photographs obtained before and after heat treatments. The cell edges of pitchblende range continuously from 5.470 to 5.395 A. The decrease is due to oxygen entering interstitial positions in the UO_2 structure with a consequent change of U^4 to the smaller U^6 ion. The lowest cell edge represents a composition of near $UO_{2.6}$; the solid solution range of laboratory-prepared cubic oxides ceases at about $UO_{2.2-2.3}$. Oxidation is not uniform throughout a pitchblende specimen and this together with a reduction in grain size results in loss of definition in the powder pattern. The term metamict is not applicable in this connection.

The cell dimensions of U_3O_8 increase as oxygen enters the structure.

It is not unusual to observe that the cell edge of a mineral species varies with the locality. This may be attributed to one or more of several causes, such as differences in chemical composition, atomic arrangements or the like. However, except in the case of zoned crystals and like phenomena, one does not expect this variation in different portions of the same specimen. In this respect is pitchblende an oddity, for not infrequently no single cell size can be regarded as characteristic for a particular locality.

It has been reported in the literature and frequently observed in this laboratory, that pitchblende may give a weak and diffuse x-ray powder pattern or actually on occasion, no pattern at all. In our opinion no satisfactory explanation has been offered to account for this.

The present investigation was concerned with the two problems outlined above. At the outset it was decided to exclude from the present study, specimens of uraninite. The terms pitchblende and uraninite are here employed in the most widely accepted usage. Both terms refer to

[1] Extracted from a thesis for the M.A.Sc. degree, University of Toronto.

the mineral with the ideal composition UO_2 and the fluorite-like structure. Pitchblende applies to material which is formed from hydrothermal solutions. It is usually fine-grained and seldom crystallized and contains only minor amounts of the rare earth elements and thorium. Uraninite is characteristically a syngenetic mineral in granitic igneous rocks. It is frequently crystallized and contains appreciable amounts of the rare earth elements and thorium. The cell edge of uraninite is characteristically longer than that of pitchblende, approaching that of thorianite. This is in part due to thorium entering the structure and substituting for uranium. The role of the rare earth elements in the UO_2 structure is not fully understood. Thus to reduce the problem of the variation in cell dimensions to simple proportions it was decided to confine the study to pitchblende which is relatively free of extraneous elements.

We are indebted to Dr. H. V. Ellsworth and Dr. S. C. Robinson, senior members of the Radioactivity Laboratory of the Geological Survey of Canada, Ottawa. Dr. Ellsworth kindly assisted us in working out the details of the procedure for the chemical analysis of the uranium specimens. Most of the specimens used in this study were collected by Dr. Robinson.

The value $CuK\alpha_1 = 1.5405$ A has been used in the calculation of spacings and cell dimensions in this paper. Cell constants extracted from other papers have been converted to A units if originally given in kX or mistakenly as A units.

Experimental Investigation

Six specimens from the Lake Athabaska district, Canada were chosen for study, an effort being made to obtain a range from fresh through to highly altered material. Their descriptions follow:

No. 1—Nicholson Mine. Pitchblende in masses up to ½ inch across. Colour black to steel gray, H. 5, density 8.20, brittle, fracture conchoidal. The pitchblende appeared fresh although bright canary yellow alteration products occurred in minor fractures.

No. 2.—Nicholson Mine. Pitchblende as a cement in ferruginous quartzite breccia. Colour dull black, H. 4½, density 7.12, less brittle than No. 1, did not fracture easily. The pitchblende appeared to be altered along fractures and in contact with the breccia where it was somewhat softer.

No. 3.—Martin Lake. Pitchblende as veinlets 2 or 3 mm. wide in coarsely crystalline, reddish calcite gangue. Colour black, H. 4½, density 5.55, fracture conchoidal.

No. 4.—Martin Lake, No. 2 flow. Pitchblende along shear planes in highly altered andesite which was dull brownish red due to the presence of much hematite; also as disseminations throughout the rock in fine grains and patches. It was relatively soft, density 7.16, and was accompanied by abundant yellow and green alteration products.

No. 5, Donaldson Group. Pitchblende in minute fractures and as small irregular patches about 1 mm. in diameter in a highly altered rock, reddish brown due to abundant hematite. Colour dull black, earthy, soft, density 4.50. Yellow alteration products occurred along some fractures.

No. 6, A. B. C. Group. Pitchblende as dull, soft, earthy patches and veinlets in a highly altered, crumbly mafic rock which was brownish red due to abundant hematite. Density 4.10.

The occurrence of pitchblende in the six specimens as tiny veinlets and as fine disseminations, its intimate association with gangue minerals and the presence of abundant alteration products made it difficult to separate enough material for chemical analyses. However, careful crushing, sizing and washing, followed by hand picking under the binocular microscope produced concentrates weighing between 0.4 and 0.8 grams of at least 75% purity. The selected material was dried and ground as finely as possible in an agate mortar in preparation for the chemical analysis.

The separation of hexavalent uranium from tetravalent uranium was based on the relative solubilities of UF_6 and UF_4. Determination by titration with permanganate solution was not considered feasible due to the presence of iron.

The weighed samples were placed with approximately 15 cc. of concentrated H_2F_2 in covered 20 cc. platinum crucibles into which nitrogen was continuously passed. The attack was allowed to continue for 4 days at a temperature of between 50 and 60° C. The crucibles were not permitted to go dry. At the conclusion of the treatment the contents were filtered, the UF_6 (yellow) being in solution while the UF_4 (green) remained as a residue. This residue was thoroughly washed with cold water and the washings added to the filtrate.

The filtrate and residue were separately dried and converted to chlorides which were then dissolved in a weak solution of HCl in freshly boiled water (to ensure expulsion of CO_2 which would tend to prevent complete precipitation of uranium). The uranium, iron, aluminium, etc., were now precipitated with NH_4OH and filtered. NH_4Cl was added to help the precipitation. The precipitate was then washed with a weakly ammoniacal solution, redissolved with HCl and the solution made up to 250 cc. An excess of $(NH_4)_2CO_3$ was then added to this solution and the precipitation of the iron-aluminium group carried out by the addition of NH_4OH, the uranium remaining in solution. The precipitate of iron and aluminium hydroxides was filtered off, washed, redissolved and reprecipitated as above. The filtrate from this second precipitation was then added to the first. The precipitation was repeated 3 times where an excess of iron and aluminium was present. The combined filtrates containing uranium were then acidified with HCl and boiled for 2 hours to expel all CO_2. The solution was then made up to 250 cc. with freshly boiled water and the uranium precipitated with NH_4OH, as ammonium uranate. NH_4NO_3 was added to help the precipitation. The precipitate

was filtered, ignited and weighed as U_3O_8. These weights were then calculated to hexavalent or tetravalent uranium and the results for each sample reported as the percentage of hexavalent uranium of total uranium.

Sample No.:	1	2	3	4	5	6
U^6 % of total U	17.4	20.2	40.2	60.0	78.5	85.0

Three *x*-ray powder photographs were prepared from each sample under the following conditions:

1) in the natural state
2) after heating in vacuum for $\frac{1}{2}$ hour
3) after heating in air for 5 minutes

The vacuum heatings were conducted in 7 mm. diameter silica glass tubes, the vacuum being maintained during heating by a continuously operating pump. Heating in air was carried out in open silica crucibles. A Meker burner with a flame temperature of near 1100° C. raised the temperature of the sample to about 900° C. For comparison purposes a sample of UO_2 supplied by Eldorado Mining and Refining, Port Hope was photographed under similar conditions.

Experimental Results

It was at once apparent that the degree of weathering in the 6 samples is an indication of the U^6/total U ratio, that is to say, to the degree of oxidation. The ratio is low for hard, compact material and high for those specimens which are loosely aggregated and consequently soft. The physical disintegration of the specimen which is a consequence of weathering, and the resulting finely divided products of weathering, are largely responsible for the decrease in density (Table 1).

The interpretation of the *x*-ray powder photographs is presented in Table 1. All samples except No. 6 with U^6/total U = 85.0% gave the typical pitchblende pattern when photographed in the natural state. A comparison of the prints (Figs. 1–7) shows a fairly regular change in the quality of the pattern with composition. As the ratio U^6/total U increases, back reflections become weaker and more diffuse, then low angle reflections become weak and diffuse and finally with U^6/total U = 85.0% none of the characteristic pitchblende diffraction lines appeared within normal exposures times. It is evident from Table 1 that the cell edges decrease as the ratio U^6/total U increases, from $a = 5.470$ A for synthetic UO_2 down to $a = 5.405$ A for pitchblende where U^6/total U = 78.5%. It appears therefore, that the quality of the powder pattern, the cell edge and the state of aggregation of the specimen are all related to the degree of oxidation.

TABLE 1. *X*-RAY POWDER DATA FROM PITCHBLENDE BEFORE AND AFTER HEAT TREATMENTS[1]

No.	U^6 wt. % of Total U	Density	Untreated	Heated ½ Hour in Vacuum	Heated 5 Minutes in Air
	Synthetic UO_2		UO_2 *a* 5.470	UO_2 *a* 5.446	U_3O_8—two cells sharply defined and of about equal intensity *a* 3.85, 3.93; *c* 4.12
1	17.4	8.20	UO_2 *a* 5.466 plus one faint, unidentified line	UO_2—clean, sharp *a* 5.446	U_3O_8—intensity relations of two cells anomalous *a* 3.87, 3.98; *c* 4.14 plus a few extra, unidentified lines
2	20.2	7.12	UO_2 *a* 5.465 plus one very faint, unidentified line	UO_2—sharp, strong *a* 5.416 plus very faint trace of 'X'	U_3O_8—intensity relations of two cells anomalous *a* 3.88, 3.97; *c* 4.14 plus a few extra, unidentified lines
3	40.2	5.55	UO_2—back reflections very weak and diffuse *a* 5.435	UO_2—sharp, strong *a* 5.406 plus weak 'X' lines but stronger than in #2	'X' essentially, diffuse plus one faint UO_2 line plus faint U_3O_8(?)
4	60.0	7.16	UO_2—back reflections very weak and diffuse *a* 5.445	'X'—strong plus UO_2—diffuse and not as strong as 'X' *a* 5.395	'X'—sharp, strong plus one faint UO_2 line
5	78.5	4.50	UO_2—back reflections very diffuse—low angle reflections diffuse *a* 5.405	UO_2—sharp, strong *a* 5.405 plus U_3O_8—strong; single cell *a* 3.94; *c* 4.17	U_3O_8 essentially; intensity relations of two cells anomalous; two cells not well defined *a* 3.94, 4.04; *c* 4.17
6	85.0	4.10	no pattern	U_3O_8—strong; single cell *a* 3.92; *c* 4.17 plus UO_2—sharp, very weak *a* 5.405	U_3O_8—single cell *a* 3.92; *c* 4.17 plus faint UO_2 lines

[1] The error of measurement in the pitchblende patterns ranges from ±0.002 to ±0.005 A for the more highly oxidized specimens. The values for U_3O_8 are considered to be accurate to ±0.01 A.

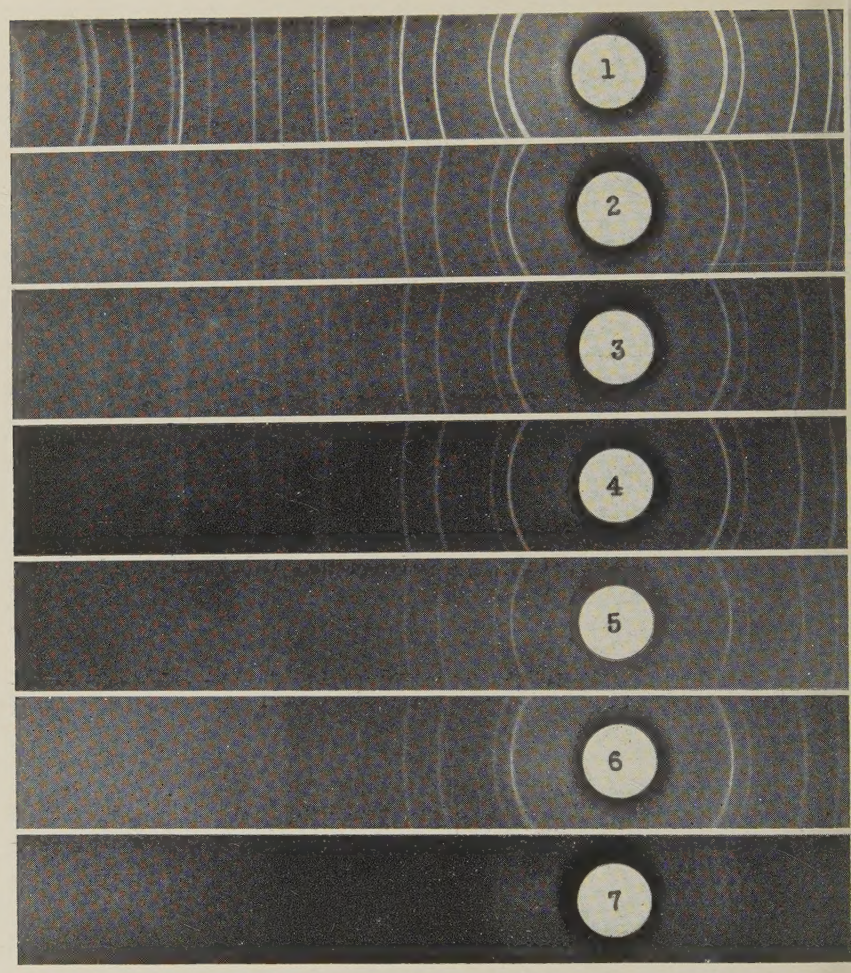

FIGS. 1–7. *X*-ray powder contact prints (1° θ=1 mm.). Untreated material. Fig. 1. Synthetic UO_2. Figs. 2–7. Pitchblende (samples 1–6 of Table 1).

After heating for $\frac{1}{2}$ hour in vacuum, all the samples now gave the pitchblende pattern (Figs. 8–14) with the diffraction lines somewhat strengthened and sharpened. Furthermore, the cell edges were reduced for all specimens where the cell edge of the untreated material was higher than $a=5.405$ A. Synthetic UO_2 and sample 1 with 17.4% U^6 of total U gave a clean pattern. The patterns of samples 2, 3 and 4 show extra diffraction lines which are least intense in sample 2 and strongest in sample 4. The compound responsible for this extra pattern has not been identified and will be referred to as compound 'X.' The patterns of samples

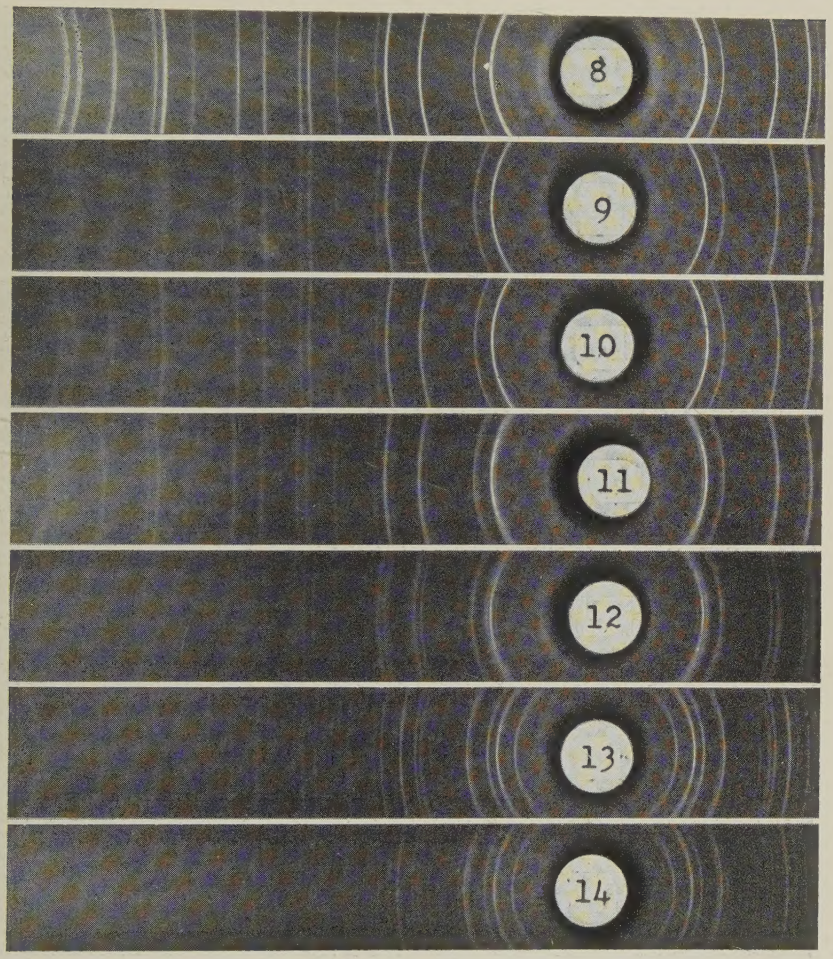

FIGS. 8–14. *X*-ray powder contact prints (1° θ=1 mm.). Heated $\frac{1}{2}$ hour in vacuum. Fig. 8. Synthetic UO_2. Figs. 9–14. Pitchblende (samples 1–6 of Table 1).

and 6 also show extra diffraction lines but are here due to a "one cell" type U_3O_8. This extra pattern is more prominent in sample 6, which has the highest U^6 content. To summarize: pitchblende low in U^6 gave after heating in vacuum, only the UO_2 pattern or with traces of the unidentified oxide 'X.' In pitchblende with a U^6/total U ratio of near $\frac{1}{2}$, this extra unknown pattern is strong. Pitchblende relatively high in U^6 gave a U_3O_8 pattern in place of the unknown, along with a UO_2 pattern.

None of the samples gave a UO_2 pattern after heating in air for 5 minutes (Figs. 15–21). Synthetic UO_2 and pitchblende low in U^6 (samples 1 and 2) and relatively high in U^6 (samples 5 and 6) gave the U_3O_8 pattern,

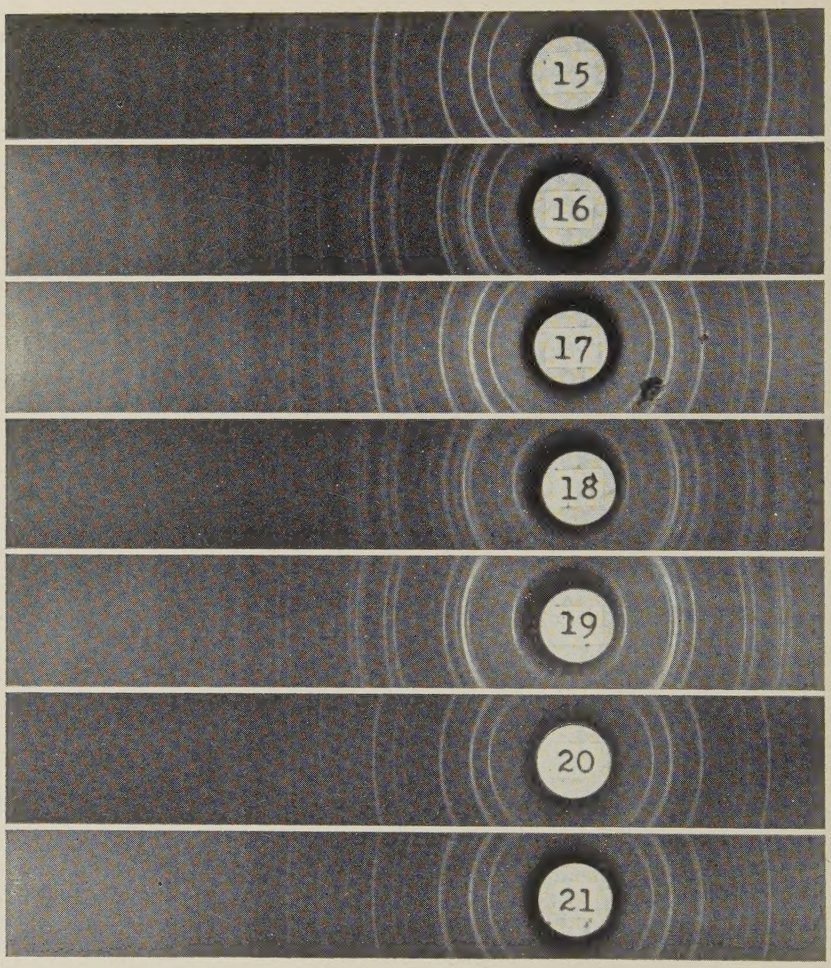

FIGS. 15–21. *X*-ray powder contact prints (1° θ=1 mm.). Heated 5 minutes in air. Fig. 15. Synthetic UO_2. Figs. 16–21. Pitchblende (samples 1–6 of Table 1).

the cell edges increasing with increasing availability of U^6 in the untreated material. All the U_3O_8 patterns were of the "two cell" type except that from sample 6 with the highest U^6 content. Samples 3 and 4 with a U^6/total U ratio of near $\frac{1}{2}$ again gave the pattern of the unidentified oxide 'X.'

DISCUSSION OF THE RESULTS

The UO_2 solid solution series:

Although it is known that the cubic UO_2 phase with the fluorite structure exists over a range of composition, there is uncertainty as to the ex-

tent of this range and the constitution of the oxides within it.

Biltz and Müller (1927) found that between UO_2 and $UO_{2.226}$ oxygen is taken up without change in volume of the oxide. Beyond this point the volume increases regularly with no discontinuity at the composition $UO_{2.67}$ ($=U_3O_8$). They were not able to detect any difference between the x-ray patterns of $UO_{2.226}$ and UO_2. Jolibois (1947) established the existence of another phase intermediate in composition between UO_2 and U_3O_8. He concluded that the oxidation of UO_2 at 220° C. ceases at

Table 2. Cell Sizes of Cubic Uranium Oxides

	$UO_{1.75}$	$UO_{2.0}$	$UO_{2.1}$	$UO_{2.2}$
Rundle, etc. (1948)	—	5.4690	—	—
Alberman & Anderson (1949)	—	5.468	—	5.441
Katz & Rabinowitch (1951)	—	5.4695	5.448	5.444
Zachariasen (in Katz & Rabinowitch, 1951)	5.488	—	—	—

$UO_{2.33}$ and continues to U_3O_8 only above 300° C. The intermediate compound $UO_{2.33}$ (or U_3O_7) gave an x-ray diffraction pattern like UO_2 but with additional lines. Grønvold & Haraldsen (1948) determined the symmetry of this compound as tetragonal with $a=5.38$, $c=5.55$ A and declared that its composition was $UO_{2.40}$. They felt that the cubic phase extends to $UO_{2.33}$. Alberman & Anderson (1949) found that UO_2 takes up oxygen to $UO_{2.19}$ below 250° C. without change of structure or cell dimensions. At this composition they observed that the symmetry becomes tetragonal, the c/a ratio increasing progressively from $UO_{2.19}$ to $UO_{2.3}$. The low temperature oxides in the range $UO_{2.0-2.3}$ were found to be unstable above 750° C. On annealing at temperatures above 750° C., the oxides $UO_{2.0-2.19}$ changed in part to a cubic β phase ($UO_{2.19}$) with a fluorite-like structure having $a=5.44$ A as compared to $a=5.468$ A for pure UO_2; the oxides $UO_{2.19-2.3}$ broke down to $\beta UO_{2.19}$ and U_3O_8.

These data indicate that the low temperature oxygenation of $UO_{2.0}$ in the laboratory is limited by the formation of the tetragonal phase. The upper limits assigned by Jolibois and by Alberman & Anderson to the cubic phase differ by a surprisingly large amount. There appears to be reason to believe that the limits may depend on the physical condition of the sample undergoing oxidation and the laboratory methods employed. The data also clearly establish that solution of oxygen into the UO_2 structure followed by annealing, reduces the cell size. Table 2 gives cell sizes for oxides of various compositions as determined by different observers.

Rundle and his associates regard the higher cubic oxides as having a uranium-deficient lattice, resulting in a smaller cell and a lower density than has UO_2. Alberman & Anderson, in analogy to other anomalous fluorite mixed-crystal systems, favour the view that these oxides have an oxygen-rich lattice, with oxygen occupying interstitial ($\frac{1}{2}00$) positions. A U^4 cation is simultaneously replaced by the smaller U^6 cation for each oxygen ion so incorporated. This results in a decrease in cell size and an increase in density. Filling of all the ($\frac{1}{2}00$) positions by oxygen would raise the composition to $UO_{2.75}$. Density measurements by Biltz & Müller of oxides between $UO_{1.992}$ and $UO_{2.349}$ are not conclusive but are in better agreement with the idea of an oxygen-rich lattice.

The variation in the cell edges of natural pitchblende may be plausibly explained with reference to the above observations on the artificial cubic oxides. Table 1 points conclusively to a close relationship between cell edge and the U^6/total U ratio in the sample. Recent observations by Kerr (1951) have led him to a similar conclusion. He noted that "sooty" pitchblende gives lower lattice constants than hard pitchblende and he surmised that because "sooty" varieties show a higher UO_3 content, the low lattice constants are connected with the increase in UO_3. Our data indicate that the relationship is roughly linear, the cell edge decreasing with increase of the ratio U^6/total U. Evidently, in analogy to the artificial UO_2 system, oxygen enters interstitial positions in the structure as oxidation proceeds. The consequent change of U^4 to the smaller U^6 ions results in a regular decrease in lattice dimensions.

The present data show that the oxidation of pitchblende differs in two respects from the oxidation of artificial cubic uranium oxides in the laboratory.

(1) Low temperature oxygenation has no effect on cell edges within the solid solution limits of the artificial cubic UO_2 phase. This must represent an anomalous, perhaps metastable condition in the structure since according to the view of Alberman & Anderson, solution of oxygen should result in a smaller cell. Presumably the metastable condition is "corrected" by annealing for the cell edge is reduced from 5.468 to 5.44 A. Our data indicate that natural pitchblende on the other hand, has a range of cell edges grading from 5.470 through 5.44 to 5.405 A. A survey of published cell constants for pitchblende shows that the gradation is continuous between the limits. This suggests that when oxidation occurs in the fullness of geological time and at atmospheric temperatures the UO_2 structure maintains a more stable condition while accommodating interstitial oxygen, than is possible under laboratory conditions of oxygenation. It has been shown in this study that when pitchblende is heated in vacuum, some reduction in cell size usually takes place. This may rep-

resent a final stabilizing of the structure and/or the introduction of additional oxygen which is always available in oxidized pitchblende.

(2) The upper limit of solid solution in the artificial cubic phase, which was given as $UO_{2.226}$ (Biltz & Müller), $UO_{2.33}$ (Jolibois), and $UO_{2.19}$ (Alberman & Anderson) is represented by a cell with dimensions $a = 5.44$ A after annealing (Table 2). The cells of certain natural uranium oxides reach markedly smaller dimensions. The lowest value recorded in this study, 5.395 A, is comparable with the lowest recorded in the literature;

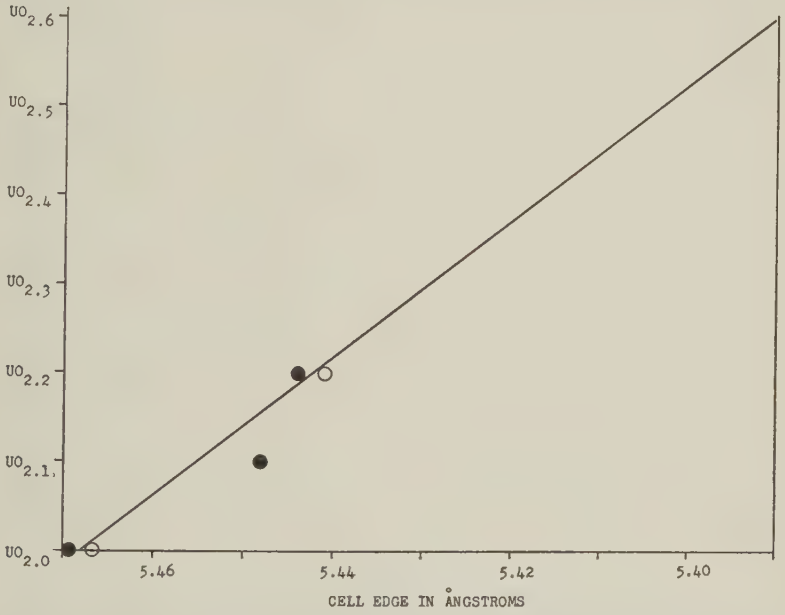

Fig. 22. Cube edge values of Alberman & Anderson, 1949 (open circles) and Katz & Rabinowitch, 1951 (filled circles) plotted against composition and extrapolated linearly to $a = 5.39$ A.

Kerr[1] (1950) gives 5.3965 A as the smallest of 33 determinations. This indicates that in nature the solid solution series extends well beyond the upper limits recorded for artificial uranium oxides. In terms of the cell edges of oxides of known composition our lowest values may be extrapolated to represent a composition of near $UO_{2.6}$ (Fig. 22). It is a reasonable assumption that certain highly oxidized pitchblende specimens reach the composition $UO_{2.75}$ with all of the ($\frac{1}{2}$00) interstitial positions

[1] In a table compiled to show the range of cell constants in pitchblende and uraninite, values are given without designation of the unit of measurement in both kX and A units.

filled by oxygen. The tetragonal phase has not been discovered in nature. Evidently the slow oxidation of pitchblende in nature at low temperatures permits a more complete saturation of the UO_2 structure by oxygen than is possible with laboratory methods which invariably result in the formation of the tetragonal phase before the process is half completed.

It should be pointed out that although the measured cell edges of pitchblende furnish a rough estimation of the ratios O/U and U^6/total U in the UO_2 structure, these ratios are not necessarily representative of the composition of the pitchblende sample as a whole. Heating in vaccum results in the appearance of extra diffraction lines characteristic of the unknown oxide 'X' or of U_3O_8 which become more prominent as the U^6/total U ratio of the specimen increases. It may be presumed that there is present an excess of U^6 perhaps as amorphous or finely crystalline UO_3. On heating in vacuum it is reduced in part to the oxide 'X' or to U_3O_8. At the same time as is evidenced by a lowering of the cell edge, oxygen is freed to enter the UO_2 structure, although the reduction in cell edge may in part be due to a rearrangement of the interstitial oxygen.

Conybeare & Ferguson (1950) have attempted to relate the degree of oxidation of pitchblende samples to the quality of their x-ray powder patterns before and after ignition. They have interpreted their observations on the basis of a statement in Dana (1944) which summarizes the conclusions of Goldschmidt & Thomassen (1923):

"Natural uraninite containing much UO_3 through oxidation is apparently structurally identical with UO_2 . . . but on ignition out of contact with oxygen it may recrystallize in part or entirely to U_3O_8, while pure UO_2 remains unchanged."

Conybeare & Ferguson have assumed that the converse of the statement that refers to pure UO_2 is true—namely, that pitchblende which gives only the UO_2 pattern after ignition is pure UO_2. Table 1 shows that pitchblende with as much as 17.4% U^6 of total U gave the present authors a sharp UO_2 pattern after ignition in vacuum. The results of Conybeare & Ferguson show no relationship between cell dimensions and composition and this can be attributed directly to faulty procedure. To fulfill the condition of ignition in the absence of oxygen, these authors heated their samples in covered crucibles; experience in this laboratory has shown that this favours oxidation and that it is necessary to perform the ignition under continuous evacuation by a pump. It is probable too, that they have overlooked the presence and reducing effect of finely disseminated hydrocarbons which we have found to be extremely common in some of the localities they studied.

Recently Wasserstein (1951) has suggested that "there is a progressive reduction in the size of the unit cell of uraninite-thorianites with time".

Wasserstein has postulated that radiogenic lead, resulting from the decay of uranium, substitutes for uranium in the UO_2 structure and causes a shrinkage of the cell because the ionic radius of Pb^4 is smaller than that of U^4. The shrinkage was said to range between 0.0025 and 0.0041 A per hundred million years. Assuming that such substitution occurs and this is by no means certain, its effect if any will be masked by the much more pronounced effect of the introduction of oxygen and change of U^4 to U^6. It is interesting to note that according to Wasserstein's theory, the variation in cell edges (5.466 to 5.405 A) of the 6 Lake Athabaska specimens studied means that these specimens from the one deposit range in age from 1×10^8 to approximately 20×10^8 years. Dana (1944, p. 618) gives the calculated age of the Great Bear Lake pitchblende deposits as approximately 13×10^8 years.

"Metamict" Pitchblende:

The term metamict was originally used by Brögger (1896) to describe the state of non-crystallinity of a number of minerals which however, often showed perfect crystal form. He inferred that a dislocation of the structure had occurred subsequent to crystallization. The disorder did not appear to be connected with weathering since the minerals were glassy, broke with a clean, conchoidal fracture, showed no zoning of the non-crystallinity from the core of a crystal outward and occurred commonly in fresh-appearing, granitic igneous rocks. Subsequent work by various observers has shown that an ordered structure can be produced by ignition either in vacuum or in air. But with the exception of certain specimens of gadolinite the product of ignition is cryptocrystalline and single crystal x-ray studies can therefore not be undertaken. In only a few cases is it assured that the original structure is restored by ignition. One of these exceptions concerns fergusonite; Barth (1926) obtained the same cell constants on ignited, metamict fergusonite as on artificially prepared material. The majority of the metamict minerals have not been prepared artificially and thus there can be little direct evidence that the original structure is restored. However, indirect evidence is not lacking. For example, Arnott (1950) was able to index the powder pattern of euxenite from Mattawan township, Ontario (ignited at 1000° C. in air) in terms of Brögger's morphological axial ratios on Scandinavian euxenite. The resulting cell dimensions together with the measured density of ignited material gave rational cell contents with the chemical analysis of euxenite from Sabine township, Ontario.

The process responsible for the loss of crystallinity is not fully understood. It is known that the majority of the minerals are multiple oxides of columbium, tantalum and titanium and contain appreciable amounts

of the rare earth elements, uranium and/or thorium. Cation substitution is both complex and abundant. Hence it appears that the disorder is connected with the presence of elements subject to radioactive decay within atomic structures rendered unstable by reason of multiple substitution for few cation positions.

Unfortunately, the casual observer in the field of metamict minerals frequently has acquired little more background than the knowledge that metamict minerals give at best, only weak diffractions. Diffuse and faint diffractions become synonymous with the metamict state. He is inclined to view with suspicion such weakly diffracting substances as opal, which never reached a sufficient degree of crystallinity for strong diffraction, and certain limonites which by the method of their formation as oxidation products of other iron minerals, are too fine-grained for effective diffraction. It is evident from the foregoing paragraphs that in neither case is the term metamict applicable. The term implies a type of crystal imperfection which is not to be confused with fine-crystalline materials that are the products of imperfect crystallization or decomposition.

It might be expected that in view of its high uranium content, pitchblende should exist in the metamict state. In fact Conybeare & Ferguson (1950) having obtained certain weak and diffuse diffraction patterns, have announced the existence of metamict pitchblende. It was mentioned above that the present authors noted a considerable variation in the diffracting power of different pitchblende samples and actually one sample gave no pattern before ignition. However, a direct relationship between the quality of the pattern, its UO_3 content as determined by chemical analyses, and the state of aggregation was evident. The quality of the pattern declined as the UO_3 content increased and the specimen itself assumed an ever-increasing weathered appearance. Clearly then, the quality of the patterns of our samples are directly related to the degree of oxidation. Conybeare & Ferguson (1950, p. 404) observed that "all the metamict pitchblendes . . . show varying degrees of oxidation, whereas the specimens from Black Lake and Great Bear Lake are crystalline and differ markedly in their degrees of oxidation." It is certain, therefore, that in the Conybeare & Ferguson samples, oxidation too is responsible for the loss of definition in the diffraction patterns and they are in fact not metamict.

It may be postulated that oxidation will affect the quality of pitchblende x-ray patterns in one or more of three ways:

1. Surface oxidation and oxidation by solutions (Kerr, 1951) is known by actual observations to affect the state of aggregation of pitchblende by reducing the grain size. Evidently the diffracting units become so small that diffraction occurs over a relatively wide angular range. It is reason-

able to believe that the range may reach such proportions in the highly oxidized specimens that the loss of definition is complete and no diffraction pattern is obtained.

2. Chemical analyses of different zones of a uraninite crystal from Quebec (Ellsworth, 1932) and another from Norway (Dana, 1944, p. 616) clearly show that the U^6 content increases outward from the core. It follows that the O/U ratio in the UO_2 structure and therefore the cell edge, will vary throughout the specimen. To test this, *x*-ray powder patterns were obtained of material scraped from the surface of an old laboratory specimen of pitchblende and of fresher material immediately below. The former gave a slightly smaller cell edge. Consequently the average *x*-ray powder sample may consist of a range of oxides, each with a characteristic cell edge and hence a different Bragg angle of reflection for each plane resulting in broadened diffraction lines.

3. As oxidation proceeds with the introduction of more oxygen in the interstices of the UO_2 structure, it is possible that some distortion of the structure will take place, resulting in some loss of definition of the powder pattern.

It is not our intention to suggest that a metamict form of pitchblende cannot exist. We do feel that the basis of future descriptions must be more substantial than comparisons of powder patterns of materials before and after ignition. It might be expected that metamict pitchblende if it does exist, should be glassy like the typical metamict minerals. But here a word of caution is in order. Certain black, glassy materials from the Lake Athabaska uranium area produce before and after ignition, diffraction patterns which suggest the metamict state. Some of these materials are "thucholite" which has been shown by Davidson & Bowie (1951) to be a hydrocarbon enclosing grains or crystals of pitchblende, often too fine-grained and sparse for effective diffraction. It was observed in this laboratory that heating such material in air has the effect of sharpening the UO_2 pattern, oxidation of the pitchblende being forestalled by the reducing effect of the hydrocarbon. This material could easily be mistaken for metamict pitchblende.

The U_3O_8 solid solution series:

U_3O_8 is perhaps the most easily prepared of the anhydrous oxides of uranium. Despite this, the compound has not yet been identified as a natural product and as a result, its properties are not as well known as those of UO_2.

The symmetry of U_3O_8 was originally described as orthorhombic by Zachariasen (1944; in Katz & Rabinowitch, 1951) and by Grønvold (1948) with the cell dimensions:

a	*b*	*c*	
6.71	3.99	4.15 A	Zachariasen (1944)
6.716	3.977	4.144 A	Grønvold (1948)

Other determinations made at Columbia University (in Katz & Rabinowitch, 1951, p. 271) agree closely with the above values. Grønvold's observations were made on *x*-ray powder photographs only; it is likely that Zachariasen and the Columbia University observers also used the pow-

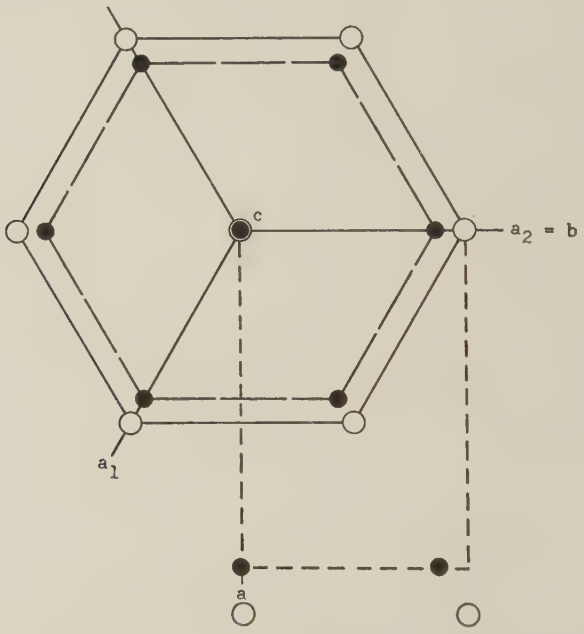

FIG. 23. The relationship between the two hexagonal U_3O_8 cells of Milne (1951) and the unreal orthorhombic cell chosen by earlier observers to account for the multiple *x*-ray powder pattern. The difference in the *a* dimensions of the hexagonal cells has been exaggerated.

der method since no mention of single crystals is made. Milne (1951), working in this laboratory with lath-like crystals obtained sharp Weissenberg films clearly showing hexagonal symmetry. They indicated that the crystals are actually multiple, consisting of two cells oriented with their *a* and *c* directions coinciding and with identical *c* dimensions:

$$a = 3.87, 3.94; \; c = 4.15 \text{ A}$$

Milne noted and this has been confirmed during the present study, that

the majority of U_3O_8 powder patterns show the double cell. It is evident that the previous observers worked with the double pattern for their orthorhombic cell shows the following relationship to the two hexagonal cells:

Orthorhombic	Hexagonal
$d(200)$	$d(10\bar{1}0)$ small cell
$d(020)$	$d(11\bar{2}0)$ large cell
$d(001)$	$d(0001)$ both cells

Fig. 23 depicts the three cells and shows that the orthorhombic cell is not a real one. The orthorhombic elements may be converted to the proper hexagonal ones by the formulae: a(hex., small) = a(orth.)/2cos 30°; a(hex., large) = b(orth.); c(hex.) = c(orth.).

Milne's hexagonal cell contains $\frac{1}{3}[U_3O_8]$. He suggested that the true hexagonal c dimension is actually 3×4.15 A, the measured value being a strong pseudo-period resulting from the arrangement of uranium atoms in the structure.

Zachariasen (1948; in Katz & Rabinowitch, 1951, p. 277) has described as UO_3(I) a compound obtained by heating amorphous anhydrous UO_3 to 500° C. for 8 hours under 20 atmospheres of oxygen pressure. It is instructive to compare its cell constants with those of Milne's large hexagonal cell of U_3O_8:

	Symmetry	a	c	calc. density
UO_3(I)	hexagonal	3.963 A	4.160 A	8.34
$\frac{1}{3}[U_3O_8]$	hexagonal	3.94	4.15 A	8.37

The measured densities of U_3O_8 are distinctly higher than those for UO_3:

U_3O_8	UO_3
8.300 (Biltz & Müller, 1927)	6.04 for $UO_{3.07}$ (Biltz & Müller, 1927)
8.34 (Grønvold, 1948)	7.07 for $UO_{2.92}$

They agree well with the calculated values for both U_3O_8 and Zachariasen's UO_3(I). The evidence strongly suggests that Zachariasen's amorphous UO_3 was actually reduced to the "single cell" type U_3O_8 phase with the loss of some oxygen during the heating procedure, rather than recrystallized to another form of UO_3. Highly oxidizing conditions apparently favour production of the "single cell" type; Milne reported that only one sample of U_3O_8, prepared by heating uranyl nitrate in air

at 220° C. for several days, resulted in a simple structure. In this study only those specimens high in U^6 (samples 5 and 6) produced a "single cell" type U_3O_8 during heating experiments.

It appears certain that the "single" and "double" type patterns of U_3O_8 are responsible for the following confusion:

"According to Boulle and Domine-Berges (1944) the *x*-ray diffraction pattern of the comparatively easily-oxidizable preparations of U_3O_8, obtained at low temperatures (lower than 350° C.) from oxalate or trioxide, is somewhat different from that of the (practically non-oxidizable) microcrystalline product obtained at high temperatures" (Katz & Rabinowitch, 1951, p. 272).

Milne (1951) has offered two suggestions to account for the "two cell" structure of U_3O_8. Both depend upon the introduction of oxygen into the structure. According to Milne this may enlarge the *a* dimension of the cell, with a higher oxide confined to the outer boundaries of grains and crystals where solution of oxygen is most likely. On the other hand, the introduction of oxygen with its consequent change of U^4 ions to the smaller U^6 ions, may result in a shrinkage of the cell as it does in the case of the UO_2 structure. Milne felt that both suggestions called for two similar oxide structures with greater and less oxygen than the resultant U_3O_8.

The majority of the U_3O_8 patterns produced by the heating experiments in this study show the "two cell" effect. Using the powder data given by Milne, the cell sizes were determined from the $(20\bar{2}0)$ and the (0003) reflection arcs. Due to the quality of the films, the accuracy of these determinations are no better than ± 0.01 A. The results show an obvious relationship between the cell sizes and the state of oxidation of the pitchblende:

	a'	a''	c
synthetic UO_2 for 10 min. in air	3.85	3.93	4.12
pitchblende—17.4 % U^6 for 5 min. in air	3.87	3.98	4.14
pitchblende—20.2 % U^6 for 5 min. in air	3.88	3.97	4.14
pitchblende—78.5 % U^6 for 5 min. in air	3.94	4.04	4.17

The unit cells of U_3O_8 formed by heating samples low in U^6 are distinctly smaller than those formed from pitchblendes that are highly oxidized. These observations support the view that the composition of the U_3O_8 structure is not constant; that the U_3O_8 structure exists over a solid solution range. Contrary to the case of the UO_2 structure, solution of oxygen in the U_3O_8 structure increases the cell size, the expansion being confined largely to the *a* dimension. This was confirmed by the reduction of UO_3 to U_3O_8 in vacuum:

	a'	a''	c
after heating ½ hour in vacuum	3.91	3.98	4.16
after heating 1 hour in vacuum	3.89	3.98	4.14

The data presented above are in keeping with the results of a tensimetric analysis by Biltz & Müller (1927) who found that the U_3O_8 structure exists over a solid solution range, the molecular volume increases regularly with oxygen solution. The data also lend support to the first of Milne's suggestions to account for the "two cell" effect: that the introduction of oxygen which may be confined largely to the outer boundaries of grains or crystals, increases the cell size of the higher oxide. Milne's view that the two oxides should have respectively more and less oxygen than the resultant U_3O_8 is not upheld by the new data since it is clear from the variation in cell dimensions given above and from the tensimetric data of Biltz & Müller that the composition of U_3O_8 may depart considerably from the ideal.

Katz and Rabinowitch (1951, p. 277) have reported that the lattice constants of two samples of partly deoxygenated UO_3 ($UO_{2.82}$ and $UO_{2.96}$) were not intermediate between those of $UO_{2.67}$ and $UO_{3.00}$. The values as reported are given here in the left hand portion of Table 3. For purposes of comparison, Katz & Rabinowitch have converted the hexagonal ele-

Table 3. Lattice Constants Reported by Katz & Rabinowitch (p. 278)

	Orthorhombic			Hexagonal		
	a	b	c	a'	a''	c
1. $UO_{2.67}$	6.70	3.98	4.14	3.87	3.98	4.14
2. $UO_{2.82}$	6.90	3.91	4.15	3.91	3.98	4.15
3. $UO_{2.96}$	6.90	3.91	4.15	3.91	3.98	4.15
4. $UO_{3.00}$	6.864	3.963	4.160	3.963		4.160

1. Zachariasen from U_3O_8 (p. 271). 2, 3. Fried & Davidson (p. 278). 4. Zachariasen, obtained by heating amorphous UO_3 at 500° C. for 8 hours under 20 atmospheres of oxygen pressure (=UO_3(I) of Zachariasen) (p. 277).

ments of $UO_{3.00}$ (UO_3(I)) to the orthorhombic setting which was believed to be correct for U_3O_8. The right hand portion of Table 3 gives the elements in the proper "two cell" hexagonal setting which, on the basis of Milne's single crystal study, is known to be correct. It has already been pointed out that Zachariasen's UO_3(I) is very likely a "one cell" type U_3O_8. It is immediately evident that in this setting the lattice constants

of $UO_{2.82}$ and $UO_{2.96}$ are in fact intermediate between $UO_{2.67}$ and $UO_{3.00}$. This lends some support to our contention that the lattice dimensions of the U_3O_8 structure increase with solution of oxygen. Actually Katz & Rabinowitch were on insecure footing in this comparison of lattice constants. The compositions of the two intermediate oxides were apparently precisely determined by Fried & Davidson. But in stating that the first sample had the composition $UO_{2.67}$, Katz & Rabinowitch have ignored the tensimetric data of Biltz & Müller which showed that the U_3O_8 structure exists over a wide range of composition and have assumed that this particular sample had the ideal composition U_3O_8 (or $UO_{2.67}$). Furthermore, as was stated earlier, the evidence suggests that Zachariasen's UO_3(I) is actually a "one cell" type U_3O_8 with an O/U ratio of less than 3.

Much research on the U_3O_8 solid solution series remains to be done. For example, while it is now known that the cell size increases with the O/U ratio, exact data relating the composition of the structure with the cell size are lacking. The difficulties in supplying this information are obvious. Most U_3O_8 samples show the "two cell" effect and chemical analyses of such material will therefore, represent the composition of a mixture of two oxides. The mechanism leading to the "two cell" structure and the physical relations of the two cells to each other require clarification. It was noted in this study that the two cells are sharply defined when prepared by heating synthetic UO_2 in air. When prepared from some natural pitchblende the doublets representing reflections from similar planes in the two cells appear as continuous bands possibly indicating a gradation of composition between the two cells. At other times intensity anomalies are apparent. Certain planes of the smaller cell may give more intense reflections than do similar planes of the larger cell; on the other hand reflections in the same pattern may indicate that the larger cell is the dominant one.

The unknown oxide "X":

There is every reason to believe that the unknown pattern produced by heating samples 3, 4 and 5 for $\frac{1}{2}$ hour in vacuum and samples 4 and 5 for 5 minutes in air, represents an anhydrous oxide of uranium. The results of heating the six samples in vacuum suggest that its O/U ratio is intermediate between the ideal ratios for UO_2 and U_3O_8. (See next page, top.)

It appears that under these heating conditions, pitchblende low in U^6 gives only the UO_2 pattern; with increasing U^6, the unknown pattern also appears and this is replaced by the U_3O_8 pattern in pitchblendes with an excess of U^6.

Two oxides intermediate between UO_2 and U_3O_8 are mentioned in the literature:

U^6 % of total U	After heating ½ hour in vacuum
17.4	strong UO_2
20.2	strong UO_2 plus faint trace of 'X'
40.2	strong UO_2 plus weak 'X'
60.0	strong 'X' plus diffuse UO_2
78.5	strong UO_2 plus strong U_3O_8
85.0	strong U_3O_8 plus weak UO_2

1) The existence of a homogeneous phase U_2O_5 has been suggested by a number of observers, most recently by Rundle, Baenziger, Wilson & McDonald (1948). It was asserted by the latter observers that the compound was formed by heating together equal quantities of UO_2 and U_3O_8. The new phase gave a somewhat different diffraction pattern than U_3O_8 but the dimensions of its pseudo-cell are almost identical with those obtained by Zachariasen (in Katz & Rabinowitch, 1951) and Grønvold (1948) for U_3O_8:

$a=4.135$	$b=3.956$	$c=6.72$ A	(Rundle, etc.; 1948)
$c=4.14$	$b=3.98$	$a=6.70$ A	(Zachariasen, 1951)
$c=4.136$	$b=3.969$	$a=6.703$ A	(Grønvold, 1948)

Our attempts to form U_2O_5 according to the directions of Rundle, etc., were unsuccessful; an x-ray powder pattern showed that a mixture of UO_2 and U_3O_8 was still present. The U_3O_8 pattern is complex and somewhat obscures the simple UO_2 pattern. Brewer (in Katz & Rabinowitch, 1951, p. 255) has suggested that this may have led Rundle, etc., to regard their product as a single phase. This is supported by the U_3O_8-like cell constants which they derived. There is reason therefore, to doubt that these observers produced a phase distinct from UO_2 and U_3O_8. However persistent reports in the early literature claiming its existence cannot be lightly dismissed and the possibility remains that our compound 'X' is U_2O_5.

2) Jolibois (1947) prepared the compound $UO_{2.33}$ ($=U_3O_7$) by the low temperature oxygenation of UO_2. He observed that it gave a diffraction pattern almost identical with that of UO_2 but interpreted it as a new phase, U_3O_7. Grønvold & Haraldsen (1948) found that oxidation of UO_2 at 200 to 250° C. gave a tetragonal phase with $a=5.38$ A, $c=5.55$ A. Alberman & Anderson (1949) have also prepared this compound at temperatures below 300° C. and found that it exists between $UO_{2.19}$ and $UO_{2.30}$, the tetragonal character becoming more pronounced with increasing O/U.

We have prepared this phase by heating UO_2 at 250° C. with free access of air for periods ranging up to 6 hours. The effects of heating for ½ hour were a broadening of the diffraction lines from planes involving

both the a and c axes. After 1 hour, the broadened lines had split into two separate lines, the separation becoming more apparent with continued heating. After 6 hours, the tetragonal phase was essentially the same but faint U_3O_8 lines had appeared.[1] This latter pattern gave the cell constants $a = 5.38$, $c = 5.54$ A in excellent agreement with the data of

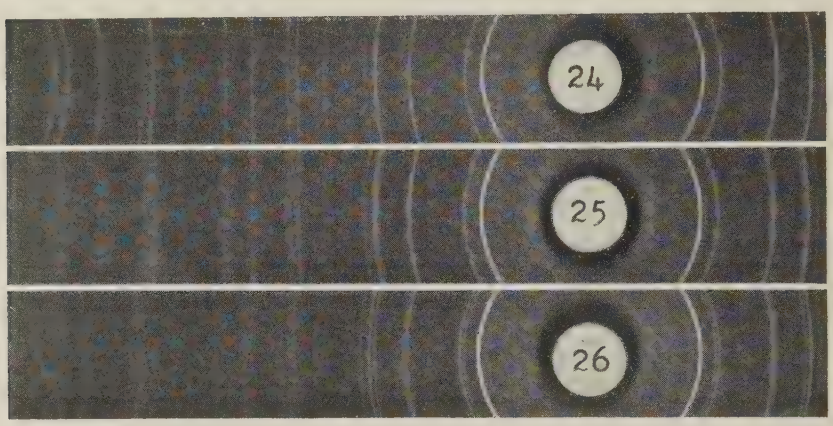

FIGS. 24–26. X-ray powder contact prints (1° $\theta = 1$ mm.). Fig. 24. Synthetic UO_2. Fig. 25. Synthetic UO_2 after heating for $\frac{1}{2}$ hour in air at 250° C. Fig. 26. Synthetic UO_2 after heating for 6 hours in air at 250° C. (= tetragonal phase).

Grønvold & Haraldsen and Alberman & Anderson. The powder data agree well with those given by Jolibois. This indicates that the various observers were working with the same compound. A comparison of the powder patterns (Figs. 25, 26) with that of our unknown however, shows no similarity.

Alberman & Anderson found that the tetragonal phase is not stable at elevated temperatures, breaking down at temperatures above 750° C. to βUO_2 and U_3O_8. This is in contrast to the compound 'X' which was produced at high temperatures. It is possible that a form of U_3O_7, stable at high temperatures, can exist but it must be added that the tensimetric data of Biltz & Müller did not indicate the existence of another phase intermediate in composition between UO_2 and U_3O_8.

The identity of compound 'X' must await further research. For its future recognition the usual x-ray powder data are given in Table 4.

[1] Jolibois stated that oxygenation of the tetragonal phase below 300° ceased at $UO_{2.33}$ and continued to U_3O_8 only above 300° C. The present study shows that U_3O_8 is formed at a lower temperature. There is no reason to doubt that U_3O_8 will form at even lower temperatures with prolonged heating.

TABLE 4. COMPOUND 'X'—X-RAY POWDER DATA[1]

I	d meas.	I	d meas.	I	d meas.	I	d meas.
6	5.95	1	2.69	4	1.892	1	1.377
4	3.36	1	2.49	3	1.852	1	1.341
10	3.21	1	2.44	2	1.687	1	1.290
2	3.17	1	2.23	3	1.662	1	1.252
2	3.04	1	2.07	2	1.612		
1	2.95	5	1.989	1	1.568		
5	2.75	2	1.949	1	1.528		

[1] Powder spacings calculated for the wavelength Cu $K\alpha = 1.5418$ A.

REFERENCES

ALBERMAN, K. B., & ANDERSON, J. S. (1949): The oxides of uranium, *Journ. Chem. Soc.*, Supp. issue, No. **2,** 303.

ARNOTT, R. J. (1950): *X*-ray diffraction data on some radioactive oxide minerals, *Am. Mineral.*, **35,** 386.

BARTH, T. F. W. (1926): The structure of synthetic, metamict, and recrystallized fergusonite, *Norsk. Geol. Tidsskrift*, **2,** 23 (in *Min. Abs.* **3,** 346).

BILTZ, W., & MÜLLER, H. (1927): Systematic doctrine of affinity. XLI, Uranium oxides, *Zeit. Anorg. Chem.*, **163,** 257.

BRÖGGER, W. C. (1896): Ueber die verschiedenen Gruppen der amorphen Körper, *Zeits. Kryst.*, **25,** 427.

CONYBEARE, C. E. B., & FERGUSON, R. B. (1950): Metamict pitchblende from Goldfields, Saskatchewan and observations on some ignited pitchblendes, *Am. Mineral.*, **35,** 401.

DANA, J. D., & E. S. (1944): *The system of mineralogy* **1,** ed. 7, by C. Palache, H. Berman & C. Frondel, New York.

DAVIDSON, C. F., & BOWIE, S. H. U. (1951): On thucholite and related hydrocarbon-uraninite complexes, *Geol. Surv. Great Britain*, No. **3,** 1.

ELLSWORTH, H. V. (1932): Rare element minerals of Canada, *Geol. Surv. Canada, Econ. Geol. Series*, **11.**

GRØNVOLD, F. (1948): The crystal structure of U_3O_8, *Nature*, **162,** 70.

GRØNVOLD, F. & HARALDSEN, H. (1948): Oxidation of uranium dioxide (UO_2), *Nature*, **162,** 69

JOLIBOIS, P. (1947): A new oxide of uranium, U_3O_7, *Compt. rend.*, **224,** 1395 (in *Chem. Abs.*, **41,** 5406).

KATZ, J. J., & RABINOWITCH, E. (1951): *The chemistry of uranium*, Part 1, ed. 1, New York.

KERR, P. F. (1950): Mineralogical studies of uraninite and uraninite-bearing deposits *Interim Technical Report*, United States Atomic Energy Commission.

KERR, P. F. (1951): Natural black uranium powder, *Science*, **114,** 91.

MILNE, I. H. (1951): Studies of radioactive compounds: III —Uranouranic oxide (U_3O_8), *Am. Mineral.*, **36,** 415.

RUNDLE, R. E., BAENZIGER, N. C., WILSON, A. S. & MCDONALD, R. A. (1948): Structures of the carbides, nitrides and oxides of uranium, *Journ. Am. Chem. Soc.*, **70,** 99.

WASSERSTEIN, B. (1951): Cube-edges of uraninites as a criterion of age? *Nature*, **167,** 380.

STUDIES OF RADIOACTIVE COMPOUNDS:

V—SODDYITE[1]

D. H. Gorman,[2] *University of Toronto, Toronto, Canada.*

Abstract

New observations are made on the rare uranium silicate mineral soddyite. The formula $5UO_3 \cdot 2SiO_2 \cdot 6H_2O$ is established as the most plausible. New crystallographic data are recorded: orthorhombic, $a=8.32$, $b=11.21$, $c=18.71$ A; space group *Fddd*. Powder data are presented which are in agreement with cell dimensions. Soddyite is optically negative, $2V=84°$, $\alpha=1.650$, $\beta=1.685$, $\gamma=1.712$, $X=c$, $Y=b$, $Z=a$, pleochroic, X colorless, Y very pale yellow, Z pale yellow-green; dispersion negligible, in disagreement with previous ob-observations of $r>v$ strong.

Soddyite is a rare hydrous uranium silicate mineral, having an extremely limited geographical distribution. It was first described by Schoep (1922) from Kasolo, Belgian Congo. In subsequent papers, Schoep (1923a, b; 1927, 1930) gave more detailed descriptions, and nothing more on it appeared in the mineralogical literature until Gevers, Partridge & Joubert (1937) reported its occurrence in Namaqualand, Africa. Namaqualand material was not available to the author. Five specimens of soddyite from Kasolo served as material for this study.

Physical Properties

Soddyite occurs as idiomorphic crystals often in groups or clusters, which are sometimes divergent. It also occurs as flat blades or fibres of the cross-fibre type in fissures; also massively intergrown with curite. Larger crystals up to a millimeter in length are generally mosaical, and usually totally opaque, or have at the most a mere selvage of transparent material. Smaller crystals, which are usually tabular are translucent and sometimes quite transparent except for a cloudiness towards the centre. Zoning of the transparent and opaque material, as shown in Fig. 1, is common.

The color is greenish-yellow for the cross-fibre type, canary yellow for the opaque material and amber yellow for the transparent crystals. It is readily distinguished from the orange-red of curite and the slightly brownish hue of kasolite. The streak is pale yellow. The transparent selvages on opaque crystals have a vitreous to adamantine lustre. The opaque varieties are sub-vitreous to dull. Massively it is earthy. The hardness is between 3 and 4 on Mohs' scale. The density of a clean cluster of crystals weighing approximately 18 mg. gave 4.70 ± 0.01 as measured on

[1] Extracted from a thesis for the degree of Doctor of Philosophy in the University of Toronto.

[2] Holding a National Research Council of Canada Studentship.

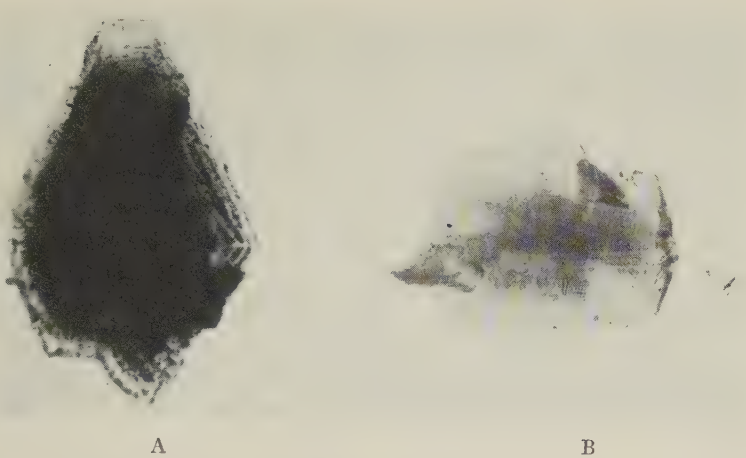

A B

FIG. 1. Soddyite. A—Crystal elongated in [001] showing zoning of transparent and opaque material. B—Crystal elongated in [110] showing murkiness toward the centre. Both photomicrographs taken with plane polarized light, ×112.

the Berman balance. This compares well with Schoep's determination of 4.627 by the pycnometer method. Two cleavages were noted: (001) perfect, (111) good. No visible fluorescence was observed from soddyite under long or short wave ultraviolet excitation.

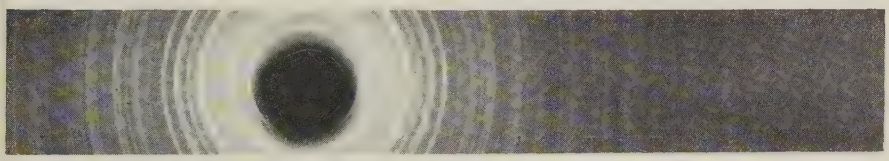

FIG. 2. Soddyite. *X*-ray powder photograph using Cu/Ni radiation ($\lambda = 1.5418$ A); camera radius 57.3 mm; actual size print.

X-RAY CRYSTALLOGRAPHY

For the *x*-ray powder photography a camera of radius 57.3 mm. and nickel filtered copper radiation were used. Spacing was based on $\lambda = 1.5418$ A. Powder photographs obtained from all types of euhedral crystals both translucent and opaque and from the cross-fibre type of soddyite proved to be identical. A print of the pattern, actual size, is shown in Fig. 2, and the powder data are presented in Table 1.

A single crystal, with no visible mosaic texture, was selected and mounted so as to rotate about the *c* axis. A sharp rotation photograph showed a large *c* period with a strong pseudo-period of $\frac{1}{3}c$. When the *Z* factor was subsequently calculated as 3, a tentative explanation of the

TABLE 1. SODDYITE—$5UO_3 \cdot 2SiO_2 \cdot 6H_2O$: *X*-RAY POWDER DATA

Orthorhombic, *Fddd*; $a=8.32$, $b=11.21$, $c=18.71$A; $Z=3$

I (Cu)	*d* (meas)	*hkl*	*d* (calc)	*I* (Cu)	*d* (meas)	*hkl*	*d* (calc)	*I* (Cu)	*d* (meas)	*hkl*	*d* (calc)
9	6.28	111	6.28	7	3.00	133	2.99	5	2.10	333	2.11
3	4.79	022	4.81	5	2.82	040	2.80	3	2.05	153	2.04
10	4.57	004	4.67	8	2.73	224	2.71	5	1.990	119	1.985
		113	4.56	8	2.49	206	2.49	5	1.918	422	1.917
2	3.80	202	3.80	1	2.33	008	2.34	6	1.867	155	1.867
9	3.36	131	3.37	2	2.28	226	2.28			246	1.864
		220	3.34	½	2.22	311	2.21				

I (Cu)	*d* (meas)	*I* (Cu)	*d* (meas)	*I* (Cu)	*d* (meas)	*I* (Cu)	*d* (meas)
3	1.771	½	1.386	4	1.088	½	0.903
3	1.710	4	1.365	1	1.046	½	0.892
2	1.681	½	1.344	1	1.022	2	0.875
4	1.654	3	1.275	½	0.999	½	0.861
2	1.606	4	1.228	½	0.984	½	0.833
½	1.557	4	1.155	3	0.946	2	0.819
3	1.524	½	1.142	½	0.931	1	0.803
½	1.502	½	1.121	1	0.912	½	0.796
4	1.412						

pseudo-period presented itself. It is conjectured that there is a threefold disposition of the heavy uranium atoms or uranium groupings along the *c* axis.

The *a* and *b* lengths were obtained from excellent Weissenberg photographs, which also showed clearly orthorhombic symmetry. The space group proved to be the rather unusual *Fddd*. The extinction conditions imposed by such a space group are (*hkl*) present only with *h*, *k*, *l*, all odd or all even; (00*l*), (0*k*0), (*h*00), (*hk*0), (0*kl*), (*h*0*l*) present only with all indices even and half the sum even. In Table 2 the single crystal data are presented.

TABLE 2. SODDYITE: *X*-RAY SINGLE CRYSTAL DATA

a 8.32 A ± .01	orthorhombic 2/m 2/m 2/m	space group *Fddd*
b 11.21	$a:b:c=0.742:1:1.669$	$Z=3$
c 18.71	$p_0:q_0:r_0=2.249:1.669:1$	

A rotation photograph was also taken about [110], the elongation direction of some crystals. The period determined was 7.00 A, which is in good agreement with 6.99 A calculated from *a* and *b*. As a further check

on cell dimensions and space group the first 17 lines of the powder photograph were indexed and their spacings calculated. The excellent agreement of measured and calculated spacings may be seen in Table 1.

Morphological Crystallography

Schoep has noted in all his papers that soddyite crystals were not amenable to accurate goniometric work. Nevertheless he was able to determine the orthorhombic symmetry and an axial ratio of $a:b:c = 0.7959:1:1.6685$. This is only in fair agreement with the axial ratio obtained in this study by x-ray work. Undoubtedly this discrepancy is due to the poor quality of the crystals which both Schoep and the present writer have observed. It is evident from the variation in measured angles for the form (111) as shown in Table 3 that an axial ratio calculated from goniometric measurements cannot be as accurate as that calculated from excellent x-ray measurements.

Table 3. Soddyite: Measured and Calculated Two Circle Angles

	$\phi(111)$	$\rho(111)$	$\phi(111)-\phi(\bar{1}11)$
Schoep (1923a)			107°
Schoep (1923b)	52° 02′	67° 01′	
Schoep (1930)	51° 29′	69° 32′	
Gorman	53° 07′ (meas)	70° 21′ (meas)	106° 14′ (meas)
	53° 25′ (calc)	70° 44′ (calc)	106° 50′ (calc)

Individual crystals of soddyite invariably have an acute dipyramid form. They show a change in habit from an elongation in [001], through equidimensional, to a platy type elongated in the [110] direction, but nevertheless dipyramidal. It appears as if opposite faces of the dipyramid have been compressed and the crystal attenuated in [110]. It is this platy, elongated habit, thought by Schoep (1922) to show a prism form, that has led George (1949) and other observers to describe this elongation as [001]. The transition in habit is clearly shown in Fig. 3.

The dominant form is the dipyramid (111) which on some crystals is terminated by the basal pinacoid (001). Other faces with ϕ values the same as that of (111) and ρ values varying from 74° 25′ to 79° 04′ were observed, although their goniometric signals were poor. These faces when plotted on the gnomonic projection could not be given simple indices, and the writer hesitates to impute any indices, regardless of complexity to faces giving such poor signals, especially when aberration caused by striations had to be considered. The crystals are heavily striated parallel to the trace of the basal pinacoid (001). These striations are due in part

to an oscillation between dipyramids with varying ρ angles, but in the main to oscillation between (111) and (11$\bar{1}$).

The platy crystals less frequently exhibit (111) but rather are formed by dipyramids with ρ values greater than that of (111). Of these ρ values 74° 45′ occurs most frequently. When the less platy types possess these possibly vicinal faces, barrel shaped crystals result from the continuous change in ρ angles.

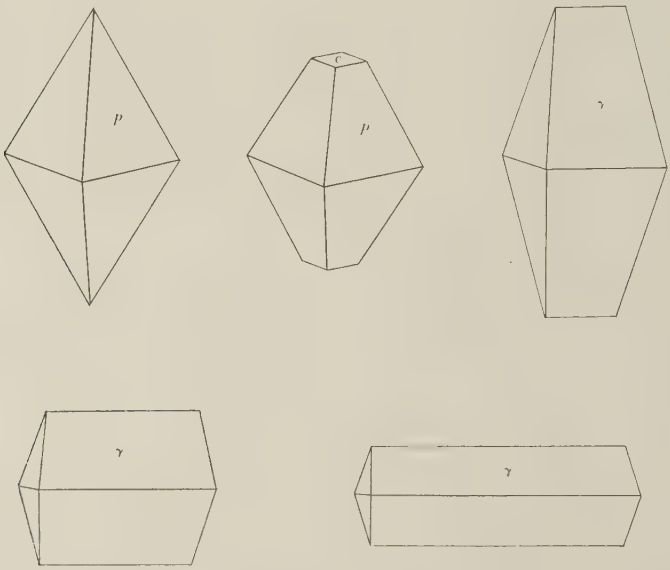

FIG. 3. Soddyite. Showing habit change from elongation in [001] to [110]; and forms: c(001), p(111), γ (dipyramid with ϕ the same as 111, and ρ varying from 74°25′ to 79°04′).

Schoep (1930) records the forms (113) and (114), neither of which appeared on the score of crystals measured in this study; nor was any indication of such faces seen when myriads of crystals were observed under the binocular microscope.

Schoep (1930) observed no cleavage, nor does he mention cleavage in any of his other papers. George (1949) records (010) and (100). Gevers, Partridge and Joubert (1937) describe a perfect (100) and a good domal cleavage, assuming that the bladed crystals are elongated in [001]. In the new orientation, with the bladed crystals elongated in [110], the cleavages become perfect (001) and good (111), both of which were observed here. It was difficult to distinguish between a crystal and a cleavage fragment since the cleavage planes are equivalent to the prominent crystal faces, and very few incipient cracks are present.

Optical Properties

Some difficulty was encountered in determining the optical constants of soddyite because of the murky, pebbly appearance of the more abundant material. This may account for the discrepancy between the indices of refraction originally given by Schoep (1923a) and those recorded by more recent workers. However, there is good agreement among the recent workers, and Professor Schoep does indicate in his own hand on a copy of his original article in the University of Toronto Library that his indices are within wide limits. Some of the optical data as determined by various observers are given in Table 4.

Table 4. Soddyite: A Comparison of Some Optical Data

	α	β	γ	Sign	2V
Kasolo					
Schoep (1923a)	1.645	1.662	—	Pos.	Large
Larsen & Berman (1934)	1.650	1.68	1.71	Neg.	Near 90°
George (1949)	1.650	1.685	1.715	Neg.	Large
Gorman (1952)	1.650	1.685	1.712	Neg.	84° (calc)
Namaqualand					
Gevers, etc. (1937)	1.654	1.685	1.699	Neg.	Near 70°

The correct optical orientation $X=c$, $Y=b$, $Z=a$ follows from the new morphological setting. Most of the material available was weakly pleochroic: X colorless, Y very pale yellow, Z pale green-yellow. There was a stronger pleochroism in some of the cross-fibre type. In Becke line tests no appreciable dispersion was observed, in contrast with the other authors listed in Table 4, who report strong dispersion $r>v$.

Chemistry and Mode of Occurrence

Table 5 shows three analyses made by Schoep on soddyite from Kasolo. Also given are the average of the three analyses according to Schoep, the theoretical compositions calculated for two suggested chemical formulae along with the molecular ratios derived therefrom. Schoep chose $12UO_3 \cdot 5SiO_2 \cdot 14H_2O$ as more likely than $5UO_3 \cdot 2SiO_2 \cdot 6SiO_2$ (advocated by Wherry, 1922) since the weight percentages calculated for it are in slightly better agreement with his average analysis.

The weight of the cell contents was calculated from the cell dimensions and the measured density. This figure, with the atomic proportions derived from analysis 3 in Table 5 led to $3[5UO_3 \cdot 2SiO_2 \cdot 6H_2O]$ as the cell contents most compatible with the chemical data. The derivation of the cell contents is presented in Table 6. The calculated Z factor of 3 is ap-

Table 5. Chemical Data on Soddyite (After Schoep)

	1	2	3	4	5	6	7	8
UO_3	85.53	85.13	85.79	85.87	86.10	86.25	0.300	0.300
SiO_2	7.86	7.88	7.61	7.87	7.50	7.30	0.131	0.125
H_2O	—	—	6.16	6.26	6.30	6.50	0.350	0.350
			99.56	100.00	99.90	100.05		

1, 2, 3. Soddyite, Kasolo; anal. Schoep (1930). 4. Schoep's average of analyses 1, 2 and 3. 5, 6. Schoep's calculated weight percentages for $12UO_3 \cdot 5SiO_2 \cdot 14H_2O$ and $5UO_3 \cdot 2SiO_2 \cdot 6H_2O$ respectively. 7, 8. Schoep's molecular proportions for 5 and 6 respectively.

parently related to the pseudo-period of $\frac{1}{3}$ which was previously noted. The calculated specific gravity of 4.75 compares well with the measured value of 4.70.

Wildish (1930) has reported the U^6 content of soddyite as 43.98% determined by the emanation method, and 44% by the gravimetric method The material analysed was certainly not soddyite, but quite possibly kasolite, which has a U^6 content of roughly 40%. These two minerals are similar in color and not easily distinguished in the hand specimen, by those not familiar with their crystal morphology.

As noted at the beginning of this paper, soddyite is both rare and limited in occurrence. It has been reported from only two localities: Kasolo, in the Belgian Congo of Africa, and the Norrabees pegmatite area south of the Orange River, Namaqualand, Africa. At Kasolo it forms a massive intimate mixture with curite. The cross-fibre or cross-bladed type always occurs as fissure fillings in the soddyite-curite complex. Euhedral crystals and crystal clusters are found associated with needles of sklodowskite on curite, the soddyite seemingly formed after

Table 6. Analysis and Cell Content of Soddyite

	1		2	3	4
UO_3	85.79	U	14.88	14.94	15
SiO_3	7.61	Si	6.26	6.29	6
H_2O	6.16	O	56.79	57.00	57
	99.56	H_2O	18.52	18.60	18
			96.45	96.83	96

[1] Analysis by Schoep on Kasolo material. 2. Atoms per unit cell. 3. Atoms per unit cell based on O=57. 4. Ideal cell content for $3[5UO_3 \cdot 2SiO_2 \cdot 6H_2O]$.

the curite and before the sklodowskite. Kasolite, the lead bearing hydrous uranium silicate is another associated mineral.

Schoep has pointed out that there seems to be an intimate association of lead and non-lead species at Kasolo, for example curite-soddyite, curite-becquerelite, and kasolite-soddyite, the lead bearing species having formed first as an alteration of uraninite. The paragenesis at the Nicholson Mine, Lake Athabaska, Canada appears analogous, although no soddyite has as yet been found there.

The Namaqualand soddyite as reported by Gevers, Partridge and Joubert (1937) occurs in pegmatites, as a bladed incrustation on quartz, associated with malachite.

Soddite was the original name given to this mineral by Schoep in honor of Professor F. Soddy of Oxford University. Billiet (1926) changed it to soddyite, the change being approved by Schoep, who used this more euphonious synonym in all his later publications.

Acknowledgements

I wish to record my thanks to Dr. V. B. Meen and Dr. G. Switzer for the loan of specimens of this rare mineral; to Dr. E. W. Nuffield for criticisms; and to the National Research Council of Canada, my patron, for allowing the publication of this work.

References

Billiet, V. (1926): Over de bepaling van becquerelite, janthiniet,—van de immersie method van Becke, *Natuur. Tijd. Ant.*, **7,** 112.

George, D. (1949): Mineralogy of uranium and thorium bearing minerals, *U.S.A.E.C., R.M.O.*, **563,** 195.

Gevers, T., Partridge, F., & Joubert, G. (1937): The pegmatite area south of Orange River, Namaqualand, *Mem. Geol. Surv. South Africa*, **31,** 172.

Larsen, E. & Berman, H. (1934): The microscopic determination of the non-opaque minerals, *U.S.G.S.* Bull. **848,** 183.

Schoep, A. (1922): La soddite, nouveau minéral radioactif, *Compt. Rend. Acad. Sci. Paris*, **170,** 1066.

——— (1923a): Sur les formes des cristeaux de soddite et sur leur properties optiques, *Bull. Soc. Belge. Geol. Brux.*, **23,** 83.

—— (1923b): Les minéraux uranifère du Congo Belge, *extrait du Bull. Soc. Belge. Geol. Brux.*, **33,** 181.

——— (1927): Kristallografische mededeelingen, kristallen van kasoliet, soddyiet en brochantiet, *Natuur. Tijd. Ant.*, **9,** 1927.

——— (1930): Les minéraux du gîte uranifère du Katanga, *Ann. Musee Congo Belge*, ser. 1, 1, fasc. 2, 26.

Tutton, A. (1922): *Crystallography and practical crystal measurement*, Vol. 1. London.

Wherry, E. (1922): Soddite (abstract), *Am. Mineral.*, **7,** 179.

Wildish, J. (1930): Origin of protactinium, *Jour. Am. Chem. Soc.*, **51,** 163.

SYNTHESIS AND *X*-RAY STUDY OF URANIUM SULPHATE MINERALS[1]

R. J. Traill, *Queen's University, Kingston Canada.*

Abstract

Attempts have been made to synthesize uranium sulphate minerals. Artificial zippeite having optical properties in agreement with the natural mineral has been prepared. Physical, chemical, optical and *x*-ray data for zippeite and four other synthetic products are presented.

Artificial zippeite is monoclinic. Space group $C2/m$. Unit cell dimensions: $a=8.81$, $b=14.13$, $c=8.85$A, $\beta=104°15'$. Cell contents: $2[(UO_2)_3(SO_4)_2(OH)_2\cdot 8H_2O]$. Calculated specific gravity 3.68, measured 3.66. Optical properties: biaxial negative; $nX=1.655$, $nY=1.717$, $nZ=1.765$; X=colorless, Y=pale yellow, Z=yellow; orientation, $X=b$, $Z\wedge a=3°$.

The optical properties and *x*-ray powder pattern of uranopilite from Goldfields, Saskatchewan, are appended.

Introduction and Acknowledgments

In the summer of 1950, the writer began a research program which had as its objective the synthesis and *x*-ray study of the uranium sulphate group of minerals. Johannite, medjidite, uraconite, uranochalcite, uranopilite, beta-uranopilite, voglianite, and zippeite are names which occur in mineralogical literature for uranium sulphates. Johannite is well established and the only mineral of this group for which the results of morphological and *x*-ray studies have been published (Peacock, 1935, and Hurlbut, 1950). The optical properties of uranopilite, recorded by Nováček (1935), have proved to be consistent and have enabled the mineral to be identified in specimens from widespread localities. Chemical analyses by Nováček suggest a composition of $(UO_3)_6SO_3\cdot 16$–$17\ H_2O$ for uranopilite but this composition has not been confirmed. Beta-uranopilite is considered by Nováček to be a dehydration product of uranopilite. Some confusion exists as to the chemical composition and optical properties of zippeite. Nováček (1935) suggested a composition of $(UO_3)_2SO_3\cdot nH_2O$ with n varying from three to eight. He noted that the refractive indices of zippeite varied over a wide range, and ascribed this variation to the changes in water content. Frondel (1951) suggests that the name zippeite be reserved for a mineral which he has found to give constant optical properties and a distinctive powder diffraction pattern. The descriptions which are recorded for medjidite, uraconite, uranochalcite, and voglianite are so vague that these names have little meaning

[1] Extracted from an unpublished M.Sc. thesis by R. J. Traill: Synthesis and *X*-ray Study of Uranium Sulphate Minerals—Queen's University, 1951. This work was carried out with the aid of a bursary and a grant (to L. G. Berry) from the National Research Council (Canada) 1950–51, and is published with the permission of the Council

today and cannot be applied to new occurrences of uranium sulphate minerals (Dana, 1951). Crystallographic data on uranopilite and zippeite are lacking, and the optical and chemical properties of these minerals require clarification.

The uranium sulphate minerals occur as clusters of tiny crystals commonly intergrown with other minerals. Museum specimens of these minerals are rare and the labels attached to the specimens are unreliable. Only rarely can material suitable for *x*-ray studies be found. The most likely way of establishing the definitive description of such minerals is by the synthesis and *x*-ray study of materials having physical, chemical and optical properties similar to those of minerals occurring in nature.

The research program was carried out in the laboratories of the Department of Geological Sciences, Queen's University, Kingston, under the supervision of Dr. L. G. Berry. Uranium oxide compounds were obtained through the courtesy of the Eldorado Mining and Refining Company. *X*-ray powder films were kindly loaned for comparison by the U. S. Geological Survey (Trace Elements Laboratory). To the abovementioned persons and institutions the writer wishes to express his sincere appreciation for assistance rendered.

Synthesis

General Considerations. Uranyl salts are characterized by the bivalent ion UO_2. Normal uranyl sulphates have a molecular ratio of $UO_2:SO_4=1:1$. The suggested compositions of uranopilite and zippeite, respectively, may be written as $(UO_2)_6SO_4(OH)_{10}\cdot 12H_2O$ and $(UO_2)_2SO_4(OH)_2\cdot 4H_2O$ showing molecular ratios of $6UO_2:1SO_4$ and $2UO_2:1SO_4$. If the concept of a uranyl radical is retained, these minerals must be regarded as basic uranyl sulphates and their formulas may be rewritten as $UO_2SO_4\cdot 5UO_2(OH)_2\cdot 12H_2O$ and $UO_2SO_4\cdot UO_2(OH)_2\cdot 4H_2O$. The synthesis experiments conducted by the writer were therefore directed towards obtaining basic uranyl sulphates.

The problem of synthesis is complicated by the consideration that the material produced must be suitable for *x*-ray studies. To determine the unit cell constants of a compound by means of *x*-rays a single crystal of the compound is usually required. For this reason the crystallization of artificial material should take place slowly enough so that single crystals develop instead of clusters of crystal intergrowths. Crystals having dimensions of from 0.1 to 0.5 mm. are most suitable for *x*-ray studies.

Three methods of synthesis have been used successfully for the production of artificial minerals. The first method, that of crystallization from a fusion, is not applicable to the problem at hand because of the

hydrous nature of the products sought. The other two methods, which may be included under the term hydrosynthesis, are of practical value in this problem. One method involves crystallization from aqueous solution under elevated conditions of temperature and pressure, and may be termed pressure bomb synthesis. The other type of hydrosynthesis involves crystallization by evaporation or precipitation under conditions of moderate temperature and atmospheric pressure. This method may be termed synthesis at atmospheric pressure.

Pressure Bomb Synthesis. The pressure bomb method of synthesis has been used successfully in recent years to produce artificial minerals of many different types. The main disadvantage of using this method is the fact that conditions existing in the pressure bomb do not simulate those which are present during the formation of naturally-occurring uranium sulphate minerals. Many substances, however, have been produced artificially under conditions that are unlikely to exist in nature. Furthermore, the physical-chemical relationships which exist in a bomb of this type are not clearly understood, and the products of chemical reactions under pressure bomb conditions are generally anticipated rather than predicted. The main reason for the increasing popularity of this method of synthesis lies in the nature of the products obtained. It has been found that the products are commonly well crystallized and highly satisfactory for study by x-ray methods. If the required products are formed but are not well crystallized, then a simple alteration of the test conditions will generally produce satisfactory material.

A series of pressure bomb experiments were carried out to test the reactions of sulphuric acid solutions of varying strengths on oxides of uranium. Four well-crystallized compounds were produced and studied by optical and x-ray methods (Traill, 1951). The four compounds were deep green in color and non-fluorescent, and therefore, probably uranous salts. Compounds of this type are unlikely to occur in nature and thus are of little interest in this investigation.

Synthesis at Atmospheric Pressure. Uranium sulphate minerals are formed in nature by the supergene alteration of uraninite. Three processes may be effective in forming the secondary minerals. In the first process, materials contained in circulating solutions react with the uraninite to form secondary minerals by direct alteration. No transportation of uranium is involved in this process. Secondly, the uraninite may be taken into solution by circulating waters and precipitated in the form of secondary minerals by reaction with suitable precipitating agents. The third process involves solution of the uraninite by circulating waters and deposition of secondary minerals as the result of evaporation of the uranium-bearing solutions.

In the first process, a long period of stable conditions and probably some catalytic action would be required to permit the transfer of sulphate ions to take place from the solution to the uraninite. This process is of doubtful value as a method of laboratory synthesis.

Chemical compounds produced by precipitation, as in the second process operative in nature, are generally very fine grained. Material precipitated in the laboratory can sometimes be made more coarsely crystalline by allowing the precipitation to take place slowly at a temperature approaching the boiling point of the solution and by retaining the temperature of the solution near the boiling point for a considerable length of time. Precipitation from solution, as applied to laboratory synthesis is perhaps the most likely way of producing a compound of the required chemical composition. The problem of obtaining the compound in a form suitable for *x*-ray and optical studies is the main drawback in using this process.

The third process, that of crystallization from solution by evaporation, is ideally suited for the formation of good crystalline material. A decrease in the rate of evaporation will generally result in an increase in the size of the crystals formed. The main problem involved when this process is used in the laboratory is that of obtaining the particular solution which will yield crystals of the desired compound. A further difficulty arises in the fact that a single solution may yield several different compounds depending on the physical conditions which are operative during crystallization. These problems arise almost invariably in the crystallization of hydrated compounds.

With the above-mentioned thoughts in mind, the writer carried out about 50 synthesis experiments at atmospheric pressure. Space does not permit detailed descriptions of the various combinations of chemicals and procedures which were used. Those experiments which yielded materials of interest are summarized briefly in Table 1, further details are given in the writer's unpublished thesis (Traill, 1951).

Identification of Products. The products resulting from each experiment were examined as completely as their nature permitted, within the limitations imposed by the means at the disposal of the writer. In some cases, the information obtained led to positive identification of the compounds, in others it was insufficient and the compounds were not identified. Very little data on uranium sulphates has been published and thus the positive identification of synthetic products by comparison with the published properties of known compounds could not be achieved until exhaustive investigations had been carried out.

The indices of refraction were obtained by immersion in standardized index oils. Specific gravity determinations were made on well-crystal-

TABLE 1. SUMMARY OF SYNTHESES AT ATMOSPHERIC PRESSURE

Reference Number	Materials Used		Procedure Adopted	Results Obtained
E-1-5	$UO_2SO_4 \cdot 3H_2O$	2 gm.	A saturated solution was evaporated slowly at 95° C. in an Erlenmeyer flask closed by a rubber stopper with a capillary opening. (E-1-5 to E-3-4)	Compound W
	Na_2O_2	0.5 gm.		
	H_2SO_4 (conc)	5 cc.		
	Water	25 cc.		
E-1-6	$UO_2SO_4 \cdot 3H_2O$	2 gm.		Copper sulphate and Compound W
	$CuSO_4$	0.8 gm.		
	Na_2O_2	0.5 gm.		
	H_2SO_4 (conc)	5 cc.		
	Water	25 cc.		
E-3-2	Uranyl hydrate			Compound Y
	$CuSO_4$			
	H_2SO_4 (1:6)			
E-3-3	Uranyl hydrate			Compound X and Compound Y
	H_2SO_4 (1:6)			
	H_2O_2 (30%)	5 cc.		
E-3-4	Uranyl hydrate			Compound Y
	H_2SO_4 (1:6)			
	$CaCO_3$			
E-5-1	Uranyl hydrate	2 gm.	Evaporation in a crystallizing dish at 30° C.	Compound Y
	H_2SO_4 (.05 M)	100 cc.		
C-1	$UO_2SO_4 \cdot 3H_2O$		NH_4OH added to give pH 4.5. The ppte. was kept at 95° C. for two weeks.	Fine-grained product gave a powder pattern close to that of zippeite.
	Water			
C-5	Ur. nitrate	5.02 gm.	NH_4OH added. Evaporation at 25° C. in a crystallizing dish.	Compound Z
	Cu nitrate	2.41 gm.		
	K_2SO_4	3.48 gm.		
	Water	50 cc.		
C-9	Ur. nitrate	3.58 gm.	Evaporation in a crystallizing dish at 30° C.	Compound Y
	K_2SO_4	.62 gm.		
	Water	50 cc.		
C-10	$UO_2SO_4 \cdot 3H_2O$		NH_4OH added to give pH 3.5. Evaporation in a crystallizing dish at 25° C.	Compound V
	Water			

TABLE 1 (*Continued*)

Reference Number	Materials Used	Procedure Adopted	Results Obtained
C-11	Ur. nitrate 5.02 gm. K_2SO_4 .29 gm. Water 50 cc.	NH_4OH added to give pH 3.3 Evaporation in a crystallizing dish at 25°C.	Crystals of zippeite formed after several weeks.
C-12	Uranyl hydrate 1 gm. Water 50 cc. H_2SO_4 (a few drops)	NH_4OH added to give pH 4.1 Evaporation in a crystallizing dish at 30°C.	Compound V.
C-13	Same as C-12	Same as C-12 but pH 3.6	Compound V.
C-14	Same as C-12	Same as C-12 but pH 2.6	Compound V.
C-17	Uranyl hydrate 1 gm. K_2SO_4 .5 gm. Water 50 cc. HCl (a few drops)	Same as C-12 but pH 2.6	Compound Z.
C-18	Uranyl hydrate 1 gm. K_2SO_4 1 gm. Water 50 cc.	Same as C-12 but pH 3.0	Compound U and Compound Z.
C-19 C-20 C-21	$UO_2SO_4 \cdot 3H_2O$ $BaCl_2$ sol'n. Water	Removal of $SO_4^=$ by ppt'n as $BaSO_4$. Filtrate evaporated at 30°C.	Compound W.
C-26 C-27	Uranyl sulphate solution	NH_4OH added to give pH 4.3 (C-26), 4.1 (C-27)	Fine-grained zippeite formed overnight.

lized material by means of the Berman balance. The Weissenberg goniometer and the Buerger precession camera were used for single-crystal x-ray studies. Accepted standard procedures of chemical analysis were adopted. Uranium was determined gravimetrically by precipitation with ammonia as the diuranate and ignition to U_3O_8. The sulphate content was obtained by precipitation as barium sulphate. Water was determined by the Penfield method for compounds easily deprived of their water, after first mixing the sample with anhydrous sodium tungstate to retain the oxides of sulphur.

SYNTHETIC ZIPPEITE

Artificial zippeite was obtained in suitable crystalline form as the product of synthesis experiment C-11. An aqueous solution of uranyl nitrate and potassium sulphate in the molecular ratio of 6:1 was ad-

justed to a pH of 3.3 with ammonium hydroxide and allowed to stand at room temperature for a period of two months. The crystalline product was then examined and found to possess the optical properties of the mineral zippeite. Several x-ray powder diffraction photographs were taken to ensure the homogeneity of the product. The observed intensities and measured spacings were similar to those obtained from pattern TE 288 of the U. S. Geological Survey Trace Elements Section labelled synthetic zippeite (said to be identical with film TE 251 of natural zippeite). In experiment C-1, a uranyl sulphate solution to which ammonium hydroxide had been added yielded a fine-grained orange precipitate on standing at 95° C. for 12 hours. The precipitate and solution were maintained at that temperature for two weeks. The material gave a powder pattern similar to artificial zippeite but was too fine grained to be identified optically. In experiments C-26 and C-27, fine-grained artificial zippeite crystallized from uranyl sulphate solutions at pH's of 4.3 and 4.1, at 30° C. The material was unsuitable for single-crystal studies.

Clusters of tiny crystals of artificial zippeite are orange yellow in color, but individual crystals have a distinctly greenish tinge. The crystals occur as flat (010) plates with elongate, doubly-terminated, rhombic outlines.

When examined under the polarizing microscope, the crystals are observed to be invariably twinned. Two individuals make up the twin by reflection across the (001) plane. There is no evidence of zoning. A doubly-terminated (010) plate shows a fourling made up of the two individuals when viewed under crossed nicols. The two individuals give acute bisectrix figures indicative of monoclinic symmetry and the optic orientation $x=b$ and $Z\wedge a=3°$. In the parallel position, the trace of the twin plane disappears giving rise to apparent orthorhombic extinction conditions with $X=b$, $Y=c$, $Z=a$. Additional optical properties are listed in Table 2, together with the properties of the natural mineral.

The specific gravity was determined by immersion in thallium malonate-thallium formate solutions. The density of the solution in which the material remained suspended was measured on the Berman balance using a cube of galena as a standard. A value of 3.66 was obtained for the specific gravity.

Rotation, zero and first layer Weissenberg films were taken about the axis of elongation (a axis) of a twinned crystal. Precession photographs were also taken using the b axis as the precessing axis. The systematic absences of diffraction spots conformed with the criteria of monoclinic space group $C2/m$. The unit cell dimensions in Angstrom units are as follows:

$$a = 8.81, \quad b = 14.13, \quad c = 8.85, \quad \beta = 104° 15'.$$

TABLE 2. OPTICAL PROPERTIES OF NATURAL AND ARTIFICIAL ZIPPEITE

		1	2	3	4	5
Indices of Refraction	nX	1.64	1.655	1.66	1.66	1.655
	nY	1.718	1.72	1.715	1.72	1.717
	nZ	1.766	1.77	1.76	1.765	1.765
Optic Sign		(−)	(−)	(−)	(−)	(−)
Pleochroic Formula	X	colorless				colorless
	Y	pale yellow to yellow				pale yellow
	Z	yellow				yellow
Extinction		parallel				parallel or inclined at 3°.
Orientation		Z parallel to elongation				$Z \wedge a = 3°$.

1. Anmerk 67071, Frondel (1951).
2. Joachimsthal 69051, Frondel (1951).
3. Joachimsthal 125, Frondel (1951).
4. Joachimsthal 6233, Frondel (1951).
5. Artificial zippeite, Traill (1951).

β was obtained by direct measurement on the zero layer precession film.

The chemical analyses of zippeite by Nováček (1935) show the presence of considerable calcium. It seems likely that the material analysed by Nováček contained uranopilite and gypsum in addition to zippeite. The variability of his analyses and optical properties could thus be accounted for. Earlier analyses by Lindacker (1857) are also unreliable. Two chemi-

TABLE 3. ARTIFICIAL ZIPPEITE: CHEMICAL ANALYSIS AND CELL CONTENT

	1	2	3	4	5		6	7
UO_3	74.52	75.70	75.11	73.29	72.70	U	6.03	6
SO_3	13.50	13.25	13.36	13.04	13.56	S	3.83	4
H_2O	13.81	14.21	14.01	13.67	13.74	O	47.43	48
	101.83	103.16	102.48	100.00	100.00	H	35.70	36

1. Analysis by writer.
2. Analysis by writer.
3. Average of analyses 1 and 2.
4. Average analysis reduced to 100 per cent.
5. Ideal composition for $2[(UO_2)_3(SO_4)_2(OH)_2 \cdot 8H_2O]$.
6. Cell content of zippeite, $M = 2353$.
7. Ideal cell content for $2[(UO_2)_3(SO_4)_2(OH)_2 \cdot 8H_2O]$.

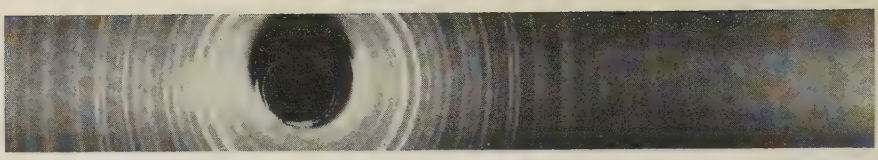

FIG. 1. X-ray powder photograph of artificial zippeite. Cu radiation, Ni filter. Camera radius $90/\pi$ (1 mm. in film $= 1°\theta$).

cal analyses of artificial zippeite were made by the writer (Table 3), and used as a basis for calculation of the unit cell contents.

The unit cell dimensions combined with the measured specific gravity give the molecular weight of the cell contents $M = 2353$. In Table 3, this value has been used to determine the atomic content of the unit cell from the average analysis. The computed cell content agrees closely with the ideal figures, clearly indicating a cell content $2[(UO_2)_3(SO_4)_2(OH)_2 \cdot 8H_2O]$. The calculated specific gravity for this cell content is 3.68, in close agreement with the measured value 3.66.

The x-ray powder diffraction pattern of artificial zippeite is shown in Figure 1. Observed intensities and measured spacings, together with the calculated spacings indexed to a minimum $d = 2.00$, are listed in Table 4. Close agreement is reached between the measured and calculated spacings.

Other Synthetic Uranium Sulphates

The synthesis experiments at atmospheric pressure (Table 1) yielded crystals of six compounds in addition to zippeite. The six greenish-yellow compounds exhibited brilliant greenish fluorescence when viewed in ultra-violet light. All were soluble in water. None of these compounds are known to occur as minerals.

The synthetic products, V, W, Y, and Z, were identified as uranyl sulphate compounds which are listed in Gmelins (1936). A search of chemical literature failed to reveal any comprehensive descriptions of the properties of these compounds. The writer, therefore, has included in this paper a summary of the properties of the four synthetic products (Table 5), and the data obtained from their powder photographs (Table 6). The properties which are recorded in Gmelins agree reasonably well with the corresponding values in Table 5. A discrepancy, however, is found in the specific gravity of compound W (uranyl sulphate trihydrate). The measured and calculated values of 3.84 and 3.88 (Table 5) disagree with the value 3.280 recorded in Gmelins and other handbooks.

Only small amounts of compounds U and X were available for study, and chemical analyses could not be undertaken to establish their identities. The crystallographic, optical, x-ray data, and brief descriptions of

TABLE 4. *X*-RAY POWDER PATTERN: ARTIFICIAL ZIPPEITE = $2[(UO_2)_3(SO_4)_2(OH)_2 \cdot 8H_2O]$

Monoclinic $C2/m$; $a = 8.81$, $b = 14.13$, $c = 8.85$ A, $\beta = 104°15'$

I (Cu)	*d* (meas)	*hkl*	*d* (calc)	*I* (Cu)	*d* (meas)	*hkl*	*d* (calc)	*I* (Cu)	*d* (meas)	*hkl*	*d* (calc)
2	8.42	001	8.58			023	2.65			$\bar{2}04$	2.15
1	7.69	110	7.32	2	2.64	$\bar{3}12$	2.65			$\bar{2}43$	2.15
10	7.02	020	7.06			$\bar{1}51$	2.63			242	2.15
½	6.24	$\bar{1}11$	6.25			113	2.49	2	2.14	203	2.14
2	5.47	021	5.48			151	2.49			004	2.14
		002	4.29			$\bar{1}33$	2.49			400	2.13
3	4.27	$\bar{2}01$	4.27	4	2.48	311	2.48			$\bar{4}02$	2.13
		200	4.26			$\bar{2}42$	2.48			312	2.11
1	3.87	$\bar{1}31$	3.89			$\bar{3}31$	2.48			$\bar{4}21$	2.10
		022	3.67			241	2.47	1	2.09	$\bar{3}33$	2.09
1	3.65	220	3.64			$\bar{1}52$	2.36			062	2.07
		$\bar{2}21$	3.64	2	2.34	060	2.35			$\bar{2}61$	2.07
9	3.48	$\bar{2}02$	3.50			$\bar{3}32$	2.34			024	2.05
		201	3.49			133	2.23			223	2.05
9	3.13	$\bar{2}22$	3.14	½	2.23	152	2.23			$\bar{2}24$	2.05
		221	3.12			331	2.22	2	2.04	420	2.04
3	2.85	003	2.86			043	2.22			$\bar{4}22$	2.04
		240	2.72	3	2.19	$\bar{4}01$	2.20			$\bar{1}53$	2.04
		$\bar{2}41$	2.72			$\bar{1}14$	2.19			$\bar{3}51$	2.03
½	2.70	$\bar{2}03$	2.71								
		202	2.70								
		150	2.70								

I	*d*(meas)	*I*	*d*(meas)	*I*	*d*(meas)	*I*	*d*(meas)	*I*	*d*(meas)
6	1.96 A	1	1.53 A	½	1.30 A	1	1.11 A	½	0.95 A
1	1.87	1	1.50	2	1.26	1	1.09	½	0.94
1	1.81	½	1.46	2	1.24	1	1.07	1	0.93
5	1.75	1	1.42	½	1.21	1	1.06	½	0.92
5	1.69	2	1.39	½	1.20	½	1.04	½	0.90
½	1.63	1	1.37	1	1.18	1	1.01	1	0.89
½	1.59	½	1.35	1	1.16	1	0.99		
4	1.56	1	1.31	½	1.14	1	0.98		

the two compounds are recorded in the writer's unpublished thesis but will not be presented here.

APPENDIX: URANOPILITE FROM GOLDFIELDS, SASKATCHEWAN

Through the generosity of Dr. S. C. Robinson of the Geological Survey of Canada, the writer obtained a specimen of pitchblende richly encrusted with a bright yellow mineral. The yellow mineral was studied optically, and a powder pattern was obtained. Both the optical proper-

Table 5. Summary of Uranium Sulphate Synthetic Products

Compound	V	W	Y	Z
Cell contents	$4[UO_2SO_4 \cdot (NH_4)_2SO_4 \cdot 2H_2O]$	$8[UO_2SO_4 \cdot 3H_2O]$	$4[2UO_2SO_4 \cdot H_2SO_4 \cdot 5H_2O]$	$4[UO_2SO_4 \cdot K_2SO_4 \cdot 2H_2O]$
Space group	$P2_1/n$	$Pbnm$	$Pmnn$	$Pmnb$
Unit cell dimensions a	20.53 A	12.58 A	12.86 A	11.55 A
b	7.30	17.00	12.99	13.78
c	7.74	6.73	11.57	7.28
β	99°25′			
Specific gravity (measured)	3.07	3.84		3.33
Specific gravity (calculated)	3.10	3.88	3.16	3.31
Chemical analysis	UO_3 52.90 SO_3 30.13 NH_3, H_2O 17.90 100.93	UO_3 69.13 SO_3 19.01 H_2O 13.78 101.92	UO_3 57.46 SO_3 26.54 H_2O n.d.	UO_3 48.74 SO_3 27.31 K_2O qual. H_2O 6.98
Indices of refraction nX	n.d.	1.574	1.555	n.d.
nY	1.555	1.589	1.586	1.529
nZ	1.600	1.593	1.586	1.575
Pleochroic formula X	colorless	colorless	colorless	not pleochroic
Y	colorless	pale green	pale yellow	
Z	pale green	greyish green	pale yellow	
Orientation		$Z=c$	$Z=c$	

ties and the powder diffraction data are in agreement with those of the mineral uranopilite.

The mineral has a silky lustre which gives the crust a velvety appearance. It emits a bright greenish fluorescence when viewed in ultra-violet light. The crust is made up of bundles of tiny fibres grouped together in the form of rosettes and also intergrown in a completely random manner. Because of the fibrous habit, the writer was unable to select a single crystal for study by single-crystal x-ray methods.

Several powder diffraction photographs were taken using Cu radiation, and the material was found to give a distinctive pattern (Table 7).

TABLE 6. *X*-RAY POWDER PATTERNS (Cu radiation, Ni filter)

Compound V		Compound W		Compound Y		Compound Z	
I	*d*(meas)	*I*	*d*(meas)	*I*	*d*(meas)	*I*	*d*(meas)
10	6.71 A	6	6.76 A	1	8.34 A	2	7.38 A
4	5.91	1	5.72	2	7.02	10	6.81
7	5.28	1	5.51	10	6.32	2	6.07
7	4.98	10	5.01	4	5.61	10	5.54
6	4.48	4	4.37	2	5.15	1	5.22
3	3.93	1	4.10	½	4.44	5	4.58
3	3.77	9	3.99	4	4.27	5	4.44
2	3.59	3	3.49	3	4.00	6	3.65
9	3.38	3	3.41	½	3.71	3	3.51
3	3.21	3	3.34	½	3.48	3	3.43
7	3.06	1	3.22	1	3.40	4	3.30
7	2.87	2	3.05	6	3.19	5	3.08
½	2.73	2	2.95	1	3.08	5	3.00
½	2.64	6	2.79	½	3.02	1	2.88
4	2.56	1	2.71	1	2.87	2	2.73
½	2.45	1	2.58	5	2.76	1	2.65
1	2.38	8	2.50	1	2.70	2	2.51
5	2.33	½	2.44	3	2.61	2	2.37
4	2.25	½	2.37	½	2.49	2	2.30
3	2.17	5	2.32	½	2.39	4	2.23
1	2.10	1	2.24	1	2.34	1	2.19
5	2.06	1	2.21	2	2.22	1	2.13
2	1.99	2	2.14	4	2.13	1	2.09
1	1.93	2	2.07	2	2.04	2	2.04
1	1.89	1	1.99	1	1.98	3	1.96
½	1.85	1	1.96	1	1.92	2	1.87
½	1.82	2	1.90	1	1.88	2	1.80
3	1.77	2	1.85	2	1.84	2	1.76
2	1.73	7	1.79	1	1.80	2	1.72
1	1.70	2	1.74	1	1.75	2	1.69
1	1.69	1	1.68	3	1.70	4	1.65
2	1.65	1	1.63	½	1.66	1	1.62
2	1.62	1	1.59	½	1.59	1	1.59
2	1.59	3	1.56	2	1.55	2	1.52
½	1.56			1	1.51	2	1.48
½	1.54			1	1.47	1	1.41
½	1.50			3	1.43	1	1.40
1	1.44			3	1.40	1	1.37

Table 7. Uranopilite: *X*-ray Powder Pattern (Cu radiation, Ni filter)

I	*d*(meas)	*I*	*d*(meas)	*I*	*d*(meas)	*I*	*d*(meas)
3	8.76 A	½	3.95 A	6	2.88 A	2	2.14
3	7.97	½	3.82	2	2.72	1	2.11
10	6.97	3	3.60	4	2.66	4	2.00
5	5.87	1	3.47	½	2.56	2	1.95
6	5.44	1	3.34	½	2.49	½	1.89
1	5.07	1	3.24	½	2.40	3	1.81
2	4.60	1	3.03	½	2.33		
9	4.21	1	2.95	½	2.24		

A powder pattern of uranopilite (TE 604) was borrowed from the Trace Elements Section of the U. S. Geological Survey for comparison with that of the mineral from Goldfields. The measurements obtained from the two patterns showed good agreement.

Rotation films were taken about the axis of elongation of several tiny bundles of fibres. The films yielded a value of 8.91 A for the lattice period along the axis of elongation.

For the mineral from Goldfields, the writer determined the following optical properties: indices of refraction, $nX = 1.620$, $nY = 1.624$, $nZ = 1.630$; strong dispersion; not pleochroic; inclined extinction, $Y \wedge$ elongation $= 16°–17°$. These properties are in close agreement with the properties of uranopilite recorded by several investigators and summarized by George (1949).

References

Dana, J. D. & E. S. (1951): *System of Mineralogy* **2,** by C. Palache, H. Berman & C. Frondel, New York.

Frondel, C. (1951): Personal communication.

George, d'Arcy (1949): Mineralogy of uranium and thorium bearing minerals, *U. S. Atomic Energy Commission Technical Information Division.*

Gmelins (1936): *Gmelins Handbuch der anorgischen Chemie.*

Hurlbut, C. S. (1950): *Am. Mineral.*, **35,** 531–535.

Lindacker (1857): *Vogl. Min. Joach.*, Ed. 5, 667.

Nováček, R. (1935): *Věstnik Král, čes. spol. nauk II*, 1–36.

Peacock, M. A. (1935): *Zeits. Krist.*, **90,** 112–119.

Traill, R. J. (1951): Synthesis and *x*-ray study of uranium sulphate minerals, M.Sc. thesis, *Queen's University, Kingston.*

UNIT CELL AND SPACE GROUP DATA FOR CERTAIN VANADIUM MINERALS

W. H. Barnes and M. M. Qurashi,[1] *Division of Physics, National Research Council, Ottawa, Canada*

Abstract

The present status of x-ray diffraction data on vanadium minerals is reviewed briefly. Unit cell and space group data for metahewettite, metarossite, melanovanadite, descloizite, pyrobelonite, brackebuschite, and a new (unnamed) iron vanadate are presented. A brief reference to hewettite and some remarks on the structure of metahewettite are included.

Introduction

Although some twenty or thirty minerals containing vanadium as a primary constituent have been reported (for example, see Dana-Ford, 1947, Hey, 1950, or Mellor, 1947), relatively few of them have been satisfactorily characterized crystallographically. This is due primarily to the fact that many, particularly those containing the lighter metals, are so poorly formed that single crystals suitable for goniometric or x-ray investigation are excessively small, rare, or unobtainable, and even their powder diffraction lines often are weak and diffuse. Optical and x-ray studies of the generally better crystallized vanadates of the heavier metals also have been restricted due to the high absorption of both light and x-radiation in many species.

It is not surprising, therefore, that, in spite of the number of simple compounds of vanadium whose structures are known, or for which at least the unit cell constants and space groups have been determined (Lukesh, 1950), very few structural data are available for the vanadium minerals. These do include, however, a suggested structure for vanadinite, $Pb_5Cl(VO_4)_3$, (Hendricks, Jefferson & Mosley, 1931), and one for (synthetic) sulvanite, Cu_3VS_4, (Lundquist & Westgren, 1936). Unit cell data, not always including the space group, have been obtained for ardennite (a vanadio-silicate of Al and Mn, containing As) (Gossner & Strunz, 1932), pascoite, $2CaO \cdot 3V_2O_5 \cdot nH_2O$, (Berman, 1942), descloizite, $(Zn,Cu)PbVO_4(OH)$, (Bannister, 1933), pyrobelonite, $(Mn,Pb)_2VO_4(OH)$, (Strunz, 1939; Richmond, 1940), brackebuschite, $(Pb,Mn)_2VO_4(OH)$, (Berry & Graham, 1948), pucherite, $BiVO_4$, (de Jong & de Lange, 1936), hummerite, $Mg_2K_2V_{10}H_{32}O_{44}$, (Weeks, Cisney & Sherwood, 1951; Weeks, 1951), and montroseite, $2FeO \cdot V_2O_3 \cdot 7V_2O_4 \cdot 4H_2O$, (Weeks, Cisney & Sherwood, 1951; Weeks, 1951).

Identical powder photographs have been reported by Bannister (1933) for the zinc-copper-lead hydrous vanadates, descloizite, cuprodescloi-

[1] National Research Laboratories Postdoctorate Fellow. NRC 2727

zite, psittacinite, eusynchite, deschenite, and mottramite. That from chileite was slightly different but Bannister considers that the specimen probably was not pure. Strunz (1939) has confirmed these results, except in the case of chileite, which he did not examine. Bannister (1933) concludes that a complete isomorphous series exists between descloizite, $ZnPbVO_4(OH)$, and mottramite, $CuPbVO_4(OH)$, in which $Zn+Cu=4$ atoms per unit cell (with some degree of substitution by Fe and Mn), and he recommends that all names be dropped except "descloizite," $(Zn,Cu)PbVO_4(OH)$, for the Zn-rich members of the series and "mottramite," $(Cu,Zn)PbVO_4(OH)$, for the Cu-rich varieties. Strunz (1939) also has pointed out the structural correspondence of aræoxene, $ZnPb(V,As)O_4(OH)$, with descloizite. On the basis of single crystal rotation photographs, Strunz (1939) considers that pyrobelonite, $(Mn,Pb)_2VO_4(OH)$, is isostructural with descloizite, but, from powder photographs, he concludes that brackebuschite, $(Pb,Mn)_2VO_4(OH)$, is completely different. On the other hand, Richmond (1940), who also classifies pyrobelonite with descloizite on the basis of x-ray data, suggests, on chemical grounds, that pyrobelonite and brackebuschite form a series, with which Berry & Graham (1948) are not in agreement.

The status of the copper-calcium hydrous vanadates, calciovolborthite, volborthite, and their varieties (Mellor, 1947; Strunz, 1939) is very confused and their compositions are uncertain. On the basis of powder photographs, however, Strunz (1939) concludes that volborthite probably is identical with tangeite, which is structurally similar to the minerals of the descloizite group. "Tangeite," however, is synonymous with calciovolborthite and Hey (1950) lists it as a member of the descloizite group. He considers it improbable that volborthite should be similarly classified.

In addition to the obvious importance of the structural types, and the coordination number of vanadium, a number of other features of the vanadium minerals are of interest. For example, in the calcium vanadates, $xCaO \cdot yV_2O_5 \cdot nH_2O$, the ratio $x:y$, passes from 1:3 in hewettite and metahewettite (Hillebrand, Merwin & Wright, 1914), through 2:3 in pascoite (Hillebrand, Merwin & Wright, 1914), and 1:1 in rossite and metarossite (Foshag & Hess, 1927), to 2:1 in pintadoite (Hess & Schaller, 1914), with the value of n uncertain in most cases. The water content of hewettite and metahewettite is very sensitive to changes in atmospheric humidity but the two minerals are not interconvertible by this means. On the other hand, metarossite ($n=2$) appears to be a dehydration product of rossite ($n=4$) from which it is obtained on standing in air, while rossite crystallizes from aqueous solutions of either rossite or metarossite.

With fernandinite, $CaO \cdot 5V_2O_5 \cdot V_2O_4 \cdot 14H_2O$, (Schaller, 1915), and melanovanadite, $2CaO \cdot 3V_2O_5 \cdot 2V_2O_4 \cdot nH_2O$, (Lindgren, Hamilton & Palache, 1922), the calcium vanadates become more complex chemically with the appearance of vanadium in two valence states.

The replacement of calcium by copper commences in calciovolborthite and volborthite, lead occurs with copper in mottramite and substitution of zinc for the latter in an isomorphous series is ideally complete with descloizite. In place of copper and zinc, manganese is found with lead in pyrobelonite and in brackebuschite.

The descloizite group of vanadates is linked through the arsenious descloizite, araeoxene, to isomorphous arsenates such as conichalcite (higginsite), $CuCaAsO_4(OH)$, (Strunz, 1939; Richmond, 1940; Berry 1951), thus inviting direct *x*-ray structural investigation of the tacit assumption sometimes made that certain arsenates and vanadates are necessarily isomorphous and isostructural.

To complete this brief summary, mention must be made of the several interesting uranium vanadates and of a few vanadium minerals that contain cations other than those already mentioned, such as barium, iron, aluminium, and bismuth (for details, see Hey, 1950, Dana, 1947, or Mellor, 1947).

In spite of the unprepossessing nature of much of the available material, a systematic structural examination of vanadium minerals has been started in this laboratory. At present the uranium vanadates are not being included, nor are hummerite and montroseite, which are under study elsewhere (Weeks, 1951).

The present paper covers unit cell and space group data for metahewettite, metarossite, melanovanadite, descloizite, pyrobelonite, brackebuschite, and a new (unnamed) iron vanadate. A few notes on hewettite and a preliminary discussion of the structure of metahewettite are included. A preliminary structure for pucherite, $BiVO_4$, is described in a separate paper (Qurashi & Barnes, 1952).

Metahewettite and Hewettite

Hillebrand, Merwin & Wright (1914) describe metahewettite and hewettite as hydrous calcium vanadates with the same composition, $CaO \cdot 3V_2O_5 \cdot nH_2O$, in which n has a maximum value of 9 and a probable minimum of 3. The water content was found to be very sensitive to changes in atmospheric humidity, and significant differences in the behaviour of the two minerals were observed during progressive dehydration at room temperature and above 100° C. Metahewettite and hewettite apparently are not interconvertible by change in water content. In the absence of crystals suitable for goniometric measurement, Hille-

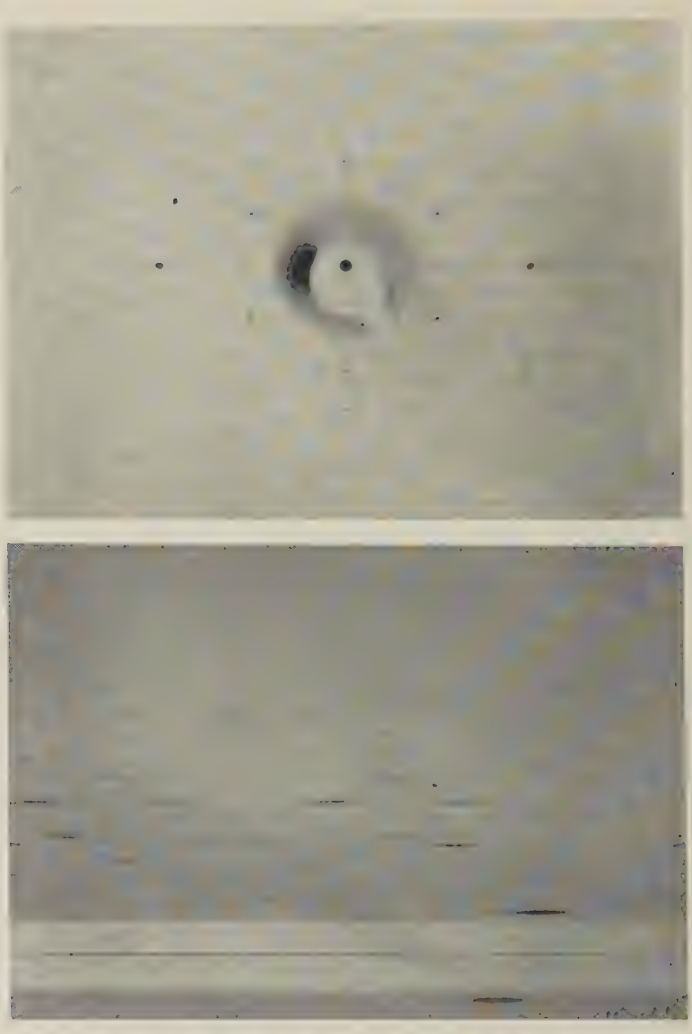

FIG. 1 (top). Metahewettite. Precession photograph of zero level (approximately normal to [101] axis) showing double set of reciprocal lattice points, $(hlk)^*$, $(hlk)^*$. (Mo, 36 hrs.)

FIG. 2. Metahewettite, zero level, *b* axis, Weissenberg photograph. (Cu, 50 hrs.)

brand, Merwin & Wright (1914) concluded from the general outlines and the observable optical properties that both minerals probably are orthorhombic.

The present *x*-ray investigation of metahewettite is based on material from the Cactus Mine, Yellow Cat District, Grand County, Utah (Harvard No. 98019). The metahewettite cleaves readily to yield lath-like crystals, and sheaves of crystals, of rectangular cross section. Ex.

tinction is parallel to the long axis and the faces of most laths are striated in the direction of this axis. The high negative birefringence, with X perpendicular to the large faces of the laths (Hillebrand, Merwin & Wright, 1914) suggests that the oxygen atoms in the structure probably lie in sheets parallel to these faces.

Preliminary precession photographs with the x-ray beam coincident with the long axis of the specimens showed short, diffuse arcs, indicating multiple crystals with a helical twist, or a range of orientation, about this axis.

One of the difficulties in handling metahewettite crystals is longitudinal cleavage into excessively thin specimens when any attempt is made to reduce the length of the laths. A crystal (approximately, $500\times40\times5\mu$) finally was obtained and mounted on the precession instrument with the long axis horizontal (*i.e.*, at right angles to the direction of the x-ray beam). Precession photographs gave a translation of 3.614A[1] along this (b) axis, with $a=12.18$ A and $c=7.80$ A, each at 90° to the b axis. The c^* axis was found to be perpendicular to the large faces of the laths, thus identifying these faces as {001}. The value of β^*, obtained as the difference between the precession instrument dial readings when the x-ray beam was normal to a^*b^* and when it was normal to c^*b^*, was approximately 90°, high accuracy being impossible due to the diffuse nature of the reflections and the insensitiveness of the a^*b^* and c^*b^* nets on the photographs to small changes in dial setting.

Assuming $\beta^*=90°$, however, the position of the [101]* axis was calculated and a zero level precession photograph was taken with [101]* vertical and b^* horizontal. This picture is reproduced in Fig. 1. Although some of the spots are very weak and are difficult to observe in the print, the original negative shows two distinct reciprocal lattice nets with a marked difference in the intensities of the spots defining the two nets. The vertical rows are common to both nets but the reciprocal lattice spacings in the vertical direction are not equal. They differ from that calculated for [101]*, on the assumption that $\beta^*=90°$, by about $\pm4\%$, which is more than ten times the probable error of measurement, whereas their mean is close to the calculated value. This suggested that the crystal was really monoclinic with $\beta^*\simeq90°$ and was twinned with c^*(or a^*) common to the two individuals. On this basis the two reciprocal lattice spacings were identified with [101]* and $[\bar{1}01]$*, respectively, and β^* was obtained from the relationship, $(t^*_{101})^2-(t_{\bar{1}01})^2=4a^*b^*\cos\beta^*$. From this, $\beta=95°15'$.

[1] All precession photographs of the minerals discussed in this paper were taken with Mo $K\alpha$ radiation ($\lambda=0.7107$ A), while Cu $K\alpha$ ($\lambda=1.5418$ A) was employed for the Weissenberg films.

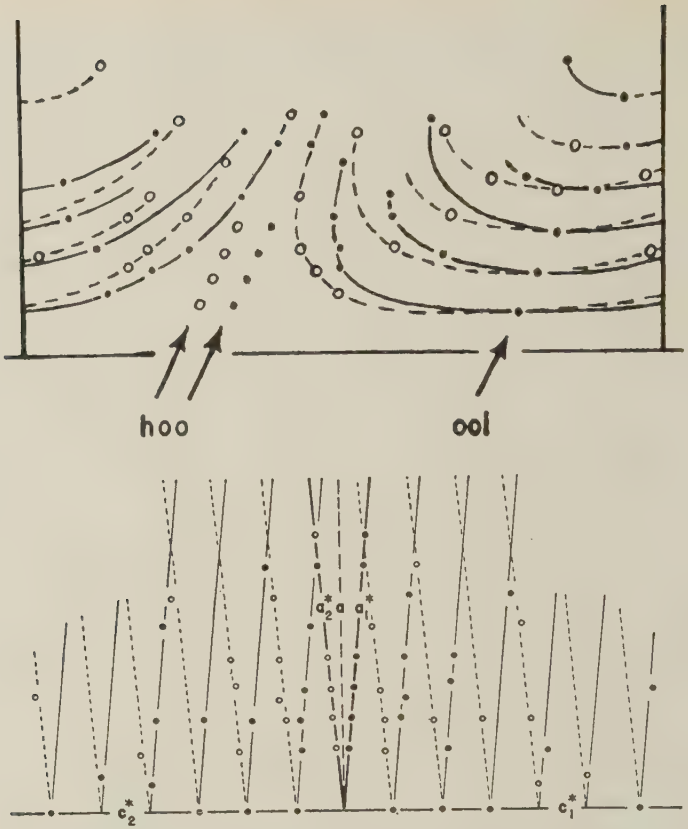

FIG. 3. Metahewettite; *a* (top), streaks of Fig. 2 reduced to spots; *b* (bottom) corresponding reciprocal lattice net with points of one twin shown as open circles and points of the other as closed circles.

The crystal was then transferred to the Weissenberg goniometer and a good rotation photograph about the *b* axis was obtained. The corresponding Weissenberg photographs, however, were comparatively poor, each diffraction spot being drawn out into a streak representing an angular distortion of the crystal of about $\pm 5°$. The upper half of the *b* axis, zero level, Weissenberg picture is reproduced in Fig. 2. Fig. 3a shows how the same photograph appears when the streaks are reduced to spots at their mid-points. The reciprocal lattice corresponding to these spots is plotted in Fig. 3b from the actual measurements of the Weissenberg film of Fig. 2. Both the twinning with a common *a* axis and the coincidence of the c^* axes are immediately apparent from these figures. The disentanglement of the streaky reflections due to one twin from

those due to the other in Fig. 2 was aided by the fact that the reflections from one twin are only about 75% as strong as those from the other. The unit cell constants obtained from the Weissenberg photograph agree to within 0.2% with those from the precession pictures.

Hillebrand, Merwin & Wright (1914) give the density of metahewettite as 2.942 when there are 3 moles of water per formula unit and 2.511 when there are 9 moles of water. Using the first value, the number of formula units per cell (Z) is $0.93 \simeq 1$, in agreement with 3 H_2O per formula unit. Although this does not determine the water content precisely, it does fix the maximum for the metahewettite crystal under investigation. The molecular volumes of $CaO \cdot 3V_2O_5 \cdot 9H_2O$ and $CaO \cdot 3V_2O_5 \cdot 3H_2O$, calculated from the foregoing values for the densities, are 505 A^3 and 370 A^3, respectively. The difference, 135 A^3, represents the increase in molecular volume due to the introduction of 6 H_2O, or about 23 A^3 per water molecule. Since this value has been obtained from experimental density data, it seems reasonable to take 25 A^3 as a rough estimate of the unit cell volume occupied by one molecule of water in these, and related, minerals, particularly when compared with the molecular volume of liquid water, which is approximately 30 A^3.

Comparison of the zero and upper level precession photographs indicates a screw axis (2_1) as the only space group criterion; otherwise the diffraction symmetry is $2/m$ with the diffraction symbol $2/m$ P-/-. However, since the formula unit, $CaO \cdot 3V_2O_5 \cdot 3H_2O$, contains only one Ca and there is only one formula unit per unit cell, the screw axis cannot be a real symmetry element because it would require the presence of at least two atoms of calcium in the unit cell. The extinction, ($0k0$) when k is odd, probably is due to some structural pseudosymmetry, although it should be noted that its recognition, even with a precession angle of 30°, depends on the absence of two reflections, (010) and (030), only, higher orders (with k odd) being beyond the range of the precession instrument even with molybdenum radiation. A statistical survey (Howells, Phillips & Rogers, 1950) of the reflection intensities indicates a centred ($h0l$) zone with possible pseudocentring of the unit cell as a whole. The probable space group of metahewettite, therefore, is $P2$.

These unit cell and space group data for metahewettite, with those for metarossite, are given in Table 1 for comparison with Ketelaar's results (Ketelaar, 1936) on vanadium pentoxide. If the original b and c axes of vanadium pentoxide are interchanged (as they are in Table 1) it will be observed that the unit cell dimensions of metahewettite and of vanadium pentoxide are strikingly similar except for the length of the c axis, which is almost twice as long in metahewettite.

The upper level, b axis, Weissenberg photographs of metahewettite

show the same twinning effect as does the zero level film. Hence b^* (and b), in addition to a, is common to both twins, and (001), therefore, is the composition plane.

An interesting feature of the intensities observed on the upper level Weissenberg films is that $S_{h,k+2,l} \simeq S_{hkl}$ (where $S_{hkl} = F_{hkl}/f_{hkl}$), while no simple relationship exists between $S_{h,k+1,l}$ and S_{hkl}. All atoms, therefore, must have $y \simeq 0$ or $\frac{1}{2}$, which would thus account for the apparent extinction of $(0k0)$ when k is odd. Patterson sections were made at $y=0$ and $y=\frac{1}{2}$ and some success in their interpretation was achieved by using the structure of V_2O_5 as a guide.

Harker-Kasper inequalities, as developed by Grison (1951), were next applied to the $h0l$ projection and refinement was effected by a special technique applied to the regions of negative electron density. By these means it was possible to identify all peaks in the projection. It is of interest to note that nineteen oxygen atoms can be recognized, in further agreement with three moles of water in the formula unit, $CaO \cdot 3V_2O_5 \cdot 3H_2O$.

At present the structure appears to be made up essentially of sheets of V_2O_5 chains, alternating in the z direction with layers, each composed of atoms of calcium (at $x=\frac{1}{2}$, $z=\frac{1}{2}$) and vanadium (at $x=0$, $z=\frac{1}{2}$) bonded together through their oxygen atoms and the water molecules. This arrangement is consistent with the optical properties and the cleavage, and is now being refined.

Hewettite is even more difficult to examine than is metahewettite. The material for the present study came from Minasragra, Cerro de Pasco, Peru (Harvard No. 96258). The crystals are microscopically small and, like metahewettite, often consist of multiple growths with the needle axes almost parallel, or they may have a helical twist about the long axis. Precession photographs with the x-ray beam normal to the long axis of one specimen (obtained by cleaving an obviously composite crystal) show that the length of this (b) axis in hewettite is identical (within 0.2%) with the length of the b axis in metahewettite. The largest, apparently single, crystal that was isolated, however, had linear dimensions of only about $100 \times 8 \times 3\mu$. With the x-ray beam again normal to the long axis, no reflections from this crystal could be observed on precession films even after exposures of 10 hours. However, a b axis, zero level, Weissenberg exposure of 70 hours did bring up a few weak, streaky reflections, which correspond with the most intense ones on the corresponding metahewettite film. It is probable, therefore, that hewettite, like metahewettite, is monoclinic with unit cell constants of the same order of magnitude as those of metahewettite.

Powder photographs of different portions of the Utah metahewettite,

taken with several different x-radiations over a period from March to July (*i.e.*, in both dry and damp laboratory atmospheres) show essentially identical d spacings and relative intensities. They can be indexed satisfactorily on the basis of the unit cell constants given in Table 1. Several powder photographs of different portions of the Peru hewettite obtained in August with copper and with cobalt radiation also are essentially identical but the positions and relative intensities of some of the lines show significant differences from the metahewettite pattern. Indexed to correspond with the latter, they indicate that the lengths of the a and c axes of hewettite may differ by 5% or 10% from the corresponding values for metahewettite.

One powder pattern of hewettite, however, which was obtained about five weeks earlier, is not identical with the others, nor does it represent simply a mixture of hewettite and metahewettite. It is possible, therefore, that the cell dimensions, if not the structure, of hewettite may be particularly sensitive to changes in atmospheric humidity.

Metarossite

Rossite and metarossite have been described by Foshag & Hess (1927), but none of their specimens were suitable for goniometric measurement. Both minerals, however, are soluble in water and good crystals of rossite, $CaO \cdot V_2O_5 \cdot 4H_2O$, were obtained by recrystallization. No pyramid faces were present on these crystals so that the axial ratios could not be determined but Foshag & Hess were able to establish that rossite is triclinic and they measured the axial angles and refractive indices. No optical measurements were possible on metarossite other than the lowest refractive index (α), the other two indices being too high. Foshag & Hess regard rossite and metarossite as distinct hydrates, $CaO \cdot V_2O_4 \cdot 4H_2O$ (rossite) and $CaO \cdot V_2O_5 \cdot 2H_2O$ (metarossite), and they consider that the change from one to the other is a discontinuous process. Rossite transforms gradually into metarossite, the stable form, even on standing under ordinary laboratory conditions. Rossite is obtained from aqueous solutions of either rossite or metarossite.

The specimen of metarossite (Harvard No. 90650) employed in the present investigation came from near Thompson's, Utah. It contains very small platy crystals, lamellar perpendicular to $(10\bar{1})$. Good precession photographs with reasonably sharp spots were obtained. The cell is triclinic and the unit cell constants are given in Table 1. The volume of the unit cell is 324 A^3.

Taking the density of rossite, $CaO \cdot V_2O_5 \cdot 4H_2O$, as 2.45 (Foshag & Hess, 1927), the molecular volume is 210 A^3. Assuming 25 A^3 as the volume of one molecule of water in the unit cell (see section on *Meta-*

hewettite and Hewettite), the volume of a rossite molecule with $2H_2O$ would be approximately $210-(2\times25)=160$ A^3. If there is similar packing in metarossite, $CaO\cdot V_2O_5\cdot 2H_2O$, this represents its molecular volume also, and the number of molecules per cell is equal to (vol. unit cell)/(mol. vol.) $=324/160=2.02$. Since the unit cell of metarossite is triclinic and there are two molecules per cell, the probable space group is $P\bar{1}$.

TABLE 1

	Vanadium Pentoxide*	Metahewettite	Metarossite
Cell contents	$2[V_2O_5]$	$CaO\cdot 3V_2O_5\cdot 3H_2O$	$2[CaO\cdot V_2O_5\cdot 2H_2O]$
System	orthorhombic	monoclinic	triclinic
a	11.48± .01 A	12.18± .02 A	6.21_5± .005 A
b	3.55± .005 A	3.61_4± .005 A	7.06_5± .005 A
c	4.36± .005 A	7.80±0.03 A	7.76_9± .005 A
α	90°	90°	92°58′±10′
β	90°	95°0′±20′	96°39′±10′
γ	90°	90°	105°47′±10′
S.G.	*Pmn*	*P*2 (probable)	$P\bar{1}$ (probable)

* Ketelaar, 1936, after interchange of a and c axes. A units presumably should be read kX.

A significant feature of the unit cell dimensions is that whereas the c axis is approximately the same in metarossite and in metahewettite, the a axis of metarossite is about one-half the length of the a axis of metahewettite and the length of the b axis of metarossite is almost twice the length of the corresponding axis in metahewettite. In metarossite, extinction is nearly parallel to the b axis; it is parallel to b in metahewettite. There is slight distortion about the b axis of metarossite as shown by short streaks ($\pm1°$) on the b axis Weissenberg films but it is not so extreme as in metahewettite (Fig. 2). A few weak spots appear on the very long exposure, b axis, Weissenberg films of metarossite, which indicate twinning with $(10\bar{1})$ as the composition plane, compared with (001) in metahewettite.

The most interesting feature of the observed intensities on the metarossite films is that the general (hkl) reflections with k odd are appreciably weaker than are those with k even, indicating considerable structural similarity with metahewettite.

MELANOVANADITE

Lindgren, Hamilton & Palache (1922) assign melanovanadite to the monoclinic system, but optical measurements were difficult due to very strong absorption and goniometric observations were hampered by

curved and striated faces. The original analysis of the material after it had been exposed to warm dry air for several months showed virtually no water content and gave a formula of $2CaO \cdot 3V_2O_5 \cdot 2V_2O_4$. Later, after prolonged exposure to a warm damp atmosphere, a total water content of 16.6% was found, of which 5.9% was retained above 105°C. These percentages correspond to 11 H_2O and 3.5 H_2O per formula unit, respectively.

The present x-ray study has been made on the type material from Minasragra, Peru.

Precession photographs show clearly that the cell is triclinic. The unit cell constants for the primitive cell are $a = 6.36_0 \pm .01$ A, $b = 16.86 \pm .02$ A, $c = 6.27_9 \pm .01$ A, $\alpha = 90°0' \pm 15'$, $\beta = 101°50' \pm 10'$, $\gamma = 93°10' \pm 15'$. The volume of this cell is approximately 658 A^3.

Individual crystals not only were too small for a density determination using the Berman balance but accurate measurements were impossible even by the flotation method. The latter, however, did indicate considerable water content compared with the specific gravity of 3.477 given by Lindgren, Hamilton & Palache (1922) for the original anhydrous material. From this value for the specific gravity the molecular volume of $2CaO \cdot 3V_2O_5 \cdot 2V_2O_4$ is 473 A^3. If the present crystals were assumed to be anhydrous, the number of molecules per unit cell (Z) would be 658/473 = 1.39. They must, therefore, contain some water. Hence, assuming one molecule per cell, the difference between the molecular (unit cell) volume actually observed and the molecular volume of anhydrous $2CaO \cdot 3V_2O_5 \cdot 2V_2O_4$ is 658 − 473 = 185 A^3. Again, as in the case of metarossite, if the volume occupied by one H_2O molecule in these minerals is approximately 25 A^3, the number of molecules of water per unit cell (and formula unit) of the melanovanadite specimen under investigation is $185/25 \simeq 7$. This is in the middle of the range, $2CaO \cdot 3V_2O_5 \cdot 2V_2O_4 \cdot 3.5$ to 11 H_2O, cal-

TABLE 2. MELANOVANADITE

	X-ray data (this paper)	Goniometric data (Lindgren, Hamilton, Palache, 1922)
System	triclinic	monoclinic
S.G.	$B1$	—
Z	2	—
a	$7.97_0 \pm .015$ A	—
b	$16.86 \pm .02$ A	—
c	$9.81_0 \pm .015$ A	—
$a:b:c$	0.4727:1:0.5819	0.4737:1:0.5815
α	87°55′ ± 10′	90°0′
β	90°45′ ± 10′	91°22′
γ	92°30′ ± 20′	90°0′

culated from the data of Lindgren, Hamilton & Palache (1922). There is thus one molecule per cell and the space group is probably $P1$.

It is convenient, however, both from the structural point of view and for direct comparison with the results of Lindgren, Hamilton & Palache (1922), to express the cell constants in terms of the centred cell, $B1$, as shown in Table 2.

The difference of approximately $\pm 2°$ in the interaxial angles between the x-ray and goniometric values is not surprising in view of the large dispersion of the ϕ and ρ data reported for the goniometric measurements.

The most interesting feature of the observed intensities is that reflections from $(hk0)$ are either absent or very weak when $h/2+k \neq 2n$, indicating a considerable degree of pseudosymmetry.

Brackebuschite, Pyrobelonite, Descloizite

The minerals of the adelite-descloizite group, $ABXO_4(Z)$, have been discussed in detail elsewhere (Bannister, 1933; Strunz, 1939; Richmond, 1940). There appears to be general agreement that descloizite, (Zn, Cu) $PbVO_4(OH)$, and pyrobelonite, $(Mn, Pb)_2VO_4(OH)$, are closely related, but, whereas Richmond (1940) considers that brackebuschite, $(Pb, Mn)_2VO_4(OH)$ in which $Pb:Mn \simeq 2:1$, forms a chemical series with pyrobelonite, $(Mn, Pb)_2VO_4(OH)$ in which $Mn:Pb \simeq 3:2$, Strunz (1939) concludes that brackebuschite is completely different in structure from the minerals of the descloizite group and Berry & Graham (1948) consider that it belongs to the chemical type $A_3(XO_4)_2 \cdot nH_2O$.

In preparation for structure determinations of the vanadates of the descloizite group, the unit cell constants and space groups of brackebuschite, pyrobelonite and descloizite have been redetermined.

Precession photographs of brackebuschite crystals, from the Sierra de Cordoba, Argentina (Harvard No. 96255), with the x-ray beam normal to the needle axis show clearly that the unit cell is monoclinic, with b coincident with the long axis of the crystals. Zero and upper level photographs with a and c as precession axes were obtained. The a^*c^* nets were photographed by mounting a smaller crystal with b as the precession axis. Measurement of a complete set of zero level films gave the unit cell dimensions, $a = 7.68_1$ A, $b = 6.15_5$ A, $c = 8.88_0$ A, with $\beta = 111° 50'$. Inspection of zero and upper level photographs shows a 2_1 axis along b but no other characteristic space group extinction. The space group, therefore, is either $P2_1/m$ (C_{2h}^2) or $P2_1$ (C_2^2). These results are in good agreement with those obtained by Berry & Graham (1948), $a = 8.92$ A, $b = 6.16$ A, $c = 7.69$ A, $\beta = 111° 47'$, after interchanging a and c.

For comparison with pyrobelonite and descloizite it is convenient, however, to choose a B centred cell for brackebuschite by taking the

[102] direction of the primitive cell as the c axis of the centred cell. The dimensions of the new cell are $a=7.68_1$ A, $b=6.15_5$ A, $c=2\times8.26_2$ A, with $\beta=86°15'$ and space group $B2_1/m$ (or $B2_1$).

Richmond (1940) gives the unit cell constants for pyrobelonite as orthorhombic, $a=7.84$, $b=9.45$, $c=6.09$ (no units, but they are probably kX), with space group $D_{2h}^{16}-Pnam$ (no reasons being given for eliminating $C_{2v}^{9}-Pna2$) and $Z=4$. For direct comparison with brackebuschite it is necessary to interchange Richmond's b and c axes, thus making the space group $Pnma$, or $Pn2a$, the former incidentally being the standard structure orientation for D_{2h}^{16}.

Strunz (1939), independently, finds pyrobelonite to be orthorhombic with $a=6.22$ A, $b=9.57$ A, $c=7.74$ A (although it is probable in this

TABLE 3

	S.G.	a	b	c	β
Brackebuschite (B. & Q.)	$B2_1/m$	7.68_1	6.15_5	$2\times8.26_2$	86°15′
Brackebuschite (B. & G.)	$B2_1/m$	7.69	6.16	2×8.30	86°20′
Pyrobelonite (B. & Q.)	$Pnma$	7.66_3	6.19_1	9.52_2	90°0′
Pyrobelonite (S.)	$Pnma$	7.74	6.22	9.57	90°0′
Pyrobelonite (R.)	$Pnma$	7.84	6.09	9.45	90°0′
Descloizite (B. & Q.)	$Pnma$	7.60_7	6.07_4	9.44_6	90°0′
Descloizite (B.)	$Pnma$	7.56	6.05	9.39	90°0′

case also that the units are kX). He does not mention its space group specifically but apparently assumes that it is the same as that of descloizite, D_{2h}^{16}, determined by Bannister (1933).

Bannister (1933) reports descloizite as orthorhombic with $a=6.05$ A, $b=9.39$ A, $c=7.56$ A (again, probably kX) and space group $V_h^{16}(D_{2h}^{16}-Pmcn)$ with $Z=4$. Richmond (1940) interchanged the a and c axes of Bannister, thereby obtaining the orientation $Pnam$, although it appears in his paper (Richmond, 1940, p. 451) as $Pnma$.

As with Richmond's orientation for pyrobelonite, it is desirable to reorientate the unit cells of Strunz for pyrobelonite and of Bannister for descloizite to $Pnma$. This simply involves changing their a, b, and c axes to b, c, and a, respectively.

Precession photographs of crystals of pyrobelonite from Långban, Sweden (Harvard No. 94831), and of descloizite from Los Lamentos, Chihuahua, Mexico (Harvard No. 91040) confirm the orthorhombic cells and the space group ($D_{2h}^{16}-Pnma$, or $C_{2v}^{9}-Pn2a$) found by Richmond and Bannister.

The unit cell data are collected in Table 3 where their sources are

identified as B. & Q. (this paper), B. & G. (Berry & Graham, 1948, after interchange of a and c and conversion to $B2_1/m$), S. (Strunz, 1939), R. (Richmond, 1940), B. (Bannister, 1933). It should also be noted that neither the space group $B2_1/m$ nor $Pnma$ has been determined uniquely; they may be $B2_1$ and $Pn2a$, respectively. Axial lengths are in A for B. & Q. data; apparently A for B. & G. data (wave-lengths not given), and probably kX in the others.

The variations in cell dimensions, even after conversion of (S.), (R.), and (B.) data to A, among the values for pyrobelonite and between those for descloizite are not unreasonable, in view of the somewhat variable composition of these minerals.

Very few crystals of brackebuschite were available for the present work and they were too small for an accurate determination of the density. Since the composition and unit cell dimensions, however, are so closely related to those of pyrobelonite and of descloizite it may be assumed that the number of formula units in the primitive cell is the same, namely, $Z=4$, which agrees with the result of Berry & Graham (1948) obtained from a measured specific gravity of 6.05. The B centred cell, therefore, must have $Z=8$.

Not only does the orientation of pyrobelonite and descloizite corresponding to $Pnma$, as in Table 3, emphasize the closeness of their axial lengths (particularly a and b) to the corresponding ones of brackebuschite, but direct comparison of corresponding precession axis reciprocal lattice levels brings out some important relationships.

Thus, the zero level a^*b^* nets of brackebuschite are almost identical (including relative intensities) with the zero level a^*b^* nets of pyrobelonite. The zero level b^*c^* nets of the two minerals are very much alike, but there is only a general similarity between the zero level a^*c^* nets. It is apparent, therefore, that, although the structures of brackebuschite and pyrobelonite cannot be identical, they must be related. The close correspondence of the x-ray diffraction effects is not nearly so apparent in powder photographs on which Strunz (1939) based his conclusions.

Corresponding zero and upper level reciprocal lattice nets along all three principal directions in pyrobelonite and descloizite are so nearly identical as to leave no doubt that the two minerals must have the same structure, at least insofar as the metal atoms are concerned. A general survey of intensities indicates that the coordinates of the heavy Pb atoms in both structures are approximately $\frac{1}{8}$, y, $\frac{1}{6}$; $\frac{7}{8}$, $\frac{1}{2}+y$, $\frac{5}{6}$; $\frac{3}{8}$, $\frac{1}{2}+y$, $\frac{2}{3}$; $\frac{5}{8}$, y, $\frac{1}{3}$. If the space group is $Pnma$ (and not $Pn2a$), then $y=\frac{1}{4}$.

Iron Vanadate

Thin platy hexagonal crystals of an iron vanadate (possibly, $FeO \cdot 2V_2O_4$) from Goldfields, Saskatchewan, have been studied with the pre-

cession instrument. The specimens were collected by Dr. S. C. Robinson, Geological Survey of Canada. The mineral has not yet been described in the literature nor has it been named.

The unit cell is hexagonal with $a = 5.85_4 \pm .005$ A, and $c = 9.29_5 \pm .010$ A normal to the plates. The diffraction symbol is $6/mmmC\text{-}/--c$ so that the space group is $C\bar{6}2c$ (D_{3h}^4), $C6mc$ (C_{6v}^4), or $C6/mmc$ (D_{6h}^4). A piezoelectric test was negative which means that none of these space groups can be eliminated on this basis.

The most interesting feature of the c axis, zero level, photographs is the appearance of an hexagonal "sub-cell" whose a axes coincide with orthohexagonal (b) axes of the true cell and have a length $\frac{1}{6}\ b$ (*i.e.*, $1/2\sqrt{3}\ a$). Furthermore, from the intensities of the general ($hk \cdot l$) reflections it appears that $S_{hk.l} \simeq S_{h+2,\ k+2,.,l}$ from which it can be shown that all, or most, of the atoms must be at the corners of the "sub-cell," which constitute twelve points in the true cell. Considering only the c glide (which is common to all three possible space groups) there are four sets of equivalent points as follows: (a) two-fold: $00z$; $00,\ \frac{1}{2}+z$, (b) two-fold: $\frac{1}{3}\ \frac{2}{3}\ z$; $\frac{2}{3}\ \frac{1}{3},\ \frac{1}{2}+z$, (c) six-fold: $0\ \frac{1}{2}\ z$; $0\ \frac{1}{2},\ \frac{1}{2}+z$; $\frac{1}{2}\ 0\ z$; $\frac{1}{2}\ 0,\ \frac{1}{2}+z$; $\frac{1}{2}\ \frac{1}{2}\ z$; $\frac{1}{2}\ \frac{1}{2},\ \frac{1}{2}+z$. (d) six-fold: $\frac{1}{3}\ \frac{1}{6}\ z$; $\frac{1}{6}\ \frac{1}{3},\ \frac{1}{2}+z$; $\bar{\frac{1}{6}}\ \frac{1}{6}\ z$; $\frac{1}{6}\ \bar{\frac{1}{6}},\ \frac{1}{2}+z$; $\bar{\frac{1}{6}}\ \frac{1}{3}\ z$; $\bar{\frac{1}{3}}\ \bar{\frac{1}{6}},\ \frac{1}{2}+z$.

The $h0 \cdot l$ projection offers the best hope of resolution of the atoms and is now under investigation.

Acknowledgments

Grateful acknowledgment is made to Professor Clifford Frondel for the specimens of metahewettite, hewettite, metarossite, melanovanadite, brackebuschite, pyrobelonite, and descloizite, and to Dr. S. C. Robinson for the specimen of the new iron vanadate.

References

Bannister, F. A. (1933): The identity of mottramite and psittacinite with cupriferous descloizite, *Min. Mag.*, **23,** 376–386.

Berman, H. (1942): private communication from Dr. C. Frondel.

Berry, L. G. & Graham, A. R. (1948): *X*-ray measurements on brackebuschite and hematolite, *Am. Mineral.*, **33,** 489–495.

Dana, E. S. (1947): *Textbook of Mineralogy*, ed. 4, revised by W. E. Ford, New York. The best general reference undoubtedly is Dana's *System of Mineralogy*, vol. 2, 1951, a copy of which, however, had not been received when this paper went to press.

de Jong, W. F. & de Lange, J. J. (1936): *X*-ray study of pucherite, *Am. Mineral.*, **21,** 809.

Foshag, W. F. & Hess, F. L. (1927): Rossite and metarossite; two new vanadates from Colorado, *Proc. U. S. Nat. Museum*, **72,** art. 11.

Gossner, B. & Strunz, H. (1932): Über strukturelle Beziehungen zwischen Phosphaten (Triphylin) und Silikaten (Olivin) und über die chemische Zusammensetzung von Ardennit, *Zeit. Krist.*, (A) **83,** 415–423.

Grison, E. (1951): De l'usage des inégalités de Harker-Kasper, *Acta Cryst.*, **4,** 489, 490.

Hendricks, S. B., Jefferson, M. E. & Mosley, V. M. (1931): The crystal structures of some natural and synthetic apatite-like substances, *Zeit. Krist.*, (A) **81,** 352–369.

Hess, F. L. & Schaller, W. T. (1914): Pintadoite and uvanite, two new vanadium minerals from Utah, *Jour. Wash. Acad. Sci.*, **4,** 576–579.

Hey, M. H. (1950): *Chemical index of minerals*, London.

Hillebrand, W. F., Merwin, H. E., & Wright, F. E. (1914): Hewettite, metahewettite and pascoite, hydrous calcium vanadates, *Proc. Am. Phil. Soc.*, **53,** 31–54.

Howells, E. R., Phillips, D. C. & Rogers, D. (1950): The probability distribution of x-ray intensities. II. Experimental investigation and the x-ray detection of centres of symmetry, *Acta Cryst.*, **3,** 210–214.

Ketelaar, J. A. A. (1936): Die Kristallstruktur des Vanadinpentoxyds, *Zeit. Krist.*, (A) **95,** 9–27.

Lindgren, W., Hamilton, L. F. & Palache, C. (1922): Melanovanadite, a new mineral from Mina Ragra, Pasco, Peru, *Am. Jour. Sci.*, Ser. 5, **3,** 195–203.

Lukesh, J. S. (1950): The crystal chemistry of the vanadium compounds, Schenectady. Private communication, manuscript. This useful compilation brings together data scattered through Wyckoff's *The Structure of Crystals* (vols. 1 & 2) and *Crystal Structures*, the *Strukturbericht* (vols. 1 to 7), and *Chemical Abstracts* (through 1948).

Lundquist, D. & Westgren, A. (1936): The crystal structure of Cu_3VS_4, *Svensk. Kem. Tidskr.*, **48,** 241–243.

Mellor, J. W. (1947): *A comprehensive treatise on inorganic and theoretical chemistry*, vol. 9, London.

Qurashi, M. M. & Barnes, W. H. (1952): A preliminary structure for pucherite, $BiVO_4$, *Am. Mineral.*, **37,** 423–426.

Richmond, W. E. (1940): Crystal chemistry of the phosphates, arsenates, and vanadates of the type $A_2XO_4(Z)$, *Am. Mineral.*, **25,** 441–479.

Schaller, W. T. (1915): Four new minerals, *Jour. Wash. Acad. Sci.*, **5,** 7.

Strunz, H. (1939): Mineralien der Descloizitgruppe, *Zeit. Krist.*, (A) **101,** 496–506.

Weeks, A. D., Cisney, E. A., & Sherwood, A. M. (1951): Hummerite and montroseite, two new vanadium minerals from Montrose County, Colorado, *Am. Mineral.*, **36,** 326, 327.

Weeks, Alice D. (1951): private communication.

A PRELIMINARY STRUCTURE FOR PUCHERITE, $BiVO_4$

M. M. Qurashi[1] and W. H. Barnes

Division of Physics, National Research Council, Ottawa, Canada.

Abstract

The unit cell of pucherite, $BiVO_4$, is orthorhombic with $a=5.33_2$ A, $b=5.06_0$ A, $c=12.02$ A and $Z=4$. The space group is *Pnca*. A preliminary structure is described with Bi and V at $\frac{1}{4}0z$; $\frac{3}{4}0\bar{z}$; $\frac{1}{4}, \frac{1}{2}, \frac{1}{2}+z$; $\frac{3}{4}, \frac{1}{2}, \frac{1}{2}-z$, ($z_{Bi}\simeq 0.108$; $z_V\simeq 0.39_2$). Eight O are in 000; $\frac{1}{2}00$; $0\frac{1}{2}\frac{1}{2}$; $\frac{1}{2}\frac{1}{2}\frac{1}{2}$ and $00\frac{1}{2}$; $\frac{1}{2}0\frac{1}{2}$; $0\frac{1}{2}0$; $\frac{1}{2}\frac{1}{2}0$. The remaining 8 O are in general positions with $x\simeq -\frac{1}{3}\frac{1}{6}$, $y\simeq\frac{1}{4}+\frac{1}{3}\frac{1}{0}$, $z\simeq\frac{1}{4}-\frac{1}{3}\frac{1}{6}$.

Introduction

Pucherite, $BiVO_4$, is better crystallized, and has been characterized more satisfactorily (Dana, 1947), than many of the vanadium minerals (Barnes & Qurashi, 1952). Single crystals, however, are very small and curved faces are common.

In a short note, de Jong and de Lange (1936) report axial lengths, from x-ray rotation photographs of material from Schneeberg, Saxony, as $a=5.38$ A, $b=5.04$ A, $c=11.98$ A, with an estimated accuracy of ± 0.03 A. The wave-length of the Fe radiation employed is not given but presumably A should be replaced by kX units. They assumed the cell to be orthorhombic in agreement with the morphological data, and calculated a value of 6.57 for the specific gravity if there are 4 formula units per cell. They point out that this differs appreciably from 6.25, the value given in the literature. Owing to lack of suitable material, de Jong and de Lange were unable to determine the specific gravity of their material, nor were they able to fix the space group.

Through the courtesy of Professor Clifford Frondel a specimen of pucherite, also from the type locality, Schneeberg, (Harvard No. 101703), was obtained for a structure determination as part of a general programme on the vanadium minerals.

Unit Cell and Space Group

Throughout this investigation, a Buerger precession instrument was employed with Mo $K\alpha$ radiation ($\lambda=0.7107$ A).

The unit cell was found to be orthorhombic, in agreement with the assumption of de Jong and de Lange (1936), with $a=5.33_2\pm .005$ A, $b=5.06_0\pm .005$ A, $c=12.02\pm .01$ A. The length of the a axis is about 1% smaller than that found by de Jong and de Lange but the lengths of the other two axes are almost the same. If the specific gravity is taken as 6.25 the number of formula units per cell (Z) is 3.77 which not only shows that there are 4 $BiVO_4$ per unit cell but also confirms doubts regarding the

[1] National Research Laboratories Postdoctorate Fellow.

NRC 2726

validity of the experimental value for the specific gravity. Single crystals were so small that an accurate redetermination of the specific gravity on suitable material was not possible even by the flotation method. The calculated density is 6.63 g/ml. It is possible, of course, that some degree of substitution of Bi or V by other atoms might account for the discrepancy between the calculated values and 6.25.

Comparison of upper level with zero level precession films reveals the presence of an n glide perpendicular to a, a c glide perpendicular to b, and an a glide perpendicular to c. The space group is thus uniquely established as $Pnca$ (D_{2h}^{14}), retaining the same orientation as that used by de Jong and de Lange (1936).

Preliminary Structure

With $Z=4$, there are 4 Bi, 4 V, and 16 O to locate in the unit cell.

In space group $Pnca$ there are three possible 4-fold positions and one general 8-fold position. The metal ions, therefore, must be in the 4-fold positions.

In addition to the characteristic space group extinctions, $(0kl)$ if $k+l$ odd, $(h0l)$ if l odd, $(hk0)$ if h odd, the general (hkl) reflections are very weak (only about 0.01 the intensity of the strong ones) when $(k+l)$ is odd. Thus most of the atoms, including the Bi and V, must be in the special 4-fold positions.

Intensities were estimated visually from multiple film exposures and a preliminary inspection suggested that the heaviest atoms, Bi, were in special positions (c), $\frac{1}{4}\ 0\ z$; $\frac{3}{4}\ 0\ \bar{z}$; $\frac{1}{4}, \frac{1}{2}, \frac{1}{2}+z$; $\frac{3}{4}, \frac{1}{2}, \frac{1}{2}-z$, with $z\simeq\frac{1}{8}$.

Patterson projections on $h0l$ and $0kl$ verified the Bi positions and gave $z=0.10_8$. The four V atoms were found to occupy the same type of positions but with $z\simeq 0.39_2$. Eight O atoms were located in special positions (a), 000; $\frac{1}{2}\ 00$; $0\ \frac{1}{2}\ \frac{1}{2}$; $\frac{1}{2}\ \frac{1}{2}\ \frac{1}{2}$, and (b) $00\ \frac{1}{2}$; $\frac{1}{2}\ 0\ \frac{1}{2}$; $0\ \frac{1}{2}\ 0$; $\frac{1}{2}\ \frac{1}{2}\ 0$. The remaining eight O atoms are in the general positions (d), x, y, z; $\frac{1}{2}+x, \frac{1}{2}-y, \frac{1}{2}-z$; $\bar{x}, \frac{1}{2}+y, \frac{1}{2}-z$; $\frac{1}{2}-x, \bar{y}, z$ (and these with changed signs), where $x\simeq-\frac{1}{30}$, $y\simeq\frac{1}{4}+\frac{1}{30}$, $z\simeq\frac{1}{4}-\frac{1}{30}$.

The preliminary structure so obtained is shown projected along the c and b axes in Fig. 1a. It gives very good agreement with the observed (hkl) intensities, the weak ones from planes with $k+l\neq 2n$ being due solely to the eight oxygen atoms in the set of general positions. Furthermore, the perfect {001} cleavage of pucherite is accounted for by the weak Van der Waals' bonds between oxygens across the planes at $z=\pm\frac{1}{4}$.

It is hoped to refine the structure by Fourier projections, and to obtain the oxygen parameters more accurately from an independent analysis of the intensities of the (hkl) reflections with $k+l\neq 2n$.

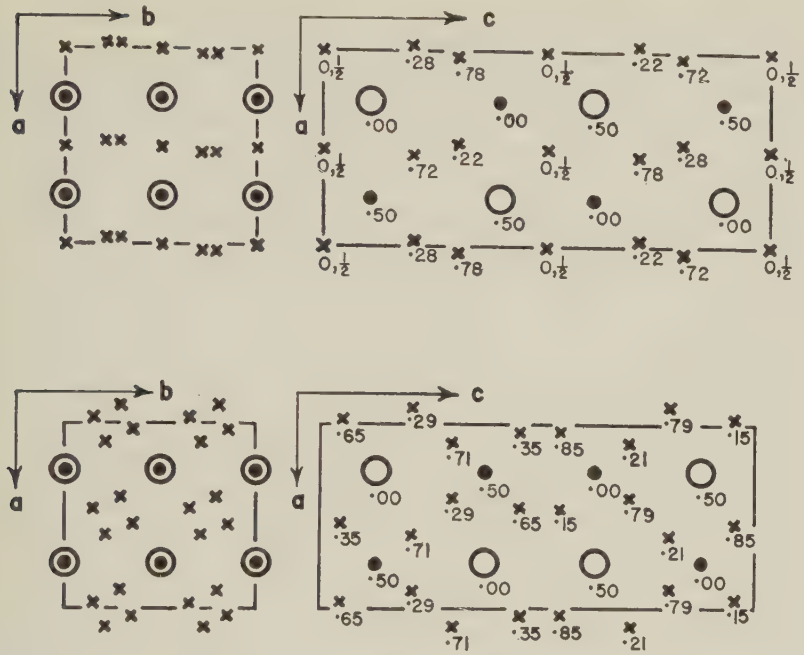

FIG. 1. *a* (top), Pucherite, $BiVO_4$; *b* (bottom), tetragonal $BiAsO_4$ (after Mooney, 1948). Large open circles, Bi; solid circles, V or As; crosses, O.

DISCUSSION

Although it is difficult to draw reliable conclusions about the oxygen coordination around the metal ions until the parameters of the oxygens in general positions are fixed more accurately, the preliminary structure indicates that both bismuth and vanadium are present in pucherite as tetravalent ions with the oxygen ions grouped somewhat closer around the smaller vanadium ions than they are around the larger bismuth ions.

The pucherite structure may be compared directly with that proposed by Mooney (1948) for tetragonal bismuth arsenate, $BiAsO_4$. This crystal has the scheelite structure, space group $C_{4h}^6-I4_1/a$, with $a=b=5.08$ A and $c=11.70$ A. The axial lengths, therefore, are very close to the corresponding ones of pucherite. The cell volume of the vanadate, however, is about 7% larger than that of the arsenate in spite of the smaller ionic radius of vanadium. This suggests a somewhat more open coordination in pucherite.

The bismuth arsenate cell is shown in Fig. 1b in the same projections as those of pucherite in Fig. 1a. For purposes of comparison the origin of Mooney's cell has been shifted to $\frac{1}{4}$, 0, $\frac{1}{8}$. There is some superficial simi-

larity between the two sets of projections, particularly in the positions of the metal ions, but examination of their y coordinates in Fig. 1 shows that they form a face-centred lattice in the vanadate as against the body-centred lattice in the arsenate. This is presumably connected with the different types of oxygen coordination in the two structures. It should be mentioned, however, that tetrahedral coordination of the AsO_4 groups was assumed in working out the structure of bismuth arsenate (Mooney, 1948); it was not derived from the intensity data.

References

Barnes, W. H. & Qurashi, M. M. (1952): Unit cell and space group data for some vanadium minerals, *Am. Mineral.*, **37**, 407–422.

Dana, E. S. (1947): *Textbook of Mineralogy*, ed. 4, revised by W. E. Ford, New York, p. 702. *System of Mineralogy*, vol. 2, 1951, data in personal communication from Dr. C. Frondel.

de Jong, W. F. & de Lange, J. J. (1936): *X*-ray study of pucherite, *Am. Mineral.*, **21**, 809.

Mooney, R. C. L. (1948): Crystal structure of tetragonal bismuth arsenate, $BiAsO_4$, *Acta Cryst.*, **1**, 163–165.

SOME FACTORS INFLUENCING FLUORESCENCE IN MINERALS

D. J. McDougall, *McGill University, Montreal, Canada.*

Abstract

In addition to composition and the exciting wave length, several other factors may have a bearing on the presence of absence of fluorescence in minerals.

A group of sixty-three minerals, of which about one third were fluorescent at room temperature were cooled with dry ice. This treatment served to intensify the fluorescence of many of the luminescent minerals and initiated fluorescence in an additional twenty specimens. The technique of estimating the percentages of minerals in rocks by their fluorescence can be expanded by the use of low temperatures, as is shown by the occurrence of fluorescence in the microcline of certain granites when chilled.

Fluorescence is quenched by heating the mineral, and may also be quenched in certain minerals by crushing. Water added to powdered minerals may either serve to activate fluorescence, or modify an existing fluorescence.

The packing index of ionic minerals is suggested to have some relationship to the presence or absence of fluorescence in minerals. Finally, a summary of the types of luminescence and empirical rules for the occurrence of luminescence are given.

A survey of recent mineralogical and petrological literature on the occurrence of fluorescence in minerals shows that the emphasis has been on the study of two controlling factors. These are the establishment of the exciting wave length, or range of wave lengths, by which the maximum emitted light is produced (Smith and Parsons, 1938), and the activating agent or impurity which is believed to be the cause of the fluorescence (Brown, 1934). However, temperature and agents other than those just noted can control the presence or absence of fluorescence, the intensity of the emitted light, and on occasions, even modify the colour. As early as 1859, Becquerel conducted experiments on several minerals involving temperature changes, and more recently, Pringsheim (1943) has noted the effect of changes in physical conditions in the study of artificial phosphors. Unfortunately, most of the recent studies of naturally occurring fluorescent minerals suggest that the writers have either ignored or have been unfamiliar with many of the techniques developed in the study of phosphors. Two exceptions may be cited, Haburlandt and Köhler (1934) who studied scapolite fluorescence using low temperatures, and Smith (1945) who notes briefly that temperature changes may have a noticeable effect on the fluorescence of minerals. It seems necessary, therefore, to re-emphasize that agents other than composition and wave length can be important in the production of luminescence in minerals. The effect of temperature change should be noted in particular, since under conditions of moderately wide natural temperature ranges, quite different results can be obtained from the same specimens. In addition, a knowledge of this effect may frequently be of use in the somewhat lim-

ited practical application of luminescence to mineralogical and petrological studies. Other physical changes which may have an effect on the luminescence of minerals are the reduction of the minerals to a powder and the wetting of powdered minerals with water or other liquids.

The writer has performed a series of experiments which illustrate the effect of temperature, powdering and wetting on a number of minerals. Most of the experiments duplicate work on artificial phosphors, but to the writer's knowledge there has been little or no reference to anything of a similar kind in any of the more recent mineralogical publications in English. Since the experiments were only intended to be exploratory, simple equipment and techniques were used. The exciting radiation was obtained from a Mineralight which supplies ultraviolet light in the vicinity of 2500 Å, with some shorter and longer wave lengths and some visible light. Solid CO_2 (dry ice) with a temperature of about $-50°$ C. provided low temperatures and a bunsen burner provided elevated temperatures. No attempt was made to record exact temperatures.

Effect of Temperature Change on Fluorescence

Change of temperature proved the most effective of the techniques employed. In general increasing the temperature of a mineral quenches temporarily any fluorescence which may be present, and reducing the temperature either temporarily increases the intensity of fluorescence if present, or, for a large number of the minerals used, actually initiates an appreciable brief luminescence. As might be expected, there were several exceptions to this general statement, ranging from a permanent quenching when the mineral altered to another form at high temperature, to the non-appearance of fluorescence in certain minerals at low temperature. Whether or not this failure to produce luminescence is a true exception remains somewhat doubtful, since there is a possibility that still lower temperatures might prove effective.

The general results are in accord with an observation by Kröger (1947) that in artificially prepared tungstates and molybdates, with a temperature range between $+200°$ C. and $-200°$ C., the various compounds show a fluorescent response which increases from zero to a maximum with falling temperature. Some of the compounds prepared by him show fluorescence in a range of about 50° above and below room temperature, but others may not develop the phenomena until the temperature is about $-100°$ C.

Table 1 lists in brief form observations of the effect of the reduction of temperature on the fluorescence of a group of sixty-three minerals. Some were selected because they showed fluorescence at room temperature, but most of the others were chosen in order to include a diverse group of the more common minerals.

TABLE 1

	Mineral	Description	Source	Room Temp.	Low Temp.
Strong Fluorescence at Room Temperature					
1	Calcite (4.0)	Opaque, white	Probably Franklin Furnace	Very bright pink fluor.	No appreciable change.
2	Scapolite (5.2)	Yellow-green	Ontario (?)	Bright yellow-orange fluor.	No appreciable change.
3	Scheelite (5.8)	Creamy-white	Source unknown	Bright bluish white fluor.	No appreciable change.
4	Willemite (4.7)	Light green	Franklin Furnace	Intense green fluor.	No appreciable change.
Moderate Fluorescence at Room Temperature					
5	Calcite (4.0)	Opaque, orange brown	Source unknown	Salmon-pink fluor.	No appreciable change.
6	Fluorite (6.2)	Purple, good penetration twins set in finely xline base	Alston Moor, Cumberland, Eng.	Blue fluor. over most of specimen, some pink fluor. partic. in base.	Blue probably intensified, pink more prevalent, partic. in dihedral angles between twins
7	Scapolite (5.2)	Yellowish-green	Source unknown	Patchy yellowish fluor.	Stronger and more widespread fluor.
Pale Fluorescence at Room Temperature					
8	Albite (4.9)	Greyish white	Lake Athabaska, Sask. (supplied by D. Blake)	Pale yellowish white over parts of xls.	Strong white over most of xls.
9	Anglesite	Dull grey	Eureka Hill, Tintic. Dist., Utah	Greyish yellow fluor.	Intense yellow fluor.
10	Calcite (4.0)	Transparent white	Source unknown	Pale pink fluor.	Slightly brighter fluor.
11	Calcite (4.0)	Grey with some xls. of cinnebar	California	Golden fluor in some parts of calcite, pale pink in others.	Golden fluor, intensified and pink more prevalent.
12	Diopside (5.9)	Dull brown with xls. of titanite	Lewis Co., N.Y.	Pink splotches	Intense pink fluor.
13	Gypsum (4.7 incl. H_2O)	Transparent, pale yellow	Source unknown	Pale green fluor.	May be slightly brighter green, pale green phosphorescence persists for about 1 sec. after U.V. source removed.
14	Sylvite (5.6)	Greyish white	Source unknown	Scattered pink spots	Pink brighter and more prevalent.
15	Wolframite	Vitreous black	Redruth, Cornwall	Patches of yellow fluor.	More extensive golden yellow patches.
Doubtful Fluorescence at Room Temperature					
16	Albite 4.9)	White, opalescent	Source unknown	Very doubtful pink	Bright pink fluor. spots
17	Cassiterite (6.0)	Brown (in quartz with sulphides)	Zinnwald, Bohemia	Faint yellow fluor. assoc. with fract. surfaces of xls.	Strong golden yellow over most of cassiterite xls.
18	Chrysotile (5.4)	Yellow green (fluffed fibres grey white)	Templeton, Ottawa Co., Que.	Doubtful yellowish green fluor. (none on fluffed fibres)	Slightly intensified yellow green fluor.
19	Labradorite (?)	Glassy white, opalescence	Source Unknown	Streaks of pinkish fluor.	Pale pink over entire mineral
20	Orthoclase (Adularia) (5.0)	Semitransparent, glassy white	Arendal, Norway	Very pale pink fluor.	Very strong pink fluor.
21	Perthite	Reddish brown with visible inter growth	Source unknown	Very pale pink fluor.	Very bright pink fluor.
22	Pyromorphite	Orange and yellow green	Source unknown	Doubtful orange fluor. on orange parts of specimen	Orange fluor. brighter
23	Scheelite (5.8)	Grey white	Source unknown	Doubtful bluish pink fluor.	Pronounced pink fluor.
No Fluorescence at Room Temperature					
24	Apatite (5.3)	Brown	Ontario	No fluor.	Pale orange fluor. in streaks parallel to c axis
25	Aragonite (4.3)	Light grey, xline	Herrengrund, Hungary	No fluor.	Doubtful bluish white fluor.
26	Barite (5.1)	Yellowish-white	Brookfield, Colchester Co., N.S.	No fluor.	Pale creamy white fluor.
27	Barite xl. in dolomite (5.1 & 4.3)	Transparent brown in yellow brown	Source unknown	No fluor.	Coppery red fluor. in dolomite around base of barite

TABLE 1 (*Continued*)

	Mineral	Description	Source	Room Temp.	Low Temp.
28	Beryl (5.1)	Brownish green xl.	Source unknown	No fluor.	Patches of yellowish fluor.
29	Carnotite	Light yellow	Montrose Co., Calif.	No fluor.	Doubtful grey-green fluor.
30	Chromite (5.9)	Greenish black	Selukwe S. Rhodesia	No fluor.	Very numerous tiny orange specks
31	Cleavelandite	Creamy white	Source unknown	No fluor.	Pale pink fluor.
32	Corundum (7.2)	Brownish xl.	Transvaal	No fluor.	Patchy pale yellow fluor.
33	Cryolite with galena & chalcopyrite (6.2)	Grey white	W. Greenland	No fluor.	Very pale pink fluor. patches
34	Crysotile in serpentine (5.4)	Yellowish-green in dark green	Thetford Mines, Megantic Co., Que.	No fluor.	Doubtful creamy fluor. in crysotile
35	Dolomite (4.3)	Brownish yellow	Pascalis Township, Que.	No fluor.	Flecks of pinkish fluor.
36	Gypsum (4.7 incl. H_2O)	White, semitranslucent	Source unknown	No fluor.	Streaks of orange yellow fluor. parallel to cleavage
37	Halite (5.8)	White, translucent cube	Source unknown	No fluor.	Doubtful bluish white fluor.
38	Lazulite (5.7)	Dark green	Graves Mt., Georgia	No fluor	Extremely doubtful pink fluor.
39	Oligoclase	White	Source unknown	No fluor.	Pale orange splotches
40	Orthoclase (5.0)	Creamy brown, carlsbad twin	Lewis Co., N.Y.	No fluor.	Patchy pink fluor.
41	Rock salt (5.8)	Brown, semi-translucent	Cheshire, Eng.	No fluor.	Scattered pink fluor. spots
42	Siderite (4.4)	Brown, xline	Source unknown	No fluor.	Scattered pale orange fluor. specks
43	Torbernite	Grey green	Cornwall, Eng.	No fluor.	Scattered greenis fluor. specks
	No fluorescence at Room Temperature or Low Temperature				
44	Aragonite (4.3)	Greyish brown, pseudo-hex. twin	Source unknown		
45	Azurite with malachite	Blue and green	Source unknown		
46	Brucite (6.7)	Pale brown, fibrous	Source unknown		
47	Chlorite (5.8)	Green, platy	Source unknown		
48	Chlorite schist with magnetite xls. (5.8 & 5.9)	Grey green	Quebec		
49	Diopside (5.9)	Greenish brown	Source unknown		
50	Fluorite (6.2)	Purple, translucent	Source unknown		
51	Garnet (6.1)	Black	Source unknown		
52	Graphite (1.7)	Black	Source unknown		
	Labradorite	Dark grey, labradorescence	Source unknown		
54	Magnetite (5.9)	Black xls.	Source unknown		
55	Manganite	Black	Source unknown		
56	Penninite	Dark green	Mill Green, Hertford Co., Maryland		
57	Quartz with free gold, pyrite tellurides (5.2)	White, opaque	Bevcourt Mine, Louvicourt Twp., Que		
58	Realgar	Reddish orange	Norris Basin, Yellowstone		
59	Rock salt (5.8)	Greyish white	Cheshire, England		
60	Sphalerite	Greyish black	Source unknown		
61	Stibnite	Metallic black	Japan		
62	Sulphur	Opaque yellow	Lakes Charles, Louisiana		
63	Tourmaline (6.0)	Black xls.	Pierpont, St. Lawrence Co., N.Y.		

Examination of this table shows that minerals which are strongly fluorescent at room temperature show no visible change when chilled. The moderately fluorescent specimens may show an intensified fluorescence on cooling, but the slightly fluorescent and doubtfully fluorescent minerals almost invariably exhibit an intensified fluorescence when their temperature is reduced. Among the specimens which show no luminescence at room temperature, about half are fluorescent to some degree when chilled. It will be noted that in several cases the fluorescence at room temperature was observed to be of a patchy or spotty nature, whereas at lower temperatures the patches were found either to increase in size, or the entire surface of the mineral became fluorescent. A similar feature was found upon chilling some of the normally non-fluorescent minerals, when a temporary fluorescence of a patchy nature developed.

Results of particular interest were obtained from specimens 6, 13, 17, and 27. Upon cooling specimen 6 (fluorite), a relationship became apparent between the fluorescence and the twinning, the pink fluorescence becoming intensified at the intersections of the crystals. Specimen 13 (gypsum), developed a short phosphorescence while below room temperature. The initial fluorescence of specimen 17 (cassiterite), showed some relationship to the fractured surfaces of the crystals, but at lowered temperature the emitted light came from the entire crystal surface. In specimen 27 (barite in dolomite), the only fluorescence noted occurred at low temperature, but it was concentrated in the dolomite around the base of the barite crystal.

Because of the possibility that initiation or augmentation of fluorescence in minerals might prove of value in estimating the percentage of minerals in rocks (Quinn, 1935), a few rock specimens of known mineral composition were cooled and examined under ultraviolet light. Most of the results were inconclusive because of the difficulty of identifying, in the hand specimen, the minerals which became luminescent. However, in a specimen of granite from Pascalis township, Quebec, consisting of quartz, oligoclase, microcline, microperthite, biotite and sphene, none of which were fluorescent at room temperature, it was observed that certain of the feldspars developed a bright pink fluorescence at reduced temperature. An uncovered thin section of this rock was prepared and the fluorescent mineral found to be microcline.

Use of a thin section in this fashion presents several problems which may make the results uncertain. Due to the opaqueness of glass to ultraviolet light a cover glass cannot be used, and, as the section is reduced in thickness to a point where the minerals can be identified, it becomes increasingly difficult to distinguish the fluorescent portions of the rock, which, in part, is due to the glass developing an orange fluorescence. If

the section is removed from the dry ice to permit close examination it warms so quickly that the fluorescence rapidly disappears. Further, the cooling caused the development of peculiar bubbles in the balsam which resemble the rune-like texture of graphic granite.

A group of hand specimens of granitic rocks from Baffin Island supplied by G. Riley were of particular interest, since they have a very pale pink fluorescence in certain of the feldspars at room temperature, but at low temperature the fluorescence has a definite pink colour,

TABLE 2

No.	*PART A* Increased Temp.	*PART B* Powdered Mineral at		*PART C* Powdered Mineral Wet with Water
		Room Temp.	Low Temp.	
1	Fluor. becomes paler and disappears, then returns quickly on cooling	Bright pink as in original mineral	Not tested	Not tested
2	Fluor. slowly becomes paler and disappears. Returns on cooling	Yellow-orange fluor. May be slightly paler than original mineral	Intense orange fluor.	Intense orange fluor.
4	Fluor. becomes paler but high temp. req'd to cause quenching. Returns rapidly upon cooling	Intense green fluor. as in original mineral	Similar to fluor. at room temp.	No appreciable change
5	Fluor. becomes paler and disappears. On cooling fluor. returns	Salmon pink as in original mineral	Not tested	Not tested
10	Fluor. quickly becomes paler and disappears. On cooling it returns slowly	Fluor. lost when mineral crushed	Doubtful white fluor.	Doubtful blue fluor.
13	Fluor. disappears very quickly and does not return on cooling	Larger grains retain green fluor. but most of powder is non-fluor.	Similar to effect at room temp.	Larger grains become brighter green, fine material very pale blue.
26	Non-fluor.	Non-fluor.	Doubtful white fluor.	Pale blue-white fluor.
35	Non-fluor.	Not tested	Not tested	Not tested
57	Non-fluor.	Non-fluor.	Non-fluor.	Distinct blue fluor.

similar to that of calcite from Franklin Furnace, N. J. One of these specimens is known to consist of 27% quartz, 6.5% adularia and anorthoclase, 32% microcline and microperthite, 27% albite, and a little mica, apatite and sphene. About 25% of the surface of the rock fluoresced and Mr. Riley tentatively identified the luminescent mineral as microcline.

The effect of the fluorescence due to increased temperature was tried on relatively few minerals, most of which were fluorescent at room temperature. The results are listed in Table 2, Part A, in which the figure in the left hand column refers to the minerals in Table 1. The general effect of increasing the temperature is a temporary loss of fluorescence in the minerals which are luminescent at room temperature, while the non-fluorescent minerals exhibit no change. No thermo-luminescent phenom-

ena were observed in the minerals tested. Specimen 6 (gypsum) which has been previously noted to develop phosphorescence at low temperature permanently lost its fluorescence when heated, presumably due to the loss of water.

Changes in Fluorescence Due to Crushing

A small group of minerals, some of which are fluorescent at room temperature, were powdered to observe the effect on their luminescing ability when in this condition, both at room temperature and low temperature. The crushing was not performed in a darkened room so that triboluminescence, if any, was not noted. At room temperature, some of the luminescent minerals showed no change when crushed but two lost their ability to emit light. A characteristic of the minerals which became non-fluorescent, which may be an important factor, is that both were transparent crystals in their original form. There was no change in the nonluminescent minerals. When the powdered minerals were cooled there was either no change from the conditions observed at higher temperature, or a very doubtful whitish fluorescence. The results are listed in Table II, Part B.

Changes in Fluorescence Due to Wetting Powders

It has been stated that some non-luminescent white powders, including crushed quartz, develop a bluish fluorescence when wet with water (Ewles, 1930). Some of the powdered minerals were treated in this fashion to duplicate this effect, if possible, and also to observe the effect on luminescent powders. The results were not uniformly good, but the non-fluorescent powders developed bluish fluorescence of varying intensities and one of the fluorescent powders changed colour to an appreciable degree. The results are listed in Table 2, Part C.

The "Packing Index" and Fluorescence

A further observation, the value of which can only be suggested at the present time, but which may be important in the examination of fluorescent minerals, is that the "packing index" (Fairbairn, 1943) appears to bear a relationship to the occurrence of fluorescence in minerals. The packing index applies only to minerals with an ionic type of bonding, but does not apply to such minerals as elements and sulphide minerals which may also show luminescent phenomena.

In Table 1, the bracketed figure beneath most of the mineral names is the packing index of that mineral. It will be noted that the fluorescent or occasionally fluorescent minerals usually have an index which lies somewhere close to 5.0, with some higher and some lower values. Most of the non-fluorescent minerals have either very high or very low values.

A frequency distribution curve of the indices given by Fairbairn has its mode at about 5.8, whereas a similar curve of the indices of minerals which have been reported to show fluorescence occasionally (DeMent, 1949), has its mode at about 4.7. This suggests that a mineral with an index close to 4.7 would be more likely to exhibit fluorescence than one with a higher or lower index. In some cases, lower indices would probably be increased by the addition of an activator, and in others equivalent changes might reduce higher values. Thus there is a possibility that the packing index may also provide an index for the occurrence of fluorescence in ionic minerals.

Causes of Luminescence

A general statement of the cause of luminescence in solid material is that an "excitant" raises the energy level of the material and the added energy is given off as visible light. These excitants include such parts of the electromagnetic spectrum as infra-red, visible, ultra-violet and x-ray radiations, as well as cathode and radium emanations, chemical reactions, heat, friction and many other factors. Commonly, long and short wave ultra-violet light is used in studying mineral fluorescence. An "activator," which is a small amount of chemical element or impurity which is foreign to the pure mineral is considered a necessary factor for a mineral to exhibit luminescence. In some cases it has been shown that if the per cent of activator is greater or less than a certain optimum range, luminescence cannot be produced (without change in temperature).

In more detail, the types of luminescent processes and empirical rules of the mode of occurrence of luminescence as found from the study of artificial phosphors are summarized below. As given they have been greatly condensed from their original form (Pringsheim, 1943).

(a) *Types of luminescent processes*

(i) Fluorescence—the spontaneous transfer of a molecule from an excited state and a high energy level to a lower energy level. The mean life is very short and practically independent of temperature.

(ii) Phosphorescence—a fraction of the excited molecules do not begin immediately to emit light by returning from the excited state, but pass instead to a metastable state from which they return to the excited state and emit light only when a quantity of energy ϵ is added by the heat movement of the surrounding medium. Thermoluminescence is a variety of phosphorescence where the value of ϵ is very high and the luminescence can only be released at elevated temperatures.

(iii) Recombination afterglow—the electrons are completely removed from the original molecules by the absorption of light. Light emission occurs when the electrons recombine with one of the excited molecules.

The luminescence of (i) and (ii) decays according to an exponential law, whereas (iii) decays according to a hyperbolic law. The exponential type is independent of the initial intensity, but the steepness of the curve increases with increasing temperature. The hyperbolic type is little affected by the temperature, but a high initial intensity produces a steep curve.

(b) *Rules*

(i) Practically no pure elements and very few simple compounds are luminescent.

(ii) Most substances with a strong luminescence are white or only slightly coloured.

(iii) Most substances become luminescent or their luminescence is strongly increased when they are cooled down to liquid air temperature. Heating to a certain upper limit which usually lies between 100° C. and 400° C. destroys the fluorescence in almost every case.

(iv) Liquid solutions are seldom phosphorescent.

(v) In the solid state many compounds show an afterglow. However, phosphorescence persisting over many hours, and "frozen in" at low temperatures is almost exclusively a property of "crystal phosphors" activated with small traces of an impurity.

(vi) The light-emissive capacity of many materials which are luminescent under normal conditions is diminished or totally suppressed by the presence of some other substance (poisons).

(vii) The question of the importance of grinding and particle size is somewhat uncertain, but it does not seem to be advisable to grind sulphide phosphors to particle sizes less than 0.1 mm, and silicate phosphors are supposed to increase in intensity with particle diameters down to 0.001 mm.

(viii) The number of impurity molecules able to activate phosphors is very large. One condition seems to be that the ionic (or atomic?) radius of the activator must be smaller than the radius of the cation of the basic lattice.

(ix) Activating impurities do not occupy analogous positions in the lattice of all phosphors. In some cases the activator ions are interstitial in the lattice and in others mix crystals are formed. In the second case there is a modification in the size of the crystal lattice and the luminescence may be dependent either on the formation of the mix crystal or the introduction of activators into the modified lattice.

Conclusions

Luminescence resulting from excitation with short ultra-violet light can be initiated or intensified in many minerals when they are cooled

with dry ice. This is in agreement with observations made on artificial phosphors and is directly attributable to the reduction of the activity of the molecules as a result of the reduced temperature. It seems probable that a content of "activator" which is less than the optimum required for fluorescence at room temperature serves to produce luminescence at lower temperatures. Patchy fluorescence is probably caused by widely scattered activator centres. Raising the temperature has an opposite effect and fluorescence is temporarily quenched unless the mineral is altered by the high temperature, in which case the luminescence may be permanently destroyed. Most of the results obtained from a varied group of specimens can be explained in this manner but a few appear to be more complex and additional factors probably have some bearing on the distribution of the fluorescence.

Temporary low temperature luminescence may occasionally prove valuable for the recognition of some minerals in rocks, particularly where megascopic identification is difficult or impossible.

Some minerals when crushed have their luminescence greatly diminished or destroyed. The reason for this is uncertain, but it may be related to the optical properties of the mineral. Wetting of crushed luminescent minerals may change the fluorescent colour, or, in the case of non-fluorescent powders, may produce a distinct blue luminescence.

It is suggested that the packing of ions within the crystal lattice may bear some relationship to the occurrence of luminescence in minerals with an ionic type of bonding.

A fairly complete summary of the types of luminescence and empirical rules for the occurrence of luminescence has been included in the discussion. The summary refers particularly to artificial phosphors and chemical solutions, but in large measure can be applied to minerals as well. No similar modern summary has been found in the easily available mineralogical or petrological literature, and it is believed that it may be of value, particularly as an introduction to the examination of fluorescence in minerals.

Acknowledgments

Members of the Geology Department, McGill University, particularly Professors John S. Stevenson and J. E. Riddell, showed much co-operation and interest by giving permission to use equipment and mineral specimens from the Departmental collections and offering many helpful suggestions. The constructive criticism of several of the graduate students and the free use of specimens on which they had done microscopic work is also gratefully acknowledged.

References

Becquerel, E. (1859): *Ann. Chem. Phy.*, **55,** 98–101.

Brown, W. L. (1934): Fluorescence of manganiferous calcites, *Univ. Toronto Studies,* Geol. Ser. **36,** 45–54.

DeMent, J. (1949): *Handbook of Fluorescent Gems and Minerals,* Mineralogist Publishing Co.

Ewles, J. (1930): Water as an activator of luminescence, *Nature,* **125,** 706–707.

Fairbairn, H. W. (1943): Packing in ionic minerals, *Bull. Geol. Soc. America,* **54,** 1305–1374.

Haburlandt, H. & Köhler, A. (1934): Fluoreszanalyse von Skapolithes, *Chemie der Erde,* **34,** 139–144.

Kröger, F. A. (1947): Fluorescence of tungstates and molybdates, *Nature,* **159,** 674.

Pringsheim, P. (1943): *Luminescence of Liquids and Solids.* Interscience Publications.

Quinn, Alonzo (1935): A petrographic use of fluorescence. *Amer. Min.*, **20,** 466–468.

Smith, E. S. C. & Parsons, W. H. (1938): Studies in mineral fluorescence. *Am. Min.*, **23,** 513–521.

Smith, F. G. (1945): Fluorescence as related to minerals. *Univ. Toronto Studies,* Geol. Ser. **49,** 41–54.

ROBINSONITE, A NEW LEAD ANTIMONY SULPHIDE*

L. G. Berry, *Queen's University, Kingston, Ontario*
Joseph J. Fahey, *U. S. Geological Survey, Washington, D.C.*
Edgar H. Bailey, *U. S. Geological Survey, San Francisco, Calif.*

Abstract

Crystals of robinsonite are triclinic, with probable space group $P\bar{1}$; $a=16.51$, $b=17.62$, $c=3.97$A, $\alpha=96°04'$, $\beta=96°22'$, $\gamma=91°12'$. Slender prismatic [001], striated [001]; also massive, fibrous to compact. Cleavage was not observed; fracture is irregular; brittle, H 2.5–3. Measured specific gravity: 5.27 (artificial crystals), 5.20, 5.25 (natural fragments), 5.34 (artificial fused material), and 5.28 (indirect determination on natural material). Composition and cell content is $7PbS \cdot 6Sb_2S_3$ with calculated specific gravity 5.40. Strongest x-ray powder lines: 4.08A(6), 3.97(6), 3.41(10), 3.19(6), 3.04(6), 2.74(5), 2.68(5).

Robinsonite occurs as a primary mineral with pyrite, sphalerite, stibnite, and boulangerite in small pieces in oxidized ore bodies at the Red Bird mercury mine, Pershing County, Nevada.

Introduction

In 1943 while investigating quicksilver deposits in Nevada, one of the authors (E.H.B.) collected a sample at the Red Bird mine in Pershing County, Nevada, that he suspected of being zinkenite or jamesonite. He sent it, with several other samples, to Washington for identification. An x-ray powder picture taken by Joseph M. Axelrod of the U. S. Geological Survey Laboratories in Washington did not match any pictures found in the literature. This was subsequently confirmed by Martin A. Peacock of the University of Toronto.

Owing to the pressure of other work, nothing more was done on the problem until 1946, when the powder pattern obtained by Professor Peacock was found to be identical with one of several unidentified patterns obtained by Dr. S. C. Robinson[1] at Queen's University during his investigation of the synthesis of lead antimony sulphides (Robinson 1947, 1948a,b). A small specimen was sent to Queen's University for x-ray study; later some of the same material was analyzed in the U. S. Geological Survey (J. J. F.) and proved to be a mixture of boulangerite and the unknown sulphosalt referred to Robinson as "mineral X" with composition close to $7PbS \cdot 6Sb_2S_3$. In 1950, additional artificial material was prepared at Queen's University.

The name robinsonite is given to this new mineral in honor of Dr. Robinson, whose synthesis made its identification possible.

Occurrence (E. H. B.)

The Red Bird mine, where the robinsonite was found, is one of the less

* Publication authorized by the Director, U. S. Geological Survey.

[1] Now Mineralogist, Radioactivity Laboratory, Geological Survey of Canada, Ottawa.

productive of several quicksilver mines in Pershing County, Nevada. It is in sec. 33, T. 27 N., R. 34 E., on the south slope of Buffalo Mountain at an elevation of about 5,500 feet, and can best be reached by travel over 23 miles of gravel road extending eastward from Lovelock, Nevada. The geology of the mine is described in a report of the strategic minerals program of the U. S. Geological Survey (Bailey & Phoenix, 1944).

The geology of a large region about the Red Bird mine is not well known, although the local geology has been mapped and studied in detail. The rocks consist of a thick sequence of Upper Triassic and Lower Jurassic sediments, which includes limestone, dolomitic conglomerate, sandstone, and shale, and locally these are intruded by small diabasic dikes believed to be late Jurassic in age. The quicksilver ore bodies in the district occur only in the limestone and dolomite beds, generally along faults of small displacement or beneath shale, and they contain cinnabar as the principal ore mineral.

Much of the ore of the Red Bird mine consists of pulverulent cinnabar closely associated with bindheimite, limonite, goethite, cerussite, hemimorphite, and various oxides of antimony. The primary ore is found in the oxidized ore bodies only in small pieces. It consists of pyrite, sphalerite, stibnite, boulangerite, and the new mineral robinsonite. The gangue minerals identified are quartz, calcite, and tarnowitzite, a plumbian aragonite.

The analyzed sample was obtained from a specimen of approximately oval shape, with major and minor axes about 9 and 5 cm respectively and weighing about 650 g. A slab about 1 cm thick was cut through the center and parallel to the longer axis. The core of the slab, which is composed of boulangerite and robinsonite, is lead gray speckled by small inclusions of quartz, usually rimmed by tiny crystals of pyrite. A few small areas of bindheimite are also seen within the boulangerite-robinsonite mass. This mass is completely rimmed by about a centimeter of the alteration product bindheimite. Small inclusions of minium, the red oxide of lead, are found in the bindheimite.

Synthetic Material (L. G. B.)

Robinson (1948a,b) obtained material, referred to as "mineral X" and giving an x-ray powder pattern identical with that of the mineral described here, by pyrosynthesis from the elements, by hydrosynthesis from alkaline solutions, and by heat treatment (below the melting point) of hydrosynthetic crystals of fuloppite and zinkenite. The material is described as follows:

"The artificial crystals are acicular to bladed, longitudinally striated, and without visible end faces. They are terminated by irregular fracture, and there is no evidence of cleav-

age. In polished section . . . strongly anisotropic, the polarization colors are bluish gray, creamy white and brownish gray; the standard etch reactions are the same as those given by Short (1940) for boulangerite. Distinction is possible with practise by the use of 1:1 KOH solution which etches mineral X in four minutes, boulangerite in ten minutes.

"The molal ratios obtained by means of the Cambridge polarograph for mineral X are Pb:Sb=3.3:6.5 and 4.2:7.9; both are near the proportions in $PbS \cdot Sb_2S_3$ as in zinkenite, and not far from $7PbS \cdot 6Sb_2S_3$."

In 1950 new fusions of Pb, Sb, and S in the proportions of $7PbS \cdot 6Sb_2S_3$ were made at Queen's in evacuated silica-glass tubes. The resulting crystalline buttons appeared homogeneous in polished section and revealed only the x-ray powder pattern of robinsonite. In these fusions the vitreosil tubes of 7-mm bore were kept as short as possible and the whole tube heated in a furnace to prevent condensation of volatiles at the colder end of the tube. This new artificial material has now been analyzed (Table 5).

Physical Properties (J. J. F.)

The specific gravity of the new mineral was necessarily determined by an indirect procedure, because robinsonite is in intimate association with boulangerite, as shown in Fig. 1, and with other materials (quartz, pyrite) that are insoluble in HCl. Using a fused-silica Adams-Johnston

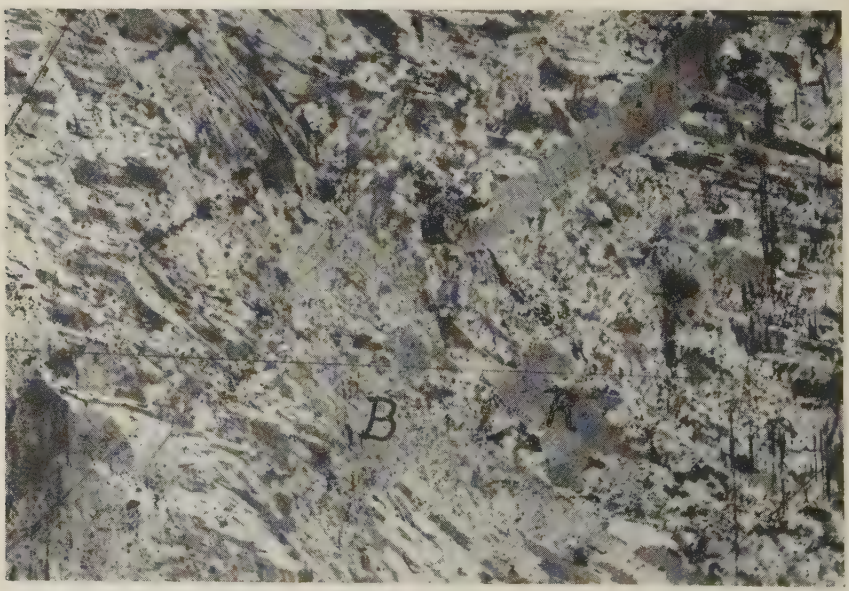

Fig. 1. Photomicrograph of polished section of robinsonite and boulangerite etched with 40% KOH solution applied for 4 minutes. Magnification 100×. The robinsonite (dark) marked "R" on the photograph, is etched; the boulangerite (light), marked "B," is not etched under these conditions. The small black areas are pits in the section.

pycometer of 5-ml capacity, the specific gravity of the sample was determined and found to be 4.790. The "Insol in HCl" portion (19.14% of the sample) was then obtained and its specific gravity (2.762) measured in the same manner. The specific gravity of boulangerite, 6.2, was taken from the literature. From these figures and from the percentages of the three constituents—robinsonite, boulangerite, and insoluble—the specific gravity of robinsonite was computed to be 5.28 at 4° C.

Robinson (1947, 1948b) measured several small samples of the artificial crystals on a Berman balance and found the specific gravity to be 5.27. A similar determination on a fragment from a natural specimen, which did not show boulangerite in polished section or by x-ray, yielded the value 5.20 (Robinson, 1947).

The new artificial material analyzed here (Table 5) gives a specific gravity of 5.34, which is in good agreement with the values given above. The hardness, 2.5–3, the bluish lead-gray color, and the metallic luster are the same as those of boulangerite.

X-ray Measurements (L. G. B.)

Robinson (1948b) described the artificial crystals of "mineral X" [=robinsonite] as "acicular to bladed, longitudinally striated, and without visible end faces. They are terminated by irregular fracture, and there is no evidence of cleavage." From Weissenberg photographs about the axis of elongation, Robinson obtained dimensions for a triclinic unit cell. Previous experience with triclinic crystals has indicated that the

Table 1. Lattice Dimensions of Robinsonite[1]

	Rotation and Weissenberg (Robinson, 1948b)	Precession camera	
		Measurements	Calc. values
$d(100)$	—	16.40 A	
$d(010)$	—	17.52	
$d(001)$	—	3.92	
α^*	84°25′	83°46′	
β^*	83°11′	83°28′	
γ^*	87°52′	88°07′	
a	16.5 A	16.3 A	16.51 A
b	17.7	17.7	17.62
c	3.99	3.97	3.97
α	95°22′	96°17′	96°04′
β	96°39′	96°40′	96°22′
γ	92°06′	—	91°12′

[1] Using CuKα, 1.5418 A and mass factor, 1.6602.

values of α and β are subject to some error when obtained from films about one axis (c) only. Therefore the cell dimensions of Robinson's original crystal were redetermined with the precession camera.

The crystal was first adjusted with the needle axis, c, as the precessing axis. The zero and first-level films yielded values for $d(100)$, $d(010)$ and γ^*, and using the orientation of the pattern on the film, the crystal was readjusted with (100) normal to the spindle of the camera. Several trial cone-axis films were used to locate the b axis as precessing axis and the angle between this axis and the needle axis, read on the drum of the precession camera, is a rough value for α. The zero-level film about b yielded values for $d(100)$, $d(001)$ and β^*. The a axis was located and used as the precessing axis in a similar way, yielding values for $d(010)$, $d(001)$ and α^*. The measurements from the precession films are given in Table 1 together with the values obtained by Robinson (1948b) from the rotation and Weissenberg films about c. The measured spacings and starred angles were obtained directly from zero-level precession films about each axis. These measurements yielded the final calculated values in the last column. The measured values of a, b, and c that were obtained from cone-axis films (in column 2) are not very accurate. The measured values of α and β were read on the drum of the camera and represent the angle through which the crystal was turned from c-axis precession position to the b- and a-axis position respectively.

The natural material, unfortunately, is quite unsuitable for single-crystal study. However, several x-ray powder photographs show patterns that are identical with patterns of the artificial material. One natural crystal fragment yielded a rotation pattern with rather poor diffraction spots that is identical with the rotation pattern from artificial crystals. The crystal was too poor to yield Weissenberg pictures.

The x-ray powder pattern for robinsonite is given by Robinson (1948b). In Table 2 the intensities, measured θ°, and d values are listed for the natural material measured on the original film taken by Professor Peacock at the University of Toronto in 1944 and for the artificial crystals averaged from two visibly identical films taken by Robinson in 1947. The measured spacings agree with one or more calculated spacings down to a spacing of 3.0, and the intensity I (W) of the diffractions for each set of planes observed on Weissenberg and precession camera films is given in the last column. The film of the natural material is very heavily exposed and the films of the artificial crystals are rather lightly exposed; this difference in exposure would probably account for slight differences in intensities. The close similarity clearly establishes the identity of the natural and artificial materials.

TABLE 2. ROBINSONITE—$7PbS \cdot 6Sb_2S_3$: *X*-RAY POWDER PATTERN
Triclinic $P\bar{1}$; $a=16.51$, $b=17.62$, $c=3.97$ A, $\alpha=96°04'$, $\beta=96°22'$, $\gamma=91°12'$, $Z=1$

Red Bird mine, Nevada			Artificial crystals			Artificial single crystal		
I	θ(Cu)	*d*(meas.)	*I*	θ(Cu)	*d*(meas.)	(*hkl*)	*d*(calc.)	*I*(W)
¼	6.0°	7.4 A	¼	6.0	7.4 A	$(2\bar{1}0)$	7.522	w
						(210)	7.333	w
½	7.4	6.0	½	7.3	6.1	$(22\bar{0})$	6.082	m
						(220)	5.885	w
½	8.15	5.44	½	8.15	5.44	(300)	5.469	w
						(130)	5.443	w
—	—	—	½	8.6	5.16	(310)	5.156	w
½	10.2	4.35	1	10.1	4.40	(040)	4.378	w
8	11.0	4.04	7	10.9	4.08	(400)	4.100	w
						$(3\bar{3}0)$	4.055	s
8	11.35	3.92	7	11.2	3.97	$(41\bar{0})$	3.963	s
						$(33\bar{0})$	3.923	m
						$(12\bar{0})$	3.916	m
6	11.75	3.79	5	11.7	3.80	$(24\bar{0})$	3.810	s
6	12.15	3.66	6	12.1	3.68	$(\bar{2}01)$	3.706	w
						$(\bar{2}11)$	3.692	s
						(420)	3.666	s
						(050)	3.502	s
5	12.85	3.47	3	12.75	3.49	$(3\bar{4}0)$	3.474	w
						$(15\bar{0})$	3.449	m
						$(4\bar{3}0)$	3.408	s
						$(15\bar{0})$	3.402	m
10	13.15	3.39	10	13.05	3.41	$(2\bar{1}1)$	3.398	m
						(201)	3.391	s
						$(\bar{3}01)$	3.374	s
						$(\bar{1}31)$	3.307	w
						(121)	3.295	m
—	—	—	½	13.6	3.28	$(\bar{2}11)$	3.264	m
						$(2\bar{3}1)$	3.261	m
						(250)	3.260	w
6	14.05	3.18	6	14.0	3.19	$(5\bar{1}0)$	3.205	s
						$(25\bar{0})$	3.183	s
						$(\bar{2}21)$	3.054	s
						$(44\bar{0})$	3.041	s
8	14.75	3.03	6	14.7	3.04	$(5\bar{2}0)$	3.039	s
						$(30\bar{1})$	3.028	m
						$(3\bar{3}1)$	3.018	s

Red Bird mine			Artificial			Red Bird mine			Artificial		
I	θ(Cu)	*d*(meas.)	*I*	θ(Cu)	*d*(meas.)	*I*	θ(Cu)	*d*(meas.)	*I*	θ(Cu)	*d*(meas.)
—	—	—	1	15.1°	2.96 A	3	23.05°	1.969 A	½	23.0°	1.973 A
2	15.55	2.88 A	1	15.45	2.89	6	24.45	1.862	2	24.45	1.862
2	15.95	2.81	½	15.85	2.82	4	25.55	1.787	2	25.5	1.791
8	16.25	2.75	8	16.35	2.74	2	26.7	1.716	1	26.55	1.725
8	16.8	2.67	7	16.7	2.68	½	27.75	1.656	½	27.65	1.661
1	17.35	2.59	3	17.35	2.59	1	29.15	1.583	1	29.05	1.588
—	—	—	½	17.75	2.53	2	32.15	1.449	—	—	—
2	19.3	2.33	3	19.2	2.34	2	35.05	1.342	1	35.05	1.342
2	19.85	2.27	½	19.9	2.26	1	36.2	1.305	½	36.05	1.310
1	20.75	2.18	½	20.6	2.19	1	37.15	1.276	½	37.05	1.279
—	—	—	1	21.25	2.13	1	38.15	1.248	—	—	—
4	21.4	2.11	3	21.6	2.09	2	40.0	1.199	—	—	—
3	21.1	2.05	1	22.2	2.04	1	53.8	0.955	—	—	—
½	22.55	2.01	—	—	—	½	58.25	0.907	—	—	—

Chemical Composition (J. J. F.)

A sample of the specimen was prepared for chemical analysis by breaking up into pea-sized pieces selected portions of a sawed slab about a centimeter thick, care being taken to avoid areas of high quartz content. This material was then ground to pass an 80-mesh sieve and that retained on 200 mesh was freed of quartz with methylene iodide. The heavy portion was washed free of methylene iodide with acetone and then allowed to dry in air at room temperature. This material was used for the chemical analysis and the determination of the specific gravity.

Table 3. Chemical Analysis of Robinsonite and Boulangerite from Nevada
[Joseph J. Fahey, analyst]

	Per Cent
Pb	36.72
Hg	0.13
Sb	27.44
As	0.48
S	15.15
H_2O	0.90
Insol. in HCl	19.14
	99.96

The sample (2.0875 g) on which the specific gravity was determined was treated in a 500-ml Erlenmeyer flask with 100 ml of H_2O and 300 ml of concentrated HCl. The flask was placed on a steam bath for one hour and then removed and allowed to remain at room temperature overnight. The solution was then filtered through a weighed Munroe crucible and the residue washed with HCl (3+1). The filtrate plus the washings was made up to 500 ml and aliquots were taken for the determination of Pb and Sb, the former being weighed as $PbSO_4$ and the latter determined by titration with permanganate. The residue on the crucible was washed with NH_4OH (1+1) followed by H_2O to remove the As_2S_3, dried for one hour in an oven at 75° C. weighed, and recorded as "Insoluble in HCl" in the analysis. The ammonia solution was acidified with HCl and the arsenic was precipitated with H_2S, filtered on a Monroe crucible, heated for one hour in an oven at 500° C, and then weighed as As_2S_3. Sulphur was determined by wet oxidation with bromine in nitric acid and weighed as $BaSO_4$ in the usual way. A separate sample was analyzed for Hg, which was collected as an amalgam on a preweighed gold bar. Water was determined by the Penfield method. The figure for water (0.90%) recorded in Table 3 was obtained by deducting the water con-

tained in the insoluble portion (0.24%) from total water (1.14%). The rigorous treatment necessary to obtain the "Insol in HCl" portion probably resulted in a water determination on this portion that is a little low. Hence the figure given for H_2O in the analysis would be correspondingly a little too high, probably by several tenths of one percent.

TABLE 4. PERCENTAGE OF ROBINSONITE AND BOULANGERITE IN THE HCl-SOLUBLE PORTION OF THE SAMPLE

	Robinsonite $7PbS \cdot 6Sb_2S_3$	Pb and Sb in the sample computed to sulphides and calculated to 100%	Boulangerite $5PbS \cdot 2Sb_2S_3$
PbS	45.1%	52.6%	63.8%
Sb_2S_3	54.9	47.4	36.2
	40.1 ←	100.0	→ 59.9

In Table 4 the formula percentages of PbS and Sb_2S_3 in robinsonite and boulangerite are listed with the determined percentages of these two constituents in the analyzed sample, after calculation to 100%. By computation based on the PbS content, the HCl-soluble portion of the sample (approximately 80%) is found to consist of 40.1% of robinsonite and 59.9% of boulangerite. By computation based on the Sb_2S_3 content, these same percentages (40.1% and 59.9%) of robinsonite and boulangerite respectively are obtained.

The ratio of $Pb:Sb_2 = 7:6$ as reported by Robinson is confirmed by the Pb and Sb_2 determinations made on a sample of synthetic robinsonite (Table 5) that appeared homogeneous in polished section and gave an x-ray powder pattern identical with that given by the natural material. A spectrogram by K. J. Murata showed only negligible quantities of impurities.

TABLE 5. PARTIAL CHEMICAL ANALYSIS OF SYNTHETIC ROBINSONITE
[Joseph J. Fahey, analyst]

		Ratios
Pb	$38.6\% \div 207.21 = 0.1863 \div 0.0262 = 7.11$	7
Sb_2	$37.5\% \div 243.52 = 0.1540 \div 0.0262 = 5.88$	6
Specific gravity = 5.34 at 4° C.		

CONCLUSIONS

Artificial crystals of lead antimony sulphide, "mineral X," prepared by Robinson (1947, 1948a,b) by dry fusion of the elements in vacuo and by hydrosynthesis in a bomb, a fusion in vacuo of the elements in the

proportion $7PbS$ to $6Sb_2S_3$, and an unidentified mineral from the Red Bird mine, Pershing County, Nevada, all give identical x-ray powder patterns. Robinson gives the composition as $PbS \cdot Sb_2S_3$ or $7PbS \cdot 6Sb_2S_3$. The homogeneous fusion, later analyzed, clearly indicates the latter composition. The crystals are triclinic with $a = 16.51$, $b = 17.62$, $c = 3.97$ A, $\alpha = 96°04'$, $\beta = 96°22'$, $\gamma = 91°12'$. The unit cell contains $7PbS \cdot 6Sb_2S_3$ with calculated specific gravity 5.40, which is in good agreement with the measured values, 5.27, 5.20 (Robinson), 5.34 (artificial fusion), and 5.28 (indirect determination on natural material), thus confirming the cell content.

Acknowledgments

The authors are indebted to the late Martin A. Peacock, of the University of Toronto, and to Joseph M. Axelrod, of the U. S. Geological Survey, for their help in the identification of robinsonite by means of x-ray powder pictures; to Esper S. Larsen, 3d, of the U. S. Geological Survey, who made the etched section in Fig. 1, and to K. J. Murata, U. S. Geological Survey, who made a spectrogram of the analyzed sample.

References

Bailey, E. H., & Phoenix, D. A. (1944): Quicksilver deposits in Nevada, *Nevada Univ. Bull.*, **38,** no. 5, 159–160, 167–168.

Robinson, S. C. (1947): The lead-antimony-sulphur system, mineralogy and mineral synthesis—Ph.D. thesis, *Queen's University, Kingston.*

——— (1948a): Synthesis of lead sulphantimonites: *Econ. Geology,* **43,** 293–312.

——— (1948b): Studies of mineral sulphosalts, XIV—Artificial sulphantimonites of lead, *Univ. Toronto Studies, Geol. Ser.*, **52,** 54–70.

STUDIES OF MINERAL SULPHO-SALTS: XVI—CUPROBISMUTHITE

E. W. Nuffield, *University of Toronto, Toronto, Canada.*

Abstract

Study of the type specimen from the Missouri mine, Park county, Colorado (U.S.N.M. 92902) has shown that cuprobismuthite, which has been regarded as a mixture of emplectite and bismuthinite, is a valid species. The unit cell is monoclinic, $C2/m$ with $a=17.65$, $b=3.93$, $c=15.24$ A; $\beta=100\frac{1}{2}°$. Most probable cell contents $12[CuBiS_2]$ and then dimorphous with emplectite.

A "probably new mineral" associated with quartz, chalcopyrite and wolframite at the Missouri mine, Hall's Valley, Park county, Colorado was the subject of a short description by Hillebrand in 1884. The mineral occurred both as dark bluish gray grains in the quartz matrix and as small, deeply striated prismatic crystals in numerous cavities. A specific gravity determination of a quantity of the crystals gave 5.75, recalculated to 6.31 to correct for the presence of 4.43% quartz and 6.97% chalcopyrite. The material offered little opportunity for precise analytical work but two analyses, one of the crystals and the other of the compact material were completed with the following results:

	Bi	Ag	Cu	Fe	Zn	S	Total
I—crystals	60.80	0.89	15.96	2.13	0.10	19.94	99.82
II—grains	63.42	4.09	12.65	0.59	0.07	18.83	99.65

Presumed by Hillebrand to include: I—6.97% chalcopyrite after deducting 4.43% gangue; II—1.91% chalcopyrite after deducting 59.75% gangue. Sulphur content was calculated for each analysis.

The analyses clearly indicated that the mineral was essentially a bismuth sulpho-salt of copper, assuming apart from visible chalcopyrite and non-metallic gangue, that the analytical samples consisted of one mineral. The relative proportions of the metallic elements led Hillebrand to suggest the composition $3(Cu,Ag)_2S \cdot 4Bi_2S_3$, which is distinct from that of other naturally occurring sulpho-salts of bismuth. He proposed to investigate similar material from other mines in the area before conferring a name upon the mineral or even definitely claiming it to be a new species, but nothing further was forthcoming.

The data of Hillebrand were classified by Dana (1892) in the *System of Mineralogy* without comment except to assign to the mineral the name cuprobismuthite. Scheiderhöhn & Ramdohr (1931, p. 378) reported the occurrence of cuprobismuthite at Arnsberg, Westphalia. However, ma-

terial from Colorado for comparison purposes was not available to these authors and no chemical evidence was presented to prove that the composition from the new occurrence was identical with that assigned to cuprobismuthite.

The validity of cuprobismuthite as a new species was now seriously questioned by the work of two observers. Short (1931, p. 104) on the basis of a mineragraphic study of specimens from the type locality reported that it was identical with emplectite ($Cu_2S \cdot Bi_2S_3 = CuBiS_2$). Palache (1940) described measurable crystals of bismuthinite (Bi_2S_3) and emplectite in a specimen (U.S.N.M. 92902) which was said to be the one upon which Hillebrand founded the species. He declared that since a mixture of these substances would give the composition revealed by Hillebrand's analyses, the species had no validity. In Dana (1944) cuprobismuthite has been dropped to the rank of a discredited species.

The present author became interested in cuprobismuthite during a study of klaprothite which was supposed to have the composition $3Cu_2S \cdot 2Bi_2S_3 = Cu_6Bi_4S_9$. In an unsuccessful effort (Nuffield, 1947) to locate this mineral, numerous specimens containing Cu-Bi sulphosalt minerals were examined. The type specimen of cuprobismuthite (U.S.N.M. 92902) which had been studied by Palache was at this time on loan to Dr. Charles Milton and his associates of the United States Geological Survey. Through the kindness of Dr. E. P. Henderson and Dr. Milton the specimen was forwarded to me together with 3 *x*-ray powder spindles obtained from the specimen at the Geological Survey.

The specimen closely resembles Hillebrand's description. Gray metallic minerals, both massive and as prismatic crystals together with scattered chalcopyrite occur in a matrix of quartz. Numerous small cavities were found to be filled with tiny, prismatic crystals. The sparse wolframite mentioned by Hillebrand was located after some effort and identified by an *x*-ray powder photograph.

The massive, gray metallic material was first investigated. It was found to be composed chiefly of a mineral giving an *x*-ray powder photograph which could not be matched with patterns from the usual sources. Presumably this is the mineral that yielded the second of Hillebrand's analyses. Minor galena and tetrahedrite were also identified by *x*-rays.

X-ray powder patterns were now obtained from crystals within the cavities. Emplectite and aikinite ($PbCuBiS_3$) were readily identified. A third pattern with few diffraction lines resembled that of benjaminite ($Pb(Cu,Ag)Bi_2S_4$) while still another proved to be identical in every respect with the unidentified pattern of the massive material mentioned above. This pattern was obtained several times on carefully chosen crystals and since no variation either in relative intensities or in spacings was

observed, it must be assumed that it does not represent a mixture of minerals. The same pattern was obtained from one of the Geological Survey spindles (U.S.G.S. No. 1699) which was labelled as "bright, distinctly anisotropic from polished section 90." It might well be presumed that crystals of this type provided the data of Hillebrand's first analysis.

The crystals which gave the new pattern are very thin blades measuring about 1 mm in greatest dimension. They characteristically show a slight twisting about an axis parallel to the elongation and commonly exhibit a bluish tarnish. They are extremely fragile, shattering at the touch of a needle. Despite the small size and the twisting, a crystal was readily found that gave sharp rotation and Weissenberg films. Projection and measurement of the films led to a monoclinic cell with dimensions:

$$a=17.65, \quad b=3.93, \quad c=15.24 \text{ A}; \quad \beta=100\tfrac{1}{2}^\circ$$

In this setting, b is the axis of elongation and a is in the plane of the blades. The systematically missing diffraction spots conform to the extinction conditions (hkl) present only with $(h+k)$ even, $(h0l)$ present only with h even, which are characteristic of the space group $C2/m$.

Attempts to produce cuprobismuthite artificially by fusion of the elements in the stoichiometrical proportions represented by the formula $3Cu_2S \cdot 4Bi_2S_3$ proved unsuccessful. Only two compounds, $3Cu_2S \cdot Bi_2S_3$ (wittichinite) and $3Cu_2S \cdot 5Bi_2S_3$ (Nuffield, 1947), can be formed within the Cu-Bi-S system by this method. My colleague, Dr. F. G. Smith with an active interest in the system undertook to investigate the possibility of producing additional compounds by annealing the fusion products for several days. It was soon established that when fusion products of the elements Cu, Bi and S with Cu/Bi near 1 were annealed at temperatures between 300 and 500° C. for periods upwards of 2 days, a new, nearly homogeneous phase was formed. X-ray powder patterns of this phase proved to be identical in both relative intensities and in spacings with the unknown pattern obtained from the crystals and massive material of the cuprobismuthite specimen. It was thus ascertained that the mineral is a bismuth sulpho-salt of copper very much like Hillebrand's cuprobismuthite in composition.

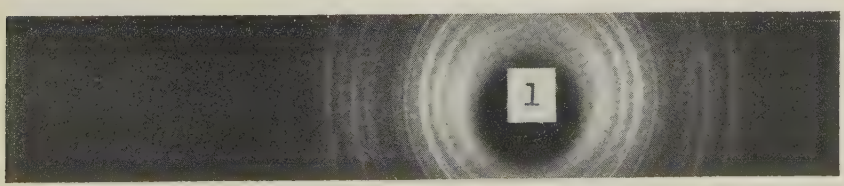

FIG. 1. X-ray powder contact print of cuprobismuthite from Park county, Colorado. Nickel filtered copper radiation; $1^\circ\theta=1$ mm.

Attempts to determine the exact composition by annealing various proportions of Cu, Bi and S and examining the products in polished sections for homogeneity were not successful. It was evident that the Cu/Bi ratio of the compound was near 1 but in no case was an absolutely homogeneous product produced. A portion of the purest product gave a density of 6.47 grs./cc. on the Berman balance (as compared to Hillebrand's corrected value, 6.31) and this value was used to calculate the approximate weight of the cell contents:

$$MW \times Z = \frac{\text{volume of cell} \times \text{density}}{1.6602} = 4049.3.$$

The composition $3Cu_2S \cdot 4Bi_2S_3$ or $Cu_6Bi_8S_{15}$ proposed by Hillebrand for cuprobismuthite has a molecular weight of 2534.32, which is clearly incompatible with the calculated value of 4049.3. However, there are three formulas which have a Cu/Bi ratio near 1 and are at the same time compatible with the calculated weight of the cell contents:

Cell Contents	Mol. Weight×Z	Calc. Density
$7Cu_2S \cdot 6Bi_2S_3$ or $Cu_{14}Bi_{12}S_{25}$	4199.48	6.69
$6[Cu_2S \cdot Bi_2S_3]$ or $12[CuBiS_2]$	4040.28	6.44
$5Cu_2S \cdot 6Bi_2S_3$ or $Cu_{10}Bi_{12}S_{23}$	3881.08	6.18

There can be little doubt therefore, that Hillebrand's cuprobismuthite is identical with the mineral studied and described by the present writer, and that it is a valid species with a composition near to that assigned to it by Hillebrand. It is likely that both Short and Palache overlooked it in their studies of type material because of the discovery of the chemically similar mineral emplectite, which had not been noted by Hillebrand.

Hillebrand's results from the analysis of the crystals are in fair agree-

Table 1. Comparison of Weight Percentages

	I	II	III	IV	
Cu	21.19	18.88	16.38	14.58	15.54
Ag	—	—	—	0.96	
Zn	—	—	—	0.11	
Bi	59.72	62.08	64.62	65.50	
S	19.09	19.04	19.00	18.85	
	100.00	100.00	100.00	100.00	

I–III. Calc. weight percentages. I. $Cu_{14}Bi_{12}S_{25}$. II. $CuBiS_2$. III. $Cu_{10}Bi_{12}S_{23}$. IV. Cuprobismuthite crystals; anal. Hillebrand. Fe deducted as $CuFeS_2$ and analysis recalc. to sum 100%.

ment with the latter two of the three suggested formulas. Table 1 compares the calculated weight percentages for the three formulas with the weight percentages of this analysis, summed to 100% after deducting iron as chalcopyrite. But because of the impure nature of the material, the analysis does not lend itself to the calculation of the exact formula. However the possible cell contents $6[Cu_2S \cdot Bi_2S_3] = 12[CuBiS_2]$ are worthy of further consideration. The cell contents of emplectite are $2[Cu_2S \cdot Bi_2S_3]$ (Hofmann, 1933) and its cell while orthorhombic in symmetry, has dimensions remarkably similar to those of the monoclinic cell of cuprobismuthite:

	a	*b*	*c*	β	Cell Volume	Density
Emplectite[1]	6.14	3.90	14.54	—	348.2	6.43 calc.
Cuprobismuthite	3×5.88	3.93	15.24	100½°	3×346.5	6.47 meas.

[1] The cell constants of Hofmann have been converted to Angstrom units.

The *b* and *c* dimensions compare directly while the *a* dimension of emplectite is roughly ⅓ that of cuprobismuthite suggesting similar structural arrangements. The cell volumes are almost exactly in the proportions of 1 to 3. Furthermore, the densities of the two minerals are almost identical. Since it is known that cuprobismuthite has a Cu/Bi ratio of near 1, it is not unreasonable to suggest that its chemical formula is in fact $Cu_2S \cdot Bi_2S_3$ and that the mineral is therefore dimorphous with emplectite. Since it is produced artificially by annealing the constituents, it is evidently the form which is stable at high temperatures. Emplectite cannot be produced by simple fusion or by annealing and may therefore represent the variety which is formed at low temperatures in nature. The final proof of the composition must however, wait on the results of fu-

TABLE 2. CUPROBISMUTHITE, $12[CuBiS_2]$—*X*-RAY POWDER DATA[1]

Monoclinic, $C2/m$; $a = 17.65$, $b = 3.93$, $c = 15.24$ A, $\beta = 100\frac{1}{2}°$

I	*d* meas.	*I*	*d* meas.	*I*	*d* meas.	*I*	*d* meas.
2	6.15	10	3.07	½	2.49	3	1.957
2	4.32	½D	2.95	½D	2.30	½	1.877
3D	3.64	½D	2.86	2	2.17	½	1.829
½	3.46	6	2.73	2	2.09	3	1.719
4	3.25	½	2.59	½	2.00		

D—diffuse line.

[1] For Ni filtered, Cu radiation (Cu $K\alpha_1 = 1.5405$ A).

ture analyses of pure material. It is hoped that the x-ray powder data of Table 2 will aid in the discovery of more favourable occurrences.

References

Dana, E. S. (1892): *System of Mineralogy*, ed. 6, New York.

Dana, J. D. & E. S. (1944): *System of Mineralogy* **1,** ed. 7, by C. Palache, H. Berman and C. Frondel, New York.

Hillebrand, W. F. (1884): A probably new mineral, *Am. Journ. Sci.*, **27,** Third Series, 355–357.

Hofmann, W. (1933): Strukturelle und morphologische Zusammenhänge bei Erzen vom Formeltyp ABC_2, *Zeit. Krist.*, **84,** 177–203.

Nuffield, E. W. (1947): Studies of mineral sulpho-salts: XI—Wittichenite (Klaprothite), *Econ. Geol.*, **42,** 147–160.

Palache, C. (1940): Cuprobismuthite—a mixture, *Am. Mineral.*, **25,** 611–613.

Schneiderhöhn, H. & Ramdohr, P. (1931): *Lehrbuch der Erzmikroskopie*, **2,** Berlin.

Short, M. N. (1931): Microscopic determination of the ore minerals, *U. S. Geol. Survey, Bull.* **825.**

THE CELL-EDGE OF JACOBSITE[1]

JOHN MCANDREW, *University of Toronto, Toronto, Canada.*

ABSTRACT

Jacobsite from Weabonga, N.S.W., of composition $Mn_{0.980}Mg_{0.006}Fe_{2.009}O_{4.000}$ corresponds closely to the ideal composition. A precise determination of the cubic cell-edge by extrapolation gave 8.5050 ± 0.0005 A. The great variation among cell-edge determinations of artificial preparations is discussed. It may arise from oxygen present in excess of stoichiometric formula requirements, shown to be absent from the mineral studied, or from variations in the distribution of the cations in the spinel structure of jacobsite. The smaller cell edge relative to normal type spinel structures does not necessarily indicate for jacobsite the presence of the inverse type structure.

Very few measurements of the cell-edge of naturally occurring jacobsite, the rare manganese iron spinel, have been published. Two concurring measurements of 8.44 A,[2] have been made on material containing 9.26% MgO from Jacobsberg by Johannsen (1928) and Wickman (1947). The cell edge of the material of composition $MnFe_2O_4$ is known however only for the artificial compound, and the measurements by different workers range from 8.48 A to 8.59 A.

A new occurrence of jacobsite shown by chemical analysis to be exceedingly close to the ideal stoichiometric composition $MnFe_2O_4$ has recently been described from Weabonga, N.S.W., by Stillwell & Edwards (1951). Through the courtesy of Drs. Stillwell & Edwards a portion of their analysed sample was obtained for the present *x*-ray investigation.

Sharp *x*-ray powder patterns were obtained of this Weabonga jacobsite on 57.3 mm. diameter and 114.59 mm. diameter powder cameras of the design described by Parrish & Cisney (1948), in which errors due to film shrinkage and inexact knowledge of the radius of the camera are eliminated. The patterns first obtained showed that all but a very small amount of grinding produced particles too fine to give sharp back diffraction rings.

A portion of the sample was also examined on a North American Philips Norelco Geiger Counter *X*-ray Spectrometer. Sharp peaks were obtained, in excellent agreement with the powder patterns. As the Norelco unit utilizes a much larger sample than the powder camera this indicated any possible inhomogeneity in composition of the jacobsite, such as zoning, was sufficiently small to have no determinable effect on the lattice spacings. The powder patterns, which were made on a minute

[1] Extracted from a thesis for the Ph.D. degree, University of Toronto.

[2] Throughout this paper measurements are given in angstrom units, converted where necessary from the original values in the references cited. In the absence of a statement of the wavelength used, particularly before 1943, the measurements although usually specified as being in A were presumed to be in kX.

amount of material, may thus be safely taken as representative of jacobsite of the composition found by analysis.

The interplanar spacings and indexing of all but the weakest lines of the x-ray powder pattern for higher diffraction angles on the large camera are given in Table 1, together with the lattice parameter calculated from each spacing. The table shows in the back diffraction region a slight but definite increase of the cell-edge calculated from the lines of the powder pattern with increasing angle of diffraction. As is well known, this arises from systematic offsetting of the diffraction lines, and the error in the lattice parameter measurement can be greatly lowered by extrapolation back to $\theta = 90°$. The parameter values calcultaed from the high angle lines of the pattern were extrapolated against each of the functions $\cos^2\theta$ (Bradley & Jay, 1932), $\cot\theta\cos^2\theta$ (Buerger, 1942), and

$$\frac{1}{2}\left(\frac{\cos^2\theta}{\sin\theta} - \frac{\cos^2\theta}{\theta}\right) \text{ (Nelson \& Riley, 1945).}$$

In each case a straight line was obtained within the limits of measurement error. However plotting against $\cos^2\theta$ gave the best linear extra-

Table 1. Jacobsite, Weabonga, N.S.W. Stronger Lines at Higher Diffraction Angles of the X-ray Powder Pattern on the 114.6 mm Diameter Camera. Fe Target, Mn Filter

d(meas)	hkl	a
1.634	(333), (531)	8.490
1.501_5	(440)	8.494
1.295_3	(533)	8.494
1.281_0	(622)	8.4972
1.226_7	(444)	8.4990
1.1062 α_1	(553), (731)	8.4970
1.0629 α_1	(800)	8.5032
.98202 α_1	(555), (751)	8.5045
.98205 α_2	(555), (751)	8.5048

polation, and was used for the final extrapolation (fig. 1). The parameter obtained by this extrapolation was $8.505_0 \pm 0.0005$ A, and those from the other extrapolations were in agreement, within this estimated error, The measurements were made for the specimen at 27°C., and the wavelengths of the x-rays from the iron target were taken as $K_{\alpha_1} = 1.93597$ A, $K_{\alpha_2} = 1.93991$ A, $K_\alpha = 1.9373$ A.

The complete x-ray powder pattern of jacobsite from the 57.3 mm diameter powder camera is given in Table 2. This is in excellent agreement with that from the larger camera, although the figures show a greater scatter, as is to be expected.

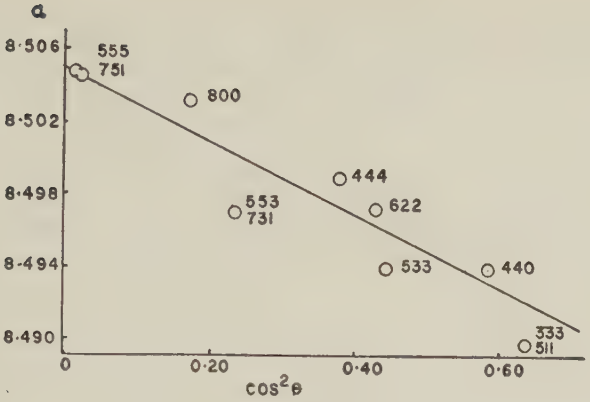

FIG. 1. Extrapolation against $\cos^2\theta$ of the lattice parameter.

Comparison of the cell-edge obtained for naturally occurring $MnFe_2O_4$ with that given by other investigators on artificial preparations is difficult because of striking variation among the latter. The following measurements[1] have been collected from the literature, with errors as estimated by the respective authors—

$8.505_0 \pm 0.0005$ A	naturally occurring, this paper.
8.442 ± 0.002 A	Clarke, Ally & Badger (1931).
or 8.474 ± 0.002 A	Clarke, Ally & Badger (1931).
$8.482 \pm (0.004)$ A	calculated from Mason (1947).
8.532 ± 0.005 A	Passerini (1930).
8.589 ± 0.002 A	Holgersson (1927).

The cell-edge from Mason was obtained by interpolation between measurements on artificial preparations with Mn:Fe atomic ratios of 30:60 and 20:70. The values given by Holgersson and Passerini may not be quite as precise as indicated, for at the time when these measurements were made the nature of the systematic errors was not fully known. The measurement of Clarke, Ally, & Badger, which is that given in the 7th edition of Dana's *System of Mineralogy* (1944) needs further consideration. In their original paper the value of 8.457 ± 0.002 A is given. This figure was obtained by averaging all values calculated from lines with θ in the range 6° to 25° recorded on their film, which was measured with a scale reading directly in lattice spacings. The accuracy they claim is therefore probably far greater than that actually obtained. The two values listed above were obtained by conversion, firstly to A units from the wavelength 0.712 "A" stated for the Mo radiation used, secondly

[1] See footnote at commencement of this paper.

Table 2. Jacobsite, Weabonga, N.S.W.: *X*-ray Powder Data
Fe target, Mn filter; $a = 8.505_0$ A

I	*d*(meas.)	*hkl*	*d*(calc.)	*I*	*d*(meas.)	*hkl*	*d*(calc.)
4	4.94	111	4.910	½	1.435	531	1.438
4*	3.11	—	—	¼	1.339	620	1.345
4	3.01	220	3.007	2	1.296	533	1.296
10	2.558	311	2.564	½	1.278	622	1.282
¼	2.449	222	2.455	1	1.225	444	1.227
1*	2.410	—	—	¼	1.191	551, 711	1.191
6	2.123	400	2.126	½	1.134	642	1.136
1	1.739	422	1.736	4	1.107_5	553, 731	1.1073
6	1.636	333, 511	1.637	2	1.062_4	800	1.0631
¼*	1.549	—	—	$3\alpha_1$	0.9820	555, 751	0.9820
6	1.501	440	1.503	$1\alpha_2$	0.9820	555, 751	0.9820

* Extraneous lines, absent from another pattern of the same specimen.

from the wavelength 0.70783 kX then known for MoK in which the scale may well have been calibrated.

Nevertheless there remains to be accounted for a distinct range of 8.48 A–8.59 A in values of the parameter obtained by different workers. Two possibilities present themselves for consideration in this respect; firstly variation of chemical composition, as known for some spinels, by the presence of oxygen in excess of the stoichiometric formula requirements; secondly by variation in arrangement of the cations in the atomic structure, which is also well known for some members of the spinel group.

In the normal structure of an AB_2O_4 spinel (Bragg, 1915), the unit cell with 32 O contains 8 *A* cations occupying the equiposition 8(*a*), in tetrahedral coordination with the oxygen, and 16 *B* cations in the 16(*d*) equipositions, in octahedral coordination with the oxygen. In some spinels (Barth & Posnjak, 1932) the cations occupy the same two equipositions, but 8 *B* cations fill the 8(*a*) positions, and $8A+8B$ cations are distributed at random through the 16 (*d*) positions.

Furthermore, the spinel structure has been long known as capable of existing with a deficiency of metal constituents below the stoichiometric requirements of the formula AB_2O_4. With this there is a commensurate replacement of the *A* or lower valency cation by the *B* or higher valency cation to maintain over-all electrostatic neutrality, and a corresponding decrease in the cell dimensions. Thus magnetite when oxidized at up to 300° C. may vary continuously in composition from Fe_3O_4 to $Fe_{8/3}O_4$, retaining the same structure, but with a uniform decrease in the cell edge from 8.40 A to 8.32 A (Hägg, 1935), and a similar change is known when Al_2O_3 is "dissolved" in $MgAl_2O_4$ (Hägg & Söderholm, 1935). It may

be noted that the structural formula for these composition variations may be expressed as $B_2(B_x A_{1-3x/2})O_4$ with x, between 0 and $\frac{2}{3}$ for the above examples, indicating the amount of vacant cation positions in the lattice.

The artificial preparations of $MnFe_2O_4$ on which the cell dimensions quoted above were measured, were all made by heating at up to 1300° C. in air preparations containing Mn and Fe in the atomic ratio 1:2. In none of these preparations was a check made on the Mn+Fe:O ratio after heating. Therefore addition of oxygen beyond the formula requirements may well have occurred, with a corresponding increase in charge of some of the cations. The product would give an x-ray powder pattern of the spinel type but with a slightly lower cell dimension than that of composition $MnFe_2O_4$.

The presence of such defects in the lattice may be determined from the chemical analysis. The atomic ratio of total cations to oxygen will be 3:4 for a structure without vacant cation positions, and a structure with the vacant positions will have a lower cation:oxygen ratio. The analysis of the Weabonga jacobsite (Stillwell & Edwards, *op. cit.*) was recalculated in atomic ratios relative to 0=4.000, and gave the formula $Mn_{0.980}Mg_{0.006}Fe_{2.009}O_{4.000}$. The ratio of total cations to oxygen was 2.995:4.000, or, within the limits of error of analysis, 3:4. The lattice parameter for this material therefore represents that of $MnFe_2O_4$ without appreciable vacant cation positions. Similar calculations were made for five other analyses of naturally occurring jacobsite. In each the cation:oxygen ratio was very close to 3:4, being so within the probable limits of error of the chemical analysis.

Finally it remains to consider the influence of the structure type on the cell dimensions of the spinel. Verwey & Heilmann (1947) have recently pointed out that, in going from the spinel series (aluminates) to the chromite series (chromites) to the magnetite series (ferrites) there is a regular increase in cell dimensions. For spinels having the normal structure the increase is about 0.23 A and 0.12 A respectively. In contrast, the ferrites $CuFe_2O_4$, $MgFe_2O_4$, and $FeFe_2O_4$, shown to have the inverse structure by Barth & Posnjack (1932), Verwey & Heilmann (1947) and Verwey, Haayman, & Romeijn (1947) respectively, have a much smaller increase in cell dimension above that of the corresponding chromites and aluminates.

For the latter two ferrites the increase is about 0.06 A above the corresponding chromites. In the series $MnAl_2O_4$—$MnCr_2O_4$—$MnFe_2O_4$ the increases 0.23 A and 0.06 A respectively were therefore taken by Verwey & Heilmann to indicate the inverse structure for $MnFe_2O_4$.

As the scattering powers to x-rays of Mn and Fe are closely similar,

Table 3. Lattice Dimension Differences in the Spinels

B	Al		Cr		Fe	Structure of
$r(B^{3+})$	0.57		0.64		0.67	the ferrite
A						
Zn	8.08	0.23	8.31	0.12	8.43	normal
Cd	—	—	8.58	0.12	8.70	normal
Cu	8.08	(0.24	—	0.06)	8.38	inverse
Mg	8.08	0.24	8.32	0.05	8.37	inverse
Fe	8.13	0.22	8.35	0.05	8.40	inverse
Mn	8.27	0.23	8.50	0.01	8.51	?
				(0.06	8.56)	Holgersson.

Modified from Verwey & Hilemann (1947).

the intensities of the x-ray diffraction beams do not enable a distinction between the two when present together in the one crystal structure, and such indirect reasoning was necessary to determine which of the cation positions each occupied in the jacobsite structure.

In $MnFe_2O_4$ the inverse structure would contain Fe^{3+} in 8(a) and $Mn^{2+}+Fe^{2+}$ occupying 16(d). An alternative possibility is an arrangement with the small Mn^{4+} in 8(a), and Fe^{2+} in 16(d). In this arrangement, corresponding to $Mn^{4+}Fe_2^{2+}O_4$, the equipositions 8(a) are occupied by ions of lower radius than in an inverse $Fe^{3+}(Mn^{2+}Fe^{3+})O_4$ structure. These positions of tetrahedral coordination, which in the latter arrangement contain Fe^{3+} of radius about 0.70 A, are occupied by Mn^{4+} of radius about 0.55 A. The 16(d) equipositions are occupied by Fe^{2+} of radius about 0.83 A, in place of $Mn^{2+}+Fe^{3+}$ with a maximum radius of 0.90 A. Therefore this alternative structure would give an increase of cell dimension over the normal $MnCr_2O_4$ structure equally small if not smaller than that for the inverse $Mn^{2+}Fe_2^{3+}O_4$ structure.

This second possibility is actually a normal type structure, and the two cannot be readily distinguished on the basis of cell size. A third possible arrangement of cations is with 8 Mn^{3+} filling the 8(a) positions, and 8 $Fe^{2+}+8$ Fe^{3+} occupying the 16(d) sites at random. However as, according to Verwey & de Boer (1936), the Mn^{4+} ion is relatively stable, and the Mn^{2+} ion much more stable than the Mn^{3+} ion, it is unlikely that the Mn^{3+} ionic state would exist in the presence of both Fe^{2+} and Fe^{3+} ions.

At elevated temperatures where the thermal vibrations in the lattice are relatively large, a more general random distribution of the cations in jacobsite, or a partial change from one to the other of the possibilities

given above may occur. If this were the case, small variations in the lattice dimensions may occur in $MnFe_2O_4$ after heating, varying with the heating and rate of cooling or quenching of the material. A similar change in cation arrangement at high temperatures has been deduced for Fe_2AlO_4 by Verwey, Haymen, and Romeijn (1947) as the reason for variation in the electrical conductivity with heat treatment.

In conclusion, the cell-edge values for artificial $MnFe_2O_4$ cannot be taken as representative of a spinel of composition corresponding to this formula until the cation: oxygen ratio of the preparations is shown by analysis to be 3:4. The variation among the reported cell-edge values may well be due to the formation of defect structures by varying oxygen content in excess of formula requirements, acquired at elevated temperatures. The Weabonga jacobsite, of cell-edge reported above, is however substantially free from such structural defects. Nevertheless, the different cation arrangements which are geometrically possible cannot be distinguished by either intensities of the coherent *x*-ray diffractions, or by consideration of the cell size, and a variation between these arrangements may well occur. Such a change offers a second explanation of variations in cell dimensions observed in the artificial preparations by different workers, and may be the reason for the high value of 8.589 A measured by Holgersson.

A portion of the analysed Weabonga jacobsite was kindly made available by Drs. Stillwell and Edwards for the *x*-ray examination. The study was carried out at the University of Toronto while holding a Studentship of the Science and Industry Endowment Fund and the Commonwealth Scientific and Industrial Research Organization of Australia.

References

Barth, T. F. W., and Posnjak, E. (1932): Spinel structures, with and without variate atom equipoints, *Zeits. Krist.*, **82,** 325–341.

Bradley, A. J. & Jay, A. H. (1932): A method for deducing accurate values of the lattice spacing from *x*-ray powder photographs taken by the Debye-Scherrer method, *Proc. Phys. Soc.*, **44,** 563–579.

Bragg, W. H. (1915): The structure of the spinel group of crystals, *Phil. Mag.*, **30,** 305–315.

Buerger, M. J. (1942): *X-ray crystallography,* John Wiley & Sons, New York.

Clark, G. L., Ally, A. & Badger, A. E. (1931): The lattice dimensions of spinels, *Amer. Jour. Sci.*, **222,** 539–546.

Dana, J. D. & E. S. (1944): *System of Mineralogy* **1,** ed. 7, by C. Palache, H. Berman & C. Frondel, New York.

Hägg, G. (1935): Die Krystallstruktur des magnetischen Ferrioxyds, *Zeit. Physik. Chem.*, **B29,** 95–103.

Hägg, G. & Söderholm, G. (1935): Die Krystallstruktur von Mg-Al-Spinellen mit Al_2O_3 Überschuss und von γ-Al_2O_3, *ibid.*, **B29,** 88–98.

Holgersson, Sven (1927): Röntgenographische Untersuchungen der Mineralien der

Spinell-gruppe und von synthetisch dargestellten Substanzen von Spinell-typus, *Lunds Univ. Arsskr., M. F. Avd.*, (2) **23,** 9. *Kungl. Fysiogr. Sallsk. Handl. N.F.*, **3,** 1–112.

Johannsen, K. (1928): Mineralogische Mitteilungen, *Zeits. Krist.*, **68,** 107–118.

Mason, Brian (1947): Mineralogical aspects of the system Fe_3O_4—Mn_3O_4—$ZnMn_2O_4$, *Amer. Min.*, **32,** 426–441.

Nelson, J. B. & Riley, D. P. (1945): An experimental investigation of extrapolation methods in the derivation of accurate unit cell dimensions of crystals, *Proc. Phys. Soc. Lond.*, **57,** 160–177.

Parrish, W. & Cisney, E. (1948): An improved *x*-ray diffraction camera, *Philips Tech. Review*, **10,** 157–167.

Passerini, L. (1930): Ricerche sug'i Spinelli: II, I composti: $CuAl_2O_4$; $MgAl_2O_4$; $MgFe_2O_4$; $ZnAl_2O_4$; $ZnCr_2O_4$; $ZnFe_2O_4$; $MnFe_2O_4$, *Gazz. chimica ital.*, **60,** 389–399.

Stillwell, F. L. & Edwards, A. B. (1951): Jacobsite from the Tamworth district of N.S.W., *Mineral. Mag.*, **29,** 538–541.

Verwey, E. J. W. & de Boer, J. H. (1936): Cation arrangement in a few oxides with crystal structures of the spinel series, *Recueil Trav. Chim. Pays-Bas*, **55,** 531–540.

Verwey, E. J. W., Hayman, P. W., & Romeijn, F. C. (1947): Physical properties and cation arrangement of oxides with spinel structures. II. Electronic conductivity, *Jour. Chem. Phys.*, **15,** 181–187.

Verwey, E. J. W., & Heilmann, E. L. (1947): Physical properties and cation arrangement of oxides with spinel structures. I. Cation arrangement in spinels, *Jour. Chem. Phys.*, **15,** 174–180.

Wickman, F. E. (1947): A redetermination of the space group of jacobsite, *Geol. Fören. Förh.*, **69** (3), 363–366.

AUROSTIBITE, $AuSb_2$; A NEW MINERAL IN THE PYRITE GROUP[1]

A. R. Graham[2] and S. Kaiman[3]

Mines Branch, Ottawa, Canada.

Abstract

A new mineral identical with the intermetallic compound $AuSb_2$ has been found in gold ores from the Giant Yellowknife mine, Northwest Territories, and from the Chesterville mine, Larder Lake, Ontario. In the former locality it occurs in dolomitic carbonate and quartz with gold, freibergite, stibnite, jamesonite, chalcostibite, bournonite, arsenopyrite, pyrite, chalcopyrite, and sphalerite; in the latter in quartz with gold, freibergite, galena, tennantite, bournonite, chalcopyrite, sphalerite, arsenopyrite, gersdorffite, and pyrite. In polished section the mineral is galena-like with a slight pinkish tinge; in hand specimen minute anhedral grains show a bornite-like tarnish. The standard etch reactions in the order of reactivity are: HNO_3, $FeCl_3$, HCl, KOH positive; $HgCl_2$ and KCN negative. The hardness is C-. The composition of the mineral was determined by comparing its x-ray powder pattern with that of the synthetic compound, and was checked by microchemical tests. The crystal structure is pyrite type; the unit cell containing Au_4Sb_8 has $a=6.646 \pm 0.003$ kX (synthetic 6.644 ± 0.003 kX); the single Sb parameter is 0.386 ± 0.007. The calculated gravity is 9.91 compared with 9.98 measured on synthetic material.

Discovery

The mineral later identified as the natural counterpart of the artificial compound $AuSb_2$ was first observed by the senior author in rich gold ore specimens from the Giant Yellowknife mine, N.W.T. which had been submitted for examination to the Mineragraphic Laboratory of the Mines Branch. Rounded anhedral grains less than 200 microns in diameter showing a bornite-like tarnish were noticed on one hand specimen adjacent to hackly masses of native gold. The x-ray powder data obtained from these grains proved to be unlisted in available mineralogical publications. An identical powder pattern was later obtained from galena-like grains of similar dimensions and association noticed by Mr. W. E. White of the Mineragraphic Laboratory, in a polished section of gold ore from the Chesterville mine, Larder Lake, Ontario. The coincidence of two widely separated localities containing the same unidentified mineral in such an interesting association impelled the authors to establish its identity.

[1] Published by permission of the Director-General of Scientific Services, Dept. of Mines and Technical Surveys.

[2] Mines Scientist, Mineral Dressing and Process Metallurgy Division, Mines Branch, Dept. of Mines and Technical Surveys.

[3] Mineralogist, Radioactivity Division, Mines Branch, Dept. of Mines and Technical Surveys.

Identification Procedure

Since insufficient pure material was available for quantitative analysis, even spectrographically, the investigation was pursued on the basis of the x-ray data alone. The pattern could be indexed completely on the basis of a simple cubic structure, with cell-edge about 6.6 kX, using the Hull-Davey cubic crystal analyzer. This cell-edge compared most favourably with that listed in the cubic crystal structure tables of Knaggs, Karlik, and Elam (1932) for the artificial compound $AuSb_2$. Search of metallurgical references located x-ray powder data on $AuSb_2$ given by Bottema and Jaeger (1932) which were identical with those of our mineral. The existence of $AuSb_2$ as a mineral was consistent with the mineral assemblages in the ores from both localities, which included native gold, and antimony-bearing minerals. Microchemical tests on the mineral confirmed the presence of gold and antimony.

The artificial compound has been well established as the only intermediate compound in the binary system Au-Sb. It was described as a synthetic product by Vogel (1906) during investigations of certain metallic systems. Oftedal (1928), using x-ray powder methods, determined its structure as pyrite-type, giving a value of 3/8 for the single Sb parameter. Nial, Almin, and Westgren (1931), Bottema and Jaeger (1932) and Grigorjew (1932), all agreed within experimental error concerning the phase relations in the Au-Sb system, and confirmed the existence of $AuSb_2$ as an intermetallic compound with distinctive physical properties. This work as summarized in Hansen (1936) shows that in the system Au-Sb an eutectic point exists between Au and $AuSb_2$ at about 25% Sb, and a temperature of 360° C. A triple point among melt, $AuSb_2$, and Sb occurs at about 54% Sb and a temperature of 460° C. The compound with stoichiometric composition 55.2% Sb dissociates at the latter temperature to a mixture of gold-rich liquid and solid Sb. Little solid solution of either gold or antimony in $AuSb_2$ is shown. Bottema and Jaeger gave evidence of three polymorphous modifications of $AuSb_2$ with inversion temperatures at about 355° C. and 405° C.

As further confirmation of the identity of the mineral, several attempts were made to synthesize pure $AuSb_2$ by dry fusion of stoichiometric proportions of Au and Sb. Various techniques were employed in an endeavour to homogenize the product. These included sintering under argon at atmospheric pressure just below the dissociation temperature, and very slow cooling of a melt under the same conditions. The most successful convenient method was found to be repeated fusion and solidification in evacuated and sealed silica glass tubes small enough to prevent condensation of distilled antimony upon unevenly heated walls.

Microscopic examination at high magnification of polished sections of

all products showed evidence of incongruent melting of the compound in narrow selvages of a yellow and white eutectic mixture on the boundaries of coarse white grains of a main phase. Small blebs of unreacted antimony were enclosed in the main phase. The more successful fusions had less than 1% unreacted antimony and eutectic, a proportion insufficient to alter materially the composition of the main homogeneous product. The latter gave an *x*-ray powder pattern identical with that listed for $AuSb_2$ and with that of the mineral under study.

The name "aurostibite" was selected to indicate the composition of the mineral, and a more complete mineragraphic and crystallographic description attempted.

Occurrence and Physical Properties

Search of the available specimens from both the Giant Yellowknife and Chesterville mines located minute amounts of aurostibite in three polished sections and one hand specimen from the former locality, and in one polished section and two hand specimens from the latter. The mineral assemblages from both localities were quite similar. The type specimen from Giant Yellowknife is a two-inch fragment of grayish-white impure vein quartz, somewhat fractured, and containing partly absorbed inclusions of chloritized and silicified wall-rock heavily mineralized with fine euhedral arsenopyrite. The walls of narrow vugs in the vein quartz are coated with minute imperfect rhombohedral crystals of dolomitic carbonate and thin flakes of sericite mica less than $\frac{1}{4}$ mm. across. Among the carbonate crystals in these vugs scattered grains of hackly gold varying in size from about 20 microns up to 1 or 2 mm. occur accompanied by rounded iridescently tarnished separate grains of aurostibite up to about 350 microns in greatest dimension. Certain of the gold grains appeared to be thinly coated with tarnished gray aurostibite; thinner layers of aurostibite may account for rusty-brown tarnish occurring on other gold grains. Occasionally, films of gold appeared to be interleaved between laminae of the mica. From these relationships, it could be inferred that the gold and aurostibite were late in the sequence of mineral deposition, and that the deposition of aurostibite probably continued after that of gold.

The polished sections of Giant Yellowknife ore confirm the occurrence of aurostibite and gold closely related to a late period of carbonate, quartz and sericite deposition in a series of fractures cutting clear quartz. The clear quartz itself has apparently filled fractures in an earlier milky quartz, which has been largely absorbed and recrystallized. The latter now appears as irregular grayish-white blocks floating in the clear quartz matrix. Both the early grayish and the later clear quartz contain irregu-

lar masses of bournonite, chalcopyrite, sphalerite, and bladed and fibrous masses of jamesonite and chalcostibite, more or less closely associated with masses and strings of arsenopyrite and pyrite crystals. The wall-rock inclusions appear to be mineralized exclusively with disseminated euhedral crystals of pyrite and arsenopyrite. Single grains of gold and aurostibite occur scattered in quartz and carbonate immediately adjacent to fractures in the clear quartz. Small areas and elongated masses

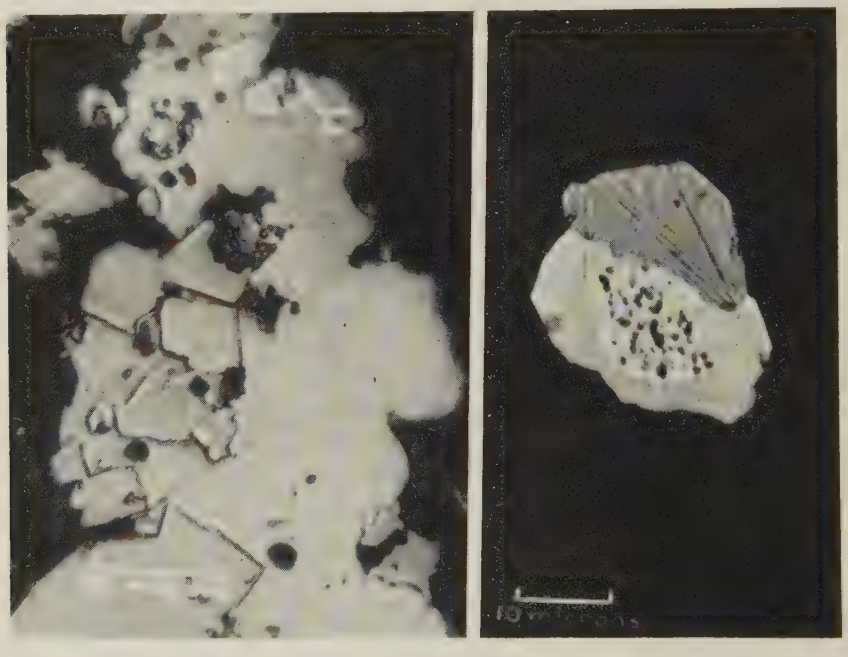

FIGS. 1, 2. Aurostibite, $AuSb_2$. Fig. 1, (left) ×800: Polished section of ore from Giant Yellowknife Mine, N.W.T. Light gray euhedral crystals with high relief are arsenopyrite; the light gray groundmass is aurostibite slightly etched with 1:1 HCl; white areas in upper right hand corner are native gold; black areas are holes in the section, and carbonate and quartz gangue. Fig. 2, ×1200: Polished section of ore from Chesterville Mine, Ontario. The stippled area is native gold; the white smooth-polished area is aurostibite; the medium gray area is freibergite; the black field is quartz gangue.

of aurostibite up to 350 microns in size lying in carbonate-filled fractures enclose or partly armour gold grains and euhedral arsenopyrite (Fig. 1). Grains of freibergite, sphalerite, and minute areas of a highly anisotropic gray-white mineral resembling stibnite were observed close to aurostibite, but without direct evidence of deposition sequence. The observed relationships in the polished sections agree with those in the hand specimen. Deposition of gold and aurostibite must have begun ap-

proximately simultaneously, while partial armouring and inclusion of gold by aurostibite indicates persistence of deposition of the latter.

In the two hand specimens from the Chesterville locality, the aurostibite occurs sparsely as minute grains embedded in clear dark quartz near and attached to small hackly masses of bright yellow gold. Where gold is undisturbed below the surface of clear quartz, coatings of light gray aurostibite and darker gray freibergite partly armour some of the extremities of the irregular gold grains. Deformation of the gold during excavation of samples with a needle point usually caused rupture and loss of the brittle coatings. The aurostibite from Chesterville did not show the bornite-like tarnish characteristic of that from Giant Yellowknife: the grains in hand specimen were difficult to distinguish visually from the other gray minerals present.

The polished section of Chesterville ore reveals sparse grains of aurostibite up to 250 microns in diameter in clear quartz closely associated with gold, freibergite, chalcopyrite, jamesonite, and galena. This clear quartz, as in the Giant Yellowknife specimen, has largely absorbed and recrystallized an older, less transparent, milky-white quartz which is now mineralized with pyrite, arsenopyrite, gersdorffite, chalcopyrite, sphalerite, and tetrahedrite. An elongated body of dark impure quartz traverses the length of the sectioned fragment, containing coarse (up to 3 mm.), fractured, subhedral pyrite, euhedral arsenopyrite, and euhedral to anhedral gersdorffite, which have been partly replaced by minor chalcopyrite, sphalerite, and tetrahedrite, and seamed by veinlets of gold. On both sides of this body, which might represent a nearly absorbed fragment of mineralized wall-rock, irregular areas of the later quartz carry quantities of free gold, aurostibite, freibergite, jamesonite, galena, chalcopyrite, and tennantite.

After the initial fracturing or shearing, the sequence of events appears to have begun with a primary surge of mineralization, consisting of milky quartz accompanied by pyrite, arsenopyrite, gersdorffite, chalcopyrite and sphalerite, which silicified and mineralized the inclusion of wall-rock. Fracturing later permitted the entry of the clear quartz, accompanied by more chalcopyrite and tetrahedrite, bournonite, jamesonite, and tennantite. This age of quartz re-crystallized and partly absorbed the fractured blocks of early white quartz. Further fracturing shattered the clear quartz, and further chalcopyrite, with sphalerite, galena, freibergite, gold, and aurostibite were deposited in and near these fractures as fillings and replacements.

Gold appears to have been deposited in the wall-rock inclusion sparingly in and around the fractured pyrite, arsenopyrite and gersdorffite, while in larger quantities it forms an interlocking stockwork generally

following the late fractures in the clear quartz. Freibergite and gold in the clear quartz show mutual boundaries indicating contemporaneity. Several grains of freibergite attached to gold grains are surrounded and partly replaced by aurostibite, which also partly armours adjacent gold grains (Fig. 2). Where aurostibite and gold occur with chalcopyrite, both send apophyses into it. No aurostibite was recognized in the area of the wall-rock inclusion.

The tests usually employed for identification of minerals in polished section reveal interesting diagnostic properties for aurostibite. The visual reflectivity and colour closely resemble those of galena. A slight pinkish tinge was noticeable on direct comparison with neighbouring galena in the Chesterville sections, but without such direct comparison, the colour may be described as galena-white. Its hardness, estimated by needle scratch, is C-, slightly harder than gold. As polished with magnesia, using a variation of the Sampson-Patmore technique, little relief is evident among gold, aurostibite, and freibergite, although the white, smooth-polishing aurostibite contrasts well with the stippled surface produced upon the yellow gold, and with the medium-gray, smooth-polishing freibergite. Aurostibite is quite brittle, in contrast to the soft-

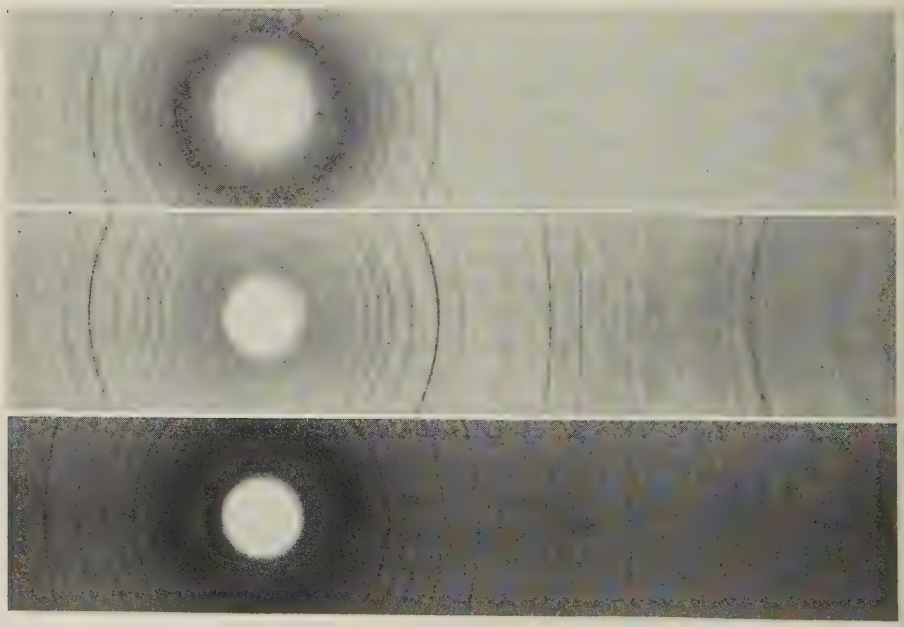

FIG. 3. Powder photographs, CuKα-radiation, Ni filter. Full size contact prints. (1°6 = 1 mm. in film.) 1. Aurostibite, Giant Yellowknife Mine, N.W.T. 2. Artificial $AuSb_2$. 3. Pyrite, Lynn Lake, Manitoba.

ness and malleability shown by many of the tellurides often associated with gold. There is no apparent cleavage.

Etch reactions according to the technique used by Short (1940) place aurostibite in a sub-group not listed in his tables. HNO_3 (1:1) reacts rapidly to form an iridescent coating. HCl (1:1) gives a dark-brown stain; on the synthetic compound the reagent drop "sweats," forming an aureole of lesser drops, which produce a brown to iridescent halo. The reaction on the mineral may be negative when the drop also covers adjacent carbonate gangue. $FeCl_3$ (20%) immediately forms an iridescent coating. KOH (40%) slowly forms a light brown coating and accentuates polishing scratches. $HgCl_2$ (5%) and KCN (20%) give no reactions. These etch reactions were essentially the same on both natural and synthetic material.

No gravity measurements were made on natural material; that measured on synthetic $AuSb_2$ is 9.98.

Crystallography

The close analogy in relative spacings and intensities of *x*-ray diffractions registered on the powder photograph with those of pyrite left no doubt that the crystallographic description of aurostibite is pyrite-type, class $2/m\ \bar{3}$, space group $Pa3$, with a unit-cell content of Au_4Sb_8. The cell-edge of the natural material, calculated from the measurements of six back reflections, is 6.646 ± 0.003 kX. Our artificial product gave $6.644 \pm .003$ kX by the same method. These values are included in the table of old and new values of the cell-edge of $AuSb_2$ (Table 1).

Table 1. Cell-Edge of $AuSb_2$

Investigators	Cell-edge (kX)
Oftedal (1928)	6.636 ± 0.001
Nial, Almin, and Westgren (1931)	6.647 ± 0.005
Bottema and Jaeger (1932)	6.636
Graham and Kaiman (1951)	6.644 ± 0.003
Graham and Kaiman, on aurostibite (1951)	6.646 ± 0.003

The Sb parameter was refined from the approximate value of 3/8 obtained by Oftedal (1928) on his artificial product, to 0.386 ± 0.007 in the natural mineral. The method employed to obtain this value was the usual one of calculating relative intensities (neglecting temperature and absorption factors) over a generous range of parameter values, comparing them with those observed, and selecting the best fit. The final calculated and observed relative intensities are listed with the powder diffraction

TABLE 2. AUROSTIBITE—$AuSb_2$: *X*-RAY POWDER PATTERN IN kX
Cubic, $Pa3$; $a = 6.646$ kX; $Z = 4$

θ (Cu)	d (meas)	d (calc)	hkl	I (obs)	I (calc)	θ (Cu)	d (meas)	d (calc)	hkl	I (obs)	I (calc)
11.60	3.82	3.837	111	1	1.9	50.20	1.001	1.002	226	½	0.6
13.375	3.32	3.323	002	5	6.5	51.00	0.989	0.991	063	½	0.4
15.00	2.97	2.972	021	4	4.8				245		
16.48	2.71	2.713	112	3	4.2	51.73	0.979	0.980	136	½	0.4
19.14	2.34	2.350	022	4*	3.9	55.58	0.932	0.931	117	1*	0.4
22.62	1.999	2.004	113	10	9.0				155		
23.67	1.914	1.919	222	1	1.4	56.56	0.921	0.922	046	½	1.3
24.75	1.836	1.843	023	1	1.9	57.46	0.912	0.913	027	1*	0.7
25.70	1.773	1.776	123	2	2.3				146		
30.355	1.521	1.525	133	½	1.0	58.265	0.904	0.904	127	1	0.8
31.26	1.482	1.486	024	1	1.3				255		
32.14	1.445	1.450	124	1	0.9				336		
32.94	1.414	1.417	233	½	0.4	59.94	0.888	0.888	246	2	1.5
34.615	1.353	1.357	224	1	1.3	62.65	0.865	0.865	137	5	3.5
37.02	1.277	1.279	115	3	3.3				355		
			333			64.65	0.851	0.851	065	1	0.7
38.65	1.231	1.234	025	1	1.0				346		
			234			65.55	0.844	0.844	237	1	0.8
39.39	1.211	1.213	125	½	0.6				156		
40.86	1.175	1.175	044	2*	1.9	67.71	0.831	0.831	008	2*	0.9
43.16	1.124	1.123	135	½	0.5	72.52	0.806	0.806	028	2	1.7
43.97	1.107	1.108	006	1	1.0				446		
			244			73.92	0.800	0.800	128	2	1.8
45.52	1.078	1.078	116	1	0.8				247		
			235			75.45	0.794	0.794	356	½	0.9
47.17	1.048	1.051	026	½	0.6	78.95	0.783	0.783	228	4*	3.0
49.47	1.011	1.014	335	2*	1.1				066		

* Observed intensities probably increased by coincident diffractions from free gold.

data in Table 2. The value 0.386 is identical with that quoted by Parker and Whitehouse (1932) for the S parameter in pyrite. Multiplying their calculated distances of closest approach, Fe—S = 2.26 kX, S—S = 2.14 kX, by the ratio of the cell-edges of aurostibite and pyrite (6.646/5.405) gives the theoretical values Au—Sb = 2.78 kX, Sb—Sb = 2.63 kX. Calculated geometrically from the cell-edge of aurostibite using 0.386 as the Sb parameter, the actual distances of closest approach are Au—Sb = 2.78 kX, Sb—Sb = 2.62 kX, in good agreement with the above values. The Sb—Sb distance in the structure is considerably less than the shortest Sb—Sb distance 2.87 kX in the structure of the element (Strukturbericht, **1**, 27). This fact is probably the result of partial covalent bonding between the Sb atoms in the pairs.

DISCUSSION

As well as being of scientific interest as another member of the pyrite group of minerals, aurostibite has economic significance as a gold mineral relatively insoluble in cyanide solution. Antimony-bearing gold ores have

often proved refractory to ordinary ore-dressing methods in the past. It is possible that aurostibite is widespread in such ores, minutely subdivided, but perhaps in important quantities. In a personal communication Dr. Frank Stillwell of the University of Melbourne, Australia, states that a gold and antimony-bearing mineral which he suspects to be identical with aurostibite occurs in an antimonial gold ore from Costerfield, Australia. Armouring of gold by aurostibite would certainly cause losses in the ordinary cyanide mill-circuit out of all proportion to the amount of gold actually present in the mineral itself. The behaviour of aurostibite under the roasting conditions often employed in treating such ores is as yet unknown. The ease of its formation from metallic antimony and gold could undoubtedly cause trouble in improperly controlled roasting processes.

References

Barrett, C. S. (1943): *Structure of Metals*, Metallurgy and Metallurgical Engineering Series, McGraw-Hill, N. Y.

Bottema, J. A. & Jaeger, F. M. (1932): *Proc. Kon. Akad. Wetensch., Amsterdam*, **35**, 916–928.

Bragg, W. L. (1914): *Proc. Roy. Soc. London*, Series A, **89**, 468.

Buerger, M. J. (1941): Numerical Structure Factor Tables. *Geol. Soc. Amer.*, Special Papers, **53**.

Grigorjew, A. T. (1932): *Zeits. anorg. allg. Chem.*, **209**, 289–294.

Hansen, M. (1936): *Der Aufbau der Zweistofflegierung*, Springer, Berlin.

Internationale Tabellen zur Gestimmung von Kristallstrukturen, Bornträger, Berlin (1935).

Knaggs, I. E., Karlik, B., & Elam, C. F. (1932): *Tables of Cubic Crystal Structure*, London, Adam Hilger.

Lonsdale, K. (1936): *Simplified Structure Factor and Electron Density Formulae, for the 230 Space-Groups of Mathematical Crystallography*, G. Bell and Sons, London.

Nial, O., Almin, A., & Westgren, A. (1931): *Zeits. phys. Chem.* B, **14**, 81–82.

Oftedal, I. (1928): *Zeits. phys. Chem.*, **135**, 291–299.

Parker, H. M., & Whitehouse, W. J. (1932): *Phil. Mag.*, **14**, 939–961.

Short, M. N. (1940): Microscopic determination of the ore minerals, *U. S. Geol. Surv. Bull.* **914**.

Vogel, R. (1906): *Zeits. anorg. allg. Chem.* **50**, 151–157.

DECREPITATION CHARACTERISTICS OF GARNET

F. G. Smith, *University of Toronto, Toronto, Canada.*

Abstract

Forty-three specimens of garnet of various compositions and types of occurrence were heated to approximately 750° C. and the decrepitation was analysed electronically and recorded. Decrepitation is general but complex, and varies in frequency and temperature of beginning of each of several stages. A stage interpreted to be due to splitting of garnet by thermal expansion of crystalline inclusions starts at 300–700°; the average for 17 calcium garnets is 446°, and for 26 iron, magnesium, and manganese aluminous garnets is 611° C. As a working hypothesis, it is proposed that these temperatures be taken as approximately the temperatures of crystallization, correctable for the effect of pressure during formation.

Introduction

The initial development of the decrepitation technique was based upon the presumption that the temperature of filling of multiphase inclusions in crystals by the liquid phase gives a second order discontinuity in the rate of decrepitation during heating (Scott, 1948; Peach, 1949; Smith, 1952). Therefore, if a stage of decrepitation can be ascribed to the filling of liquid inclusions, the temperature of beginning of that stage is the minimum temperature of crystallization. The temperature-pressure relations during deposition are defined by the P-V-T relations of the fluid in the inclusions (Ingerson, 1947; Kennedy, 1950a, b).

Subsequent decrepitation studies have indicated that there are several other causes of decrepitation, and one which is probable (but not yet proved) is the misfit which develops in and around crystalline inclusions (Smith, 1952b). Neglecting the effect of pressure, this should cause decrepitation (when the inclusion has a greater thermal expansion than the mineral) starting at the temperature of deposition. The correction for pressure has not been determined, but it would be useful to have some of the facts of decrepitation of minerals with solid inclusions to control the calculation method.

Preliminary microscopic examination and decrepitation tests showed that metamorphic minerals usually contain an abundance of crystalline inclusions, but few, if any, fluid inclusions, and that they begin to decrepitate at temperatures too high to be reasonably ascribed to the filling of aqueous fluid inclusions. That the crystalline inclusions are responsible for the decrepitation was indicated by several tests in which transparent garnet and cordierite gave a very low rate, but impure material with abundant solid inclusions gave a high rate of decrepitation. Consequently, a number of metamorphic minerals were studied in order to select one which would be most likely to provide useful data. Garnet was

chosen because it is of widespread occurrence, in individual crystals, in a variety of rock types, of various origins, and it is not often contaminated with decomposition minerals.

A number of specimens of garnet were collected for this series of decrepitation tests. The aim was to study a number of compositional types and manners of occurrence and formation.

The reader should keep in mind that interpretation of decrepitation data is still in the formative stage, and that the discussion of the following experimental facts doubtless will be modified extensively at a later time.

Decrepitation Method

The garnet specimens consisted of metacrysts in schist and gneiss, idiomorphic crystals in pegmatite, and massive and drusy replacement material. Because of the difficulty of preparing clean crystal fragments from intergrowths of small grain size, there was a positive discrimination in the material studied, in favor of large crystal units.

Visibly clean fragments were crushed and sieved to $-40+80$ mesh size. When micaceous impurities were present, these were removed by a panning operation in water. Carbonate impurity present in some of the grossularite and andradite specimens was removed by acid treatment.

The general technique of electronic decrepitation analysis was described by Peach (1949), and Smith & Peach (1949). Modifications of the initial methods were described by Smith (1952b), and a more detailed description is being prepared for publication.

The standard decrepitation method employed was 1) to use 1 cc. of the mineral powder, spread out near the closed end of the horizontal muffle, 2) to heat at $15 \pm 5°$ C. per minute, 3) to make several runs with different sensitivity and counting rate settings so that all discontinuities of rate of decrepitation could be detected, down to the sensitivity limit of the instrument, 4) to measure the temperature of second order discontinuities of rate from the rate-time recording (with temperature fiducial marks), and 5) to correct the nominal decrepitation temperatures by an amount dependent on the heating rate using an empirical calibration made in October, 1950.

The accuracy of the decrepitation temperatures is governed principally by the selection of the discontinuities in the rate curves. The accuracy limits given below refer to the limits which enclosed repeated determinations, and were made ample enough to enclose all reasonable interpretations of the temperature of the discontinuities. The accuracy after adding the heating rate correction is within $\pm 5°$ C. determined, from the scatter of the results during calibration for the effect of heating rate.

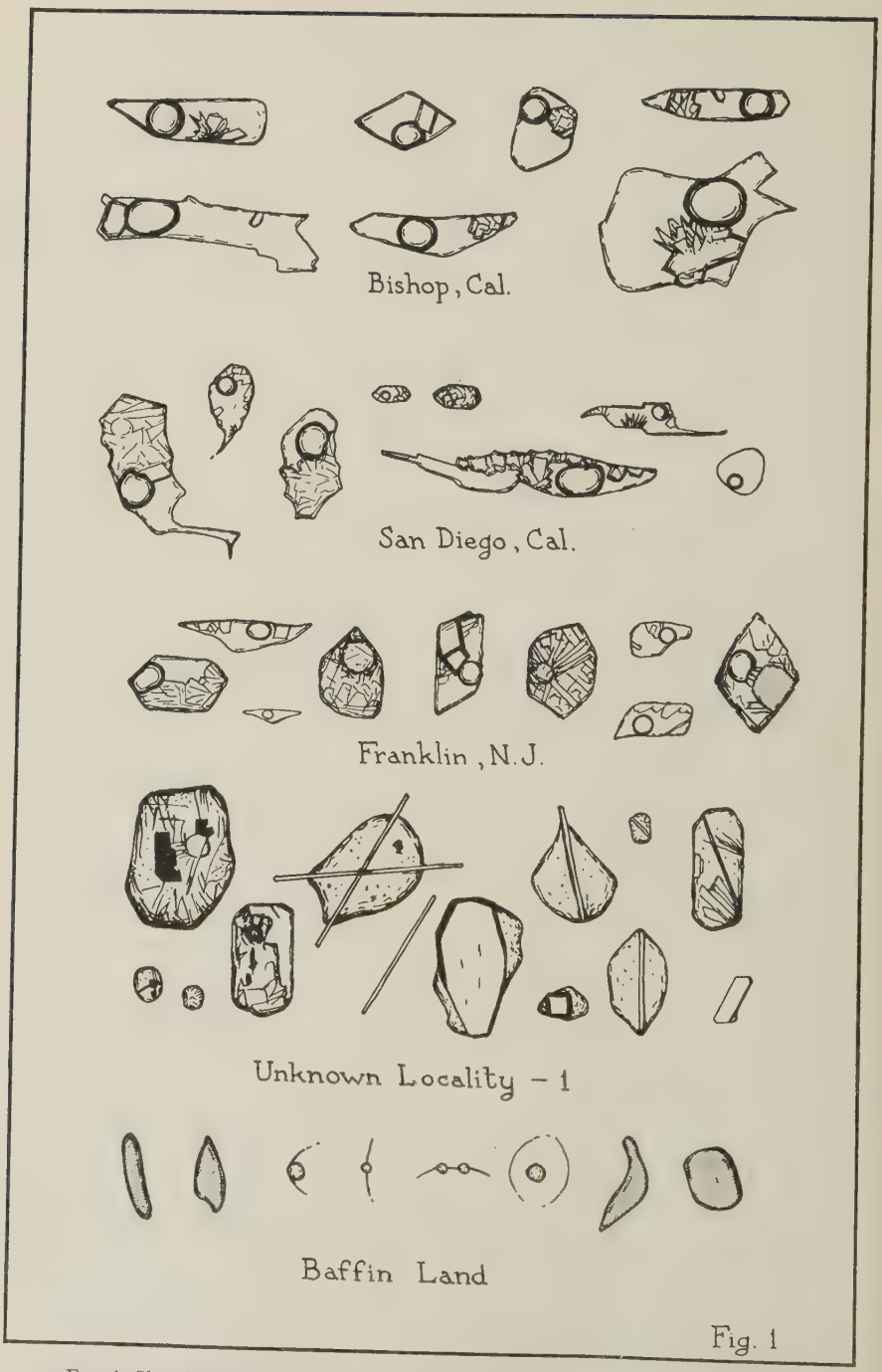

FIG. 1. Sketches of multiphase and single crystal inclusions in garnet from the indicated localities. (×400 approximately.)

Qualitative Decrepitation Data

Several experiments were undertaken to determine the optimum grain size for the decrepitation runs. It was found that $-40+80$ mesh is satisfactory, and being the same size as that used in the calibration of the instrument (using quartz), the correction for heating rate could be made readily.

Wetting the specimen during cleaning (if any) was found to give no additional decrepitation effects.

Quantitative Decrepitation Data

Notes on the specimens studied, and the decrepitation results, are given below, and the quantitative results are summarized in Table 2.

Garnet Island, Baffin Land, Canada; bright red transparent garnet (Royal Ontario Museum). Only crystalline inclusions were observed in this specimen under the microscope. Most are pleochroic (yellow-brown) and anhedral. Others are colorless, at the centre of strong optical anisotropic effects, and of radial cracks (Fig. 1). The decrepitation of this specimen was not vigorous, but a definite rate curve started at $626 \pm 30°$ and reached a peak rate about 730°.

Barton Mine, New York; clear red garnet (Royal Ontario Museum). The specimen consists of a large cracked metacryst, several inches in diameter, surrounded by a layer of massive dark green hornblende about two inches thick. Both minerals were prepared substantially pure for decrepitation. The garnet decrepitated feebly, beginning at $613° \pm 30°$, and the hornblende decrepitated more vigorously, starting at $603 \pm 20°$. Both rate curves were qualitatively similar except for the difference in rate.

Berggiesshubel, Saxony; A specimen of andradite (variety aplome) is pale greenish yellow in color, in massive form. The dodecahedral form appears in small vugs. The decrepitation of this specimen (cleaned with HCl) was vigorous. The first rate curve began at $297 \pm 15°$ and this reached a peak about 400°. Another curve began $469 \pm 10°$ and reached a peak near 650°.

Bishop, California; grossularite (essonite) (Ward's). It is massive and also vuggy. The crystals are amber yellow in color. The principal crystal form is the dodecahedron, but this is modified by several other forms.

Polished thin sections of two crystals were examined under the microscope. A large number of relatively large inclusions were seen, most of these containing a fixed bubble, a clear solution or glass, and clusters of small crystals (Fig. 1). A very small number of small inclusions were seen in which the bubble moved and in which there were no crystals. In addition, a few inclusions with no bubble were seen. Considering the ratio of

volumes of bubble and inclusions, the temperature of filling was estimated to be about 200° C., but the presence of crystals makes this estimate uncertain. One of the polished thin sections was examined while being heated under the microscope. The bubbles in 8 inclusions were found to disappear by shrinkage at $326 \pm 3°$. The crystals did not dissolve appreciably up to that temperature.

The decrepitation of this specimen, using the massive material ($-40 +80$ mesh), was vigorous. A feeble stage began at $175 \pm 10°$, a fairly vigorous stage began at $318 \pm 10°$, and this increased in rate considerably at $375 \pm 20°$. The peak rate was near 500°. No other increase was detected up to 750°, the limit of heating. The meaning of the decrepitation starting at 175° is obscure, but that beginning at 318° is evidently due to filling of the complex inclusions by the liquid phase.

Ceylon; transparent almandite (Ward's). The specimen consists of small (2 mm. to 6 mm.) purplish red crystals, nearly euhedral, some of which are water-worn. They are nearly transparent, but most contain some healed cracks. The decrepitation of this specimen was feeble and no definite rate curve was recorded in the low and intermediate temperature ranges. However, a curve began sharply at $707 \pm 10°$ with a peak rate above 750°, the limit of heating.

Charlemont, Massachusetts; almandite (Ward's). The crystals are euhedral, distorted, and of several sizes, in a fine grained chloritic schist. The color of the garnet is reddish brown and the habit is dodecahedral. Decrepitation of this specimen was found to be fairly vigorous. A double rate curve was recorded, the first starting indefinitely near 300°, but increasing somewhat near 370°, and the second starting at $628 \pm 15°$.

Some of the chloritic schist in which the garnet crystals are embedded was prepared and tested in a similar way. Virtually no decrepitation was recorded before $704 \pm 10°$ C., but at that temperature very rapid, but not loud, decrepitation began. The lag correction for this mineral may not be the same as for quartz, so that the above may be in error by as much as 20°. This probably is the decomposition temperature of the chlorite, which is known to be near this temperature from other data. From a comparison of the two decrepigraphs, it is evident that traces of chlorite in the garnet preparation did not influence the results.

Dana Township, Ontario. Several specimens of bright red garnet from a garnet mine near River Valley, Dana Township, Sudbury district, Ontario, were tested. The crystals are about one inch in diameter, with a dodecahedral habit. The outer parts of the crystals approach gem quality. The host rock is chlorite schist. A very feeble stage of decrepitation began indefinitely between 300 and 400°. A moderately vigorous stage began at $595 \pm 10°$, and increased somewhat starting at 640 ± 20. No quartz inversion rate increase was evident.

Another similar specimen from the region, obtained from the Royal Ontario Museum, started to decrepitate feebly at $400 \pm 30°$, increased in the range of the quartz inversion, and then again at $620 \pm 20°$. A slight increase in rate was noted, beginning at 702 ± 20, possibly due to chlorite impurity. The meaning of the two stages of high temperature decrepitation is uncertain. The mean of the two higher values, $630 \pm 20°$, is used in the tabular summary.

Delaware County, Pennsylvania; reddish brown almandite (Ward's). The specimen consists of a large crystal 2.5 inches across, attached to a light coloured quartz-mica bearing rock. The crystal shows evidence of crushing and healing. The crystal faces are the dodecahedron and trapezohedron. Decrepitation of this specimen began between 200 and 300° and increased in rate near 350°. The peak rate was at about 500°. Another rate curve due to rather feeble decrepitation began at $625 \pm 30°$.

Duckmaloi, New South Wales; grossularite (Ward's). The specimen is massive, but also somewhat vuggy. The garnet has a light brown color, and its habit is dodecahedral and trapezohedral. The decrepitation of this specimen was found to be vigorous, but the rate curves were complex. The first curve began between 200 and 300° and increased in rate at $300 \pm 10°$. Another increase began at $414 \pm 20°$. No other increase was recorded up to 750°, the limit of heating.

Dungannon Township, Ontario; translucent orange- and flesh-colored garnet (essonite) (Royal Ontario Museum). The garnet is in the form of an intergrowth of large crystals with a white carbonate. Microscopic examination indicated the presence of a number of solid inclusions some of which are in planar arrangement, suggesting a secondary origin. A few small inclusions were seen which may contain a bubble, liquid, and crystals. It was estimated that the liquid phase would fill this type of inclusion at $250 \pm 50°$, if the liquid is water. The decrepitation of this specimen (cleaned with HCl) was vigorous. The first rate curve began at $332 \pm 20°$, and another began at $472 \pm 30°$. The peak rate of the latter was near 610°. No other increase was noted up to 740°, the limit of heating.

Emerald Creek, Idaho; almandite (Ward's). The crystals are euhedral and show trapezohedral and dodecahedral faces. The color is a clear purplish red. Three grain sizes ($-20+80$, $-40+80$, and $-80+200$ mesh) were tested. All of the decrepigraphs were complex. Some decrepitation began very indefinitely between 400 and 500°. This was most evident in the coarsest fraction. The peak rate of this stage was near 630°. A fairly sharp increase began at $683 \pm 10°$ (682° using $-40+80$ mesh, 686° using $-20+80$ mesh). The peak rate of this curve was above 750°, the limit of heating. The finest fraction gave very little decrepitation. The grain size which gave the clearest resolution of the beginning of the high temperature stage of decrepitation was $-40+80$ mesh.

Fernwood, Idaho; almandite (Ward's). The crystals are euhedral, have a clear red color, and the crystal faces are dodecahedral, and trapezohedral. The decrepitation of this specimen was very feeble, but a high temperature curve began fairly definitely at $590 \pm 20°$ C.

File Lake, Manitoba; fairly clear, deep red garnet. The occurrence is in a band of gneiss. The crystals show the simple dodecahedral form. A very small amount of decrepitation, starting between 300 and 400°, was recorded, but a well-defined rate curve began at $617 \pm 20°$ and reached a peak rate near 720°.

Blackbird mine, Forney, Idaho; garnet (F. Ebbutt). The crystal is brownish red in color and shows trapezohedral and dodecahedral faces. The decrepitation of this specimen was very feeble. The first rate curve started indefinitely between 200 and 300° and reached a peak near 400°. Another curve began at $562 \pm 30°$.

Franklin Furnace, New Jersey; brownish yellow garnet (Ward's). It is labelled andradite (polyadelphite). The garnet is intergrown, in the form of large dodecahedral crystals, with black mica and a carbonate mineral. The faces of the garnet show some etch figures. Under the microscope, many stone-inclusions, consisting of a fine-grained aggregate of crystals, were seen (Fig. 1). Some of the inclusions contain what appears to be a small cavity within the group of crystals, and some contain undoubted bubbles, indicating the presence of a liquid or glass. The associated carbonate mineral contains an abundance of fluid inclusions which would become filled about 150°. However, most of these may be secondary.

The decrepitation of this specimen was fairly vigorous, and multiple. The first stage began sharply at $268 \pm 10°$ C., but the rate continued to increase until about 300° C. The peak rate of this stage was near 400° C. A high temperature stage began at $510 \pm 15°$ C., and the peak rate of this stage was near 670° C. The resolution of the two curves was not very good. A finer grain size ($-80+200$ mesh, cleaned with HCl) gave even poorer resolution.

Another specimen from the same locality also obtained from Ward's is labelled andradite, variety melanite. It is brownish black in color, massive, and intergrown with other minerals. The crystal habit is dodecahedral and trapezohedral. The decrepitation of this specimen was fou to be vigorous and loud, but there was some difficulty in interpreting t rate curves. The first stage of decrepitation began very indefinitely between 300 and 400° C. and reached a peak near 480°. Another stage began at $534 \pm 10°$. No other increase was recorded up to 750°, the limit of heating.

Graham County, Arizona; andradite (Ward's). The garnet is massive, but in places good crystal faces are shown (dodecahedron). The color is

pale greenish yellow. Decrepitation of this specimen began indefinitely between 200 and 300°, increased near 320°, and, after going through a peak rate near 530°, increased again at 594 ± 10° C. The intermediate temperature stage of decrepitation was more vigorous than the high temperature stage using a coarser fraction, but this was reversed using a finer fraction.

Jackson County, North Carolina; rhodolite garnet (Ward's). The garnet is in the form of subhedra in massive brown mica. The color of the garnet is pale purple. One preparation of the garnet was treated with HF to remove the associated brown mica. This also altered some of the garnet. Decrepitation of this material was very feeble. Another similar preparation of the garnet was cleaned by jigging and washing away the mica impurity. Decrepitation of this material also was very feeble, but using a large charge and fast heating rate, and increase was recorded at 660 ± 20°.

Kern County, California; andradite (Ward's). The specimen is massive and slightly vuggy. The crystal habit is dodecahedral modified by the trapezohedrons. The color of the garnet is olive green. Decrepitation of this specimen was moderately vigorous, but the rate curve was difficult to interpret. Decrepitation started about 320°, but increased considerably starting at 417 ± 20°. There appeared to be a small increase in rate beginning at 606 ± 10° but this curve soon fell again. No other increase in rate was noted up to 740°, the limit of heating. The small rate curve starting at 606 ± 10° was of unusual type. The sharp rise and fall of the curve suggest decomposition of an impurity or an inversion point. This stage of decrepitation will be considered to be anomalous.

Langban, Sweden; andradite (Ward's). The specimen is massive, but some imperfect crystals line vugs. The garnet has a light brown color. This specimen decrepitated vigorously but gave a complex decrepigraph. The first stage began at 363 ± 20°, and increased to a higher rate beginning at 440 ± 20°. The peak rate was near 560°. A much feebler stage of decrepitation started at 650 ± 20° and reached a peak rate about 700°. Several size fractions were tested, as well as both uncleaned and HCl-washed material. The best decrepigraph for resolution of the beginning of the highest temperature stage was obtained with −80+200 mesh ction. Cleaned and uncleaned material gave very similar decrepigraphs. ıe rapid rise and fall of the rate curve beginning at 650 is not like the usual decrepitation rate curves and will be considered to be anomalous.

Lowell, Vermont; grossularite (Ward's). The garnet is massive, lining cracks in a pale green, fine grained rock. The garnet has an orange color, with well developed crystal faces of the dodecahedron and trapezohedron. The decrepitation of this specimen was found to be moderately vigorous, but the rate curve was difficult to interpret. Feeble decrepita-

tion began at $189 \pm 10°$. This increased at $329 \pm 10°$ and again at $371 \pm 10°$. The peak rate was near 520°, and no other increase was recorded up to 650°, the limit of heating.

Mitchell County, North Carolina; (Ward's). The crystals are nearly euhedral dodecahedrons in a micaceous schist. The color is red and parts of the crystals are nearly transparent. The compositional variety is said to be almandite. The decrepitation of this specimen was multiple. Some low temperature decrepitation was detected. A medium temperature curve began indefinitely near 350°. A high temperature curve began fairly definitely at $648 \pm 10°$.

Mumbwa, Northern Rhodesia; brownish red garnet (Royal Ontario Museum). The crystals are well developed and complex, and appear to have grown in a drusy cavity. The exterior part of each crystal is translucent, but the interior contains abundant small inclusions. The decrepitation of this specimen (cleaned with HCl) was vigorous. The first stage began indefinitely near 220°, the second stage began at $392 \pm 20°$, and the third stage began at $466 \pm 20°$. No other rate increase was noted up to 740°, the limit of heating.

Orford, Quebec; uvarovite (Ward's). The crystals are small, and intergrown with a light colored mineral, a black mineral, and sulphide minerals. This assemblage is cut and seamed by coarse white calcite. The garnet has a bright emerald green color. The specimen was crushed, sieved, and treated with HCl to remove the abundant calcite. The residue was boiled several times with concentrated nitric acid to remove sulphides, followed by digestion in a warm mixture of HCl and HF to remove silicates other than the garnet. After washing and drying, some magnetite and/or chromite was removed with a strong magnet. Impurities still remaining were estimated to be 5 per cent of a white silicate and 5 per cent of a black mineral, probably chromite. The decrepitation of this material was vigorous, but the rate curves were complex. The first curve began sharply at $196 \pm 10°$, and reached a peak value near 265°. On the downward slope, a small increase began at $311 \pm 20°$. A vigorous stage began at $440 \pm 20°$ and reached a peak near 570°. No other increase in rate was noted up to 730°, the limit of heating.

Parry Sound, Ontario; bright red garnet (Royal Ontario Museum). The crystals, about one inch in diameter, are somewhat irregular metacrysts from a schist or gneiss. Decrepitation began at $417 \pm 20°$; another rate curve began at $660 \pm 20°$ and reached a very rapid rate.

Crow Lake, Peterborough, Ontario; (Ward's). The garnet is reddish brown in color, and probably is of the almandite compositional type. It is partly massive and partly intergrown with quartz. The crystal faces against the quartz are well developed trapezohedra. The decrepitation of

this specimen was vigorous, but the rate curves were multiple. Feeble decrepitation began between 200 and 300°, and gradually increased to a peak rate near 550°. Another increase began at 661 ± 20, with a peak rate above 750°, the limit of heating.

Plainfield, Massachusetts; spessartite (Ward's). The crystals are brownish black, subhedral and intergrown with each other and with white mica. The specimen was crushed and sieved to −10+20 mesh and then was digested in warm HF to decompose the mica. After washing and drying, the garnet was crushed and sieved to size. The decrepigraph of this specimen was complex. A feeble stage began fairly sharply at 170 ± 20°. Another rate curve began at 343 ± 20° and reached a peak rate near 500°. Another curve began at 646 ± 20°, and continued to increase above 750°, the limit of heating.

Green Monster mine, Sulzer, Prince of Wales Island, Alaska; (F. Ebbutt). The specimen is massive in the central part, but is encrusted by radially disposed zoned crystals, with excellent terminations. The color is pale amber to pale green in various bands, and the green colored parts were deposited later than most of the amber colored material. The crystal faces are the simple dodecahedron. In thin section, the optical anisotropism was considerable, and the mineral classification was doubted, but *x*-ray powder diffraction analysis by E. W. Nuffield showed that it is garnet. Microscopic examination of a polished section of this specimen disclosed few inclusions, mostly irregular groups of crystals, but some with liquid and bubble. In the latter type, small anisotropic rhomboid crystals which may be a carbonate mineral, and radiating aggregates of anisotropic acicular crystals, were seen. The bubbles were not in brownian movement. Two bubbles were seen in one inclusion of this type.

The decrepigraphs of this specimen were complex. The first stage began fairly abruptly at 318° ± 20°, and rose to a peak rate near 430°. A new rate curve began soon after the peak, at 445 ± 20°. The second curve reached a peak rate between 500 and 600° and no other increase was detected up to 740°, the limit of heating.

Roxbury, Connecticut; Two specimens of metacryst garnet (Ward's). The first specimen consists of euhedral crystals in a white quartz-mica schist. The habit is imperfectly dodecahedral and the color is red. The crystals are only partly transparent due to an abundance of solid inclusions. The compositional type is said to be almandite. The decrepitation of this specimen was vigorous. The beginning was very indefinite, but the rate appeared to increase near 350°. The peak of this stage was near 550°. Another stage began at 635 ± 10°, but increased again at 654 ± 10°. The latter was the principal discontinuity in the complex rate curve.

The second specimen consists of somewhat smaller trapezohedral crystals in a coarse white mica schist or gneiss. The color is red, and similarly the compositional type is said to be almandite. The crystals contain an abundance of solid inclusions. This specimen gave a very good decrepitation curve. A feeble stage began at $351 \pm 15°$ and reached a peak near 580°. A very sharp inflection point at $630 \pm 10°$ was the beginning of a stage of vigorous decrepitation.

The above two specimens are from the same general locality, but the differences in the host rock suggest different occurrences. However, the beginning of the high temperature decrepitation of both specimens is the same (635 and 630, $\pm 10°$). In the tables and discussions following, only one high temperature decrepitation value for the locality will be used, *i.e.*, $632 \pm 10°$, the average value.

Russell, Massachusetts; almandite (Ward's). The crystals show trapezohedral and dodecahedral faces. The color is a clear red, but an abundance of cracks filled with iron oxide stain gives the crystals a dark brown appearance. A number of solid inclusions were seen under the microscope, but no liquid inclusions. Decrepitation of this specimen was fairly vigorous. The beginning near 300° C., was indefinite, but a more definite increase began at $580 \pm 20°$.

Salida, Colorado; almandite (Ward's). The crystals are euhedral, showing the simple dodecahedron. The color is reddish brown. The crystals are coated with a dark green chloritic mineral, labelled aphrosiderite. The chloritic coating was removed from the outside of one crystal, by digesting in warm HF, before crushing and sieving to size.

Decrepitation of the garnet was vigorous, but the rate curves were multiple. The first stage of decrepitation began very indefinitely between 300 and 400° but increased in rate starting at $463 \pm 10°$. A fairly well-defined increase in rate began at $681 \pm 20°$. Decrepitation of the chloritic coating (not cleaned) was very slight until $692 \pm 20°$, when a rate curve began somewhat indefinitely. A sharper increase in rate began at $712 \pm 10°$. This reached a peak rate near 731 and then fell rapidly. After the run, the mineral had a bright bronze color. The highest temperature stage of decrepitation of the garnet is tentatively interpreted to be due to decomposition of chlorite impurity.

San Diego County, California (Ward's). The specimen consists of broken crystals of yellow to light reddish brown and transparent material. It is said to be grossularite (essonite). Under the microscope, a number of interesting inclusions were seen, consisting of a liquid, a gas bubble, and crystals (Fig. 1). Assuming that the crystals would not dissolve in the liquid during heating, it was estimated that the liquid (if water) would fill the space about 250°. The smaller inclusions appeared

to have only two phases, a liquid (or glass) and bubble, but even in the smallest of these the bubble did not move. This indicates that the liquid has a high viscosity or is a glass.

A polished thin section was heated under the microscope and the temperatures of disappearance of the bubbles in the complex inclusions were determined. The results were as follows.

Two irregular, probably primary	$235 \pm 2°$,
Two in a plane, may be secondary	$230 \pm 2°$,
One flat, may be secondary	$246 \pm 3°$.

In all of the above inclusions, the bubble moved when it was very small (above 220°), and it rose in the first four, but sank in the last one.

The decrepitation of this specimen (both treated and untreated with hydrochloric acid) was fairly vigorous, but the rate curves were very complex. A very feeble stage appeared to start at $236 \pm 10°$, but increased at $280 \pm 10°$. There appeared to be another increase between 300 and 400°, but the beginning was indefinite.

Shelby, North Carolina (Ward's). It consists of several large trapezohedral crystals, somewhat weathered and eroded on the outside. The variety is said to be almandite, and it has a clear red color. Probably the crystals are from a metamorphic rock. This specimen was divided into two parts. A crystal approximately two inches in diameter was broken and fragments from the inside half of the diameter were separated from those from the outer half of the diameter. These were crushed separately.

The outer part decrepitated vigorously starting at $280 \pm 20°$, and again at $526 \pm 10°$. The inner part decrepitated feebly, but there was a fair indication of a curve beginning at $700 \pm 30°$ C. There was no sign of a curve beginning at 526°. The decrepitation temperature of $700 \pm 30°$ is the same as that found for chlorite from Charlemont, Massachusetts, so that this may be the cause of this stage.

Snohomish, Washington; grossularite (Ward's). The specimen is massive and vuggy. The crystals are yellow and show well-developed dodecahedral faces. A polished thin section of one of the larger crystals of this specimen was examined under the microscope. A few inclusions were seen, but no details were resolved. No liquid inclusions were seen. The decrepitation of this specimen (acid washed to remove a small amount of carbonate impurity) was only moderately vigorous. A feeble stage began at $269 \pm 20°$. This increased in rate considerably at $326 \pm 20°$. The peak rate was near 450°. A very slight increase in rate took place near 700°, but it was too small to determine accurately.

South-West Africa (Ward's). The specimen consists of fragments of a large olive green crystal. The color suggests that it is probably andradite. Decrepitation of this specimen started with a very feeble stage which

began between 200 and 300°, but a sharp increase in rate began at 382 $\pm$10°. Another increase at 414$\pm$10° led to very vigorous decrepitation with a peak rate near 530°. No other increase in rate was recorded up to 750°, the limit of heating. The decrepitation temperature shown in the tabular summary is 400$\pm$20°, a mean weighted in favor of the higher of the above two temperatures.

Spokane, Washington; red almandite (G. G. Waite). The crystals are euhedral, showing the dodecahedral faces modified by the trapezohedral faces, and are from a mica schist. Under the microscope, a fragment of one crystal shows a great abundance of solid inclusions. Most of the inclusions are fairly well formed single crystals (black tablets which may be ilmenite, elongated prisms which may be quartz, pleochroic irregular prisms which may be hornblende, and other transparent unidentified minerals). No fluid or glass inclusions were seen. The decrepitation of this specimen was simple. Virtually no decrepitation was recorded until a curve began at 624$\pm$10°. The rate continued to increase to 750°, the limit of heating.

St. Just, Cornwall; andradite (Ward's). The material is massive and vuggy. The crystals are well developed dodecahedrons, very slightly modified by the trapezohedrons. The color is brown. The crystals of garnet are overgrown with a pink carbonate mineral. Under the microscope, a number of inclusions were seen in a vuggy crystal (Fig. 1). The inclusions contain an aggregate of minute crystals, also frequently a bubble. They are of the type which Sorby called stone-inclusions, since they appear to be devitrified siliceous material trapped during crystal growth. Small individual crystals are also included, and from some of these extend radial cracks.

The decrepitation of this specimen (cleaned with HCl) was fairly vigorous. The first stage began too indefinitely to determine precisely, but it appeared to be near 330°. A definite stage of vigorous decrepitation began at 410$\pm$20° and reached a peak rate near 560°. A small increase before, and decrease after, the inversion temperature of quartz indicated the presence of some of this mineral as impurity. There was a slight increase in rate beginning near 650°, but this soon reached a peak near 720°. This latter curve appears to be anomalous.

Fish-tail Lake, Wilberforce, Ontario (G. G. Waite). The garnet crystals are subhedral, in a mica-bearing gneiss. The color is a clear red. The decrepitation of this specimen was found to be complex. The first stage began very indefinitely between 200 and 300° and reached a peak near 500°. A quartz inversion curve obscured the beginning of a high temperature curve but it probably started at 610$\pm$30°.

Willsboro, New York; andradite (Ward's). The specimen consists of

fragments of large crystals, and no crystal faces were seen. The garnet, which has a light brown color, is intergrown with white wollastonite. Three grain sizes were tested (−20+80, −40+80, and −80+200 mesh). Two stages of decrepitation were found, one, which started indefinitely between 300 and 400° and reached a peak rate near 560°, and another, which started fairly sharply at 594±10°. The second stage was more vigorous than the first stage in the finest fraction, and less vigorous in the coarsest fraction.

Wrangell, Alaska (Ward's). The crystals are well developed metacrysts showing the trapezohedral and dodecahedral faces. The color is clear red, and parts of some of the crystals are transparent. The compositional type is said to be almandite. The decrepitation of this specimen was found to be very feeble, but using a large charge and fast heating rate, a fairly well defined break was found at 628±20°.

Unknown Locality—1; bright red garnet. This material is fairly clear megascopically, but contains an abundance of small solid inclusions, most of which may be sillimanite, oriented in several directions. A number of isotropic inclusions were seen, closely associated with the crystals, usually along one or both sides of elongated types. Some of the inclusions are illustrated in Figure 1. Decrepitation of this specimen began feebly between 300 and 400°, but a new rate curve began at 568±10°. This curve reached a peak rate near 660°, and qualitatively was dissimilar to decrepitation caused by quartz inversion.

Unknown Locality—2; A specimen of dull red garnet in the form of metacrysts in white mica schist, was studied. Under the microscope, a large number of solid inclusions, but no liquid or glass inclusions were seen. Decrepitation of this specimen (both with some mica impurity and after removal of practically all of the mica) was complex. Some low temperature decrepitation was recorded, but this changed to a higher rate at 339±10°. A stage of vigorous decrepitation began at 610±20°, and reached a peak rate near 715°. From comparison of the decrepigraphs of the uncleaned and cleaned material, it was concluded that a small amount of micaceous impurity does not sensibly influence the rate curves.

Unknown Locality—3. A specimen of dark red garnet, said to be pyrope of gem quality, was tested. The crystals are water-worn fragments up to 0.2 inches in diameter. Decrepitation of this material was feeble. The only significant rate curve appeared to start at 615±20° and reached a peak rate about 730°.

Decrepitation Frequency as a Function of Clarity

As the above work was being carried out, it became evident that garnet

with abundant and large solid inclusions decrepitates much more vigorously than transparent material. It is not easy to transform this working hypothesis into a numerical relation, but a few of the specimens were graded into three categories: 1) clear, 2) translucent, and 3) clouded, for comparison with the maximum rate of decrepitation. The facts are recorded below in Table 1.

TABLE 1

Locality	Clarity	Relative Maximum Rate
Unknown—3	Clear	0.25
Barton Mine	Clear	0.88
Baffin Land	Clear	0.97
Dana Twp., Ont.	Translucent	2.2
Unknown—1	Translucent	2.5
File L. Man.	Translucent	6.6
Dungannon Twp.	Clouded	11
Unknown—2	Clouded	18
Mumbwa, N.R.	Clouded	53
Parry Sound, Ont.	Clouded	200

Number and Character of Inclusions

The number of inclusions in most of the specimens is difficult to determine, because of their randomness and irregularity. However, in one specimen—from Spokane, Washington—the inclusions are of very similar size and regular shape. They are somewhat larger and less abundant than most of the inclusions seen in other specimens of garnet. A thin plate of this specimen was cut and polished to 0.295 mm. thick. By using a micrometer microscope method, the number of inclusions in the plate was determined to be 4.25 in each square, 0.1 mm. on the side. These values give the surprising total of 1,400,000 inclusions in a cubic centimeter.

(The great abundance of inclusions in most minerals casts doubt on their chemical analyses, unless the inclusions have been identified and their compositions subtracted from the total. This was discussed by Fischer (1871) at some length, but is often overlooked. Some metacrysts of garnet are more like rocks than minerals.)

Assuming that this garnet has a density of about 3.8, 0.5 cc. of the material previously prepared for decrepitation was weighed out and heated. The cumulative numbers of recorded explosions were recorded at each 20° interval. It was found that the slope of the cumulative number curve (the rate) was constant at least to 620°. The total number from 150°, when recording was started, to 620° was 850. After 650°, the

cumulative numbers increased in an exponential-like way with the following values:

t° C.	660	680	700	720	740
Cum. No.	900	1,400	2,000	3,000	4,600

The discontinuity of rate, from extrapolated intersection of the two curves, was found to be $661 \pm 10°$. This is higher than the value obtained by picking the discontinuity on the recorded rate —time curve ($624 \pm 10°$) but the two methods of graphical solution are not analogous. If the decrepitation continues at the above acceleration of rate, the number would reach 700,000, the calculated number of solid inclusions, at about 1,000°.

Another specimen of garnet –from Snohomish, Washington—also gave a relatively simple rate curve, but which started at a much lower temperature than the above, and the rate was decreasing at the highest temperature of the run. Therefore, the total number of recorded explosions in one stage of decrepitation could be determined more closely. Unfortunately, the number of inclusions could not be estimated visually. There are only a few solid inclusions in the clear amber-colored crystals lining the cavities, but the material decrepitated was the finer intergrowth underneath the clear crystals. Probably this garnet contains fewer solid inclusions than the garnet from Spokane.

Assuming a density of 3.5 for the Snohomish material, 0.5 cc. of the preparation previously used, was weighed out and heated. Feeble decrepitation took place at a constant rate up to at least 260°, by which time the cumulative number was 200. When the principal rate curve began near 326°, the number was 600, and at its peak near 450°, was 5,200. By 730° the number was 10,800.

Comparing the above two results, in the first 100° following the beginning of the higher temperature rate curves, the Spokane garnet gave approximately 6,200 recorded explosions, and the Snohomish garnet gave 2,900.

Discussion of Results

The results of decrepitation analysis of the various specimens of garnet are shown in Table 2, arranged alphabetically by location name. Under the heading of variety the compositional type is indicated as follows:

Gr (Grossularite, Ca-Al garnet),
Uv (Uvarovite, Ca-Cr garnet),
An (Andradite, Ca-Fe garnet),
Al (Almandite, Fe-Al garnet),
Py (Pyrope, Mg-Al garnet),
Rh (Rhodolite, Mg-Fe-Al garnet),
Sp (Spessartite, Mn-Al garnet).

TABLE 2

	Color	Variety	Type[1]	Decrepitation Temperatures			
				First	Second	Third	Fourth
Baffin Land, Can.	R	Al	Met			626	
Barton Mine, N. Y.	R	Al	Met			613	
Berggiesshubel, Saxony	G-Y	An	Mass		297	469	
Bishop, California	Y	Gr	Mass	175	318	375	
Ceylon	R-P	Al	Met			707	
Charlemont, Mass.	Br-R	Al	Met	(300)	(370)	628	
Dana Twp., Ont.	R	Al	Met		(350)	630	
Delaware Co., Penn.	Br-R	Al	Met	(250)	350	625	
Duckmaloi, N.S.W.	Br	Gr	Mass	(250)	300	414	
Dungannon Twp., Ont.	Y	Gr	Mass		332	472	
Emerald Creek, Idaho	R-P	Al	Met		(450)	683	
Fernwood, Idaho	R	Al	Met			590	
File Lake, Manitoba	R	Al	Met		(350)	617	
Forney, Idaho	R-Br	Al(?)	Met(?)		(250)	562	
Franklin, N. J.	Y-Br	An	Mass		268	510	
Franklin, N. J.	Bl-Br	An	Mass		(350)	534	
Graham Co., Ariz.	Y-G	An	Mass	(250)	(320)	594	
Jackson Co., N. C.	P	Rh	Met			660	
Kern County, Calif.	G	An	Mass		(320)	417	606
Langban, Sweden	Br	An	Mass		363	440	650
Lowell, Vermont	O	Gr	Mass	189	329	371	
Mitchell Co., N. C.	R	Al	Met		(350)	648	
Mumbwa, N. Rhod.	Br	Al	Mass	(220)	392	466	
Orford, Quebec	G	Uv	Mass	196	311	440	
Parry Sound, Ont.	R	Al	Met		417	660	
Peterborough, Ont.	Br-R	Al	Mass		(250)	661	
Plainfield, Mass.	Bl-Br	Sp	Mass	170	343	646	
Prince of Wales I., Alaska	Y-G	Gr	Mass		318	445	
Roxbury, Conn.	R	Al	Met	Indef.	351	632	
Russell, Mass.	R	Al	Met		(300)	580	
Salida, Colorado	Br-R	Al	Met		(350)	463	
San Diego Co., Calif.	Y	Gr	Mass	236	280	(350)	
Shelby, N. C.	R	Al	Met		280	526	
Snohomish, Wash.	Y	Gr	Mass		269	326	
South-West Africa	G	An(?)	Mass(?)		(250)	400	
Spokane, Wash.	R	Al	Met			624	
St. Just, Cornwall	Br	An	Mass		(330)	410	650
Unknown—1	R	Al	Met		(350)	568	
Unknown—2	R	Al	Met		339	610	
Unknown—3	R	Py	Met			615	
Wilberforce, Ont.	R	Al	Met		(250)	610	
Willsboro, N. Y.	Br	An	Mass		(350)	594	
Wrangell, Alaska	R	Al	Met			628	

[1] Mass (Massive or intergrown, even though it may be vuggy), Met (Metacryst type).

The decrepitation temperature tabulation is divided into four groups, according to character of rate curve and tentative interpretation of the cause of each stage. The probable limits of error of measurement are not shown in the table for the sake of simplicity, but these are recorded above if required. Approximate values are in parentheses.

The temperatures of beginning of the second and third stages of decrepitation as shown in Table 2, were grouped in 50° limits, and the number of occurrences of each value were added. The results are given in Table 3.

TABLE 3

Temperature Range	Number of Occurrences	
	Second Stage	Third Stage
150–200° C.	0	0
200–250	2	0
250–300	8	0
300–350	15	1.5
350–400	8	3
400–450	1.5	6.5
450–500	0.5	4
500–550	0	3
550–600	0	6
600–650	0	14
650–700	0	4
700–750	0	1

The values in Table 3 show four distinct relations:

1) The second stage of decrepitation begins most frequently near 325°;

2) The second stage of decrepitation does not begin much below 200° or much above 400°;

3) The beginning of the third stage of decrepitation has two peak frequencies, near 425° and near 625°;

4) The third stage of decrepitation does not begin much below 300°, or much above 700°.

When no account is taken of grouping in the above manner, all of the results show a distinct double curve of frequency of occurrence, with peaks near 340° and near 620°. Another relation which was noted during the decrepitation tests is that, in general, the ratio of rate of second stage decrepitation to the rate of third stage decrepitation is greater when the latter begins at a lower temperature. The temperature of beginning of the third stage of decrepitation also is related to the type of garnet. The average values are shown in Table 4.

The average temperature of beginning of the third stage of decrepitation of 17 calcium garnets is 446°, and that of 26 iron, magnesium, and manganese garnets is 611°. The majority of the third stage decrepitation values cannot be due to filling of aqueous fluid inclusions, because they are above the critical temperature of water. As derived in a previous paper (Smith 1952b), these values may represent the temperatures at which misfit of solid inclusions causes decrepitation. Therefore, they may represent the temperature of crystallization, subject to a small correction for the effect of pressure during formation. This interpretation is

TABLE 4

Variety	Average	Number
Grossularite	393° C.	7
Uvarovite	440	1
Andradite	487	9
Almandite	607	23
Pyrope	615	1
Spessartite	646	1
Rhodolite	660	1

strengthened somewhat by the fact that garnet of different composition (Franklin, N. J.), and garnet and related hornblende (Barton Mine, N. Y.) have similar decrepitation temperatures.

There are only a few experimental facts to which the above results can be compared. Flint, McMurdie & Wells (1941) synthesized grossularite and andradite by devitrification of glasses of the same composition in contact with steam at 500° C. and approximately 400 bars. No garnet was formed at 300°, 400°, and 600°. Pyrope was not synthesized, using similar methods. Belyankin & Petrov (1941) reported thermal effects of heating a hydrogrossularite (hibschite or plazolite—$3CaO \cdot Al_2O_3 \cdot 2SiO_2 \cdot 2H_2O$). An endothermal effect occurs at 650–690° and two exothermal effects occur at 870° and 940°. (It is possible that the feeble increase in decrepitation of some of the andradite garnets in the 600–700° range may be due to loss of water from somewhat hydrous material, this presumably giving the reported endothermic effect.) Hummel (1950) crystallized uvarovite from its constituent oxides at 855° and 1,400° C. at atmospheric pressure. Yoder (1950) did not synthesize grossularite at 600° at one atmosphere, but hydrogrossularite was formed by devitrification of calcium alumino-silicate glass in steam below 850° at 2,000 atmospheres. Yoder (1951) did not synthesize pyrope in the system MgO-Al_2O_3-SiO_2-H_2O at temperatures between 450° and 900° and pressures of steam up to

2,000 bars. It was concluded that pyrope is not stable in the high water concentrations of the experiments. Mme. Michel-Lévy (1951) crystallized spessartite from the component oxides in steam at 500° C. In order to form crystals containing some iron, higher temperatures, up to 700°, were needed, also the presence of Na_2SiF_6. No garnet was formed when the ratio of Mn to Fe in the charge was less than 1 to 9. Yoder & Keith (1951) made spessartite and yttrogarnet by devitrification of appropriate glasses at 1,080–1,970° C. at atmospheric pressure. Schairer & Yagi (1951) determined that almandite decomposes rapidly above 900° C. at atmospheric pressure.

The microscopic examination of inclusions in garnet did not disclose evidence that this mineral is formed by hydrothermal solutions. Those specimens with high temperatures of the third stage of decrepitation contain a few inclusions of glassy material, but most of the inclusions are of single crystals and aggregates of crystals. Those with low temperatures of the third state of decrepitation contain complex inclusions of an intergrowth of small crystals (probably siliceous), a liquid (probably aqueous), and a gas bubble. The three-phase type of inclusion was observed only in garnets which begin to decrepitate, in the third stage, below 550°. Inclusions with a small degree of filling, such as would be expected if deposition were in a gas phase, were not found in any of the specimens examined. The inclusion data suggest that siliceous solutions are responsible for the crystallization of garnet, but in the lower range of temperature, approaching 300°, the water content of the solutions may be substantial. The possibility of a pneumatolytic origin of garnet appears to be excluded.

There appears to be some prejudice by geological theorists against the concept of existence of siliceous magmatic derivatives down to such low temperatures as 300° C. (Ramberg, 1949). However, the experimental facts are not in disagreement. Friedman (1951) discussed the problem and showed that a silicate liquid containing Na_2O, SiO_2, H_2O, and Al_2O_3 is stable with silicate crystals down to at least 300° C. Smith (1948) determined that a complex hydrous silicate melt, approximating a granite magmatic derivative, is stable with silicate crystals down to 290° C.

Further Work

It is planned to continue this study in more specific directions, such as 1) a suite of metamorphic minerals closely associated with garnet, 2) garnet from zones representing different grades of metamorphism, and 3) growth zoning in large garnet metacrysts. The writer would like to receive specimens of garnet and related minerals from mineralogists interested in facilitating this research.

Acknowledgements

I wish to thank W. M. Little, A. D. Mutch, and P. A. Peach for assistance in the decrepitation procedure and interpretation, E. W. Nuffield for the *x*-ray diffraction analysis, and V. B. Meen, G. G. Waite, and F. Ebbutt for some of the garnet specimens. The electronic apparatus with which the determinations were made was constructed and tested under grants from the University of Toronto, and from a number of mining companies of Canada, United States, and South Africa. This assistance is gratefully acknowledged.

Conclusions

1. All of the common garnet minerals decrepitate when heated giving complex rate curves (decrepigraphs).

2. The complex decrepigraphs can be resolved into four types of curves, not all of which are evident in each decrepigraph.

3. Decrepitation starting below 250° C. is interpreted to be due to secondary inclusions and/or alteration in two specimens studied, and appears to be reasonable as an explanation in several other specimens in which a preliminary low temperature decrepitation occurs before one or more definite stages of higher temperature decrepitation.

4. Decrepitation starting between 250 and 400° C., most commonly near 325°, is interpreted to be due to filling of complex inclusions by the liquid phase, on the evidence of measured temperatures of filling, and of visual estimates of temperature of filling, under the microscope.

5. Decrepitation starting between 300 and 700° C., most commonly near 425° and 625°, is tentatively interpreted to be due to misfit of solid inclusions, on the evidence that the frequency of decrepitation increases with number of solid inclusions. This type of decrepitation gives an extended rate curve, with a peak rate between 100 and 200° from the beginning and with a much more rapid increase than decrease of rate of decrepitation.

6. Decrepitation between 600 and 700° C., which rises and falls in rate within about 50°, is tentatively interpreted to be due to loss of water from hydrogarnet.

7. The peak rate of decrepitation of the second stage generally is greater when the third stage starts at lower temperatures. The second stage is insignificant when the third stage begins in the 600–700° range.

8. The beginning of the third stage of decrepitation has an average value of 446° in the case of calcium-aluminium, calcium-iron, and calcium-chromium garnets, and 611° in the case of iron-, magnesium-, and manganese-aluminium garnets.

9. Garnets of different composition from the same locality, and garnet and associated minerals from the same rock, have very similar third stage decrepitation.

10. The experimental data on synthesis and thermal decomposition allow the working hypothesis that the temperature of beginning of the third stage of decrepitation is the temperature of crystallization (plus a correction for pressure, which has not yet been evaluated).

11. The types of inclusions in garnet suggest that siliceous liquids were present during crystallization, although aqueous solutions may also have been present during formation of some of the calcium garnets. No evidence was found for a pneumatolytic origin of any type of garnet.

References

Belyankin, D. S. & Petrov, V. P. (1941): The grossularoid group (hibschite, plazolite), *Am. Mineral.*, **26,** 450–453.

Fischer, H. (1871): *Kritische, mikroskopisch-mineralogische Studien.* Troemer, Freiburg.

Flint, E. P., McMurdie, H. F., & Wells, L. S. (1941): Hydrothermal and *x*-ray studies of the garnet-hydrogarnet series and the relationship of the series to hydration products of portland cement. *Jour. Res. U. S. Bur. Stand.*, **26,** 13–33.

Friedman, I. (1951): Some aspects of the system H_2O—Na_2O—SiO_2—Al_2O_3. *Jour. Geol.*, **59,** 19–31.

Hummel, F. A. (1950): Synthesis of uvarovite. *Am. Mineral.*, **35,** 324–325.

Ingerson, E. (1947): Liquid inclusions in geologic thermometry. *Am. Mineral.*, **32,** 375–388.

Kennedy, G. C. (1950a): Pressure-volume-temperature relations in water at elevated temperatures. *Amer. Jour. Science,* **248,** 540–564.

——— (1950b): "Pneumatolysis" and the liquid inclusion method of geologic thermometry. *Econ. Geol.*, **45,** 533–547.

Michel-Lévy, Mme M. C. (1951): Reproduction artificielle de grenats ferro-manganésifères: série almandin-spessartine. *Compt. Rend. Acad. Sciences, Paris,* **232,** 1953–1954.

Peach, P. A. (1949): A decrepitation geothermometer. *Am. Mineral.*, **34,** 413–421.

Ramberg, H. (1949): The facies classification of rocks: a clue to the origin of quartzofeldspathic massifs and veins. *Jour. Geol.*, **57,** 18–54.

Schairer, J. F., & Yagi, K. (1951): System FeO—Al_2O_3—SiO_2, *Geol. Soc. Amer.*, 1951 Ann. Meeting, Abstracts, p. 67.

Scott, H. S. (1948): The decrepitation method applied to minerals with fluid inclusions, *Econ. Geol.*, **43,** 637–654.

Smith, F. G. (1948): Transport and deposition of the non-sulphide vein minerals. III, Phase relations at the pegmatitic stage. *Econ. Geol.*, **43,** 535–546.

——— (1952a): History of inclusion thermometry. (In press)

——— (1952b): Determination of temperature and pressure of formation of minerals by the decrepitometric method. (In press)

——— & Peach, P. A. (1949): Recent advances in the laboratory study of ore. *Can. Mining Met. Bull.*, 351–353, 1949.

Yoder, H. S. (1950): Stability relations of grossularite. *Jour. Geol.*, **58,** 221–253.

——— (1951): Stability relations of clinochlore and cordierite in the system MgO—Al_2O_3—SiO_2—H_2O, *Geol. Soc. Amer.*, 1951 Ann. Meeting, Abstracts, p. 85.

——— & Keith, M. L., Complete substitution of aluminum for silicon: the system $3MnO \cdot Al_2O_3 \cdot 3SiO_2$—$3Y_2O_3 \cdot 5Al_2O_3$, *Amer. Mineral.*, **36,** 519–533.

THE FELDSPAR IN THE INTRUSIVE ROCKS NEAR BEAVERDELL, B. C.

L. Dolar-Mantuani, *The University of British Columbia, Vancouver, Canada.*

Contents

Abstract

The plagioclase and especially the potash-feldspar in the intrusive rocks near Beaverdell, B. C., were studied in considerable detail as an example for some general views on the feldspar as rock-forming minerals. General information on the Fedorov-Universal-Stage-Method as used by Nikitin is added.

Introduction

According to Reinecke (1915) two groups of intrusive rocks occur near Beaverdell, British Columbia. One is the Westkettle batholith which forms the western slope of Wallace Mountain, the second is the Beaverdell stock which intrudes the Westkettle batholith near Beaverdell. Recently W. H. White (1950) studied the silver deposits of the Beaverdell mining camp. During the preparation of his report, he asked me to determine the feldspars in a few specimens.

Although the number of thin sections examined is very small (5 thin sections of Westkettle rocks and 7 of Beaverdell rocks), data of the feldspars obtained by the Fedorov method seem to be interesting and worth publication.

General Information on the Rocks

Figure 1 made by W. H. White shows the location of rock samples described in this paper. It should be noted that the Highland Lass mine which on the map appears to be in the metamorphosed sediments and volcanic rocks of the Wallace group actually are in the underlying Westkettle rocks.

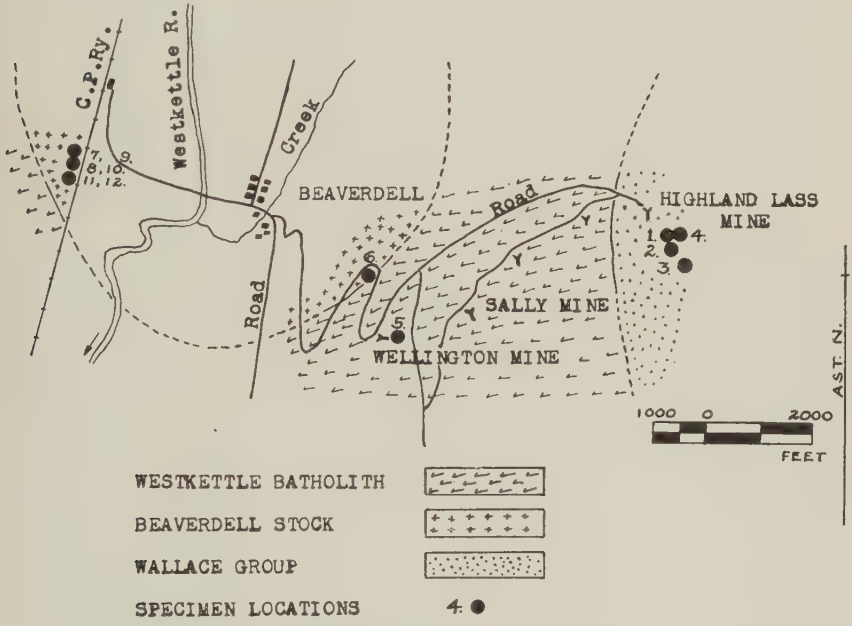

Fig. 1. The Beaverdell Silver Camp.

The following paragraph gives the classification of the samples according to Johannsen. For additional details the reader is referred to the above mentioned publication.

Thin sections No. 1, 2, and 3 represent the average quartz monzonite from the Highland Lass mine in the Westkettle rocks. Sample No. 5 is an albitic quartz monzonite from the Wellington mine, and sample No. 4 a leucocratic (albitic) quartz monzonite from the Highland Lass mine where it forms irregular tabular bodies and may represent segregations of more acid material or metasomatic alteration of the original quartz monzonite.

The other thin sections are made of mainly porphyritic rocks from the Beaverdell stock. Thin sections No. 6, 7, and 8 represent the groundmass, thin sections No. 9 and 10 the phenocrysts of specimens No. 7 and 8 respectively. Specimen No. 6 is taken right from the border, the other

two from a more internal part of the stock. The groundmass of these three samples is granodioritic; No. 6 is an almost leucocratic, No. 7 an albitic, and No. 8 an albitic and almost leucocratic porphyritic granodiorite. But all three samples are very close to the respective variations of quartz monzonites if also the amount of phenocrysts (about 10 per cent) is considered.

Thin sections No. 11 and 12 are still more leucocratic rock which occurs in small irregularly tabular bodies having gradational contact with the normal Beaverdell rock. As this sample is not described in the publication mentioned, a short description may be added. The rock is generally fine-grained in contrast to the other medium- to coarse-grained samples of the stock. It shows a very typical granophyric intergrowth of quartz with plagioclase and potash-feldspar, which could develop as result of some sort of replacement or synantetic process (H. Backlund, written communication). The constituents are: quartz 33.0%, plagioclase 36.3%, K-feldspar 29.3%, and magnesium-iron minerals (magnetite, epidote, chlorite) 1.4%. The specimen is a leucocratic (albitic) quartz monzonite. The ratio of plagioclase to K-feldspar cited above is only approximate, and the non-granophyric parts suggest that, on the contrary, K-feldspar prevails over plagioclase. Even so, the rock would be classed as a quartz monzonite as the limits for this quartz monzonite are 42% K-feldspar and 23% plagioclase. The measured percentage of constituents and the composition of the plagioclase show a very close relationship to the leucocratic Westkettle rock (No. 4 of the Highland Lass mine).

For the determination of the constituents, especially the feldspar, the Fedorov method was used in its classical application as given by my teacher, the late Prof. V. V. Nikitin. Because of some deviations and modifications of the Fedorov method found in the literature of the last years a few notes are included on the details of some determinations and the recording of the observed data as used by Nikitin who was connected with the Fedorov method from its beginning in 1893 till his death in 1942.

General Notes about the Fedorov Method

The Fedorov or the Universal-Stage method is the basic method which gives exact data on both the composition and the crystallographic habit of feldspar in thin sections of rocks. As the habit of feldspar seems to become more and more important in petrologic studies (cf. Koehler, 1949, p. 597 and Tuttle & Bowen, 1950, p. 583) their crystallographic elements should be studied carefully. In this connection some details of the work, especially with the feldspar, have to be explained.

As is generally known in using the Fedorov method, the position of the three symmetry axes of the optical indicatrix in a twinned grain are de-

termined together with the twin axis (which is deduced from the position of X, Y, and Z in both subindividuals) with the greatest accuracy. In addition it is always desirable to try to determine as exactly as possible the position of other crystallographic elements. As the measurements of the crystallographic elements are generally less sensitive than those of the indicatrix axes, the tilting angle should be read at least four times on Wright's folding arcs for the S–N axis, using a Leitz universal stage or a stage of a similar type. The crystallographic elements do not only supply additional data for determination of the composition of the plagioclases but may also be of essential use in deciding which curve, and in special cases, which part of a curve of the standard diagram should be used (e.g. for the albite twinning of the alcalic plagioclases; cf. Turner, 1937, p. 396). In the case of K-feldspar they may offer the only criterion for the kind of K-feldspar present in thin sections of rocks. But it is important to realize that in the presence of the sanidine optics with the optic plane parallel to (010) (sanidine, some adularia; Chaisson, 1950, p. 546) the coordinates of the crystallographic elements change entirely from those which are found in some classical books and diagrams (e.g. Nikitin, 1936). In these cases even the identification of (010) or (001) may be difficult. Also the angles between all crystallographic elements should be established from the observation diagram because they have to be regarded together with the coordinates of the elements for selection of the curves and poles in the standard diagram.

Thus in the present study the optic axial angles were read at least four times. The position of the emergence of the optic axis was determined using the gypsum plate. The sensitive tint was always tested by noting the colour produced by it at holes in the rock section to allow for possible anisotropism of the glass slide.

Using the findings of Nikitin (1936, p. 14) the set of hemispheres with $n=1.516$ and a liquid with $n=1.52$ was used not only for examination of feldspars but also hornblende. (The second set of hemispheres at my disposal had $n=1.649$.) In this way I had a set with following refractive indices: lower hemisphere $n=1.516$, liquid $n=1.52$, glass plate $n=1.51$–1.53 (Nikitin, 1936, p. 14), liquid $n=1.52$, slide $n=1.51$–1.53, Canada balsam $n=1.54\pm0.01$ (Winchell, 1951, p. 333), mineral?, Canada balsam $n=1.54\pm0.01$, cover glass $n=1.51$–1.53, liquid $n=1.52$, upper hemisphere $n=1.516$. The difference between the inevitable refractive indices as enumerated and that of the hemispheres with $n=1.516$ is 0.006–0.034, that with $n=1.55$ (not available to writer) is 0.000–0.040, and that with $n=1.649$ is 0.099–0.139.

For accuracy and speed the construction of the microscope and universal stage is important in every detail. During the practice with the Fedorov method the writer had occasion to work with the theodolite

microscopes of C. Leiss and R. Fuess of Steglitz, near Berlin over a period of 15 years and with the universal stage-microscope of E. Leitz, Wetzlar for two years. She found the first two models corrected according to the suggestions of Nikitin to be the most suitable ones.

Determination of the Feldspar by the Fedorov Method

The migration curves for low-temperature plagioclase. For the determination of the crystallographic elements of the feldspar and the plagioclase composition, Nikitin's standard diagram (1936, Table VII) was used. Many workers prefer Nikitin's curves for determination of low-temperature plagioclase. In this connection, Larsson (1940) states that the position of the poles of plagioclases from the Nygård-pluton and the W. Swedish hyperites correspond best with Nikitin's curves for $\perp(010)$, $\perp(001)$ and the rhombic section:

> "Nikitin's curve (for $\perp(010)$) in the majority of cases seems to answer most closely to the conditions and is, therefore, to be given preference. Also the calibration of the curve by Nikitin is likely to be the most reliable one, as it is based upon more abundant and modern sources of measurements and analyses" (p. 366).

In agreement with this Lundegårdh (1941) uses Nikitin's curves for the bytownite from the anorthosite and states that the three curves mentioned correspond best for the basic plagioclases of intrusives (1941, p. 429). But Barth & Oftedahl state "The most complete curves are those of Duparc and Reinhard and used by Winchell in his Optical Mineralogy" (1947). It seems, however, that they refer to the plagioclase curves from 1924. Nikitin's three publications in the years 1926, 1929, and 1933 (the first two in Russian, the third in German) deal with corrections of the plagioclase curves based on determinations with the Fedorov method and partly new chemical analyses (Nikitin, 1936, p. 8).

On the other hand the following statement of Kaaden cannot be accepted: "It is only logical that Nikitin (1936) used average values (for low and high temperature plagioclases) for the construction of his determination curves" (1951, p. 11). From the cursory control of Nikitin's coordinates of 14 main faces and twin axes for An_0 and An_{100} with the analogous coordinates for low and high temperature plagioclases as listed by the same author (p. 20), it follows that only two-thirds of the 24 poles of Nikitin lie closer to the high temperature poles than those listed by Kaaden as standard low temperature poles of plagioclases of the same composition. Generally the distance of Nikitin's poles to the other low temperature poles is much smaller than to the high temperature poles. Only in four cases did the former distance exceed the latter and the poles lie almost within the range of determinative errors. This shows, furthermore, that the work on the correction of curves for the determination of the composition of plagioclases has to be continued.

The main constituents of the rocks near Beaverdell are feldspars. Plagioclase and potash-feldspar are found in all sections regardless of the amount of mafics. The plagioclase grains are subhedral, those of potash-feldspar are always anhedral. A strong replacement of plagioclase by potash-feldspar and both by quartz is visible in the Westkettle rocks, and to a much smaller extent in the groundmass of the average rocks from the Beaverdell stock.

Many of the potash feldspar show perthitic structure. Although some grains, especially those of plagioclase, are heavily altered a sufficient number of grains occurs in every thin section to permit the determination of the feldspar by the Fedorov method.

Recording the data. The general symbols for the crystallographic elements are:

B—the twin axis,
D—the composition plane,
L—the twin lamellae,
S—the cleavage plane,
K—the outline face,
RS—the rhombic section,
I—the plane of regular (dusty) inclusions,
j—the core,
s—the middle part,
p—the border zone of a zoned subindividual of a twin or of an untwinned grain.

In the tables the data are arranged in columns as follows:

1. The number for reference of the particular grain in the thin section.

2. The symbol of the crystallographic element (e.g. B, D etc.). Some symbols have a number or a letter as a suffix. The number indicates to which subindividual (e.g. twin lamella) of the grain the element belongs, the letter to which zone in a zoned plagioclase. The exact crystallographic habit is easily understood from the tables for every grain examined; e.g. in grain No. 3 thin section No. 1. The composition face (D) is developed parallel to the twin lamellae (L) in both subindividuals. Beside this a second set of twin lamellae (L′) occurs to which the cleavage face (S) is parallel but visible only in the second subindividual; etc.

3. The coordinates of the crystallographic element, i.e. the values of angles between the element and the axes X, Y and Z. It is important to use a comparative standard diagram which takes into account all three angles to X, Y, and Z because only all three coordinates define the exact position of the pole in the standard diagram and control the accuracy of the work at the same time.

4. The crystallographic symbol of the element.

5. The composition in percentage of anorthite in plagioclase, or the kind of potash-feldspar.

6. The distance and the direction of the determined pole to the migration curve or the pole in the standard diagram. This distance shows the exactness of the determination, it indicates perhaps certain characteristics in the development of the feldspar in the rock, and it may offer a help in the determination of the average composition of a grain when it becomes evident that the more distant poles should be omitted.

7. The angles between the different crystallographic elements.

8. The value of the optic angles. Figures in italics indicate angles determined by the visible emergence of *both* optic axes, giving such numbers the weight two in calculation of any average.

9. The average composition of the grain. The average composition of a plagioclase grain is calculated from the different crystallographic elements in the following way: The values which result from the twin axes are taken into consideration four times; those of the composition face (if it is given for two subindividuals together in the less exact measurements) twice, and of the remaining elements once for every subindividual. The twin axes of zoned grains are naturally not used for determination of the composition as they give only the mean value of both subindividuals which are used for the determination of the twin law.

At this point the need of publication of the coördinates should be emphasized because they are directly obtained from the plotting diagram and preserve their values regardless of the eventual changes in the comparative curves of the standard diagrams. A certain change of the comparative curves is not only to be expected for the high temperature plagioclases (Koehler, 1949, p. 595) but also to a much smaller degree for the low temperature plagioclases. On the other hand the publication of extensive data offers the possibility of evaluating the conclusions and of continuing the research in related fields on the basis of work done by others.

Finally it is to be noted that for the determination of feldspar the thin sections should not be too thin. A thickness of 0.03 to 0.04 mm. is desirable. In special cases of exact determination of the crystallographic elements, especially of the potash-feldspar with their low refractive indices and birefringence, still thicker thin sections should be used. If the thin sections are not covered so that the cleavage fissures are partly filled with air, a still greater accuracy in the determination of cleavage faces is obtained (Dolar-Mantuani, 1931). But in addition normal thin sections should be made to prevent the fine twinning structure in the triclinic potash-feldspar becoming invisible.

Notes about particularities of grains are given at the end of the data for every thin section. They explain many conclusions which are made in the last two sections.

TABLE 1. DETAILED DATA ON FELDSPAR FROM THE WESTKETTLE ROCKS
Thin section No. 1

1	2	3			4	5. An %	6		7. L∧S	8. 2V	9. An %
					Plagioclase						
1	L	14°	83°	78°	⊥(010)	31	NNE	10°			31
2	D=L_1	24	66	87	⊥(010)	43	SW	3½			
	2	16	77	80½	⊥(010)	36	NNE	7			
	3j=p	20	70	88	⊥(010)	39½	SSW	2			
	s	26	65	85	⊥(010)	45½	SW	3½			1=2=40
	$B_{1/2}$	19½	71½	83	⊥(010)	40½	NNE	3			3j=39½
	$B_{1/3s}$	70	51½	45½	[001]						s=45½
	$B_{2/3j}$	82	44½	46	⊥[001] / (010)						p=39½
3	D=L_1	10½	80½	85	⊥(010)	31	N	3		1=−86°	
	2	13	77½	88	⊥(010)	33½	S	½		2=−88	
	L′=S_2	74	16½	84½	⊥(001)	33½	NW	3	87		
	$B_{1/2}$	11½	79	86½	⊥(010)	32	N	1½			32
4	D=L_1	14	77	85½	⊥(010)	34½	N	2½		1=−78	
	2	18	72	90	⊥(010)	37½	SSW	3½		2=−82	
	$B_{1/2}$	17	75	82½	⊥(010)	37	NNE	4½			36½
5	L	9	81	87	⊥(010)	29½	N	1			29½
6	D=L_1	9½	80½	88½	⊥(010)	30		0		1=−75	
	2	10½	79½	88	⊥(010)	31		0		2=−75	
	S_1	79	11½	86	⊥(001)	27	NE	1	88½		
	2	81	9	88	⊥(001)	26½	SW	2			
	$B_{1/2}$	10	80	89	⊥(010)	31	S	½			30
7	L_j	25	65½	85	⊥(010)	44½	SW	3		2j=+81	
	p	21	69	87½	⊥(010)	40	SSW	2½		p=+83	
	S_j	63	29	80	⊥(001)	41½	SE	2½	88½		j=43
	p	67	23	87	⊥(001)	35½	SE	3			p=38
					Potash-feldspar						
8	L=S	12½	77½	89½	⊥(010)	Micr	SSW	15		−80	
					or	Or	E	12½			
	L′=S′	71½	84	19	⊥(15.0.$\bar{2}$)	Micr	ENE	2⅕	83½		
					or	Or	ENE	18½			
9	S	83½	6½	87½	⊥(001)	Micr	SW	6½		90	
10	L	12	79	85	⊥(010)	Micr	SSW	11½		72	
					or	Or	WNW	12			
	L′	78	88	12	⊥(15.0.$\bar{2}$)	Micr	NW	6½	82		
					or	Or	NE	16			
11										−82	

Grain 4: As inclusion in the K-feldspar.
Grain 10: The determination of 2V is difficult as the thin section is too thin.
Grain 11: A very large grain with twin lamellae only in one corner.

Thin Section No. 2

1	2	3			4	5. An %	6		7. L∧L′	8. 2V	9. An %
					Plagioclase						
1	D=L1/2	17°	77°	79½°	⊥(010)	36½	NNE	8°		1=+83°	
	B1/2	15½	75½	84	⊥(010)	36½	NNE	3½		2=+87	36½
2	D=L1	19	71½	85½	⊥(010)	39½	NE	½		1=−74	
	2	17	73½	86½	⊥(010)	37	N	½		2=+80	
	3	11	81	84	⊥(010)	31	NNE	4½		3=−88	
	B1/2	74	44½	50	[001]	42½	NW	4½			
	B1/3	84	52	38½	⊥[001] / (010)	43	WSW	3½			
	B2/3	13½	77½	85	⊥(010)	34	N	3			39
3	L	9½	81	86	⊥(010)	30	N	2			30
4	L1=Sj	70	26	74	⊥(001)	42	NW	6½		1j=+*76*	1j=42
	s	74	17	84	⊥(001)	33	NW	3		s=+*74*	p=32½
	p	73½	16½	88	⊥(001)	33½		0		p=+*82½*	s=33
	p1	76	14	86	⊥(001)	32	NW	2½		p1=+*80½*	p=32½
					or	28	NE	2½			
	L=S2	78	13	86	⊥(001)	27½	NE	2			s=33
					or	31	NW	3½			
	L′2	16	74	86	⊥(010)	36½	N	1			p=32½
	B1s/2	76	36	57	[001]	35½	NW	1			p1=28
											2=34
5	D=L1	13½	77	88½	⊥(010)	34	S	½			
	2	18½	72	86½	⊥(010)	38½		0			
	3	12½	82	80	⊥(010)	30½	N	7			
	4	18	72	89	⊥(010)	38	SSW	2½			
	B1/2	15½	75	86½	⊥(010)	36	N	1			
	B3/4	14	77	85	⊥(010)	34½	N	2½			
	B1/3	77	27	66½	[001]	31	SE	4½			
	B2/4	75	30½	64	[001]	33	SE	4			
	B1/4	83	68	23	⊥[001] / (010)	30	NE	6			
	B2/3	87	64	26	⊥[001] / (010)	30½	NE	½			32
					Potash-feldspar						
6	L	78½	82	14	⊥(15.0.$\bar{2}$)	Micr	W	5			
					or	Or	ENE	12½			
7	L	81	84½	10½	⊥(15.0.$\bar{2}$)	Micr	WNW	8	90		
	L′	10	86½	80½	⊥(010)	Micr	SE	8			
8	L	22	77	72½	⊥(010)	Micr	W	5½	88		
	L′	76½	81½	16	⊥(15.0.$\bar{2}$)	Micr	W	3½			
9	L	17	78	78	⊥(010)	Micr	SW	6	77		
	L′	77½	84	14	⊥(15.0.$\bar{2}$)	Micr	WNW	4½			

Grain 2: A larger grain; on a margin replaced by quartz.

Grain 3: It forms an inclusion in the large chadacryst No. 8.

Grain 4: The appearance of the grain is unusual for a Carlsbad twin. The second subindividual forms only a corner of the larger subindividual. The coordinates of the twin axis correspond to those of a Carlsbad twin and so does the angle between $\perp(001)_1$ and $\perp(001)_2 = 56°$, according to $[001] \wedge \perp(001) = 28°$ (Nikitin, 1936, diagram VI) and $\rho_{(001)} - 27°02'$ (for albite; Goldschmidt, 1897). The core of the grain is very heterogeneous; Almost 14 zones are visible between "p" and "j" zones, repeating mainly the compositions of "p" and "s" zones. The difference in the composition which follows from the extinction angles is greater than that found by the Fedorov method. The data for "p_1" give a composition of An_{28} because the distances of Z, Y, and X of this zone and of the zone "p" with $An_{33\ 1/2}$ are greater than they would be in the case of An_{32}. The border "p_1" shows a parallel intergrowth of two minerals, probably andesine and quartz, perpendicular to the margin.

Grain 5: In the subindividual 3 the more peripheral part is determined. A slight zoning is visible.

Grain 6: The other set of twin lamellae is not clear enough for measurement.

Grains 7 and 8: The lamellae are measured in the part with twin texture and the optical indicatrix in that with almost homogeneous extinction.

Thin section No. 3

1	2	3			4	5. An %	6		7. L∧L′	8. 2V	9. An %
					Plagioclase						
1	D=L_1	15°	76°	86°	⊥(010)	35½	N	2°		1=+83°	
	2	20	70	89	⊥(010)	39½	SSW	3			
	3	15½	75	85	⊥(010)	36	N	2			
	$B_{1/2}$	84½	63	28	⊥[001] / (010)	34	NE	2			
	$B_{2/3}$	75	30½	64	[001]	33	SE	4			
	$B_{1/3}$	15	75	89	⊥(010)	35½	S	1½			34½
2	D=L_1	13½	77½	84½	⊥(010)	34	N	3½		1=−82	
	2	18½	71½	89½	⊥(010)	38	SSW	3		2=+80	
	$B_{1/2}$	15½	75	86½	⊥(010)	36	N	1			36
3	D=L_1	12	79	86	⊥(010)	32½	N	2	87°		
	2j	20	70	86	⊥(010)	39½	SSW	3			
	p	11	79	89	⊥(010)	32	S	1			
	L_4'	81	12	82	⊥(001)	24½	NE	3			
					or	30½	NW	8½			
	2j	67	27	78	⊥(001)	41½	NW	2			1=31½
	p	76	17	80	⊥(001)	26	NE	7			2j=40½
					or	34½	NW	7			
	$B_{1/2p}$	11½	78½	88	⊥(010)	32		0			p=33
4	D=L=S_1	18	72½	85½	⊥(010)	38	N	1			
	2	18	75	80½	⊥(010)	38	NNE	6½			
	$B_{1/2}$	18	73	80	⊥(010)	38	NNE	7			38

Potash-feldspar

5										−84
6	L	16	80	78	⊥(010)	Micr	SW	4½		
7	S	82	14½	78	⊥(001)	Micr	NW	4		−87

Grain 2: The lamellae are slightly bent.

Grain 3: In both cases the higher value is taken, corresponding to the albite twin axis (An_{32} sharp).

Grain 4: Inclusion in the microcline No. 7.

Grain 6: The grain is mainly homogeneous with a slightly developed perthitic structure. The lamellae are measured in small patches which show characteristic net texture.

Grain 7: The largest grain of microcline in the thin section. Inclusions of quartz and some slightly altered, subhedral plagioclases. *Y* shows a homogeneous, *X* a heterogeneous extinction. The twin lamellae present are not sufficiently constant for measurement. "S" is a very fine, not clearly visible cleavage.

Thin section No. 4

1	2	3			4	5. An %	6		7. L∧L′	8. 2V	9. An %
						Plagioclase					
1	L	11°	79°	88°	⊥(010)	10½°		0			10½
2	L	17	74	85	⊥(010)	2	NE	3½°		+80°	1
					or	37	N	3			
3	L_1	10½	79½	88	⊥(010)	11		0			
	$D_{1/2}$	79	25½	68	RS	1	W	1			
	$B_{1/2}$	12½	78	88	[010]	3½	NE	½			4
4	$D=L_{1/2}$	10	80	88	⊥(010)	11½		0			
	$B_{1/2}$	10	80	87	⊥(010)	11½	N	1			11½
5	$D=L_{1/2}$	6	84	89	⊥(010)	15	S	1			
	$B_{1/2}$	6½	83½	87½	⊥(010)	14½	N	½			15
						Potash-feldspar					
6	S	90	9	81	⊥(001)	Or	N	4		−83	
					or	Micr	W	10½			
7	L	18	75½	80	⊥(010)	Micr	SW	9		−79	
	L′	72	89	18½	⊥(15.0.$\bar{2}$)	Micr	NNE	7	82°		
8	S_1	12½	77½	89	⊥(010)	Micr	SE	8		1=−78	
	$B_{1/2}$	80	12	83	⊥(001)	Micr	SW	1		2=−79	
9	L	20	79½	73	⊥(010)	Micr	W	3			
10	L	71	19	88½	⊥(001)	Micr	SE	10½		−81	
	L′	72	89	18	⊥(15.0.$\bar{2}$)	Micr	NNE	6	82½		

Grain 3 and 5: The refractive index is lower than that of Canada balsam.

Grain 6: The central part is almost without lamellae.

Grain 8: "D" is parallel to (001) but it is impossible to measure it. Only two lamellae

corresponding to (010) are visible in subindividual 1 and patches of perthitic intergrowth in both. The subindividual 2 was developed in the form of a lamella.

Grain 10: The axes of the indicatrix are measured in the homogeneous part of the grain.

Thin section No. 5

1	2	3			4	5. An %	6	7. L∧S L∧L′	8. 2V	9. An %
					Plagioclase					
1	D=$L_{1/2/3}$	15½°	74½°	88½°	⊥(010)	3	NE 1°		1= 90°	
	$B_{1/2}$	76	27	67	⊥[100]	3½	NW 2½		2=−82	
					(010)					
	$B_{2/3}$	82½	70	22	[100]	3	E 2½			3½
	$B_{1/3}$	15	75	89	⊥(010)	4	NE ½			
					or	6	NW ½			
2	D=$L_{1/2}$	16	74	88	⊥(010)	2½	NE 1	88½°	1=+86	
					or	5½	NW 2			
	S_2	77	19	77	⊥(001)	8	SE 5½		2=−87	
	$B_{1/2}$	73½	18½	81½	[001]	4½	NE 1½			5
3	D=$L_{1/2}$	79	20	73	RS	1	W 1		2=+81	
	$B_{1/2}$	11	79	87½	[010]	3	NE 1½			2½
4	D=$L_{1/2}$	16	76	86	⊥(010)	1	NNE 5½		2=+82	
					or	7½	NNW 5½			
	$B_{1/2}$	16	75	82	⊥(010)	1	NNE 5½			8
					or	8	NNW 6			
					Potash-feldspar					
5	L	73	86	17½	⊥(15.0.$\bar{2}$)	Micr	W 8½			
	S	23	74	74	⊥(010)	Micr	W 8½			−76½
	S′	73	52½	43	⊥($\bar{1}$11)	Micr	WNW 4			
6	S	80½	11½	83	⊥(001)	Micr	SW 2			−86
7	S	84	11	81	⊥(001)	Micr	W 4½			
					or	Or	NE 6½			
8	L_1	23	73½	75	⊥(010)	Micr	W 9	90		
	2	15	87	75	⊥(010)	Micr	E 5			
	3	3½	88	88	⊥(010)	Micr	SSE 15			
					or	Or	NW 3½			
	4	14	79	81½	⊥(010)	Micr	SSW 7½			
					or	Or	NW 14			
	L_1′	76	84	15	⊥(15.0.$\bar{2}$)	Micr	NW 3½			
	2	75	87	15	⊥(15.0.$\bar{2}$)	Micr	N 4½			
	3	87	86	5	⊥(15.0.$\bar{2}$)	Micr	WNW 14			
					or	Or	NNE 8½			
	4	84½	84	9	⊥(15.0.$\bar{2}$)	Micr	WNW 10½			
					or	Or	NE 8½			
	$B_{1/2}$	18	80	75	⊥(010)	Micr	SW 2			
9	S	74	80	19	⊥(15.0.$\bar{2}$)	Micr	SSW 3			−80

Grain 4: The value of An_8 corresponds exactly to that deduced from $2V = +82°$.

Grain 5: A twin net occurs only in a part of the grain. The optic indicatrix is measured in the homogeneous part. "S" corresponds to an irregular and therefore not exactly determined parting. The angles between the faces are $L \wedge S = 89°$, $L \wedge S' = 55°$, and $S \wedge S' = 73°$. They correspond to the angles $\perp(010) \wedge \perp(15.0.\bar{2}) = 89\frac{1}{2}°$, $\perp(15.0.\bar{2}) \wedge \perp(\bar{1}11) = 62\frac{1}{2}°$ (Nikitin, 1936, table VI), and $\perp(010) \wedge \perp(\bar{1}11) = 63°$ (Gilbert & Turner, 1949, p. 15).

Grain 6: The extinction is mainly homogeneous. In one corner of the grain an irregular wide lamella is developed but the tilting angle for its determination is too large.

Grain 7: The grain has dusty inclusions but less than the normal plagioclase. The extinction, especially parallel to *X* is in patches and does not show twin lamellae.

Grain 8: A large oikocryst with chadacrysts of plagioclase. The indicatrix is measured in different points of the grain: 1. in a large homogeneous area; 2. in a small homogeneous area in the form of lamella; 3 and 4. in different spots which show a clear twin net. *Y* is almost perpendicular to the stage. "L" is also the composition plane of subindividuals 1 and 2.

Grain 9: Regular cleavage with dusty inclusions; only in one part the twin net is visible but it is not sufficiently clear to be measured.

TABLE 2. DETAILED DATA ON FELDSPAR FROM THE BEAVERDELL ROCKS
Thin section No. 6

1	2	3			4	5. An %	6		7.	8. 2V	9. An %
					Plagioclase						
1	L=S	7½°	86°	83½°	⊥(010)	16	N	4½°	89°	+88°	
	S′	89	13	77	⊥(001)	16	NW	2			16
2	D=L_1	9	81	87½	⊥(010)	12½	N	½			
	2	5	85	89	⊥(010)	16	S	1			
	$B_{1/2}$	3	87½	88½	⊥(010)	18	N	2			17
3	L_j	85	7½	84	⊥(001)	22½	SW	1		j=−89	j=22½
	s	89	7	83	⊥(001)	19½	SW	2		p=−88	s_1=22½
	p	80	18	75	⊥(001)	10	SE	2½			p=10
4	D=L=S_{1j}	3	88	88	⊥(010)	18½	N	1		j=+86	
	p	8½	82½	89	⊥(010)	13	S	1		p=+88	1j=18½
	2	8	82	89½	⊥(010)	13	S	1½			p=13
	$B_{1p/2}$	8	82	86	⊥(010)						2=13
5	S	88½	14½	75½	⊥(001)	15	NW	2		+88½	15
					Potash-feldspar						
6	S	89	6	84	⊥(001)	Or	NE	1		−67	
	i	88	21	69	⊥(001)	12	NW	7		i=+87	
	S′	74	73	23½	⊥(110)	Or	WNW	14½			
	i	69	86½	21½	⊥(1$\bar{1}$0)	12	NW	7			
	S″	81	45	46½	⊥(111)	Or	W	18			
	i	76	32	63	⊥($\bar{1}$11)	2½	NW	2			i=12
7	S	89	7	83	⊥(001)	Or	NE	2		−66½	
	S′	87	76	14	⊥(15.0.$\bar{2}$)	Or	SE	3½	69°		
8	S	77	13	87½	⊥(001)	Or	ESE	13		−67	
	S′	87	78	12	⊥(15.0.$\bar{2}$)	Or	W	3	75½		
9	S	85	5½	87½	⊥(001)	Or	E	5½		−68	

Grain 3: "j" is the almost euhedral main part of the zoned grain. The small zone "s" near the border is followed by a zone of the same composition as the core. "p" is the border, anhedral in relation to the nearby minerals and strongly different in composition from the other part of the grain.

Grain 4: The composition of one system of lamellae changes from one side of the grain to the other across the lamellae. The lamellae of the second system are very small and measurable on only one side.

Grain 5: No lamellae are visible in the grain but 2V is clearly positive.

Grain 6: Microperthitic structure is very clear. The included plagioclase is marked with "i." S corresponds to a fine cleavage; S′ to a parting and to one boundary of the plagioclase inclusion of the perthitic intergrowth; S is not very clearly visible and corresponds to the second boundary of the intergrowth. The symbols of the faces S′ and S″ are chosen according to the fast that their poles for the included plagioclase must lie near a curve which gives a reasonable anorthite value. This must correspond in the best way with that obtained from (001) as the face most exactly determined. The measured angles between the faces are: S∧S′=68°, S∧S″=52°, and S′∧S″=62°. The angles between these faces are: ⊥(001)∧⊥(110)=67½°, ⊥(001)∧⊥($\bar{1}$11)=54°, and ⊥(110)∧⊥($\bar{1}$11)=58½° (Nikitin, 1936, table VI).

Grain 8: S is the main cleavage; sericite inclusions are parallel to this cleavage. Perthitic inclusions are parallel to S′.

Thin section No. 7

1	2	3			4	5. An%	6		7. L∧S	8. 2V	9. An %
					Plagioclase						
1	D=L_1	19°	71½°	87°	⊥(010)	0	NW	1°		1=−85°	
	2	24	67	85	⊥(010)	0	NW	6		2=−82	
	3	24	66	85½	⊥(010)	0	WNW	6			
	4	19½	71	84½	⊥(010)	0	NW	3			
	$B_{1/2}$	68½	24½	78½	[001]	0	NE	7			
	$B_{2/3}$	24	66	87	⊥(010)	0	WNW	6			
	$B_{1/3}$	86	82	8	⊥[001]	5½	E	1½			1½
					(010)						
2	D=$L_{1/2}$	15½	75	85	⊥(010)	2	NE	3½	86½°		
					or	7	NW	3½			
	L'_1	82	8½	88	RS	8½	W	1½			
					or	10½	N	1			
	$B_{1/2}$	75	16	83½	[001]	4½	SW	1			4½
3	D=L=S_1	88	21	69	⊥(001)	11½	NW	6½		1=+86	
	p	88	23	67	⊥(001)	11	NW	8		p=+86	
	2	86½	15	75½	⊥(001)	14	NW	1½		2=+74	
	3	72½	21½	78	⊥(001)	5	SE	9½			
	$B_{1/2}$	85½	77½	17½	[100]	10		0			
	$B_{2/3}$	12½	78	86	⊥[100]	5½	NW	1½			
					(001)						
	$B_{1/3}$	80	18	75	⊥(001)	10	SE	3			9
4	D=$L_{1/2}$	17	75	82	⊥(010)	0	NE	6½		2=+87	
	$B_{1/2}$	74	17	85	[001]	1½	SW	1½			1
5	L	22	68½	86	⊥(010)	0	WNW	4		90	0

6	D=L_1	19½	70½	89	⊥(010)	0	SW	2		1=−86	
	2	8½	82	87½	⊥(010)	13½	N	½		2=−85	
	3	21½	69	85½	⊥(010)	0	WSW	3½		3=+88	
	4	9½	81	87	⊥(010)	12½	N	1		4=−79	
	$B_{1/2}$	14	76	89	⊥(010)	6½	NW	½			
	$B_{3/4}$	15	75	89½	⊥(010)	5	N	½			
	$B_{1/4}$	75	19	79	[001]	7	NNE	4			
					or						
					⊥[100] (010)	11	SE	7			
	$B_{2/3}$	75	18½	79	[001]	8	NE	3			
					or						
					⊥[100] (010)	11½	SE	7			
	$B_{1/3}$	86	79½	11	⊥[001] (010)	10	ESE	3			
					or						
					[100]	16½	E2½				
	$B_{2/4}$	89	78½	11½	⊥[001] (010)	12	E	½			
					or						
					[100]	16	W	1			8

Potash-feldspar

7	S	86½	12½	78½	⊥(001)	Or	NE	7½			
					or	Micr	NW	7½			
8	S	82½	9½	84	⊥(001)	Or	E	7	74	−76	
					or	Micr	SW	4			
	S′=I	69	83	22½	⊥(15.0.$\bar{2}$)	Micr	E	4½			
9	S	82	12	81	⊥(001)	Or	NE	9		−74	
					or	Micr	WNW	2½			
	p	84	13½	78	⊥(001)	Or	NE	9		p=−68	
10	S=I	86	85	5½	⊥(15.0.$\bar{2}$)	Or	NE	8		−62	
11	S	83½	13½	78½	⊥(001)	Or	NE	9½	74	−70	
	I	83½	85½	8	⊥(15.0.$\bar{2}$)	Or	NE	10			
12	S	87½	8	82	⊥(001)	Or	NE	4	69	−72	
	S′	90	76	14	⊥(15.0.$\bar{2}$)	Or	S	1½			
13										−67	
										−67	
14	S	77	18	78	⊥(001)	Or	NE	14	76	−55	
					or	Anor	NE	12			
	I	80	89	10	⊥(15.0.$\bar{2}$)	Or	NE	15			
15	L_p	20	85½	70½	⊥(010)	Or	NNW	20	82½		
					or	Micr	NE	4½			
	S=I_j	90	81	9	⊥(15.0.$\bar{2}$)	Or	N	3			
					or	Micr	W	15			
	p	77½	82	15	⊥(15.0.2)	Or	ENE	12½			
					or	Micr	W	4			

Grain 3: The rim "p" without inclusions has the same composition as the remaining subindividual rich in inclusions.

Grain 6: The composition planes of the subindividuals form a kind of a cross. That the subindividuals 1 and 3 have actually a different composition is not very probable because of the occurrence of very narrow lamellae which interfere with accurate determination. A larger difference in 2V is found only in subindividuals 2 and 4 and the composition obtained from the twin axis $B_{1/3}$ is similar to that from $B_{2/4}$. The composition obtained from the alternative trilling complex $\perp$ (010), [100], and $\perp$ [100]/(010) and from both complexes with (001) as composition face differ so much within each complex that the alternative trilling complexes were excluded.

Grain 9: The nonhomogeneous extinction is somewhat different in a rim-like area but the cleavage is the same in the whole grain. According to the value of 2V the rim is an orthoclase, the other part of the grain seems to be transitional to microcline.

Grain 10: 2V has been measured three times in this very heterogeneous grain.

Grain 11: The grain is subdivided into smaller grains with sutured outlines between them similar to those occurring in quartz.

Grain 13: The perthitic grain is very heterogeneous. The indicatrix was determined twice: 1. in the middle part, 2. where it borders a partly replaced plagioclase. A fine rim of dusty inclusions indicate the former size of the plagioclase. Only 2V could be obtained.

Grain 14: The extinction of the very large perthitic grain is most heterogeneous in the position with the optical axis parallel to the tube of the microscope. The indicatrix axes were measured at least four times (X—7 times). If the means of all measurements were plotted on the diagram the crossing points embrace 3° to 5° less than 90°; but the corrected projections equal 90° (Nikitin, 1936, p. 36). 2 V obtained in this way is −50°.

The very small perthitic inclusions show some twin lamellae with sharp borders but they do not allow the determination of their optical indicatrix. Therefore, the extinction angle was measured in an orientation when the lamellae—presumably being parallel to (010)—were vertical; Wahlstrom's curve "L" in his diagram (1947, fig. 22) gave as composition of the inclusion An_7.

In addition to the perthitic intergrowth some areas of the grain show a poorly defined twin structure with no sharp outlines between the lamellae. In certain extinction positions when the grain seems to be homogeneous this twinning is not visible and the perithitic intergrowth stands out.

Grain 15: The perthitic grain shows locally a twin net, especially on the borders. The optical indicatrix was measured in the central part with no lamellae and on the border with them. Therefore, the lamellae are considered only for the border. From the position of the crystallographic elements it is concluded that microcline is developed on the borders and orthoclase in the homogeneous central part. As the optical axes could not be measured, 2V was determined in the indirect way by determining the birefringence in the section Z X and in a section perpendicular to it, following Nikitin's method (1936, p. 68). 2V is deduced from Boldyrev's diagram (Nikitin, 1936, plate IV) where the relationship between 2V and the birefringences $nZ-nY$ and $nY-nX$ is considered. $nZ-nX$ in the central part is 0.0057, in the peripheral 0.0050; $2V_j = -67°$ and $2V_p = -74°$. Values for $nZ-nX$ under 0.006 are normal and were found repeatedly in potash-feldspar of different rocks, e.g. of pegmatites (Dolar-Mantuani & Koritnig, 1939) and of aplites (Dolar-Mantuani; 1938, p. 377 and 1942, p. 407).

Thin section No. 9

This thin section was made from an apparently uniform phenocryst of specimen No. 7. The slide includes two large grains separated by an irregular boundary and bounded on one side by the groundmass. Both grains are relatively rich in inclusions. Plagioclase

grains with some quartz occur in the form of an irregular strip about 1 mm. from the border to the groundmass. On an area of 4 sq. cm., measurement of inclusions gave the following results: 12.2% of mostly anhedral, partly euhedral plagioclases (maximum size 0.5 mm.), 0.8% of anhedral quartz grains with mainly different optical orientations, and 0.7% of accessories as crystals of magnetite, sphene, apatite, and some epidote as vein filling; 86.3% of K-feldspar.

Both grains of potash-feldspar show a very nonhomogeneous extinction in patches combined with extremely fine twinning texture which is best visible at larger tilting angles. The optical indicatrix was measured in four places resulting in different values for 2V. S=I is a fine but interrupted cleavage with inclusions. S′ is a parting. The pole of (15.0.$\bar{2}$) for anorthoclase is not plotted in Nikitin's diagram; it must lie very close to that of orthoclase.

Grain 1: S=I 89° 77° 13°−⊥(15.0.$\bar{2}$)−Or−SE 1°; S′ 47½° 67° 51½°−⊥(110)−Anor−SE 12°; 2V=−49°, −51°, −59°; mean −53°.

Grain 2: 2V=−60°.

Thin Section No. 8

1	2	3			4	5. An %	6		7. S∧I	8. 2V	9. An %
					Plagioclase						
1	D=$L_{1/2}$	14°	76°	88½°	⊥(010)	7	NW	½°		1=+80°	
	$B_{1/2}$	15½	74½	89	⊥(010)	4	NE	½		2=+79	5
2	D=$L_{1/2}$	20	71	84	⊥(010)	0	NW	4		1= 90	
	$B_{1/2}$	19½	70½	88	⊥(010)	0	W	1½		2=−80	0
3	D=$L_{1/2}$	14½	77½	82½	⊥(010)	10½	N	5½		2=−84	
	$B_{1/2}$	13	78	85	⊥(010)	10½	N	3			10½
5	D=$L_{1/2}$	15	75½	86	⊥(010)	7½	NW	3		1=+82	
	$B_{1/2}$	15	75½	86	⊥(010)	7½	NW	3		2=−85	7½
					Potash-feldspar						
5	S	86½	3½	89	⊥(001)	Or	SE	5½	74½°	−72	
	I	90	75	15	⊥(15.0.$\bar{2}$)	Or	S	2½			
6	S	20	88	70	⊥(010)	Micr	NE	6½	84		
	I	75½	84	16	⊥(15.0.$\bar{2}$)	Micr	NW	2½			
7	S	86	6	85½	⊥(001)	Or	ESE	4	75	−67	
	S′=I	83½	71½	20	⊥(15.0.$\bar{2}$)	Or	SE	9			
8	S	73	19½	80½	⊥(001)	Micr	W	6½		−78	

Grain 4 is a small inclusion in the large heterogeneous grain No. 8.

Grain 6: In addition to the normal cleavage a set of fine cleavage planes with dusty inclusions is developed.

Thin section No. 10

The thin section of the phenocryst includes also some groundmass. The large grain is anhedral and of the same character as described in No. 9. On the border with the groundmass the inclusions become more numerous and the potash-feldspar fills only the interstices. Very fine twin lamellae in only one direction are visible between untwinned patches with a very unhomogeneous extinction. No difference in the refractive index is visible.

At first sight it seems that the grain consists of three subindividuals. The outline between the subindividuals 1 and 2 is mainly parallel to the twinning texture of both subindividuals and only partly irregular. The outlines between subindividuals 2 and 3 is straight for a short distance, but elsewhere curved and irregular. Subindividuals 1 and 2 are twinned according to the Carlsbad twin law but 2 and 3 are not twinned. The angle between $\perp(001)_2$ and $\perp(001)_3$ is only 29°, the part of the straight border is formed by $(001)_2$, and neither the position of the faces (001) nor the extinction is symmetrical in regard to the "composition" plane. $S_2 \wedge S'_2 = 89\frac{1}{2}°$.

The optical indicatrix is measured in four places which are indicated by a, b, c, and d. 2V is the highest in subindividual 1 and measured in three places it varies very little: from −64° to $-65\frac{1}{2}°$; mean −65°. *X* bisects the angle formed by the two optic axes and demonstrates the exactness of the determination. The other optical angles are smaller ($2V_2 = -59°$ and $2V_3 = -51°$) and typical for anorthoclase. $2V_1 = -65°$ and $2V_2 = -59°$ are obtained in the same central area "c" of the grain. As the character of subindividual 1 is the same as that of subindividual 2 with which it is connected by the Carlsbad law it is also regarded as being an anorthoclase.

1	2	3			4	5	6		7. $S \wedge S'$	8.2V
					Potash-feldspar					
1a	S_1	89°	3°	87°	$\perp(001)$	Or	SE	3°		$1 = -64°$
					or	Anor	SW	$3\frac{1}{2}$		
1b	L_1	$6\frac{1}{2}$	$83\frac{1}{2}$	88	$\perp(010)$	Or	NW	$6\frac{1}{2}$		$1 = -65\frac{1}{2}$
					or	Anor	SW	4		
1c	$D = L_1$	$7\frac{1}{2}$	$82\frac{1}{2}$	88	$\perp(010)$	Or	WNW	$7\frac{1}{2}$		$1 = -65$
					or	Anor	SW	$5\frac{1}{2}$		
	2	$6\frac{1}{2}$	$83\frac{1}{2}$	89	$\perp(010)$	Or	W	$6\frac{1}{2}$		$2 = -59$
					or	Anor	SW	5		
	$B_{1/2}$	$22\frac{1}{2}$	68	$88\frac{1}{2}$	[001]	Or	NE	2		
					or	Anor	NW	$\frac{1}{2}$		
1d	S_2	$83\frac{1}{2}$	$6\frac{1}{2}$	88	$\perp(001)$	Or	SE	7		$3 = -51$
					or	Anor	SE	$4\frac{1}{2}$		
	S_3	88	$8\frac{1}{2}$	82	$\perp(001)$	Or	NE	$3\frac{1}{2}$		
					or	Anor	NW	3		
	S'_2	5	87	86	$\perp(010)$	Or	NW	5		
					or	Anor	NW	$\frac{1}{2}$		
2	S	$85\frac{1}{2}$	$85\frac{1}{2}$	6	$\perp(15.0.\bar{2})$	Or	NE	$8\frac{1}{2}$		
					or	Micr	NW	$12\frac{1}{2}$		
3	S	87	$85\frac{1}{2}$	$5\frac{1}{2}$	$\perp(15.0.\bar{2})$	Or	NE	$8\frac{1}{2}$		
					or	Micr	NW	$14\frac{1}{2}$		
4	S	90	$9\frac{1}{2}$	$80\frac{1}{2}$	$\perp(\bar{0}01)$	Or	N	4	$74\frac{1}{2}$	−68
	$S' = I$	89	83	6	$\perp(15.0.\bar{2})$	Or	N	$6\frac{1}{2}$		
					Plagioclase					
5	L	$17\frac{1}{2}$	$72\frac{1}{2}$	$88\frac{1}{2}$	$\perp(010)$	1% An		0		+86

Grain 2 has a very fine and close spaced cleavage and no lamellae; only wavy extinction is visible.

Grain 3: It is heterogeneous and similar to grain No. 1. The optical data are too scarce to

allow determination of the type of potash-feldspar. The pole for (15.0.$\bar{2}$) falls nearer to that of (an-)orthoclase than microcline.

Grain 4: Although the extinction is nonhomogeneous, no smaller 2V can be expected. No twin lamellae are visible, only a perthitic structure.

Grain 5: As inclusion in No. 1.

Thin section No. 11

1	2	3			4	5. An %	6		7. L∧L′ S∧L	8. 2V	9. An %
					Plagioclase						
1	D=L_1	10°	83°	83°	⊥(010)	13	N	5°	85°	2=+81°	
	2	13½	77	87	⊥(010)	9	NW	1½			
	3	12	78	85½	⊥(010)	11	N	2½			
	4	11	80	85½	⊥(010)	11½	N	2½			
	D′=S_1	78	31	62	⊥(001)	0	NNW	6			
	2	83	23½	67½	⊥(001)	7	NW	4½			
	3	75½	28	66½	⊥(001)	0	N	1½			
	4	83	25	66	⊥(001)	6	NW	5½			
	$B_{1/2}$	11	79	87½	⊥(010)	11	N	½			
	$B_{3/4}$	11	79	90	⊥(010)	11	S	2			
	$B_{1/3}$	88	74	26	[100]	0	SW	5½			
	$B_{2/4}$	86	67	23	[100]	0	SSW	3			
	$B_{1/4}$	79½	28½	64	⊥[100] / (010)	4	NW	7			
	$B_{2/3}$	79	25½	68	⊥[100] / (010)	7	NW	4			6
2	D=$L_{1/2}$	12½	88	86	⊥(010)	10½	NNW	2½	85		
	D′=$S_{1/2}$	80	22½	75	⊥(001)	5½	NW	1			
	$B_{1/2}$	80	19	74	⊥[100] / (010)	11½		0			10
3	D=L_1	89	13	77	⊥(001)	16	NW	1½		1=+85	
	2	88	18	72	⊥(001)	13	NW	4½		2=+84	
	$B_{1/2}$	87½	74½	16	[100]	12	SW	1½			13
4	D=L_1	15	75	90	⊥(010)	5		0		3=+85	
	2	10	80	89	⊥(010)	11½	S	1½			
	3	7½	83	87½	⊥(010)	14	N	½			
	D′=S_2	86	17	73	⊥(001)	12½	NW	2½			
	3	90	12	78	⊥(001)	18	NW	2			
	$B_{1/2}$	13	77	89	⊥(010)	8		0			
	$B_{1/3}$	80	18½	75	⊥[100] / (010)	11½	SE	1½			
					or [001]	13½	NE	3½			
	$B_{2/3}$	86	66	14½	[100]	12	NW	½			
					or ⊥[001] / (010)	14½	E	4			10
5	S	86	20	70	⊥(001)	11	NW	4½		+88½	11

Potash-feldspar

6	L	18	82	74	⊥(010)	Micr		0	86	
	L′=I	69½	88	20½	⊥(15.0.$\bar{2}$)	Micr	NE	6½		
7	D_1	85	7	85	⊥(001)	Or	E	5		1=−70
	2	82	10	84	⊥(001)	Or	E	8		2=−70
	$B_{1/2}$	83½	8½	84	⊥(001)	Or	E	6		
8	L	20	87	70	⊥(010)	Micr	NE	6	90	
	L′=S=I	70	84	21	⊥(15.0.2)	Micr	E	3½		

Grain 1: The form of the grain is similar to that of No. 6 in sample No. 7. As the poles of the twin axes $B_{1/4}$ and $B_{2/3}$ lie in the vicinity of only ⊥[100]/(010) the other two axes $B_{1/3}$ and $B_{2/4}$) can be only [100]—if only (010) is considered as D.

Grain 4: It is almost impossible to decide what twin laws occur in this grain. As the first subindividual extends through the length of the whole grain and only subindividuals 2 and 3 are divided by (001), the complex ⊥(010), [100], and ⊥[100]/(010) was chosen.

Grains 6 and 8: Both grains show a typical microcline net. Grain 6. is a part of a micrographophyric intergrowth with quartz.

Grain 7: A simple twin resembling a Carlsbad twin.

Thin section No. 12

1	2	3			4	5	6		7	8. 2V	9

Plagioclase

1	L	14°	76°	90°	⊥(010)	6% An	SE	½°		+88°

Potash-feldspar

2	D=S_1	83	13	79	⊥(001)	Micr	NW	4½		1=−80
	2	82	9	85½	⊥(001)	Micr	SW	4		2=−81
	$B_{1/2}$	86	8	82	⊥(001)	Micr	SW	6½		
3	S	80½	10	86	⊥(001)	Or	E	10		−69
4	S	89	5½	84½	⊥(001)	Or	E	1		−60
					or	Anor	W	2½		−62
5	D=S_1	86	7	84	⊥(001)	Or	E	4		
					or	Anor	NE	1		
	2	87	11	79½	⊥(001)	Or	NE	6		
					or	Anor	N	5½		
	S′=I_1	87	81	9	⊥(15.0.$\bar{2}$)	Or	NNE	4½		
	2	87	82	8	⊥(15.0.$\bar{2}$)	Or	NNE	5		
	$B_{1/2}$	89½	8	82	⊥(001)	Or	NNE	2½		
					or	Anor	NW	4		

Grain 2: The relatively large grain grades with the net structure into a granophyric intergrowth.

Grain 3: The central part of the grain is homogeneous and free of dusty inclusions which are conspicuous in the border zone.

Grain 4: The grain shows heterogeneous extinction and relatively large perthitic patches.

The optical indicatrix was measured twice. The extinction angle in the plagioclase is 12° in a section ⊥(010), giving An_8.

Grain 5: As Y_1 and Y_2 are almost parallel to the microscope tube 2V was not measurable. It can not be decided if the grain is orthoclase or anorthoclase because the heterogeneous extinction shows a kind of striation. Larger perthitic patches occur together with very fine stringers parallel to (15.0.$\bar{2}$).

Summary and Conclusions for Plagioclase

Composition of the plagioclases. Table 3 shows the composition of plagioclases in different thin sections. The variation in the composition of

Table 3: Composition of Plagioclases

Thin section	An % in unzoned grains			An % in zoned grains				
				Borders		Cores		
	Mean	Variation	No. of grains	Mean	Variation	Mean	Variation	No. of grains
1	33	29½–40	6	39	38–39½	44	43 –45½	2
2	34½	30 –39	5	28		42		1
3	35	31½–38	4	33		40½		1
4	8½	1 –15	5					
5	5	2½–8	4					
6	14½	12 –17	5	11½	10–13	20½	18½–22½	2
7, 9	4	0 –9	6					
8, 10	5	0 –10½	5					
11, 12	9	6 –13	6					

unzoned grains in any section is not very large; the greatest variation is 14% An in the leucocratic rock from the Highland Lass mine (No. 4). In the same way the zoning of plagioclases is very slight and seems not to be present in the acid rocks with the exception of the sample from the border of the Beaverdell stock. But this lack of zoning may be partly only apparent because alteration makes the zoning less conspicuous. The differences in the composition of the cores and the borders of the zoned grains are small; the borders correspond mainly to the mean of the unzoned grains.

The plagioclases of the average rock from the Highland Lass mine (No. 1, 2, 3) are acid andesines, all others are albites to acid oligoclases. The present andesines with the composition near An_{30} are not pseudomonoclinic and also the oligoclase is more acid than An_{20} which shows as a low-temperature plagioclase a pseudomonoclinic optical orientation (cf. Oftedahl, 1950). It is interesting that the composition of plagioclase from the Wellington mine (No. 5) corresponds to that from the inner part of the Beaverdell stock (No. 7–10), and that of the leucocratic rock

from the Highland Lass mine (No. 4) to that from the granophyric rock in the Beaverdell stock (No. 11, 12). The plagioclases from the border of the Beaverdell stock are not only slightly more basic but also zoned in comparison with those of the inner part.

2V: The plagioclases from the different rocks show a wide range in the values of 2V, as shown in table 4. The values over *Z* are normal in acid

TABLE 4. 2V IN PLAGIOCLASE

Thin section	1	2	3	4	5	6	7, 9	8, 10	11, 12
Mean of 2V	−84°	+82½°	+87°	+80°	+87°	+88½°	+88½°	+87½°	+85½°
Variation	−75° to +83°	−74° to +74°	−82° to +80°		−87° to +81°	−88° to +86°	−79° to +74°	−84° to +79°	+81° to +88°
No. of deter.	8	9	3	1	6	7	13	8	6

plagioclases, and those of the other two sections (No. 2 and 3) are not so surprising as 2V changes strongly in the part of An_{30-45} (especially of An_{35-41}).[1] The usual variation in 2V of plagioclases demonstrates that it is not satisfactory, in general, to depend only on values of 2V in determining the composition of plagioclases (cf. Comucci, 1948, p. 166; Kaaden, 1951, p. 15). Anomalies in the optical properties of plagioclases (and also of K-feldspars) are often found in addition to the complexity in the optical and structural properties of the feldspars; the latter is repeatedly pointed out in recent publications on feldspars (Raaz 1947, Koehler 1949, Laves 1950, Chaisson 1950, Chayes 1950, Heald 1950, and others).

Crystallographic elements (especially the twin axes): One hundred and seventy two crystallographic elements were studied during this work. The face (010) was oriented with respect to the optical elements on one hundred occasions. It is developed as twin lamellae or a distinct composition face, seldom as cleavage face. However, (001) is normally developed as cleavage face, seldom as composition face, or lamellae. Perhaps even these apparent cases of (001) as composition face or lamellae are really still less numerous, and they should be partly replaced by the rhombic section, especially if a cleavage parallel to these twin elements

[1] From −84° to +82° (respectively from −86° to +84°)—according to the average curve of 2V for the plagioclases in Nikitin's diagram (1936, fig. 39). Compare the break of the line for the relationship between *nZ* and the An-content of natural plagioclase at An_{45} described by Chayes (1950, p. 594). Also the lines for relationship between the An-content and the line separation of the *x*-ray diffraction pattern show a break in the vicinity of An_{30-40} described by Claisse (1950, p. 419).

is not visible. As is well known, it is impossible to decide in medium plagioclases and difficult to decide in unfresh albite-oligoclases (and andesine-labradorites) whether a composition face corresponds actually to (001) or to the rhombic section. Therefore, the statements on the frequency of the pericline and acline law seem to be very uncertain for a large composition range of plagioclases and conforming to this, for plagioclases in volcanic and plutonic rocks also (Kaaden, 1951, p. 62).

Table 5 shows the frequency of the different twin laws in all thin sections examined. In the second line, only the twinning is considered for which both subindividuals were measured; in the examples on the third line the relationship between the twins was deduced including the twin lamellae. With regard to the ambiguous twin laws, it may be referred to the notes of the previous chapter. The complex ⊥(010), [001], and ⊥[001]/(010) was found four times as trilling and twice as quadrilling;

Table 5. Twinning in Plagioclase

Twin law	⊥(010)	[001]	⊥[001] / (010)	[100]	⊥[100] / (010)	[010]	⊥[100] / (001)	⊥(001)
Determ. in section	in all	1–3, 5, 7	1–3, 7	5, 11	5, 11	4, 5	7	7
No. of obs.	28 (45%)	11 (18%)	9 (14%)	6 (10%)	5 (7%)	2 (3%)	1 (1½%)	1 (1½%)
No. of obs.	43 (51%)	11 (13%)	9 (11%)	6 (7%)	5 (6%)	7 (9%)	1 (1%)	1 (1%)

⊥(010), [100], and ⊥[100]/(010) twice as trilling and once as quadrilling, and ⊥(001), [100], and ⊥[100]/(001) once as trilling.

From Table 5 it follows that twinning according to the albite law is the most frequent. If also the lamellae are taken into consideration, on the assumption that they belong to the albite and pericline twins respectively, the frequency of both twin laws increases (—the pericline twins change from the sixth to the fourth highest frequency). A still greater prevalence of the albite (70%) and pericline (16%) laws is recorded by Lundegårdh (1944, p. 373) from an ultrabasic massif, where the pericline shows the second highest frequency. The order of frequency in the present rocks agrees to a certain degree with that in plutonic (and metamorphic) rocks (90 twin axes) listed by Kaaden (1951, p. 87); but an entirely different order of frequency was found in tonalites and aplitic rocks from the Pohorje massive where the order of frequency is as follows: [001], ⊥(010), [010], ⊥[001]/(010), between 27 and 17%); ⊥[100] /(010) ⊥(021), ⊥(001), [100], ⊥[010]/(001), ⊥[100]/(001) (less than 4% each); (172 twin axes; Dolar-Mantuani 1935, 1938 and 1942). Therefore, it can be said in agreement with Winchell (1951, p. 273) only generally that the twin laws with (010) as composition face are the most

frequent (if 010 is not considered which shares, e.g., with albite twins the first highest frequency in tonalites from the Pohorje massif.

Although the greatest variability in the twin laws occurs in sections No. 5 and 7 with albites as plagioclases, this is not considered as a rule because only albite twin were determined in sections No. 6 and 8 both with acid plagioclases. On the other hand the *a*-axis and its perpendicular are important as twin axes in the aplitic rock of Beaverdell (No. 11). However, the number of grains and thin sections examined is too small to show a definite correspondence between the character of the plagioclases present or the place from which the specimens came, and the kind of twin laws developed.

It may be added that the writer's present and earlier examinations of twin laws in acid andesine do not support A. L. Culson's opinion that the $\perp$[100]/(010) law is favored in plagioclases of composition An_{30-35} (quoted by Emmons, 1943, p. 113). No Albite-Ala B twins were found in thin sections No. 1, 2, and 3 (total 23 twin axes) and only three times (among 118 twin axes) in plagioclases of the tonalites from the Pohorje massif with an average composition of unzoned grains—An_{33} (Dolar-Mantuani 1935, p. 99 and 1942, p. 407).

Summary and Conclusions for Potash-Feldspar

As the potash-feldspar in the Westkettle rocks appears to be almost entirely microcline whereas that of Beaverdell show large variations, the data are divided into two groups according to the occurrence in different batholiths.

Microcline of the Westkettle rocks

The optical results for potash-feldspar in five thin sections show a rather wide variation in the values of 2V and in the position of the crystallographic elements in regard to the optical indicatrix. In addition to this many grains contain areas which lack the characteristic microcline grating and some grains do not show any twin structure. The question arises therefore, whether such grains of the potash-feldspar are still microcline on the whole or transitional between microcline and orthoclase, or an soda-potash-feldspar, e.g. of the same character as in the larvikite of Larvik.[2]

To decide to which potash-feldspar a grain belongs, the presence of lamellae, the value of 2V, and the following angles are important here:

[2] According to determinations of Nikitin (1942, p. 282) by the Fedorov method the homogeneous alkali-feldspar grains in the larvikite show $2V = -72°$ to $-80°$, and $Z \wedge \perp (010) = 4°$, $Z \wedge \perp (001) = 87°$, and $Y \wedge \perp (001) = 8\frac{1}{2}°$ to 11°. Johannsen (1939, part IV) mentions soda-orthoclase (cryptoperthite, Broegger) or soda-microcline (anorthoclase, Rosenbusch) as constituents of larvikite.

$Z \wedge \perp(010)$, $Z \wedge \perp(001)$, $Y \wedge \perp(001)$, $Z \wedge \perp(15.0.\bar{2})$, and $X \wedge \perp(15.0.\bar{2})$. After a very careful examination it was found that 13 of the 21 grains determined are undoubtedly microcline. Four of the remaining 8 grains have a high value of 2V but no twinning lamellae are visible. As two of these grains (4/8[3] and 5/6) show much better agreement in their crystallographic coordinates with those of microcline than with those of any other type of potash-feldspar the writer appears to be justified in stating that also grain 3/5 in which only the optical angle was determined, and grain 1/9 whose coordinates of (001) indeed correspond better to those of anorthoclase, are microcline.

Of the remaining four grains, grain 1/10 has a relatively low value of 2V ($-72°$) but it shows twinning structure as do grains 2/6 and 2/7. As the poles of all these grains and also of grain 5/7 lie nearer to those of microcline than orthoclase or soda-orthoclase on Nikitin's diagram, it is more likely that these grains also belong to microcline. Because gradations of orthoclase and microcline and vice versa are normally demonstrated by different values of 2V in different parts of one grain, as e.g. in some grains of the Beaverdell rocks or in potash-feldspar of a tonalite in the Pohorje massif (Dolar-Mantuani, 1935, p. 103).

Parts and grains without twin net are repeatedly reported for microcline. Winchell mentions that microcline devoid of multiple twinning is quite rare but not unknown (1951, p. 366) and Johannsen that it is even common in alkali granites (1939, part II, p. 146). Recently Higazy mentions analogous microclines with perthitic structure occurring in pegmatites of the Black Hills, Dakota (1949, p. 563). Microcline apparently without twinning could have very narrow and hence microscopically indistinct twin lamellae as Dana suggests for some anorthoclase (1932, p. 541). Recently F. Laves established it for microcline by x-ray investigations (1950, p. 550). That the lack of lamellae is connected with relatively low temperature of its origin, as suggested by Broegger for such microcline found in drusy vugs in the Langesund Fjord (quoted by Fuechtbauer, 1950, p. 248), is not established. But that twinning in the detrital microcline continues into the late outgrowth which is in optical continuity with the core of microcline from West Virginia sandstones (Heald, 1950b, p. 628), argues against this assumption.

In conclusion the potash-feldspar of the Westkettle rocks show generally values of 2V which are typical for microcline in the mainly homogeneous parts of the grains in which the determination of the optical indicatrix and, therefore, of 2V is more convenient. The optical angle is also typical of microcline in cases where the cleavage and lamellae (being

[3] The first number indicates the number of the thin section, the second of the grains in the tables of the detailed optic data.

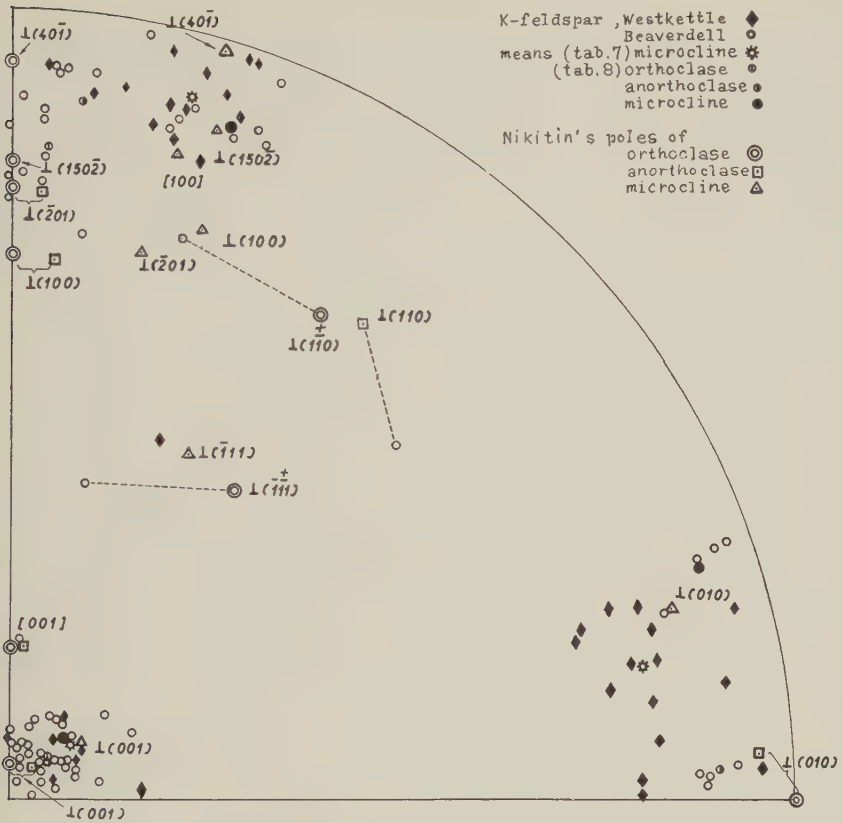

FIG. 2. The poles of the K-feldspars of the Westkettle and Beaverdell rocks shown on the one-octant diagram of Nikitin.

measured, of course, in the part with the twin net) show a relatively great distance to the microcline poles on Nikitin's diagram. Here grain 5/8 is illustrative: it shows rather good agreement for $\perp(010)$ and $\perp(15.0.\bar{2})$ with the data of microcline in the homogeneous parts of the grain and deviating data in the parts with a typical microcline net. In comparison with this grain, grain 7/15 from the Beaverdell stock is interesting because there the untwinned area shows apparently monoclinic optics (deviation for pole $\perp(15.0.\bar{2})$ of orthoclase is 3°). Laves (1950, p. 553) obtained the same result in microcline where portions of single grains were a) optically monoclinic, b) fully twinned, optically triclinic, and c) optically triclinic without observable twin lamellae. The results with the Fedorov method show therefore in accordance with the *x*-ray investigations that areas where twinning disappears completely, may be

optically monoclinic or triclinic. On the other hand the lower values of 2V for potash-feldspars in the Westkettle rocks are determined in those grains in which the poles of crystallographic elements lie nearer to those of microcline than any other feldspar.

2V: The variation of the values of 2V is from $-72\frac{1}{2}°$ to 90°, taking into account all thin sections of the Westkettle rocks. The average value is $-81°$ (16 determinations, three of them determined by emergence of both optical axes). The extreme value $-72\frac{1}{2}°$ is still 1° higher than that in the microcline of the granite of the island Maddalena in Sardinia as reported by Riva (Rosenbusch-Muegge, 1927, p. 722). Some of Spencer's microclines show still smaller axial angles but they are not typical for microcline (1937, p. 460). If the average value $-81°$ is plotted in Winchell's diagram for the microcline-analbite series (1951, p. 300, Fig. 192) about 20% of the Na-component is apparently present in the Westkettle microcline.

The crystallographic elements: The position of the different crystallographic elements is shown in the following diagram together with those of the potash-feldspar from the Beaverdell rocks.

Only four different elements are determined in the potash-feldspar of the Westkettle rocks, i.e. (010), (001), (15.0.$\bar{2}$), and once (111) (as an irregular parting face). The average coordinates of the three main faces are (number of observation in brackets):

⊥(010)	$16\frac{2}{3}°$	$78\frac{3}{4}°$	$78\frac{2}{3}°$	(14 times)
⊥(15.0.$\bar{2}$)	76	85	$15\frac{1}{2}$	(13 times)
⊥(001)	$81\frac{2}{3}$	12	83	(7 times)

The smallest variation in the coordinates was obtained for ⊥(15.0.$\bar{2}$) but the average coordinates for ⊥(001) correspond best to those of microcline as quoted by Nikitin (1936, p. 94).

Most of the data were supplied by twin lamellae (20), rather than by the cleavage plane (10). No preference could be established between the faces (010) and (001) as cleavage planes. In samples of the acid rocks, twin axes were determined twice: once in an albite and once in a Manebach twin (5/8 and 4/8 respectively).

The function of (15.0.$\bar{2}$) as a possible composition face of the microcline twinning

It is very interesting that no twin net could be determined which was composed of lamellae parallel to (010) and (001) but that the combination (010) and (15.0.$\bar{2}$) was found seven times and once that of (001) and (15.0.$\bar{2}$), (4/10). If only one set of twinning was visible it was parallel to (010) or (15.0.$\bar{2}$). As the face (15.0.$\bar{2}$) is not often mentioned in the literature, it seems to be opportune to explain its position in more detail.

The face (15.0.$\bar{2}$) which is close to (70$\bar{1}$) and (80$\bar{1}$) is more extensively described as murchisonite cleavage by Rosenbusch-Muegge in the chapter on orthoclase (1927, p. 661), although it is —according to them—very frequent also in microcline where it forms an angle of 71° to 74° with (001) (p. 721). This cleavage was described first by Lévy in the murchisonite of Dawlishland and Heavytree. The development of this cleavage can be so perfect, that it has led in the past to mistakes in the orientation of crystals. The angle of this cleavage ranges from 72°1′ to 74°15′ with (001) in (010) as given by different authors and is said to be smaller than 68° by Kraatz-Koschau and Hackman. The angle does not seem to be constant and the face is calculated as parallel to (15.0.$\bar{2}$) and (70$\bar{1}$) to (80$\bar{1}$). This murchisonite cleavage is developed especially, but not exclusively, in orthoclase of foyaitic rocks; it can be one of the faces along which the microperthitic deposition takes place. Rosenbusch points out that it may result from release of inherent tensions which are due to admixtures of a greater quantity of albite to orthoclase (in non-equilibrium space lattice) by intensive straining of the feldspar.

Dana (1932, p. 540) quotes an analogous statement of Broegger: extremely fine interlamination of albite and orthoclase exists parallel to (80$\bar{1}$) which is connected in cryptoperthites with secondary planes of parting parallel to (100) or (80$\bar{1}$).

Duhovnik (1949, p. 259) describes an intergrowth between microcline and albite in the face (15.0.$\bar{2}$) in addition to the characteristic microcline grating in sections $\perp$ [100]. He calculates the symbol of the face of the perthitic intergrowth using the angle between this face and (001) which is 73½°.

During the present study the question arose whether not only a cleavage and regular inclusions were parallel to (15.0.$\bar{2}$) but also one composition face of the cross grating twinning in microcline has the symbol (15.0.$\bar{2}$). This intersecting twinning is generally said to follow the albite and pericline twin laws. All writers agree that the composition face of the non-albite lamellae lies in the zone (100):(001) but the angle between this face and (001) ($=\sigma$) seems to vary and therefore different faces are reported as composition faces.

σ is a right angle or nearly so (Dana, 1932, p. 543). It varies from $-75°$ to 90° with the greatest frequency between $-81°$ and $-85°$, according to Boeggild (1911; Reinhard and Boechlin, 32, p. 216). σ is $-75°$ and the composition face is (15.0.$\bar{2}$) as found by Litmanowicz (1931; Reinhard and Boechlin, 1936). Reinhard and Boechlin give the same variation range $-75°$ to 90° for 30 grains, as Boeggild. The poles of the composition face migrate along the zone [010] between the $\perp$ (15.0.$\bar{2}$) and [$\bar{1}$00] (p. 221). Winchell mentions that σ is $+99°$ (1951, p. 308), respectively $-80°$

or $+100°$ (p. 269, fig. 166). In fig. 201 he sketches the trace parallel to $(40\bar{1})$.[4]

Because Winchell reports twinning on an axis normal to $(\bar{2}01)$ as often being present in (also triclinic) anorthoclase, the angles between (001) and three faces in the same zone are considered, using Goldschmidt's tables (1897, p. 144) for ϕ and ρ of orthoclase (microcline is not included) in his book).

$(001)\wedge\ (\bar{2}01) = +80°17'$ or $-99°43$
$(001)\wedge\ (40\bar{1}) = +99\ 01$ or $-80\ 59$
$(001)\wedge(15.0.\bar{2}) = +107\ 30$ or $-72\ 30$

If the sign is not taken in consideration the angles between the poles of these faces are (in brackets for microcline):

$\perp(001)\wedge\perp\ (\bar{2}01) = 80°17'$ $(79\frac{1}{2}°)$
$\perp(001)\wedge\perp\ (40\bar{1}) = 80\ 59$ (81)
$\perp(001)\wedge\perp(15.0.\bar{2}) = 72\ 30$ (72)
$\perp(001)\wedge\ [\bar{1}00] = 90$

The coordinates of these three faces for orthoclase and microcline are (of $(\bar{2}01)$ and $(15.0.\bar{2})$ —Nikitin, 1936, p. 94; of $(40\bar{1})$ calculated for orthoclase and graphically determined for microcline, by the writer):

	Orthoclase			Microcline		
$\perp(\bar{2}01)$	90°	$75\frac{1}{4}°$	$14\frac{3}{4}°$	78°	$70\frac{1}{2}°$	23°
$\perp(40\bar{1})$	90	86	4	$74\frac{1}{2}$	89	$15\frac{1}{2}$
$\perp(15.0.\bar{2})$	90	$77\frac{1}{2}$	$12\frac{1}{2}$	$73\frac{1}{2}$	$82\frac{3}{4}$	$18\frac{1}{4}$

In Fig. 2 the pole of $(40\bar{1})$ is drawn in addition to $\perp(100)$, $\perp(15.0.2)$, $[\bar{1}00]$, and $\perp(\bar{2}01)$. It lies half-way between $\perp(\bar{1}5.0.2)$ and $[\bar{1}00]$ where Reinhard and Boechlin indicate the pole of the rhombic section (1936, p. 221, fig. 5) assuming that the composition face of the pericline twin has the function of a rhombic section. As it may be seen on Fig. 2 the poles of the three faces for microcline are sufficiently distant to make the distinction among them, especially if also the interfacial angles are considered. However the distinction between $(15.0.\bar{2})$ and $(40\bar{1})$ becomes somewhat difficult if (001) is not visible or if the observations are made under inconvenient conditions. Under the same circumstances the distinction is still more difficult for orthoclase and anorthoclase, especially between the poles of $(15.0.\bar{2})$ and $(\bar{2}01)$.

From the interfacial angles it follows that Dana's data are insufficient and therefore ambiguous; Winchell's data correspond to $(40\bar{1})$, as do Boeggild's concentrations (between $-81°$ and $-85°$). It seems that the mean of poles, as they are shown on the diagram by Reinhard and

[4] Using the x-ray method Laves (1950, p. 568) makes the statement that planes (OkO) show diffuseness in a direction near [401] which corresponds to the direction in reciprocal space that connects the points $(hkl)-(\bar{h}\bar{k}l)$ of a pericline twin (in microcline).

Boechlin, would lie close to $\perp (40\bar{1})$. The value $\sigma = -75°$ reported by Litmanowicz is closer to that for $(15.0.\bar{2})$ than $(40\bar{1})$.

The poles for the composition face of microcline in the Westkettle rocks show migration around $\perp (15.0.\bar{2})$ and $\perp (40\bar{1})$; the mean value of the coordinates gives a pole at about half distance between the standard poles of both faces. As the interfacial angle σ is determined only twice in the present work, and this not with sufficient accuracy, only the coordinates can be considered for the determination of the type of the composition face. The fact that a cleavage parallel to the lamellae is visible not only in grain 1/8 but also in 11/6 and 11/8 from the Beaverdell rocks, and that the mean value of coordinates of this face in the Beaverdell rocks is close to those of $\perp (15.0.\bar{2})$, seems to justify again the statement that not only $(40\bar{1})$ but also $(15.0.\bar{2})$ must be taken into consideration as composition face of a pericline twinning in microcline.

Further work must be made to establish whether the variations in the position of the composition face are apparent and due only to difficult conditions of the determination caused by the fine twinning, or whether they depend upon the composition of microcline, or the temperature of formation as does the position of the rhombic section in the plagioclase group (Muegge 1930; Winchell, 1951, p. 268).

On the other hand it should not be overlooked that a combination of (001) and $(15.0.\bar{2})$ as twin grating was found twice in the present work but that (001) was never observed to be parallel to a single visible set of lamellae. Twin grating parallel to (010) and (001) was determined recently by G. Wilson in a microcline of a granodiorite of Gambier Island (unpublished master's thesis, 1951) and the same kind of grating seems to be present in Duhovnik's study. As the twin axes were not established and there are, in analogy with the plagioclase group, too many possibilities for multiple twinning with (001) as composition face, it is impossible to say which is the other multiple twin law in microcline in addition to the albite and pericline twin.

Similarly Winchell mentions pericline twinning with one set of "lines" at $-4°$ to $-8°$ with (001) or at $-75°$ to $-78°$ with (001) in anorthoclase (1951, p. 269). It seems that it would be better to make a distinction in form of pericline A and B—as in the Carlsbad twins—between these twins when two entirely different composition faces may be developed. But the fact that two sets of twinning lamellae which follow two faces: (001) and $(15.0.\bar{2})$ can be developed in one grain would rather, require two different names for these twinnings.[5]

[5] Cf. Barth's description of microcline-like cross-hatching in triclinic adularia, according to albite, pericline, and acline laws was confirmed by Koehler (quoted by Chaisson, 1950, p. 540).

Potash-feldspar of the Beaverdell stock

The optical data of the potash-feldspar in the seven thin sections of the Beaverdell stock were divided according to their variation into two groups: 1, from the border, 2, from the inner part of the Beaverdell stock.

K-feldspar from the border of the Beaverdell stock near the Westkettle intrusive (*Specimen No. 6*). The extremely small variation of the optical angle in the potash-feldspar in this thin section (from $-66\frac{1}{2}°$ to $-68°$, mean $-67°$) suggests that all grains of the potash-feldspar are of the same type although the crystallographic elements show a greater variation in their coordinates. The optic angle, the absence of twin lamellae or even simple twinning, the lack of crystallographic outlines, the occurrence in an intrusive rock and the fact that the poles of some elements are close to those of orthoclase in Nikitin's diagram, confirm that the potash-feldspar belongs to orthoclase and that no anorthoclase (or adularia) is present in this thin section. Nevertheless the average coordinates for $\perp$ (001) deviate 2° and less from those in anorthoclase ($\perp$ (001) —87°, 6°, 85°; Nikitin, 1936, p. 94).

At this point attention should be drawn to Nikitin's statement that an apparent deviation of the crystallographic elements from the monoclinic orientation which were determined by the Fedorov method, together with the lack of twin lamellae do not indicate that the potash-feldspar is an anorthoclase. A relatively strong deviation of a monoclinic orientation seems to follow often from determinations of sanidine or orthoclase by the Fedorov method and a small optic angle may be also found in orthoclase (Nikitin, 1942, p. 285; Spencer, 1937 and others).

Potash-feldspar from the inner part of the Beaverdell stock. Average porphyritic rocks (Specimens No. 7–10), leucocratic granophyric rock (Specimen No. 11, 12). The extremely great variation of 2V and the coordinates of the crystallographic elements required an especially careful examination. The values of 2V and the crystallographic data (twin lamellae, and coordinates of the faces, i.e. the angles mentioned at the beginning of the section dealing with microcline of the Westkettle rocks) were consulted. As most of the grains show heterogeneous extinction and perthitic intergrowth, the determinations were repeated in many cases, and the optical indicatrix measured in several places of the same grain.[6] The determination of grains of apparent anorthoclase proved especially difficult because of the fine twinning and the heterogeneous extinction which both are even more pronounced in anorthoclase than in microcline. In spite of careful examination some of the grains could not be assigned to one type of the potash-feldspar group.

[6] See notes accompanying the tables of the different thin sections.

The data were classed in three groups according to three types of potash-feldspar: microcline, orthoclase, anorthoclase, regardless of some apparently transitional values of optical data. Table 6 gives the optic angles, Table 7 the means of coordinates for three main faces. (The data of section 6 are included in the orthoclase group.) For microcline the value $-74°$ was chosen as the lower limit of 2V, for orthoclase the classical value $-70°$ with the limits $+3°$ and $-3\frac{1}{2}°$. The group of anorthoclase must be especially considered because of orthoclase with a low value of 2V. The phenocrysts of the porphyritic rock (Sections No. 9 and 10) form most of this group. In addition to the normal pink colour, the lack of crystallographic outlines, the relatively small deviation of the monoclinic optical orientation—which all characterize also the orthoclase grains of the Beaverdell rocks (cf. Table 7) —the relatively low value of 2V together with the fine twinning were determining that these grains are

TABLE 6

Thin section	2V in Orthoclase		Microcline		Anorthoclase	
	Mean	Variation	Mean	Variation	Mean	Variation
6	−67° (4)	−66½° to −68°				
7, 9	−69 (5)	−67 to −72	−75° (2)	−74° to −76°	−57½° (4)	−49° to −62°
8, 10	−69 (3)	−67 to −72	−78 (1)		−57 (2)	−51 to −65½
11, 12	−69¾ (3)	−68 to −70	−80¾ (2)	−80 to −81	−61 (2)	−60 to −62

regarded as anorthoclase.[7] From the grains in the groundmass three were added to this group: grain 7/14 with $2V = -55°$, 7/10 and 12/3 with $2V = -62°$ and $-61°$ respectively. The latter two values are still lower than 2V in the anorthoclase phenocryst 10/1. (Cf. data and notes of slide No. 10.)

In this way the variation of 2V in the three groups is relatively small and a gap results between the neighbouring limit values. Also the means of 2V are rather well distinct from each other, and seem to justify the division of the potash-feldspar into three groups, although the occurrence of anorthoclase in the groundmass of the Beaverdell rocks is not clearly proved.

The crystallographic elements are determined mostly as cleavage planes and twinning lamellae ((010) and (001)); some of the composition faces in microcline were considered as $(15.0.\bar{2})$, as established in the last paragraph. Although the poles of the parting faces with a small distance to X for orthoclase and anorthoclase migrate strongly in the diagram Fig. 2,

[7] To decide if these grains are not better classified as triclinic orthoclase by analogy with the triclinic adularia determined by Chaisson (1950) and Laves (1950) chemical analyses would be highly desirable.

the average interfacial angle being $73\frac{1}{2}°$ (variation from 69° to 76°) agrees with the angle $\perp (001) \wedge \perp (15.0.\bar{2}) = 72\frac{1}{2}°$ for orthoclase. Due to dusty inclusions of alteration material or stringers in perthites (e.g. grain 12/5) this face may be even better visible than the cleavage parallel to (001). ($\bar{1}11$) and (110) border a perthitic intergrowth and (110) is also a parting plane.

Simple twins which have the appearance of Carlsbad twins, were found to be related by the Manebach twin law in the leucocratic granophyric rock. Carlsbad twinning was recognized only in one of the two phenocrysts examined. The twin laws would indicate that the potash-feldspar in the leucocratic rock was formed at a relatively low temperature and the large crystals in the porphyritic rocks at a higher temperature, according to the statements of Koehler (1949, p. 596).

Table 7 gives the means of coordinates for all grains divided into three groups according to Table 6.

Table 7

Symbol	Orthoclase				Anorthoclase				Microcline			
$\perp (010)$					$6\frac{1}{2}°$	$84\frac{1}{2}°$	88°	(4)	$19\frac{1}{2}°$	$85\frac{1}{2}°$	71°	(4)
$\perp (001)$	85°	$8\frac{1}{2}°$	84°	(14)	$85\frac{1}{2}$	$8\frac{1}{2}$	84	(5)	$82\frac{1}{2}$	12	81	(6)
$\perp (15.0.\bar{2})$	87	79	$11\frac{1}{2}$	(9)	85	$83\frac{1}{2}$	$9\frac{1}{2}$	(3)	$72\frac{1}{2}$	84	19	(5)

That the means of these coordinates as they are shown also in Fig. 2 do not lie nearer to Nikitin's standard poles is believed to be caused mainly by unhomogeneous extinction which could be due partly to submicroscopically fine twinning. No explanation can be given using only the Fedorov method why the means of coordinates for $\perp$ (001) of orthoclase and of grains which are considered as anorthoclase, are so close to each other.

Perthitic intergrowth in the potash-feldspars

Most of the grains of potash feldspar in the samples of Westkettle and Beaverdell rocks show perthitic structure. However, the proportions of plagioclase and the type of the intergrowth do vary not only in different sections but also in different grains. The perthitic structure is more frequently visible in untwinned microcline, although sometimes it can be observed between the twinning net (samples No. 2 and 3). Evidently the presence of perthitic intergrowth is not related to absence of twinning although Higazy's statement (1949, p. 562) that the microcline portions of perthites are more homogeneous, is confirmed in the present work.

Generally it can be said that the plagioclase content is not only smaller in the perthites of the Westkettle rocks than those of the Beaverdell rocks but also that the blebs have mostly the form of regular or irregular stringers, seldom that of patches. In the Beaverdell rocks plagioclase blebs are more conspicuous and patches more common. These patches may be still regularly outlined as shown in grain 6/6 where two outline faces have the symbols (110) and ($\bar{1}11$). The face ($\bar{1}11$) is not mentioned by Alling in his table on "Cleavage in K-feldspar and orientation of perthitic blebs" (1932, p. 52). The perthitic orthoclase grain 8/7 whose patches seemed more convenient for measurement, gives an idea of the proportion of plagioclase (-9%; the length of the measured line was 27.55 mm.). It is not clear whether Reinecke's general proportions in the "microperthitic intergrowth of anorthoclase or soda-orthoclase and albite" given as 5:1 (1915, p. 48) should correspond to the large grains of the Beaverdell rocks or to the potash-feldspar in the groundmass.

The fact that both types (stringers and patches) are developed in Westkettle and Beaverdell rocks and that in all thin sections grains of potash-feldspar occur without perthitic structure, or that it is not developed uniformly, makes difficult a more exact classification on the conditions of their formation, as proposed by Alling or Anderson. On the other hand the simplified definition of the composite type as given by Wahlstrom (1950, p. 81) is too indefinite to be applied to these perthites. In general it can be said that the perthite of the Westkettle samples is mainly of the exsolution type and that replacement is probably involved in the perthite of the Beaverdell samples, assuming the variation in the form and amount of the blebs lies within the limits which so far have not been closely enough determined.

In three grains the composition of the plagioclase blebs was established using the albite lamellae (cf. Winchell, 1951, p. 299). The value An_{12} in grain 6/6 determined by the Fedorov method is the same as in the unzoned grains in the thin section. In two other grains (7/14 and 12/4) the values An_7 and An_8, respectively, are established from the extinction angle. They are close to the average composition of the plagioclases in these thin sections, being An_4 and An_6 respectively. Similarly two grains from an aplite from the Pohorje massive had included an oligoclase with An_{27} in full agreement with the average composition of the unzoned plagioclase grains (Dolar-Mantuani 1935, p. 83). These examples from different types of rocks explain why oligoclase and albite are mentioned as participating in the perthitic intergrowth in different publications and textbooks. The writer found the highest An-content being An_{34} (using the normative percentages) mentioned by Higazy (1949, p. 561) in per-

thite pegmatites but this value differs so much from the other fifteen perthites analysed (maximum $An_{12.6}$) that some special explanation seems necessary.

The occurrrence of perthitic plagioclase of the same composition as that of free plagioclase in the rock would be normal (Johannsen, 1939, Part II, p. 140). On the other hand Faessler & Tremblay (1946, pp. 62 & 66), mention an oligoclase in the replacement type of the Lauretian gneisses and albite in the exsolution perthite of the Pine Hill intrusives, both rocks having oligoclase as constituent. As the origin of the perthitic intergrowth is so variable and the composition of the examined plagioclase portion is so contradicting it is too early to make a more definite statement on the influence of the conditions of origin or of the surrounding plagioclases in the rock, on the composition of a perthite.

Conclusion

The detailed study of *plagioclases* of the Westkettle rocks show that andesine is developed in the average rock of the Highland Lass mine and albite-oligoclase in the leucocratic rock of the same mine. No evidence could be obtained that the albite which was found as the only plagioclase in the average sample of the Wellington mine, had been later introduced. Labradorite which has been reported in the rock of the nearby Sally mine (Reinecke, 1915, p. 43) could not be found in any thin section. The plagioclases from the border of the Beaverdell stock correspond to an (acid) oligoclase in agreement with Reinecke's data but from the inner part they are still more acid and correspond to an albite-oligoclase or albite.

The results of Table 5 on the frequency of the different twin laws in plagioclase demonstrate that the statement that the multiple twinning follows the albite or pericline law and the simple twinning the Carlsbad law, is too generalized in most publications. But no rule is found as yet in the order of frequency of different twin laws in relation to different types of rocks, according to these determinations and others of the writer.

The present data indicate that only microcline occurs as *potash-feldspar* in the Westkettle rocks near Beaverdell although some of the grains do not show net structure in the whole grain or in parts of them. Some deviations which are established from the normal values of 2V and of coordinates of the crystallographic elements of microcline are believed to be due to inexact determinations because of difficult conditions of observation. These data do not indicate an intergrowth of orthoclase and microcline which would be suggested by the frequently heterogeneous extinction which is typical for this type of intergrowth (Prof. M. Reinhard's written communication) neither do they confirm gradation to another type of

potash-feldspar. An "undulatory" extinction in optically triclinic microcline without observable twin lamellae is explained by F. Laves as to be produced by variation of the proportions of right and left (submicroscopical) twin positions (Laves 1950, p. 553). Provided, however, a gradation be assumed in the potash-feldspar of the Westkettle rocks on Wallace mountain, it would be from microcline to orthoclase and would be limited to only a few grains. In any case the present data do not support Reinecke's statement that only orthoclase is present in Westkettle rocks.

Detailed microscopical examinations indicate that the face $(15.0.\bar{2})$ known as murchisonite cleavage in potash-feldspars, may be the composition face in microcline twinning. As no twin lamellae were wide enough to determine the optical indicatrix of each set of lamellae of the twinning with $(15.0.\bar{2})$ as composition face, the twin axis could not be determined using the Fedorov method. Also the function of (001) obtained only twice as composition face—and this always together with $(15.0.\bar{2})$ - is not clear but argues for development of two different twin laws in addition to the albite law which form the cross grating structure of microcline.

From the border of the Beaverdell stock one section of the matrix was available. Only orthoclase was determined in this slide. The identification of large grains from this porphyritic rock would be interesting for comparison with the phenocrysts from the more central part of the Beaverdell stock.

The fine lamellar large grains of the rocks from the central part of the Beaverdell stock have special features. If their development as Carlsbad twins on one hand, and their irregular borders together with the amount, type and distribution of the inclusions in them on the other hand is considered, these large grains formed at a higher temperature and increased in size by later replacement. The anhedral border is in disagreement with the statement of Reinecke that "K-feldspar is very clear cut in outline and nearly always formed according to the Carlsbad law" (1915, p. 48). The formation of the phenocrysts at high temperature would be confirmed by the fact that they seem to be anorthoclase (c.f. Bowen & Tuttle, 1950 p. 509) and the replacement of their borders is supported by the evidence of replacement found in the described rock. But although the value of 2V varies in large limits in one phenocryst (tables and notes of sections No. 9 and 10) no evidence was found that the variation of 2V depends upon the place where it was measured or that some rim would show different characteristics in comparison with the core.

Some indications such as a relatively low 2V and striate extinction suggest that also some rare grains in the groundmass and in the granophyric

rock from the inner part of the Beaverdell stock are anorthoclase. The presence of anorthoclase in addition to orthoclase and microcline in one rock is surprising and demands a special explanation of the origin of the rock. On the other hand the observed Manebach twins in the potash feldspars and the cross-twins in plagioclases of the granophyric leucocratic rock from the Beaverdell stock would indicate a relatively low temperature at the formation of this rock (cf. the "Roc-Tourné-type" twins in authigenic albites of the "Muschelkalk" formation near Goettingen; Fuechtbauer, 1950 p. 246). To classify these potash-feldspars, especially from the granophyric rock as triclinic orthoclase would make the petrogenesis of the Beaverdell stock much simpler. As the coordinates of $\perp$ (001) and partly $\perp (15.0.\bar{2})$ are very close for orthoclase and anorthoclase in the present rocks (Table 7), further proof (chiefly using chemical tests) is needed for occurrence of anorthoclase in the Beaverdell stock.

The results also show that both orthoclase and microcline are present in some grains. No evidence could be obtained that would show whether the orthoclase grades gradually into microcline or whether it is intergrown with the latter somewhat as in the perthite the potash-feldspar and plagioclase with more or less sharply distinguishable outlines.

The type of the relatively indistinct perthitic structure in the potash-feldspar of Westkettle and Beaverdell rocks indicates that the perthite in the former rocks is of exsolution type, that in the latter of replacement type, but it is not known whether some essential difference exists between the perthitic structure in different types of potash-feldspar. It is also uncertain whether the composition of plagioclase blebs is influenced by the composition of the surrounding plagioclases as established here or by the type of origin.

The study shows some difficulties which arise using even the Fedorov method for detailed determination of the feldspar group which is seen to be more and more complicated. For the feldspars investigated, further determination on a greater number of specimens should be made to illustrate the distribution of the more acid plagioclases, their possibly special origin, and (as suggested in the study of White and Dolar-Mantuani) the closer relations between the Westkettle and Beaverdell rocks. It would be of interest to see whether some regularity can be found in the distribution or time of origin of the different types of potash-feldspar in the Beaverdell stock.

Acknowledgments

First, I want to thank Dr. W. H. White for the specimens, thin sections, and the sketch showing the specimen localities. I am indebted to

Dr. H. C. Gunning, the Head of the Department of Geology and Geography who supported my work with great understanding, active interest and partly new equipment. Funds and petrographic equipment were made available by the Department of Geology and Geography of the University of British Columbia and by a grant from the research funds of that Institution. My thanks are due to Dr. K. C. McTaggart who corrected the language of the manuscript in order to make it clearer and more easily understood to Miss H. Böttger, the Librarian of the Department who made the final corrections and to Mr. J. Dolar-Mantuani who prepared the diagram. Finally, I am much indebted to the Lady Davis foundation of Montreal whose one year fellowship (1949/50) made it possible for me to start my scientific work again after so many years when my activity was interrupted by World War II.

References

Alling, H. L. (1932): Perthites, *Am. Mineral.*, **17,** 43–65.

Barth, T. F. W. & Oftedahl, C. (1947): High-temperature plagioclase in the Oslo igneous rocks, *Trans. Am. Geophys. Union*, **28,** 102–104.

Bowen, N. L. & Tuttle, O. F. (1950): The system $NaAlSi_3O_8-KAlSi_3O_8-H_2O$, *Jour. Geol.*, **58,** 489–511.

Chaisson, U. (1950): The optics of triclinic adularia, *Jour. Geol.*, **58,** 537–547.

Chayes, F. (1950): On the relation between anorthite content and index of natural plagioclase, *Jour. Geol.*, **58,** 593–595.

Claisse, F. (1950): A roentgenographic method for determining plagioclases, *Am. Mineral.*, **35,** 412–420.

Comucci, P. (1948): Le rocce della regione di Jubdo (Africa orientale), *Acc. Lincei, Roma*, 262.

Dana, E. S. (1932): *A Textbook of Mineralogy*. 4th Ed., W. E. Ford; New York.

Dolar-Mantuani, L. (1931): Zur Charakteristik der Feldspate des Syenites vom Groeba Typus, *Min. Petr. Mitt.*, **41,** 272–307.

——— (1935): Razmerje med tonaliti in apliti Pohorskega masiva. (Sum. Das Verhaeltnis der Aplite zu den Tonaliten im Massive des Pohorje), *Geol. Anal. Balk. poluost.*, **12,** 1–164.

——— (1938): Die Porphyrgesteine des Westlichen Pohorje, *Geol. Anal. Balk. poluost.*, **15,** 281–414.

——— (1942): Tonaliti in apliti na jugovzhodu pohorskega tonalitnega masiva. (Sum. I tonaliti e le apliti nel sudest del massiccio tonalitico del Pohorje); *Razpr. mat. prir. raz. Akad. zn. um. Ljubljana*, **2,** 363–426.

——— & Koritnig, S. (1939): Die Feldspate von Schwanberg (Steiermark). *Zeits. Krist.*, A., **101,** 30–38.

Duhovnik, J. (1949): Izpremembe sestava granita in apnenca ob njunem kontaktu. (Sum. on the contact phenomena between pegmatite and marble at Lohja in S.W. Finland). *Razpr. mat. prir. raz. Akad. zn. um. Ljubljana*, **4,** 247–289.

Emmons, R. C. (1943): *The Universal Stage; Geol. Soc. Am.*, Mem. **8.**

Faessler, C. & Tremblay, L. P. (1946): Perthite as age indicator in Laurentian gneiss and Pine Hill intrusives, *Can. Min. Met., Bull.* **405,** 58–70.

Fuechtbauer, H. (1950): Die nichtkarbonatischen Bestandteile des Goettinger Muschel-

kalkes mit besonderer Beruecksichtigung der Mineralneubildungen; *Heidelb. Beitr. Min. Petr.*, **2**, 235–254.

Gilbert, C. M. & Turner, F. J. (1949): Use of the universal stage in sedimentary petrography, *Am. Jour. Sci.*, **247**, 1–26.

Goldschmidt, V. (1897): *Krystallographische Winkeltabellan.* Berlin.

Heald, M. T. (1950a): Thermal study of potash-soda feldspars; *Am. Mineral.*, **35**, 77–89.

——— (1950b): Authigenesis in West Virginia sandstones; *Jour. Geol.*, **58**, 624–633.

Higazy, R. A. (1949): Petrogenesis of perthite pegmatites in the Black Hills, South Dakota; *Jour. Geol.*, **57**, 555–581.

Johannsen, A. A. (1939): *A Descriptive Petrography of Igneous Rocks.* Chicago. 2nd Ed.

Kaaden, G. v. d. (1951): Optical Studies on natural plagioclase feldspars with high- and low-temperature optics; Dr. Thesis. *Rijks-University of Utrecht.*

Koehler, A. (1949): Recent results on investigations of the feldspars, *Jour. Geol.*, **57**, 592–599.

Larsson, W. (1940): Petrology of interglacial volcanics from the Andes of Northern Patagonia, *Geol. Inst. Bull. Upsala.* **28**, 191–405.

Laves, F. (1950): The lattice and twinning of microcline and other potash feldspars, *Jour. Geol.*, **58**, 548–571.

Lundegårdh, P. H. (1941): Bytownit aus Anorthosit von Bönskär im noerdlichen Teil der Stockholmer Scharen und seine Beziehungen zu verschiedenen Feldspatbestimmungskurven: *Geol. Inst. Bull. Upsala*, **28**, 415–430.

——— (1944): The Grovstanas region, *Geol. Inst. Bull. Upsala*, **29**, 305–388.

Nikitin, W. (1936): *Die Fedorow—Methode.* Berlin.

——— (1942), O prištevanju živcev k anorthoklazu samo na podlagi podatkov o legi optićne indikatrise, ki jih daje Fedorovlja metoda. (Sum. Ueber die Moeglichkeit die Feldspaete nur auf Grund der mittels der Fedorow-Methode erhaltenen Angaben der Indikatrixlage dem Anorthoklas zuzuordnen), *Razpr. mat. prir. raz. Akad. zn. um. Ljubljana*, **2**, 269–298.

Oftedahl, C. (1950): Note on "pseudo—monoclinic" plagioclase, *Jour. Geol.*, **58**, 596–597.

Raaz, F. (1947): "Dimorphe Mischungsreihen" oder "Isodimorphie" bei den Plagioklasen, *Akad. Anzeig. oesterr. Akad. Wiss. math.-naturw. Kl. Wien*, **4**, 4.

Reinhard, M. & Boechlin, R. (1936): Ueber die gittarartige Verzwilligung beim Mikroklin, *Schweiz. Min. Petr. Mitt.*, **16**, 215–225.

Reinecke, L. (1915): Ore deposits of the Beaverdell map-area: *Geol. Surv. Canada, Mem.* **79**.

Rosenbusch, H. & Muegge, O. (1927): *Mikroskopische Physiographie*, **1**, 2. Haelfte. Stuttgart. 5. Aufl.

Spencer, E. (1937): The potash-soda-feldspars. I. Thermal stability: *Mineral. Mag.*, **24**, 453–494.

Turner, F. J. (1947): Determination of plagioclase with the four-axis universal stage: *Am. Mineral.*, **32**, 389–410.

Tuttle, O. F. & Bowen, N. L. (1950): High-temperature albite and contiguous feldspars: *Jour. Geol.*, **58**, 572–583.

Wahlstrom, E. E. (1947): *Igneous Minerals and Rocks.* New York.

——— (1950), *Introduction to Theoretical Igneous Petrology.* New York.

White, W. H. (1950): Beaverdell: *Ann. Rep. Minister of Mines. B.C.*, **1949**. A., 138–148.

——— & Dolar-Mantuani, L. Preliminary notes on the intrusive rocks near Beaverdell, B. C. (in manuscript)

Winchell, A. N. & Winchell, H. (1951): *Elements of Optical Mineralogy.* Part II. 4th Ed. New York.

KORNERUPINE FROM LAC STE-MARIE, QUEBEC, CANADA[1]

J. P. Girault

Department of Mines of the Province of Quebec.

Abstract

This study of two varieties of kornerupine from the vicinity of Lac Ste-Marie, County of Gatineau, Province of Quebec (Canada) has furnished new data on this rare mineral. The forms observed are (010), (100) and (110). Data deduced from an x-ray powder diagram are given together with unit cell dimensions determined with the Weissenberg x-ray goniometer ($a=13.65$ and 13.69, $b=15.91$ and 15.93, $c=6.68$ and 6.68 kX, for the green and yellow varieties respectively). Two new complete chemical analyses, from which a formula of the type $R_{40} \cdot (Si, B)_{18} \cdot O_{86}$ can be deduced, are given.

The author has examined the relationships, between the chemical composition, the refractive indices, the axial angle, and the specific gravity of seven analyzed varieties of kornerupine. The relationships between kornerupine and its associated minerals at the Lac Ste-Marie occurrence were studied: kornerupine occurs with quartz, orthoclase, biotite, tourmaline, andalusite, almandite, rutile, zircon, dumortierite, etc. This deposit is found in paragneisses, of the Grenville series, which have been modified by igneous emanations.

Introduction

First found in Greenland (Lorenzen), kornerupine was later reported from a few localities: in Saxony (Sauer, Uhlig, Gossner and Mussgnug, Harker), in Madagascar (Lacroix, 1912, 1922, 1923, 1939) (Payne), in Antarctica (Mawson), in Ceylon (Hey, Anderson, & Payne), and in South Africa (de Villiers). The chemical composition of the mineral was not accurately known until boron was detected in it by Lacroix and de Gramont (1921) and until as a result of comparative studies published in 1940, Hey, Anderson & Payne showed that much of the iron is present in ferrous condition in the mineral.

The kornerupine here described was discovered in 1949 near Lac Ste-Marie, by Prof. Pierre Mauffette, of the Ecole Polytechnique in Montreal when he was mapping the area for the Quebec Department of Mines. He submitted a specimen of this mineral for identification to the Department of Mines Laboratories. Later, the writer visited Lac Ste-Marie in order to collect specimens, but he had too little time to make a full study of the mode of occurrence of the mineral.

The region is largely underlain by formations of the Grenville series, which are locally made up principally of paragneisses and crystalline limestones. Igneous intrusives of diverse composition cut the Grenville rocks intricately. A contact between the limestone and the paragneisses east of the occurrence, strikes N 50° E and dips 35° E. The kornerupine-

[1] Published by permission of the Deputy Minister of Mines of the Province of Quebec.

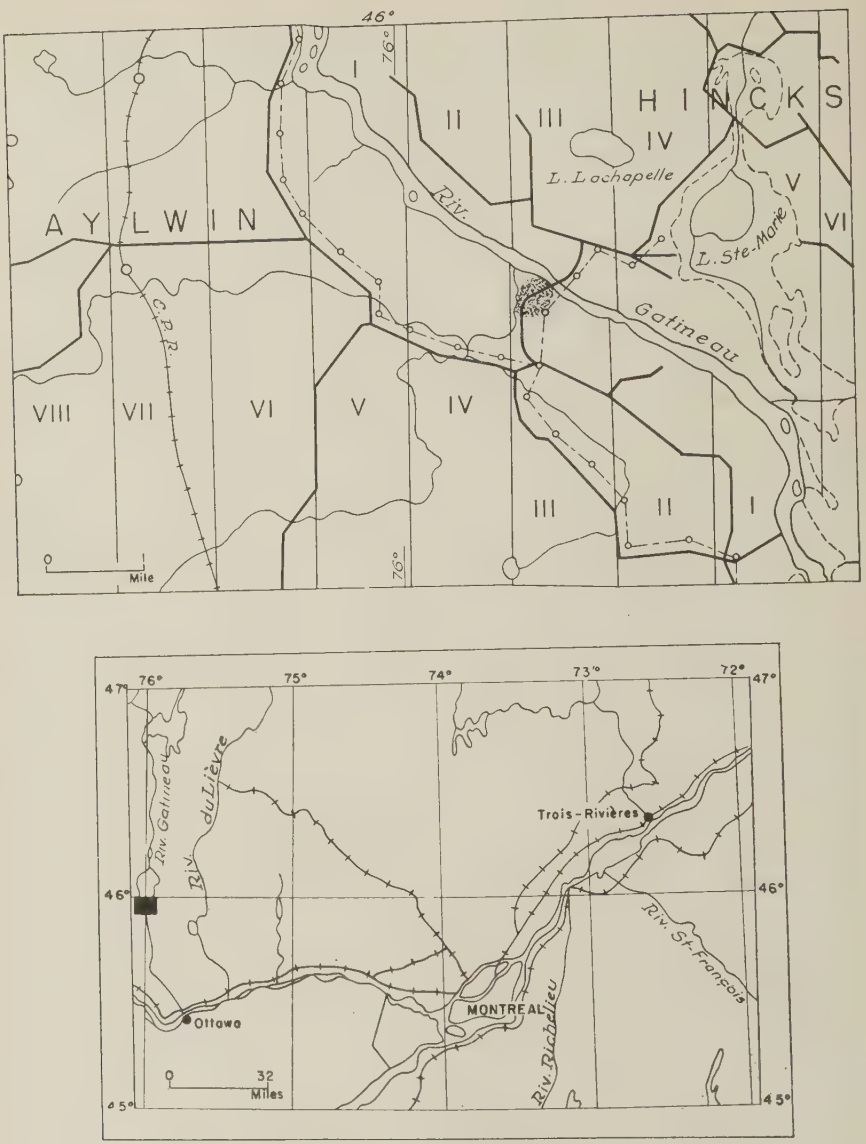

FIG. 1. Sketch showing location of kornerupine bearing rocks near Lac Ste-Marie, Quebec.

bearing rocks crop over a length of about 500 feet and a width of 100 feet.

The deposit is in the Aylwin township, Range III, Lots 15 and 16, and along the road from Kazabazua to Lac Ste-Marie, on the southwest bank of Gatineau river, near Hincks bridge (Fig. 1).

Geometric Crystallography

Two varieties with somewhat different properties have been studied. A *green* kornerupine is found in well defined dark green or black orthorhombic crystals of diverse dimensions which may be as much as two inches long and nearly $\frac{1}{2}$ inch diameter. The faces are very shiny and allow accurate goniometric measurements in spite of the slight irregularities of their surfaces. Faces (110) and (100) tend to be better developed than (010). No (001) face has been found.

The *yellow* variety occurs as fairly well defined greenish-yellow crystals, forming as much as 40 per cent of the rock. The crystals are commonly smaller than those of the green kornerupine, but they show the same crystal faces; however (100) and (010) are in some crystals better developed than (110). The faces are dull and not suitable for good angle measurements.

Table 1. Kornerupine from Lac Ste-Marie (green variety)
Measured and Calculated Angles, Orthorhombic
$a:b:c=0.8597:1:0.4198$[1] $p_0:q_0:r_0=0.4883:0.4198:1$

Forms[2]	Measured		Calculated	
	ϕ	$\rho=C$	ϕ	$\rho=C$
010	0°00′	—	0°00′	90°00′
100	90 02 (6)	—	90 00	90 00
110	49 17 (4)	—	49 19	90 00

N.B. Numbers in parentheses indicate the number of measurements.

[1] The values in which axis c enters have been calculated from x-ray diffraction data.

[2] The author has observed dull and irregular (101) and (201) faces at one end of a small crystal of kornerupine from Natal.

X-Ray Crystallography

Measurements of the unit cell dimensions of the two varieties of the kornerupine from Lac Ste-Marie, as well as of a sample from Natal, South Africa (Table 2) were made with the Weissenberg x-ray goni-

Table 2. Kornerupine, Orthorhombic, *Cmmm*?

Cell Dimensions kX[1]	Lac Ste-Marie		Natal	Ceylon[2] Hey et al (1941)
	Green	Yellow		
a	13.69	13.65	13.65	13.68
b	15.93	15.91	15.91	15.95
c	6.68	6.68	6.68	6.68

[1] Using wavelengths FeKα_1 1.93208 kX and FeKα_2 1.93601 kX.

[2] Given as A but probably really kX units.

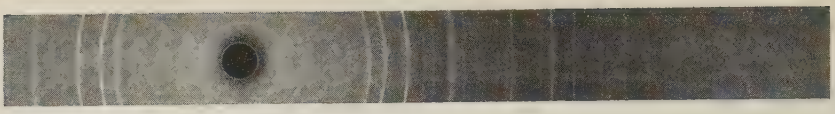

FIG. 2. Kornerupine (yellow variety) *X*-ray powder pattern, Fe/Mn radiation, Contact print of film from 114.6 mm. diam. camera reduced to $\frac{1}{2}$ size ($1°\theta = 1$ mm. on print).

ometer. An *x*-ray powder photograph was also made of the yellow kornerupine of Lac Ste-Marie (Table 3 and Fig. 2). The unit cell is base centered. Furthermore, after a short immersion in fused Na_2CO_3, crystals exhibit etch patterns indicating the presence of a plane of symmetry perpendicular to the *c* axis. These tests, together with the morphology of the crystals, lead to the belief that kornerupine probably belongs to the dipyramidal class. In this case, the only space group susceptible to accommodate the 86 atoms of oxygen present in the cell would be D_{2h}^{19}—*Cmmm*.

CHEMICAL COMPOSITION

The samples for chemical analyses were prepared from selected crystals which were crushed and screened ($-50+70$ mesh and $-70+100$ mesh). The two screen fractions were then processed separately, with

TABLE 3. KORNERUPINE (YELLOW VARIETY)—*X*-RAY POWDER PATTERN
Orthorhombic *Cmmm*?; $a = 13.65$, $b = 15.91$, $c = 6.68$kX[1]

I(Fe)	*d*(meas)	*hkl*	*d*(calc)	*I*(Fe)	*d*(meas)	*hkl*	*d*(calc)
8	10.4	110	10.36A	5	1.976	313	1.985
4	7.94	020	7.96			551	1.978
7	6.83	200	6.82			234	1.870
1	4.06	221	4.09	4	1.864	403	1.862
6	3.99	040	3.98			172	1.860
		131	3.98	4	1.795	552	1.760
7	3.42	400	3.41			712	1.674
		041	3.42	8	1.670	661	1.671
9	3.34	002	3.34			004	1.670
10	3.00	202	3.00			820	1.668
4	2.87	421	2.84	6	1.590	603	1.590
5	2.69	510	2.69			224	1.589
10	2.61	350	2.61	7	1.533	044	1.540
6	2.387	402	2.385			662	1.532
5	2.273	531	2.280	9	1.488	882	1.491
		600	2.275			590	1.483
		152	2.273			083	1.482
5	2.117	203	2.118	6	1.436	1.11.0	1.438
8	2.095	460	2.093			0.10.2	1.436
		512	2.095	8	1.406	1.11.1	1.406
6	2.069	062	2.077			2.10.2	1.405
		550	2.072			354	1.404

[1] Using wave-lengths FeKα_1 1.93208 kX and FeKα_2 1.93601 kX.

bromoform, methylene iodide, and Clerici solution (specific gravity: 3.50). The concentrates of kornerupine thus obtained were purified by hand sorting under the binocular microscope. A small quantity of rutile remained as a minor impurity. Kornerupine is very resistant to acids, especially the green variety, and FeO had to be determined by the Carius tube method.

The chemical composition of the two varieties of kornerupine from Lac Ste-Marie compared with other published analyses will be found in Table 4. Several other analyses were not considered, for the boron had

TABLE 4. SELECTED CHEMICAL ANALYSES OF KORNERUPINE

Elements	1	2	3	4	5a	5b	6a	6b	7
SiO_2	31.09	30.5	29.3	30.5	30.24	30.32	30.18	30.35	29.53
B_2O_3	3.59	2.8	2.5	3.0	3.50	3.51	3.27	3.29	3.5
Al_2O_3	38.17	37.6	40.0	35.8	40.86	40.97	41.95	42.21	40.97
Fe_2O_3	nil	3.3	nil	3.2	0.42	0.42	0.90	0.91	nil
FeO	2.55	4.8	5.0	9.1	8.52	8.52	9.10	9.15	12.22
MgO	22.51	20.7	21.0	17.6	14.87	14.91	12.48	12.56	10.90
CaO	0.51	—	—	—	0.06	0.06	0.18	0.18	—
Na_2O	1.36	trace	0.1	1.6	0.08	0.08	0.13	0.13	0.70
K_2O	0.08	trace	0.6	trace	0.00	0.00	0.00	0.00	—
H_2O+	0.10	—	—	—	0.97	0.97	1.06	1.07	0.67
H_2O-					0.00	0.00	0.00	0.00	
TiO_2	—	—	—	—	0.19	0.00	0.51	0.00	0.44
P_2O_5	—	—	—	—	0.09	0.09	0.08	0.08	0.12
Cr_2O_3	—	—	—	—	0.06	0.00	0.04	0.00	—
ZrO_2	—	—	—	—	0.00	0.00	0.05	0.00	—
MnO	—	—	—	—	trace	trace	trace	trace	0.08
		Loss: 0.2							
Total	99.96	99.9	98.5	100.8	99.86	99.87	99.93	99.93	99.13
Specific gravity	3.27	3.335 ±0.005	3.330 ±0.003	3.37 ±0.010	3.37 ±0.01		3.39 ±0.02		3.449

1 —Itrongay, Madagascar (Lacroix, 1922) "corrected in accordance with a new FeO determination" (Hey, 1941), F. Raoult, analyst. Hey, Anderson & Payne note that a new measurement of the density gave 3.29.

2 —Ceylon "normal type" (Hey, Anderson & Payne). M. H. Hey, analyst.

3 —Ceylon "optically pseudo-uniaxial type. (Hey, Anderson & Payne). M. H. Hey, analyst.

4 —"Prismatine." Waldheim, Saxony. (Hey, Anderson & Payne). M. H. Hey, analyst.

5a—Lac Ste Marie, green variety (new data). H. Boileau, analyst.

5b—Lac Ste Marie, green variety corrected for 0.19% rutile and 0.08% chromite.

6a—Lac Ste Marie, yellow variety (new data). H. Boileau, analyst.

6b—Lac Ste Marie, yellow variety corrected for 0.51% rutile, 0.05% chromite and 0.07% zircon.

7 —Port Shepstone, Natal, South Africa (de Villiers), C. J. van der Walt, analyst; "corrected in accordance with a new FeO and total iron determination" (Hey, Anderson & Payne), M. H. Hey, analyst.

not been determined (Lorenzen, Sauer, Uhlig, Gossner and Mussgnug, Lacroix (1912), or for other reasons, Hey, Anderson, and Payne (their analysis No. II).

The analyses of Lac Sainte-Marie kornerupine show about one per cent of water. The role of this water in the mineral is not clear, and accordingly experiments were undertaken to determine if possible how it occurs. Samples were heated in a Chevenard thermobalance (Duval), which allows an accurate recording of the changes of weight with rising temperature. The results with kornerupine were inconclusive as yet.

Three hypotheses concerning the state of the water were considered. These are: a) the kornerupine contains only absorbed water; b) the kornerupine holds one molecule of water; c) all the water found in the analysis is water of constitution.

Analyses 5b and 6b were recalculated to sum 100 on each of those hypotheses and the empirical atomic contents of the unit-cell were calculated. The results are shown in Table 5. Examination of this table shows that the most plausible hypothesis is that kornerupine holds one mole-

Table 5. Empirical Unit-Cell Contents of Lac Ste-Marie Kornerupine

Elements	Number of atoms					
	No molecular water		1 molecule H_2O		Total H_2O contents as molecular	
	Green	Yellow	Green	Yellow	Green	Yellow
Si	15.1	15.2	15.0	15.1	14.9	15.0
B	3.0	2.8	3.0	2.8	3.0	2.8
Al	24.3	24.8	23.9	24.7	23.8	24.5
Fe'''	0.2	0.3	0.2	0.3	0.2	0.3
Fe''	3.5	3.8	3.5	3.8	3.5	3.8
Mg	11.1	9.4	11.0	9.3	10.9	9.3
Ca	0.0	0.0	0.0	0.0	0.0	0.0
Na	0.1	0.1	0.1	0.1	0.1	0.1
P	0.0	0.0	0.0	0.0	0.0	0.0
H	0.0	0.0	2.0	2.0	3.2	3.4
O	86.0	85.6	86.1	86.1	86.3	86.3
Si+B	18.1	18.0	18.0	17.9	17.9	17.8
Al+Fe'''	24.4	25.2	24.0	25.0	24.0	24.9
Mg+Fe''	14.6	13.2	14.5	13.1	14.5	13.0
ΣR	39.1	38.5	40.6	40.2	41.7	41.5
ΣA	143.3	142.1	144.8	144.3	145.9	145.6

ΣR: sum of atoms except Si, B and O.
ΣA: sum of all atoms.

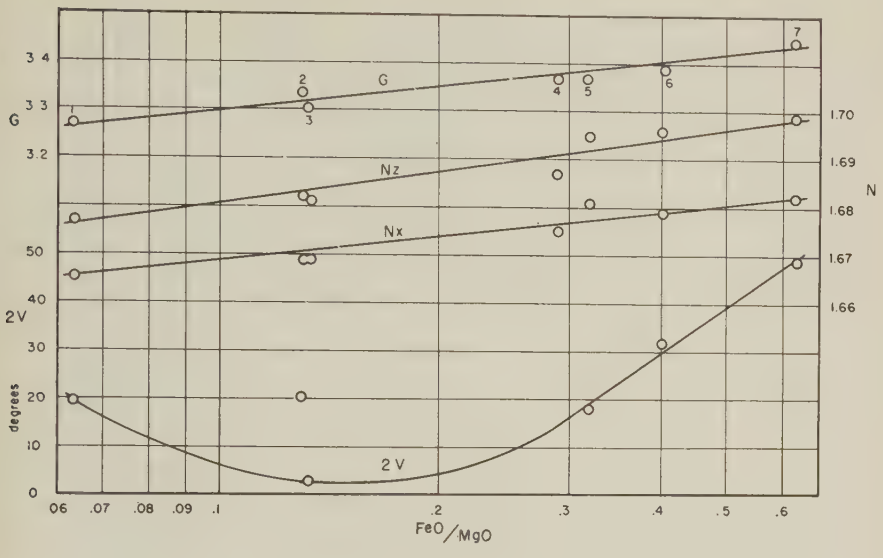

FIG. 3. Graph showing variations in optic properties of kornerupine according to the molecular ratio of FeO to MgO contents.

cule of water of constitution. With this hypothesis the number of oxygen atoms is nearest to 86, as suggested by Hey, Anderson & Payne (1941).

PHYSICAL AND OPTICAL PROPERTIES

Hardness—The hardness of the kornerupine from Lac Ste-Marie is $6\frac{1}{2}$ to 7 for the green variety,[1] and 6 to $6\frac{1}{2}+$ for the yellow.

Specific Gravity—$3.37 \pm .01$ (green) to $3.39 \pm .02$ (yellow). The yellow variety contains microscopic inclusions which makes it difficult to separate a homogeneous grain for determination.

Cleavage—(110) cleavage is imperfect in the green variety, slightly better in the yellow variety.

Fusibility—6.

Optical Properties—The two varieties of Lac Ste-Marie crystals are sufficiently large and clear cut to make it feasible to cut oriented sections from them. The optical properties (Table 6) were determined on such oriented sections. The varieties, the analyses of which are given above, were grouped in this table according to the increasing values of the ratio of molecular FeO to MgO. Figure 3 shows a close relationship between this ratio and the indices of refraction, the axial angle, and the specific gravity. The reason for the deviation of 2V of sample 2 from the curve is not at once apparent.

The yellow kornerupine shows variations from about 28° to about 36° in the value of the axial angle.

[1] Hardness measurements made with the Bierbaum Microcharacter 2100 to 2200.

Table 6. Comparative Optic Properties of Analyzed Kornerupine

No.	Origin	$\frac{FeO}{MgO}$ molecular	N_X	N_Y	N_Z	$N_Z - N_X$	2V	Pleochroism
1	Madagascar[1]	0.064	1.6650	1.6766	1.6770	0.0120	19½°	—
2	Ceylon[1]	0.130	1.669	1.681	1.682	0.013	20½°	X green; Y pale-brownish yellow, Z pale brownish green.
3	Ceylon[1]	0.132	1.669	1.681	1.681	0.012	3°	—
4	Saxony[1]	0.291	1.675	1.687	1.687	0.012	—	—
5	Lac Ste Marie (green variety)	0.321	1.681	1.694	1.695	0.014	18°	X colorless; Y colorless or pale yellowish-green, Z green.
6	Lac Ste Marie (yellow variety)	0.409	1.679	1.694	1.696	0.017	32°±	X colorless; Y colorless or very pale pink; Z pale green (in thick section, 1 mm).
7	Natal[1]	0.629	1.682	1.696	1.699	0.017	48°	X = Y colorless, Z light amber (yellow with some brown and green).

Index values are given for the D line with a precision of ±0.002 except for sample 4 (±0.004).
[1] Data from Hey, Anderson & Payne (1941).

Petrography

Green Kornerupine

The green kornerupine occurs in an injected biotite and tourmaline paragneiss, that is rich in orthoclase and relatively poor in quartz. Injected zones are parallel with the foliation and are clearly visible due to their light color against the dark background of the rock; the injected material is made chiefly of orthoclase with occasionally some large crystals of kornerupine; quartz is rare in it, tourmaline rare or absent. Kornerupine is not distributed uniformly through the rock but is found either in the immediate vicinity of the injected zones or in nests which are as much as two inches in diameter and whose limits are marked by numerous biotite flakes, and containing many sub-parallel prisms of kornerupine embedded in orthoclase with a little quartz. The crystals of kornerupine are not always parallel to the foliation. They are generally coated with biotite flakes; in the neighbourhood are also observed large areas of orthoclase with a coating of biotite (Fig. 4). Tourmaline is extremely rare as inclusions in kornerupine; on the other hand inclusions of pyrite, pyrrhotite, and biotite are fairly common; very few inclusions of rutile occur in the green variety, whereas this mineral is rather common in the yellow variety.

One thin section shows an irregular mass of andalusite, which appears to be moulded on the kornerupine. In the same section, a thin rim of quartz surrounds an apparently corroded crystal of kornerupine.

FIG. 6

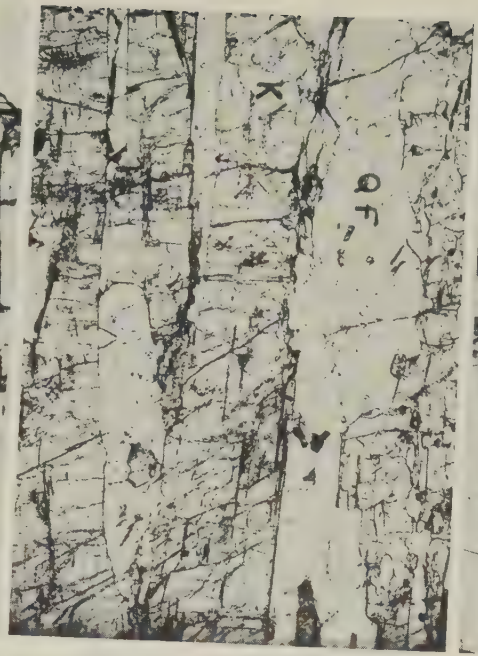

FIG. 5

FIG. 4

FIG. 4. Contact between a large crystal of green kornerupine (K) and paragneiss. Note the coating of biotite flakes around kornerupine and orthoclase (F) 9× plane polarized light.

FIG. 5. Sub-parallel crystals of yellow kornerupine (K) in a gangue of quartz with orthoclase (QF) 9× plane polarized light.

FIG. 6. Crystal of yellow kornerupine, section normal to the *c* axis 70× plane polarized light.

Tourmaline is small grains with polygonal outlines is uniformly distributed in the apparently non-injected parts of the rock. Biotite defines the foliation, and it contains many inclusions of zircon surrounded by pleochroic halos. A few grains of pyrite and pyrrhotite are also present.

Yellow Kornerupine

The rock containing the yellow variety is probably also a paragneiss, but it may originally have had a different composition from the paragneiss containing the green variety or have undergone a different process of metasomatism. Kornerupine abounds in it and is in some parts one of the main constituents of the rock. The other important minerals in this rock are quartz, and in certain places, almandite. Aggregates of tourmaline are observed in places. This rock contains less feldspar than the rock in which the green variety is found. Here and there, needles of sillimanite are sparsely disseminated. In one section, a few needles of dumortierite were seen in a grain of almandite.

Kornerupine, that is found as elongated crystals (Fig. 5) which define the foliation of the rock, is very rich in various inclusions of quartz, orthoclase, rutile, biotite, pyrite, pyrrhotite, tourmaline (rare), etc. In thin sections normal to the *c*-axis the yellow kornerupine shows good euhedral shape (Fig. 6).

Genetic Considerations

Little precise information on the geology and petrography of the kornerupine occurrences is found in the mineralogical literature. Some Madagascar kornerupine may have originated in a quartz vein, with a pegmatitic facies. The vein may be interbedded in a cordierite-rich gneiss (Lacroix 1939); in Ceylon kornerupine is found in gravels, together with zircon, garnet, and spinel (Hey, Anderson & Payne); in Natal kornerupine is accompanied by biotite and quartz with little tourmaline and grandidierite ("the nature and texture of the component minerals make it seem likely that the rock is of pegmatitic origin and that contact assimilation of iron and magnesium has played a part in its formation," de Villiers, 1940); in Saxony kornerupine is found in an albitic facies of a "granulite" together with corundum, kyanite, sillimanite, and tourmaline (Harker), etc.

It would therefore appear that kornerupine is a product of metasomatism; furthermore, the presence of boron, unsuspected by the early authors, and the usual association with tourmaline lead to the belief that the proximity of boron-bearing intrusives, such as occur near the deposit of Lac Ste-Marie, is necessary to the formation of kornerupine. For these reasons, and also because of the analogy between kornerupine and tourmaline, it would be worthwhile to investigate possible relation-

ships between these two minerals. Perhaps, elements that should normally form tourmaline end by forming kornerupine when placed in certain physico-chemical environments which must surely be very unusual in view of the rarity of this mineral.

Acknowledgments

The present study was made in the laboratories of the Department of Mines of the Province of Quebec with the permission of Dr. A. O. Dufresne, Deputy Minister, and under the direction of Dr. Maurice Archambault, Director of Laboratories, who has offered valuable suggestions during the work. Dr. F. F. Osborne, on the staff of the Department of Mines and Université Laval, has discussed the subject and kindly read and corrected the manuscript. Prof. Pierre Mauffette, of the Ecole Polytechnique de Montreal, who discovered the deposit, accompanied the writer to its location.

The author wishes to record his indebtedness to Mr. Fernand Claisse, physicist, for the *x*-ray work performed and for much kind cooperation, and also to Mr. Henri Boileau, chief-chemist, who carried out the chemical analyses presented here. Hearty thanks are due to his other colleagues of the Department of Mines who took part in this work and whose friendly cooperation was much appreciated. Thanks are also due to Prof. L. G. Berry, of Queen's University, Kingston, for his criticisms of the manuscript.

References

de Villiers, J. A. (1940): Iron-rich kornerupine from Port-Shepstone, Natal: *Min. Mag.*, **25,** 550–556.

Duval, C., *et al.* (1951): Continuous weighing in analytical chemistry: *Analytical Chemistry,* **23,** 1271–1286.

Gossner, B., & Mussgnug, F. (1928): *Neues Jahrb. Min.*, Abt. A, Beil-Bd, **58,** 227.

Harker, A. (1932), *Metamorphism,* London.

Hey, M. H., Anderson, B. W., & Payne, C. J. (1941): Some new data concerning kornerupine and its chemistry: *Min. Mag.*, **26,** 119–130.

Lacroix, A. (1912): *Comptes Rendus Acad. des Sciences, Paris,* **155,** 672.

——— (1922): *Min. de Madagascar,* **1,** 396; **2,** 102.

——— (1923): *Min. de Madagascar,* **3,** 302.

——— (1939): Observations sur quelques minéraux de Madagascar: *Bull. Soc. Fr. Minér.*, **62,** 300–304.

——— & de Gramont, A. (1921): Sur la recherche spectrale du bore et sur sa présence dans quelques silico-aluminates naturels: *Bull. Soc. Fr. Minér.*, **44,** 66–77.

Lorenzen, J. (1884): *Meddelelser om Grønland,* **7,** 19.

Mawson, D. (1940): Record of Minerals of King George Land, Adelie Land and Queen Mary Land: *Australasian Antarctic Expedition* 1911–1914, Ser. A, 4 (Geology), **12,** 360–403.

Payne, C. J. (1939): Dispersion of some rarer gemstones: *Gemmologist,* London.

Sauer, A. (1886): *Zeits. Deutsch. Geol. Gesell.*, **38,** 704.

Uhlig, J. (1910): *Zeits. Kryst.*, **47,** 215.

NOTES AND NEWS

A COBALT-NICKEL-COPPER SELENIDE FROM THE GOLDFIELDS DISTRICT, SASKATCHEWAN[1]

S. C. Robinson and E. J. Brooker

Geological Survey of Canada, Ottawa, Canada.

A number of small deposits of selenide minerals in the Goldfields District, Saskatchewan have been reported by the senior author (Robinson *Geol. Surv., Canada*, Paper 50-16, 1950). In two of these deposits, disseminated grains and small masses of a mineral ressembling pentlandite were recognized. Enough of this mineral has now been segregated to provide data for this preliminary description.

The deposits in which the mineral was found consist primarily of umangite, with minor klockmannite and traces of berzelianite, clausthalite pyrite, hematite and chalcopyrite. These minerals occur cementing the sheared and fractured host rocks and their principal alteration product is chalcomenite. Quartz is the only introduced gangue mineral and is present in very small amount. The cobalt-nickel-copper selenide is veined, embayed and replaced by umangite so that segregation of pure material is a difficult and tedious process.

Grains of the mineral are usually rounded, but a few of them show subhedral development of the cube. Crushed products contain both cubic fragments and others showing conchoidal fracture; it is probable that there is poor cubic cleavage. The mineral is brittle with a hardness of about $3\frac{1}{2}$. Specific gravity of 6.6 ± 0.2 was determined by use of a modification to the Berman balance on 7.42 milligrams of finely-divided, picked material. The mineral has a metallic lustre, is light bronze in colour and yields a black streak. It is opaque even on thin edges. In polished section, it is isotropic and its colour is light brassy bronze. Positive microchemical tests for copper, cobalt, nickel and selenium were obtained using methods described by Short (1950).

X-ray powder patterns of material from both occurrences and of pentlandite from the Worthington mine, Sudbury, Ontario, are reproduced in Fig. 1. The material used for specific gravity and *x*-ray fluorescence analysis determinations, corresponds to pattern No. 2 and comes from the western part of the Eagle group of claims. Material represented in pattern No. 1 comes from a deposit at the head of Ato Bay, on Beaverlodge Lake. The relative intensities, glancing angles and spacings for all lines on pattern No. 1 and pentlandite are given in Table 1, together with

[1] Published by permission of the Director-General of Scientific Services, Department of Mines and Technical Surveys, Ottawa, Canada.

TABLE 1. *X*-RAY POWDER PATTERNS*

Cobalt—Nickel—Copper Selenide $a_0 = 10.005 \pm 0.004$ A					Pentlandite Worthington Mine, Algoma Dist. $a_0 = 10.042 \pm 0.005$ A			
I	2θ Cu	*d*(meas)	*hkl*	*d*(calc)	*I*	2θ Cu	*d*(meas)	*d*(calc)
4	15.33	5.780	111	5.776	3	15.33	5.780	5.798
			002		½	17.71	5.009	5.021
4	25.18	3.537	022	3.537	½	25.12	3.545	3.550
½	26.61	3.350	003	3.335				
½	28.03	3.183	013	3.164				
6	29.62	3.016	113	3.017	8	29.50	3.028	0.028
7	30.99	2.886	222	2.888	4	30.88	2.896	2.899
9	35.90	2.501	004	2.501	½	35.76	2.511	2.511
1	39.24	2.296	133	2.295	3	39.15	2.301	2.304
			024		½	40.07	2.250	2.245
1	44.37	2.042	224	2.042				
6	47.20	1.926	115; 333	1.926	5	47.06	1.931	1.928
10	51.68	1.769	044	1.769	10	51.49	1.775	1.775
1	54.19	1.693	135	1.691	½	54.04	1.697	1.697
1	60.65	1.527	335	1.526	1	60.50	1.530	1.528
4	61.44	1.509	226	1.508	1	61.23	1.514	1.514
4	64.51	1.445	444	1.444				
2	66.70	1.402	155	1.401				
1	70.22	1.340	246	1.337				
2	72.46	1.304	355	1.303	2	72.27	1.307	1.307
3	75.97—	1.253	008	1.251	2	75.78	1.255	1.252
1	78.09	1.224	337	1.222				
½	81.50	1.181	228; 066	1.179	½	83.29	1.160	1.183
1	83.65	1.156	157; 555	1.155				
1	84.26	1.149	266	1.148				
4	86.94—	1.121	048	1.119				
1	89.07	1.099	119; 357	1.098	½	88.50	1.105	1.102
2	94.43	1.050	139	1.049	½	94.11	1.052	1.053
4	97.74	1.023	448	1.021	2	97.47	1.025	1.025
½	99.89	1.006	177; 339	1.006				
3	105.45	0.9680	159; 377	0.9672	½	105.08	0.9704	0.9708
½	111.17	0.9337	468	0.9290				
2	120.89	0.8855	088	0.8843	½	120.35	0.8878	0.8876
2	123.34	0.8751	179	0.8741				
½	127.95	0.8572	0.6.10; 668	0.8582				
½	130.06	0.8497	3.3.11; 379	0.8496				
½	130.91	0.8466	2.6.10	0.8456				
2	134.67	0.8347	488	0.8338				
½	137.62	0.8261	777	0.8252				
1	142.89	0.8125	2.2.12	0.8115				
1	146.29	0.8048	579	0.8036	½	145.40	0.8068	0.8047
4	153.06	0.7920	0.4.12	0.7910	1	151.86	0.7941	0.7939
1	158.92	0.7835	0.8.10; 688	0.7813				

* Radiation Cu; $\lambda = 1.5418$ A, $2\theta < 90$, $\lambda = 1.54050$ A, $2\theta > 90$, Camera 114.58 mm. Film shrinkage correction applied.

the indices for the corresponding planes and calculated spacings for the mineral being described. All lines in the powder patterns conform to a face-centred cubic lattice with a cell edge (a_0) of 10.005 ± 0.005 A. For pattern No. 1, this value is 10.004 ± 0.005 A, for pattern No. 2 it is 10.006 ± 0.004 A and for the pentlandite specimen it is 10.042 ± 0.004 A.

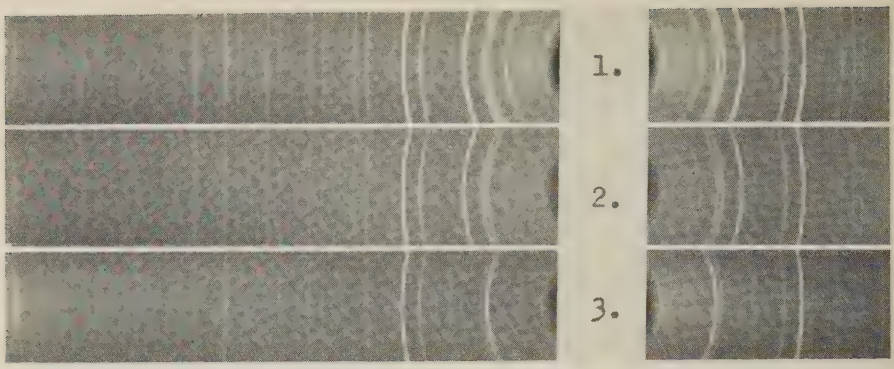

FIG. 1. *X*-ray powder photographs, filtered CuK radiation (contact prints $1°\theta = 1$ mm on film) 1 & 2 Cobalt-nickel-copper selenide; Ato Bay and Eagle group, Goldfields district, Saskatchewan. 3. Pentlandite, Worthington mine, Sudbury Ontario.

Systematically missing spectra indicate that the space group is $Fm3m$.

A preliminary *x*-ray fluorescence analysis indicates that the composition conforms to the approximate atomic formula $Co_{3.0}\ Ni_{2.0}\ Cu_{3.5}\ Se_{9.5}$. It is probable that cobalt, nickel and copper may substitute for each other in varying amount and that the mineral may conform to a general formula of the RX type. Search of the literature has not disclosed any mineral whose chemical and structural features approach closely those here described; Penroseite has a unit cell of 6.01 ± 0.01 (Bannister & Hey, *Am. Mineral.*, **22**, 319–324, 1937), and a composition conforming to the general type RX_2.

A complete chemical analysis of this mineral is to be made, that will permit calculations of the contents of the unit cell and of the specific gravity. Until this more complete description is available, it would be premature to suggest a name for this mineral.

AUTORADIOGRAPHS AS A MEANS OF STUDYING DISTRIBUTION OF RADIOACTIVE MINERALS IN THIN SECTION[1]

S. C. ROBINSON, *Geological Survey of Canada, Ottawa, Canada.*

This note describes a simple method of recognizing those grains in a thin section, that contribute to its radioactivity. General information on the subject of detecting and measuring alpha radiation by means of nuclear emulsions is fully described by Yagoda (*Radioactive Measurements with Nuclear Emulsions* 1949), and some ingenious applications of the method to the study of radioactive minerals, by Stieff & Stern

[1] Published by permission of the Director-General of Scientific Services. Department of Mines and Technical Surveys, Ottawa, Canada.

(*U.S.G.S. Trace Elements Investigations Report 127*, 1950). Recognition of radioactive minerals in thin sections is greatly facilitated where the thin section, and the autoradiograph made from it, are mounted together under the microscope. This can be done by coating the thin section with nuclear emulsion, however, alpha tracks overlying opaque or dark minerals cannot be detected in such a mount. The method here described, simply involves orienting the thin section on the autoradiograph made from it, so that the glass of the thin section and the glass of the nuclear plate (or the celluloid of the stripping film), lie between the rock slice and the emulsion, (see Fig. 1). Once so mounted, the distance between the rock slice and the emulsion is such that the alpha tracks are out of focus when examining the rock slice and vice versa. Photomicrographs of uraninite and radioactive apatite in biotite, and of the resulting alpha track pattern, are reproduced in Fig. 2. These photomicrographs were taken at the requisite focal distances, with the nuclear track plate mounted on the thin section and using a Leitz P3 objective, focal length 6.0 mm. approximately.

Procedure and Material

Kodak Nuclear Track Plates, type NTA or, Kodak Autoradiographic Stripping Film, type NTB.
Kodak D72 developer, development time, 3 minutes.
Kodak F16 fixer, fixing time, 30 minutes.

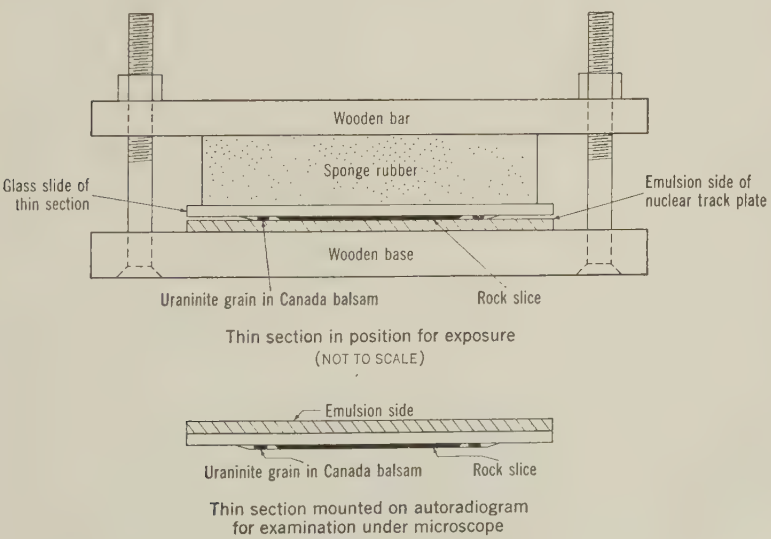

Fig. 1

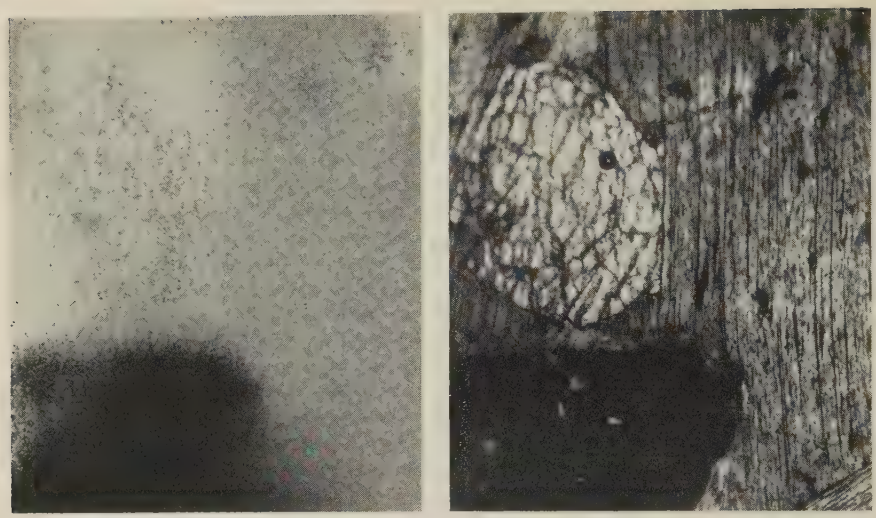

FIG. 2. Photomicrographs of a thin section (right) and corresponding autoradiograph (left). In the thin section the black area is uraninite, the white area is radioactive apatite and the remainder is biotite under plane polarized light. Magnification approximatelv 90 diameters.

Thin sections should be made without a cover glass and with all the Canada balsam removed from the exposed surface of the rock slice. In order to facilitate orientation of the thin section on the autoradiograph, two or three single grains of uraninite (or other radioactive substance), should be cemented in the Canada balsam around the rock slice and ground down with the rock slice.

For exposure, the rock surface is placed against the emulsion side of the plate or film and held there under light pressure. A simple press for this purpose is illustrated in Fig. 1. The mount is then put away in total darkness for exposure. Time of exposure depends on the radioactivity of the minerals in the rock. For uraninite, an exposure of 3 days is ample (see Fig. 2), but for weakly radioactive minerals, exposures of up to a month in duration, may be necessary.

Areas of alpha tracks from the uraninite grains will be clearly visible to the unaided eye and by means of these, the thin section may be roughly oriented and held in position, back to back, on the autoradiograph, by rubber cement (see Fig. 1). With the mount lying on the microscope stage, rock slice down, emulsion side up, the thin section may be precisely oriented on the autoradiograph under a low-power objective (Leitz, P1), before the cement sets.

The mount is studied under a medium-power objective such that the alpha tracks are out of focus when the microscope is focussed on the rock slice and vice versa. It is best to set the focus on one of the dense patches

of tracks from the uraninite and then traverse the mount to look for the weaker centres of tracks. When these are found, it is only necessary to focus down to the rock slice in order to identify the mineral that has caused them. If the mineral is opaque, it is often possible to dig enough of it out of the section with a needle, to be mounted on a glass fibre coated with vaseline, for determination by x-ray diffraction.

A METHOD FOR QUANTITATIVE RADIOACTIVITY MEASUREMENTS OF SMALL AMOUNTS OF RADIOACTIVE MINERALS[1]

H. R. Steacy, *Geological Survey of Canada, Ottawa, Canada.*

The property of radioactivity possessed by minerals containing uranium and, or, thorium may be used as an aid in identifying them, for by accurate quantitative radioactivity determinations the minerals may be grouped according to their uranium and, or, thorium contents. In some instances it is possible by radiometric measurements to determine that the mineral in question is one of a group of only three or four minerals. Of the commoner species, for example, pitchblende, uraninite, and uranothorite all show a radioactivity very much higher than other primary radioactive minerals, whereas allanite, cyrtolite, zircon, and some fergusonites show relatively low activities and euxenites and similar complex minerals usually show an intermediate degree of activity.

In the course of investigations at the Radioactivity Laboratory it has been common experience to be able to obtain only a few, hand-picked grains of a radioactive mineral from the solid specimens or recover a small amount of the mineral by separation tests. The method here described has been used effectively for the measurements of 5–10 mg. samples. The sample powder is weighed, transferred to the tip of a small glass funnel, and counted with an ordinary laboratory-type, thin end-window, Beta tube in combination with a ratemeter or scaling unit. Comparison is made against uranium standards which, in this laboratory, are made up from pitchblende and inert material.

The glass funnel is illustrated in Figure 1; small variations in its dimensions are not important. The funnel-shaped mouth serves two purposes: (1) it allows easy filling of the tip with the sample powder, and (2) it provides a firm base during the counting period.

The funnel is made from a short length of 2 mm.-bore, soft glass tubing. One end of the tubing is heated to a small globule of glass, which is blown into a bubble with a diameter about equal to that of the funnel mouth. The outer half of the bubble is reheated and blown out, and the

[1] Published by permission of the Director-General of Scientific Services, Department of Mines and Technical Surveys, Ottawa.

funnel mouth shaped with a metal tool. The stem of the funnel is cut at the required length and the tip ground flat on a glass plate with a little carborundum powder. The mouth of the funnel is also ground flat to afford a firm vertical standing position. Other materials necessary are tube of ambroid cement and a thin sheet of cellophane.

The choice of a uranium standard is determined by preliminary activity tests of the sample; the standard should, if possible, closely approximate the activity of the sample.

The samples and uranium standards are ground to pass a 200-mesh screen in order to produce a smooth sample surface and allow firm pack-

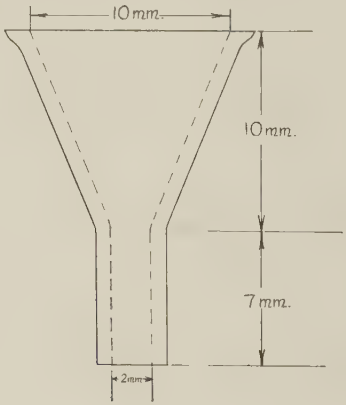

FIG. 1

ing of the materials in the funnel tip to prevent any loss of sample while handling the funnel. Using a chemical balance, equal portions of the sample and uranium standard are weighed out[2] on small sheets of glazed paper.

The technique for placing the powder in the funnel tip is as follows: a drop of ambroid cement is smeared thinly on a glass plate. The tip of the funnel is carefully touched to the ambroid and then immediately pressed firmly on a small square of cellophane. The powder is poured into the funnel and shaken down to the tip, after which the funnel is rapped sharply on the table several times to compress the powder. The cellophane is now removed as it offers some shielding to the radiation. The powder will not drop out if the funnel is handled carefully.

To carry out measurements, the funnel is inverted so that the surface

[2] A layer of sample powder 2–3 mm. thick absorbs most Beta radiation from the back layers and will not be obtained in the funnel tip with amounts as little as 5–10 mg. of sample. Accordingly, measurements are made by weight rather than volume because the latter cannot be estimated accurately and will vary with differences in the packing of the powders.

of the sample may be brought as close as possible to the mica window of the Geiger tube.[3] The time period for the sample count, or the pre-set number of impulses to be recorded, is dependent upon the activity of the sample and the desired accuracy,[4] and is left to the experience and discretion of the investigator. A background count is taken before and after a sample measurement and for a similar period of time. The average of these two background counts is subtracted from the sample count to obtain the net sample count. Calculations are made on the net sample counts.

From several samples of analysed radioactive minerals on hand, three were chosen for experimental tests by the above method. Descriptions of these three samples are given in the following table:

Product	Chemical analyses[1] UO_2	UO_3	ThO_2	Calculated approximate per cent U_3O_8 radiation equivalent[2]
No. 1—Euxenite Mattawan tp., Ont.	6.42	0.43	0.97	7.3
No. 2—Euxenite, Maberley tp., Ont.	7.25	1.51	2.64	9.7
No. 3—Uraninite, Parry Sound, Ont.	53.63	26.32	3.22	82.4

[1] Ellsworth, H. V.: Rare-element Minerals of Canada, Geological Survey of Canada, Economic Geology Series No. 11, 1932.

[2] $UO_2 \rightarrow U_3O_8 = 1.0395$
$UO_3 \rightarrow U_3O_8 = 0.98136$
$ThO_2 \rightarrow U_3O_8 = 0.25$ (approximate Beta radiation equivalent)

The samples were tested against uranium standards prepared by the Mines Branch, Department of Mines and Technical Surveys. Ten milligrams of both samples and standards were measured with an end-window

[3] The distance between the sample surface and the mica window is critical as the sample may be regarded as a point source and, therefore, obeys the inverse square law, that the intensity of radiation is inversely proportional to the square of the distance from the source. The distance should be equal in measurements of both samples and uranium standards.

[4] Since radiations from radioactive substances are random in their distribution, a large number of impulses must be recorded with the Geiger tube to ensure accuracy in sample measurements. The per cent probable error associated with counting rates is given by the formula: $67.45/\sqrt{n}$ where n is the number of recorded impulses. It may be seen from substitution in this formula that it is necessary to total approximately 4,000 impulses to reduce the statistical error to one per cent. (*See* also: Harris, R. F.: Statistical Variation Applied to Radioactive Counting, Mines Branch, Department of Mines and Technical Surveys, Topical Report No. 38, Sept. 1949.)

Beta tube in combination with a ratemeter. The mica window thickness of the Beta tube was 1–2 mg/cm². Results of measurements are as follows:

Product	Net counts/minute	Per cent U_3O_8 equivalent	Per cent U_3O_8 equivalent from chemical analyses
No. 1	190	7.6	7.3
No. 2	246	9.8	9.7
Standard sample, 8.72 per cent U_3O_8	218	—	—
No. 3	1668	82.2	82.4
Standard sample, 63.19 per cent U_3O_8	1283	—	—

The results of the uranium standards are not in agreement as measurements were made on different days and the powder surfaces were at different distances from the mica window of the Geiger tube.

The method described above is also used by the Radioactivity Laboratory of the Geological Survey of Canada for quantitative radioactivity measurements of the concentrates from concentration tests of low-grade radioactive materials.

Unaltered, primary radioactive minerals commonly have a higher specific gravity than the gangue minerals, and can often be concentrated by gravity separation. However, where a concentration of the radioactive constituents is effected on low grade samples the amount of concentrate separated is usually too small for quantitative radiometric measurements by previous methods using metal trays with small depressions to hold the sample powder. The radioactivity of concentrates in such instances was calculated from the activities and weights of the middlings and tails, and the head sample. Several errors were thus introduced which can now be eliminated by a radiometric measurement of the concentrate itself.

A METHOD FOR THE SEPARATION OF MINERAL GRAINS FROM SIZED PRODUCTS[1]

H. R. Steacy, *Geological Survey of Canada, Ottawa, Canada.*

In the course of laboratory investigations for the Radioactivity Division, Geological Survey of Canada, a quick and easy method has been

[1] Published by permission of the Director-General of Scientific Services, Department of Mines and Technical Surveys, Ottawa.

developed for the separation of mineral grains from sized products. The grains are fastened to paper with drops of a solution of acetone and celluloid and collected in a dish of acetone. The method is useful for the preparation of pure mineral samples for chemical or physical examination. It is especially suitable for the selection of grains from a non-magnetic product whose constituents approximate the same specific gravity, because in this instance magnetic and gravity separations are not applicable.

The solution is prepared with 3.8 grams of clear celluloid and 50 c.c. of C. P. acetone, which are allowed to stand overnight in an air-tight container. After stirring the mixture vigorously, small drops of the liquid should be found to form hemispheres that dry whitish in approximately 30 seconds. The viscosity may be adjusted by evaporation, or dilution with acetone, and the mixture may be stored in the original container. The writer finds it convenient to have on hand several short lengths of glass tubing drawn to a fine tip at one end, with an opening 0.25 to 0.50 mm. in diameter.

Sprinkle a little of the sized product on a sheet of glazed paper 3 inches square. The individual grains should be at least 1 mm. apart. With an 8-inch length of rubber tubing attached to one of the pipettes, a little of the liquid is drawn by mouth into the pipette. A slight, steady pressure exerted by mouth will keep the liquid at the tip of the pipette; an increase in pressure will force it out in small drops. Examine the paper under a binocular microscope, and where a desired grain is seen allow a drop of the liquid to settle over the grain. This will secure the grain to the paper. It is not necessary to move the eyes from the binocular microscope until all the liquid in the pipette has been exhausted. As many as forty grains have been selected in one observation by this method.

At the end, the residual grains are shaken off the paper, and the sheet(s) immersed in a dish of acetone. The selected grains will drop free. Most of the acetone may then be poured off and recovered. The remainder will quickly evaporate leaving the selected sample of the pure mineral.

WALKER MINERALOGICAL CLUB*

OFFICERS 1951

Honorary President, A, L, Parsons; *President*, G. G. Waite; *Secretary-Treasurer*, Mrs. Helen Bush; *Editor*, L. G. Berry; *Councillors*, M. H. Frohberg, V. B. Meen, W. Take, C. C. Stevenson, J. A. McDonald.

ABSTRACT OF PROCEEDINGS, 1951

January 18, 1951. The Walker Mineralogical Club met in the Royal Ontario Museum of Geology and Mineralogy. Major E. Taylor of Queen's University gave a brief talk on mounting mineral specimens in plaster and displayed several minerals mounted in this manner. Dr. V. B. Meen, Director of the Royal Ontario Museum of Geology and Mineralogy, then addressed the club, giving a brief history of this museum and outlining the arrangement of its specimens. The remainder of the evening was spent in examining more closely the exhibits in the gallery of Mineralogy. Refreshments were served.

February 8, 1951. Mr. D. H. Gorman of the Department of Geological Sciences of the University of Toronto spoke on Mineral Identification. Groups of mineral specimens illustrating various properties were arranged systematically and members had the opportunity of examining them. Mr. C. C. Stevenson donated the lucky door prize, native copper from Keewanan Point, Michigan.

March 8, 1951. Three graduate students working in the Department of Geological Sciences addressed the club. Mr. D. H. Gorman spoke on "The Secondary Uranium Minerals," Mr. E. J. Brooker discussed the Metamict Minerals and Mr. J. M. Andrew's topic was the Study of Opaque Minerals in Polished Surfaces.

April 19, 1951. The financial statement of the year 1951 was presented by Mr. W. M. Tovell, showing a Balance on Hand to be $348.54. Colour slides of the 1950 field trip to Gouverneur, N. Y. were shown as well as slides of individual collecting trips by members. A mineral identification contest was won by Mr. Bruce Metcalfe.

May 22, 1951. Mr. E. R. Tiffany, certified gemologist, Henry Birks and Sons, Limited, Toronto, spoke on "How a Gemologist Looks at Gem Values," and also showed colour slides taken on his recent buying trip abroad. He put on display several exceptionally fine gem stones viz: two large alexandrites, a large blue sapphire, synthetic emeralds and black and white pearls.

October 5–8, 1951. The Fifth Annual Field Trip was held at Combermere, Renfrew County. Mr. Louis Moyd acted as guide. Corundum crystals were collected at the Craigmont Corundum Mines, and from the Quadville Beryl Mines beryl crystals, black tourmaline crystals, amazonite and rose quartz. An innovation introduced to this year's hunt was a square dance held on Saturday evening.

November 22, 1951. Mr. W. M. Tovell, lecturer in the Geological Sciences, University of Toronto addressed the club on "Gold Comes in Barrels," an outline of oil developments in Canada. He illustrated his talk with slides and specimens.

December 13, 1951. Dr. P. A. Peach of the Department of Geological Sciences, University of Toronto spoke on "A Trip to Labrador" and illustrated his talk with slides. The evening concluded with a gift exchange of minerals in which all members participated.

The Peacock Memorial Prize of One Hundred Dollars Cash is offered by the Club for

* Founded in 1938 and named in honour of the late Professor T. L. Walker (1867–1942), then Professor Emeritus of Mineralogy and Petrography in the University of Toronto and Director of the Royal Ontario Museum of Mineralogy. The by-laws of the Club were published in *Am. Mineral.*, **34**, 469, 1949.

the best scientific paper on pure or applied mineralogy. A full announcement of the conditions governing the award appeared in the March–April, 1952, issue of *The American Mineralogist.* The papers must reach the secretary, Walker Mineralogical Club, 100 Queens Park, Toronto, not later than June 30, 1952.

The Council of the Walker Club wishes to acknowledge the courtesy of the Council of the Mineralogical Society of America in again making possible the publication of a Canadian number of *The American Mineralogist.*

MRS. HELEN BUSH
Secretary-Treasurer

ANNUAL MEETING

The thirty-third annual meeting of the Mineralogical Society of America will be held in Boston, Massachusetts, on November 13–15, 1952, with headquarters at the Hotel Statler.

A series of field trips is being planned for Monday, Tuesday, and Wednesday, November 10th to 12th. Various short excursions to scientific laboratories, industries, and historical sites in the Boston area are planned for the days of the meeting, November 13th–15th.

Abstracts of papers to be presented at the annual meeting must be received by the Secretary on or before *July 15, 1952.* Abstract blanks may be obtained from the Secretary.

NOMINATIONS OF OFFICERS FOR 1953

President: J. D. H. Donnay, Johns Hopkins University, Baltimore, Maryland

Vice-President: H. V. Ellsworth, Canada Geological Survey, Ottawa, Canada

Secretary: C. S. Hurlbut, Jr., Harvard University, Cambridge, Massachusetts

Treasurer: Earl Ingerson, U. S. Geological Survey, Washington, D. C.

Editor: Walter F. Hunt, University of Michigan, Ann Arbor, Michigan

Councilor: (1953–56): C. Osborne Hutton, Stanford University, Palo Alto, California.

The above Fellows have been mominated by the Council as officers of the Mineralogical Society of America for 1953. They will be voted on at the election in October 1952.

C. S. HURLBUT, JR., *Secretary*

According to the Arizona Daily Star of March 26, 1952, Dr. Maxwell N. Short, head of the Dept. of Geology and Mineralogy at the University of Arizona, died at his home in Tucson at the age of 63. Dr. Short had suffered from high blood pressure for a long time. Professor Short was one of the associate editors of *The American Mineralogist* and in 1939 was elected President of the Mineralogical Society of America.

Copies of a 12 page brochure summarizing articles and patents pertaining to the Diamond Tool Industry in 1951 are available, free of charge, from the Industrial Diamond Information Bureau, 32-34 Holborn Viaduct, London, E.C.I.

The Society of Exploration Geophysicists has elected the following officers for 1952–1953:

President: Curtis H. Johnson, assistant chief geophysicist for General Petroleum Corporation, Los Angeles, California.

Vice-President: Roy L. Lay, manager of the geophysical division of the Texas Co., Houston, Texas.

Secretary-Treasurer: Carl L. Bryan, consulting geophysicist, Shreveport, Louisiana.